THE SPEED OF VISUAL PROCESSING OF COMPLEX OBJECTS IN THE HUMAN BRAIN

Sensitivity to image properties, the influence of aging, optical factors and individual differences

Magdalena Maria Bieniek

Submitted in fulfilment of the
requirements for the degree of PhD

28 February 2014

Institute of Neuroscience and Psychology

School of Psychology

College of Science and Engineering

University of Glasgow

CENTRE FOR COGNITIVE NEUROIMAGING

University of Glasgow

ACKNOWLEDGEMENTS

First and foremost I would like to thank my supervisor Dr Guillaume Rousselet for his guidance, time and patience in taking me through the fascinating world of cognitive neuroscience. His incredible knowledge, enthusiasm and enormous dedication to doing great science will always be an inspiration to me. Thank you for encouraging me to always aim higher and for pushing farther than I thought I could go. Without your input and persistent help this work would not have been possible.

To all my friends in the School of Psychology and beyond: Chris, Kirsty, Flor, Luisa, Carl, David, Kay, Sarah, Zeeshan and especially Magda M. - you shared both the fun and the tough times with me and have made my time in Glasgow an amazing and unforgettable experience!

To all the students that I worked with over the years: Eilidh, Jen, Lesley, Terri-Louise, Santina, Sean and Hanna – you have been great and I wish to thank you for all your help with collecting data!

To Willem – thank you for your continues help and support; your immense technical knowledge has rescued me many times and your encouragement kept me going, allowing me to be where I am today.

Finally, I would like to thank the Leverhulme Trust and the School of Psychology for providing the financial support necessary for my PhD research.

ABSTRACT

Visual processing of complex objects is a feat that the brain accomplishes with remarkable speed – generally in the order of a few hundred milliseconds. Our knowledge with regards to what visual information the brain uses to categorise objects, and how early the first object-sensitive responses occur in the brain, remains fragmented. It seems that neuronal processing speed slows down with age due to a variety of physiological changes occurring in the aging brain, including myelin degeneration, a decrease in the selectivity of neuronal responses and a reduced efficiency of cortical networks. There are also considerable individual differences in age-related alterations of processing speed, the origins of which remain unclear. Neural processing speed in humans can be studied using electroencephalogram (EEG), which records the activity of neurons contained in Event-Related-Potentials (ERPs) with millisecond precision. Research presented in this thesis had several goals. First, it aimed to measure the sensitivity of object-related ERPs to visual information contained in the Fourier phase and amplitude spectra of images. The second goal was to measure age-related changes in ERP visual processing speed and to find out if their individual variability is due to individual differences in optical factors, such as senile miosis (reduction in pupil size with age), which affects retinal illuminance. The final aim was to quantify the onsets of ERP sensitivity to objects (in particular faces) in the human brain. To answer these questions, parametric experimental designs, novel approaches to EEG data pre-processing and analyses on a single-subject and group basis, robust statistics and large samples of subjects were employed. The results show that object-related ERPs are highly sensitive to phase spectrum and minimally to amplitude spectrum. Furthermore, when age-related changes in the whole shape of ERP waveform between 0-500 ms were considered, a 1 ms/year delay in visual processing speed has been revealed. This delay could not be explained by individual variability in pupil size or retinal illuminance. In addition, a new benchmark for the onset of ERP sensitivity to faces has been found at ~90 ms post-stimulus in a sample of 120 subjects age 18-81. The onsets did not change with age and aging started to affect object-related ERP activity ~125-130 ms after stimulus presentation. Taken together, this thesis presents novel findings with regards to the speed of visual processing in the human brain and outlines a range of robust methods for application in ERP vision research.

LIST OF PUBLICATIONS

Bieniek, M. M., Pernet, C. R. & Rousselet, G. A. (2012) Early ERPs to faces and objects are driven by phase, not by amplitude spectrum information: Evidence from parametric, test-retest, single subject analyses. *Journal of Vision*, 12 (13): 12, 1-24, http://journalofvision.org/content/121/13/12, doi: 10.1167/12.13.12

Bieniek, M. M., Frei, L. S., & Rousselet, G. A. (2013), Early ERPs to faces: aging, luminance and individual differences, *Frontiers in Perception Science*: *Visual Perception and visual cognition in healthy and pathological ageing, 4 (267),* doi: 10.3389/fpsyg.2013.00268.

Bieniek, M. M., Bennett, P. J.; Sekuler, A. B. & Rousselet, G. A. (in prep), ERP face sensitivity onset in a sample of 120 subjects = 87 ms [81, 94].

TABLE OF CONTENTS

1 LITERATURE REVIEW

The ease with which humans can recognise complex objects in a fraction of second is perhaps one of the most striking abilities of the human brain. When visual information travels from the retina through the primary visual cortex (V1) to higher-order cortical areas, it undergoes a number of transformations and is progressively translated into higher-level neural representations that can be used for decision-making (Wandell, 1995; DiCarlo & Cox 2007). It is still unclear what information that is available to the visual system is used by the brain to create these representations and how fast are they created. Our knowledge with regards to how factors such as development, aging and disease influence the dynamics of visual processing is also fragmented. Further, we know very little as to why human brains differ considerably in how fast they process visual information; these individual differences are only beginning to be quantified. Various scientific disciplines have contributed to the current state of knowledge about the properties and speed of object processing in the brain, from biology, through molecular and cognitive neuroscience to psychology. Multiple brain imaging methods have also been used to explore neural correlates of visual processing and one technique has been particularly useful in measuring the time course of object categorisation – EEG (electroencephalogram). In this literature review, I will first introduce EEG methodology, outline its pros and cons, and discuss areas of concern and point out potential improvements in collecting and analysing EEG data. Subsequently, I will present the theoretical and empirical developments to date with regards to visual object processing in the human and monkey brain, followed by an overview of the current state of knowledge concerning the aging brain and how various cortical and optical factors might contribute to age-related changes in visual processing speed. I will also identify the gaps and inadequacies in the existing literature and point out how the experimental work presented in this thesis addresses some of these gaps.

1.1 USING ELECTROENCEPHALOGRAPHY (EEG) TO MEASURE THE SPEED OF VISUAL PROCESSING IN THE BRAIN

Because recognition occurs so rapidly, it is essential to explore the temporal dynamics of the neuronal extraction of information necessary for image classification. This can be achieved by recording Event-Related Potentials (ERPs) contained in EEG data. Scalp EEG non-invasively records the summed activity of thousands, or even millions, of neurons in the form of tiny electrical potentials picked up from subject's scalp. EEG is particularly sensitive to post-synaptic potentials generated in superficial layers of the cortex by neurons directed towards the skull. Dendrites that are located deeper within the cortex and/or are producing currents that are tangential to the skull have much less contribution to the EEG signal. Because scalp EEG records summed neuronal activity coming from different parts of the brain, precise source localisation of EEG signal poses difficulties. Hence, EEG is considered to have a poor spatial resolution. EEG has excellent temporal resolution (in the order of milliseconds), however, allowing it to track the time course of neural activity associated with perceptual and cognitive processes (Luck, 2005).

Many methods of processing EEG data exist, and most of them typically involve basic steps such as filtering, baseline correction, epoching or artifact rejection. To increase the signal-to-noise ratio of EEG data, many trials per condition need to be recorded, which can be then time-locked to the stimulus onset and averaged. This procedure outputs mean ERP waveforms, which are typically reported in EEG studies. No consensus exists as to what the best approach is in terms of processing or statistical analyses of EEG data, but the choice of method may potentially have a significant impact on the experimental results (Rousselet & Pernet, 2011; VanRullen, 2011). I will challenge several assumptions in current EEG data analyses techniques, point out their limitations, and suggest potential improvements.

First, ERP researchers commonly restrict their data analyses to easily identifiable peaks (components) within the EEG waveform, for example P100 – a positive peak around 100 ms post-stimulus, or N170 – a negative deflection around 170 ms post-stimulus. However, this approach is problematic mainly because there is no agreement within the EEG research field regarding the exact nature of the information carried within the EEG waveform, including the exact meaning of ERP peak latencies and amplitudes. ERP components are not equivalent to functional brain components (Luck, 2005). Thus, limiting the analyses to pre-defined peaks, and discarding the potentially informative activity between peaks, misses what could have been otherwise obtained using a data-driven approach. And

since it is difficult to pin-point the exact cortical sources of EEG activity picked up from various parts of the scalp, we should not restrict the analyses to pre-defined scalp electrodes either. Using data-driven EEG data analyses procedures was encouraged already in the 80' by Lehmann (1986a; 1987; 1986b) who emphasised the importance of both temporal and spatial dimensions of EEG data. Since then many developments in data-driven analyses approaches have been introduced making these approaches an attractive and necessary direction for the future of EEG research (Rousselet & Pernet, 2011).

Including all the electrodes and all the ERP time-points into the statistical analyses significantly increases the number of comparisons one needs to perform. Thus, such analyses require robust methods that correct for multiple comparisons to help to control for Type I error – an inflated rate of possible false positives. A variety of possible ways to correct for multiple comparisons exists, including Bonferroni correction or resampling-based methods, which provide better univariate confidence intervals and, in conjunction with other techniques, can be used to control the Type I error rate. These include bootstrapping, permutations or Monte Carlo simulations. The popularity of the resampling methods has been growing recently because of their strength in utilising the characteristics of distributions of the observed data (Nichols, 2012; Eklund, Andersson, & Knutsson, 2011). However, too stringent multiple comparison corrections may boost the rate of false negatives. To deal with this problem sophisticated thresholding techniques have been introduced (Nichols, 2012) that incorporate information both on false positives and false negatives. The method combines evidence against the null hypothesis (classical p-value) with evidence that supports it (alternative p-value). The selection of multiple comparisons correction methods is currently broad and the choice should depend on the experimental design, the characteristics of data, and the estimators used (Rousselet & Pernet, 2011; Maris & Oostenveld, 2007; Litvak, et al., 2011).

Another issue comes into play when applying statistical measures to analyse EEG data. Typically, EEG studies compute the average EEG activity across trials using the mean as a measure of central tendency. They also typically report variance as a measure of dispersion, and use standard t-tests and ANOVAs for inferential statistics. However, the use of these classic statistical tools requires the data to be normally distributed and the variances to be homogeneous. If applied to data that do not meet the optimal distribution criteria, and are, for instance, skewed or contain outliers, standard statistical tools can lead to significant errors both in descriptive and inferential statistics (Wilcox, 2012). Robust alternatives to the standard tools exist, for instance trimmed mean or winsorized variance and equivalents of t-

test and ANOVA that incorporate them. These measures are robust even when optimal distribution requirements are violated, and the EEG community could greatly benefit from applying them more widely.

Recently, the cutting-edge EEG data analyses techniques tend to move away from averaging ERP activity towards single-trial-oriented approaches. This is because important information regarding the nature of neural processing is contained within each single-trial ERP and in the variability across trials. A growing number of studies use single-trial-based analyses to study the relationships between brain activity, stimulus properties and behavioural responses of subjects (Philiastides & Sajda, 2006; Schyns, Petro, & Smith, 2007; Ratcliff, Philiastides, & Sajda, 2009; Vizioli, Rousselet, & Caldara, 2010). This would have been impossible with the standard average-across-trials ERP techniques, which obstruct inter-trial variability. New techniques to estimate single-trial variability distributions are being developed, including reverse correlation techniques (Smith, Gosselin, & Schyns, 2007), Generalized Linear Models (Pernet, et al., 2011) and ICA-based approaches (De Vos, Thorne, Yovel, & Debener, 2012). The latter technique has been used in recent studies to demonstrate that the ERP activity visible ~170 ms in response to faces can be dissociated from activity ~100 ms in terms of its neural origins (Desjardins & Segalowitz, 2013), and that it is not exclusively face-related but associated with the network involved in general visual processing (De Vos, et al., 2012). Furthermore, relating behavioural and brain responses with each other, and with the information content of the stimuli, requires moving away from statistical analyses on a group level and focusing instead on individual subject data. Each brain is unique and there is evidence that ERPs are much more similar within a subject than they are across subjects. Moreover, ERPs averaged across subjects tend to not resemble any of the individual subjects' ERP patterns (Gaspar, Rousselet, & Pernet, 2011). Finally, there are considerable individual differences in the speed of visual processing in the brain (Rousselet, et al., 2010) that cannot be addressed by using group analyses approaches.

Another problem that can potentially distort EEG results is data filtering. Typically EEG data is filtered during the pre-processing stage in order to increase the signal-to-noise ratio. However, filtering can seriously distort the data – an issue that has been well documented in the literature (Luck, 2005) and recently has been brought back into the attention of the ERP research community (VanRullen, 2011; Acunzo, MacKenzie, & van Rossum, 2012; Rousselet G. A., 2012; Widman & Schroger, 2012). Non-causal high-pass filters, with cut-offs beyond a recommended 0.1 Hz, cause potential distortions in the shape of the ERP waveform (Luck, 2005; Acunzo, et al. 2005). A filter is called non-causal

if it is applied in a forward direction first and then again in a backward direction, which results in a zero-phase shift. Non-causal filtering can produce artifacts; in particular it can smear the effects in later parts of the waveforms back in time, contaminating earlier parts of the waveform with the effects that were not previously there (Acunzo, et al., 2012). Non-causal filters are prevalently used in ERP research according to non-exhaustive overviews done by Acunzo, et al. (2012) and Rousselet (2012). Acunzo, et al. (2012) reported that out of 185 scrutinized studies, 43% used filters with cut-offs higher than 0.1 Hz and half of those used cut-offs higher than 1 Hz. Rousselet (2012) reported that out of 158 studies, 21 used high-pass filters at 1, 1.5 or 2 Hz. Moreover, most ERP studies do not specify whether the filter they used was non-causal or causal. Causal filters are applied only in forward direction, hence they do not generate distortions backward in time. They can be safely used to study the latencies of the earliest effects (onsets). However, causal filters alter the phase of the signal; thus, if one is interested in the latency of peaks, non-causal filters should be applied (Acunzo, et al. 2005; Rousselet, 2012). In general though, data filtering should be kept to a minimum whenever possible and filter types and cut-offs should be carefully considered, taking into consideration the quality of the data and experimental hypotheses.

To sum up, the future of ERP vision research lies in single subject data-driven analyses techniques, using careful data cleaning procedures, robust statistical measures and experimental designs that aim to link brain activity, behaviour and the information available to the visual system on a single-trial basis. The new developments will hopefully help to create models of the visual system that incorporate the various levels of neuronal information processing, from activity of single cells to large populations of neurons. EEG has been the method of choice for the work in this thesis, which also applies several methodological improvements: parametric experimental designs, single subject data analyses, EEG data pre-processing procedures based on cutting-edge developments, and robust statistics using variety of non-parametric measures that do not rely on assumptions about data distributions. All this allows a more precise quantification of the speed of the neuronal processing underlying visual object categorisation, as reflected in the ERPs.

1.2 PROPERTIES OF THE VISUAL SYSTEM IN PRIMATE AND HUMAN BRAIN

Understanding the visual system's structure and function is vital to understanding how, when and where in the brain objects are processed and recognised. Anatomical studies of the primate brain have shown between two dozens and 40 visual and visual associative cortical areas, but their exact number is still unknown (Van Essen, 2003; Sereno & Tootell, 2005). Establishing how many visual areas are in the human brain has been proven more difficult, mostly because highly informative techniques, such as single cell recordings, neural tracers or artificially induced lesions, to name a few, are also highly invasive and cannot be routinely used in humans. However, non-invasive brain imaging techniques, primarily structural and functional magnetic resonance imaging (MRI and fMRI), have revealed more than a dozen putative human visual areas (Tootell, Tsao, & Vanduffel, 2003; Felleman & Van Essen, 1991; Nowak & Bullier, 1997; Orban, Van Essen, & Vanduffel, 2004). The exact number, location, and functionality of primate and human visual areas are the subject of ongoing research. Two main suggestions have been put forward to account for the multiplicity of visual brain regions: hierarchical processing and functional specialisation.

1.2.1 HIERARCHICAL ORGANISATION OF THE VISUAL SYSTEM

According to the hierarchical organisation hypothesis, as the visual information travels from the retina, through the lateral geniculate nucleus (LGN) and the primary visual cortex (or striate cortex/V1) to the extrastriate and higher-order visual areas, such as V4, inferior temporal cortex (IT) or medial temporal cortex (MT), it undergoes a number of transformations from very simple to increasingly more refined and complex representations (Grill-Spector & Malach, 2004; Ullman, 2006). A simplified representation of the main human visual areas is depicted in Figure 1.1. Visual signals reaching the retina are processed by at least 80 anatomically and physiologically distinct neural cell populations and 20 separate circuits, resulting in over a dozen parallel pathways that project their signals further to the cortex (Dacey, 2004). While information travels up the visual hierarchy, more and more complex visual features are being resolved. For example neurons in V1 respond to simple lines of different orientations, brightness or local contrast (Geisler, Albrecht, & Crane, 2007; Tootell, Hamilton, Silverman, & Switkes, 1988), while some neurons in the higher level visual areas in the IT cortex fire selectively when certain categories of stimuli are present, such as faces (Tsao, et al., 2006; Freiwald, et al., 2010; Logothetis & Sheinberg, 1996; Freedman & Miller, 2008).

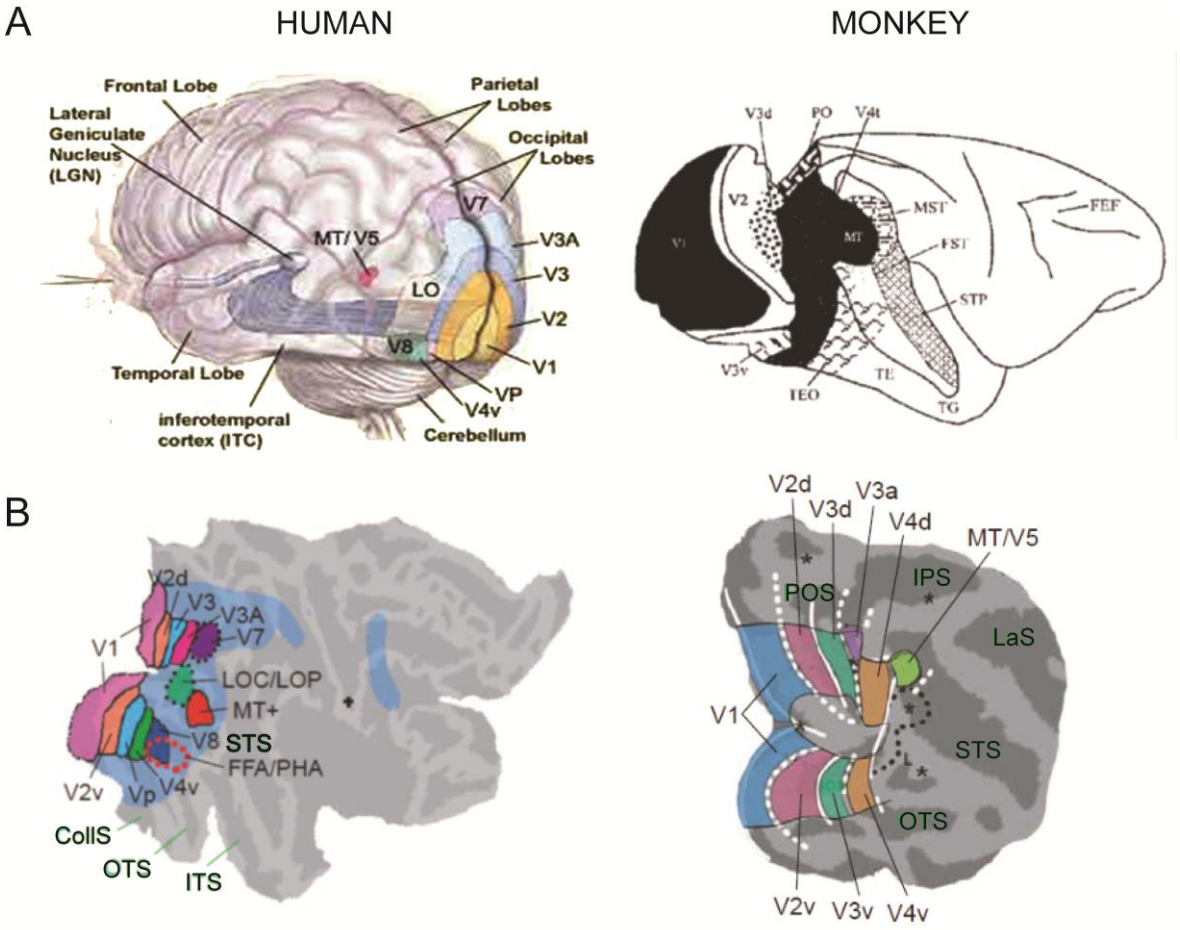

Figure 1.1. *Schematic representations of the visual areas in the human (left) and the macaque monkey brain (right). (Human brain image sourced from (Dubuc, 2014); macaque image adapted from Bullier (2003), Fig. 33.5, p. 529). (B) Flat maps of human (left) and monkey (right) visual areas; CollS: collateral sulcus, OTS: occipito-temporal sulcus, ITS: inferior temporal sulcus, POS: parieto-occipital sulcus, IPS: intraparietal sulcus, LaS: lateral sulcus, STS: superior temporal sulcus (Adapted from Orban, Van Essen, & Vanduffel (2004), Fig 1, p.317).*

The notion of a hierarchical organisation of visual pathways is supported by monkey data indicating that as information travels from the retina to the higher-order visual areas the response latencies of neurons become increasingly delayed (Bullier, 2003; Nowak & Bullier, 1997). While responses at the retina appear as early as 20 ms post-stimulus (Copenhagen, 2004), those in LGN/V1/V2 become visible between 45 – 80 ms, and the responses in IT, Superior Temporal Sulcus (STS) and most posterior regions of the temporal lobe occur between 100 – 200 ms (Nowak & Bullier, 1997). It is worthwhile to note that the reported latencies of neurons in the various areas of a monkey's visual system vary considerably among studies (Figure 1.2). For instance, median latencies of cells responding to light flashes in V1 range from 45 – 80 ms. The latency differences between two adjacent areas, for instance between V1 and V2, seem to range between 10 – 20 ms (Raiguel, Lagae, Gulyas, & Orban, 1989; Schmolesky, et al., 1998; Wang, Zhou, Ma, &

Leventhal, 2005) (Figure 1.3). The reported latency differences between V1 and V4 areas, connected through a relay in V2, tend to be around 20 – 40 ms (Maunsell & Gibson, 1992; Schmolesky, et al., 1998), or even less if bypass routes from V1 to V4 and from V2 to IT are considered (Nakamura, Gattass, Desimone, & Ungerleider, 1993). Thus, it seems that at least parts of the visual systems are organised in a hierarchical manner. However, the pure form of hierarchical hypothesis is difficult to reconcile with the findings showing that response latencies within the visual system are not always ordered as expected from their anatomical hierarchy (Felleman & Van Essen, 1991).

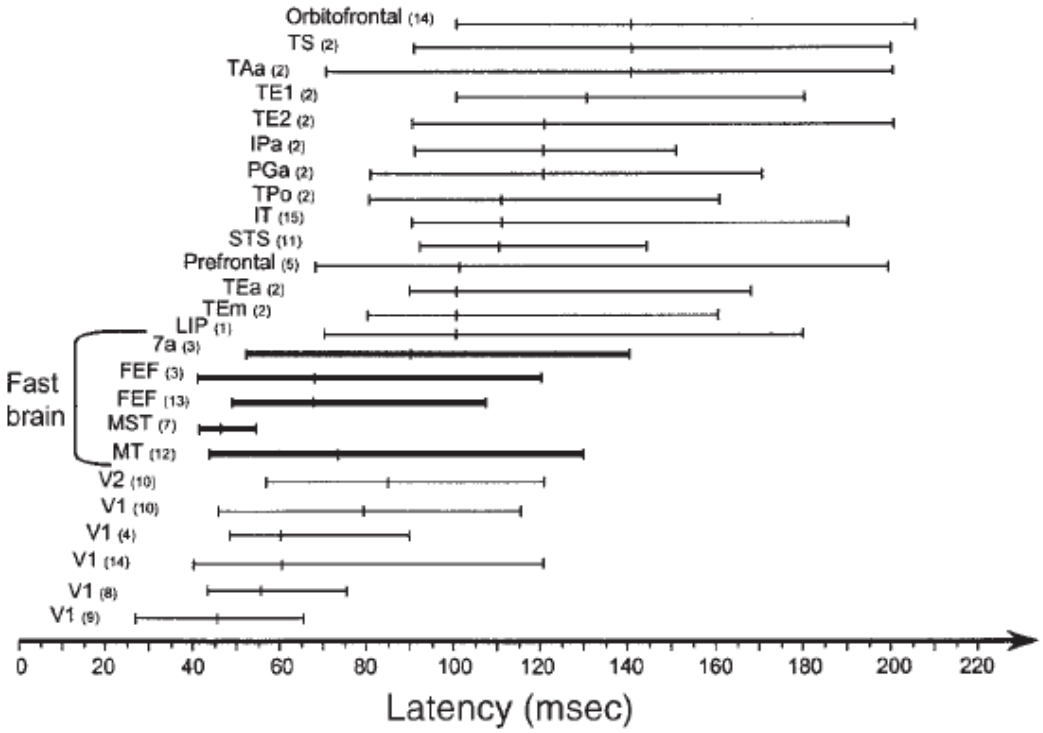

Figure 1.2. *Latencies of neurons in different cortical areas of the macaque monkey. Data from behaving monkeys in all cases except (10). Stimuli were small light flashes in all cases except (7) and (12), for which fast- moving visual pattern was used. For each area, the end points of the bar represent the 10% and 90% centiles and the tick represents the median latency. No difference was found between latencies to motion onset and to small flashed stimuli (Raiguel et al., 1999). [(1), Barash, et al., 1991; (2), Baylis, et al., 1987; (3), Bushnell, et al., 1981; (4), Celebrini, et al., 1993; (5), Funahashi, et al., 1990; (6), Goldberg and Bushnell, 1991; (7), Kawano, et al., 1994; (8), Knierim and Van Essen, 1992; (9), Maunsell and Gibson, 1992; (10), Nowak, et al., 1995; (11), Perrett, et al., 1982; (12), Raiguel, et al., 1999; (13), Thompson, et al., 1996; (14), Thorpe, et al., 1983; (15), Vogels and Orban, 1994]. (Modified from Nowak & Bullier, 1997, Fig.4, p.229).*

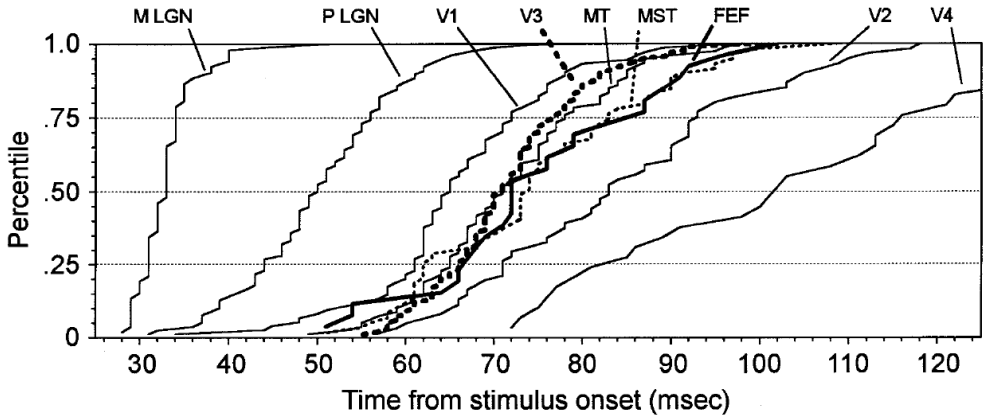

Figure 1.3. *Cumulative distributions of visually evoked onset response latencies in the LGNd, striate and extrastriate visual areas as labeled. Percentile of cells that have begun to respond is plotted as a function of time from stimulus presentation. The V4 curve is truncated to increase resolution of the other curves; the V4 range extends to 159 ms. (Reprinted from Schmolesky, et al., 1998, Fig. 2, page 3272).*

Multiple findings suggest that the information transfer across the visual pathways follows a more complex route and does not happen in a simple serial fashion - from bottom to top, or from simple to complex. For example, latencies of neuronal responses in the Frontal Eye Field (FEF) area, located anatomically close to the top of visual hierarchy, overlap with those in V1, located at the bottom of the visual hierarchy (Bichot, Shall, & Thompson, 1996). Further, the fast-cells-mediated 10 ms delay observed between monkey areas V1 and V2 is also observed between V1 and MT – an area located anatomically much further away from V1 than V2 (Raiguel, Lagae, Gulyas, & Orban, 1989). Such findings have led to multiple propositions with regards to the organisation of the visual system (Figure 1.4) and to a distinction between the so called *fast* and *slow* brain areas within it. The areas that belong to the *fast* brain include V1, V2, medial superior temporal area (MST) and FEF, with average response latencies below 80 ms, as well as MT and V4, with latencies only 10 and 20 ms larger than in V1, respectively. Areas in the temporal lobe, such as the STS or IT cortex (e.g. areas TE and TEO) represent the *slow* brain and respond with latencies above 100 ms (Nowak & Bullier, 1997; Bullier, 2003).

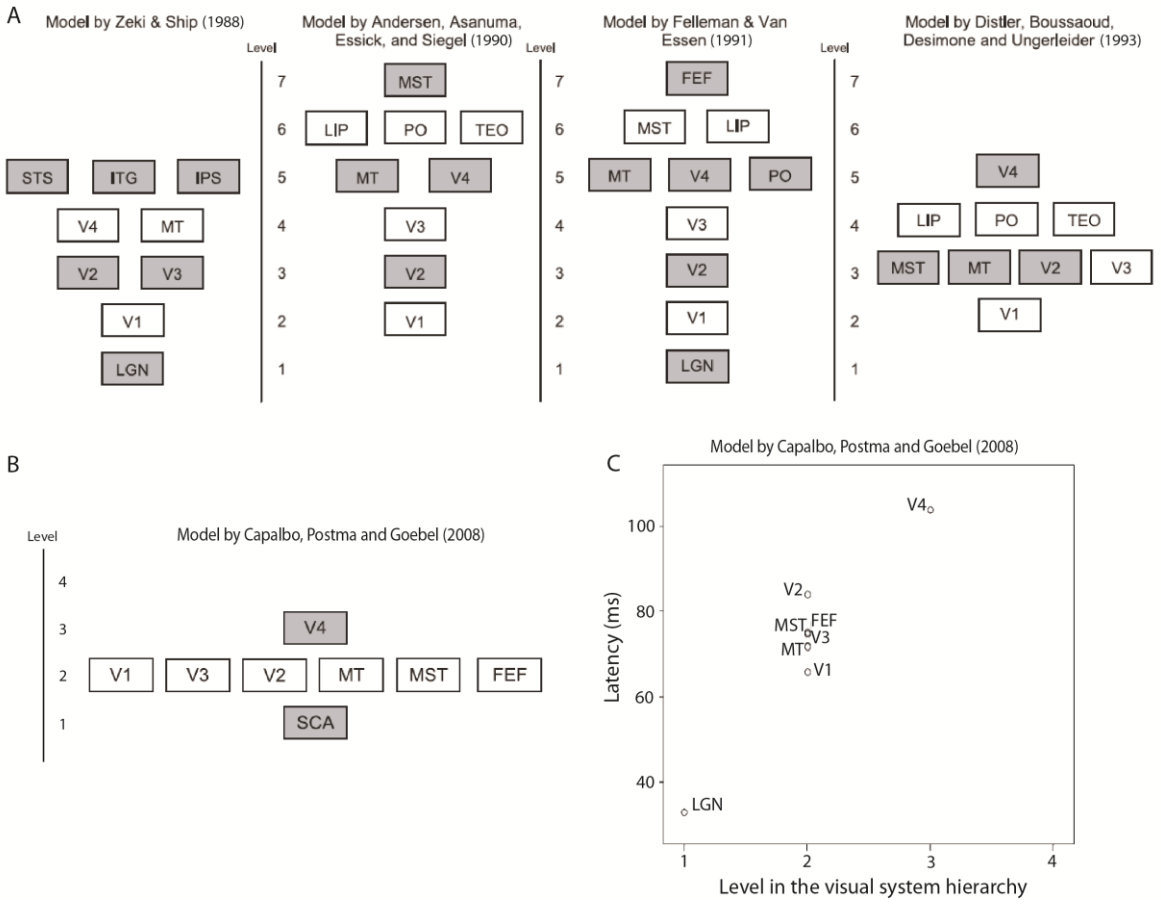

Figure 1.4. *Models of the visual system.* ***(A)*** *Hierarchies of visual areas proposed in different publications. Areas are arranged according to the figures in the original articles (Adapted from Capalbo et al., 2008, Fig.1, p.2).* ***(B)*** *Model proposed by Capalbo, et al. (2008) with response latencies of various brain regions* ***(C)*** *occupying different levels in this model (Adapted from Capalbo, et al., 2008, Fig.12, p.11 & Fig.11B, p.10).*

While relatively distant areas can activate almost simultaneously or with little delay, considerable differences in neuronal response latencies may exist within one cortical region. For instance, neurons in layer 4Cα of V1 receiving input from the magnocellular pathway have ~20 ms shorter response latencies than neurons in layer 4Cβ of V1 that receive input from the parvocellular pathway. Evidence from intracranial recordings in humans indicates that visual information is processed in parallel by several cortical areas and that a single cortical area can be involved in more than one stage of visual processing. For example, Halgren, Baudena, Heit, Clarke, & Marinkovic (1994) showed that each of the 14 studied brain regions in the temporal, occipital and parietal lobes, including fusiform and lingual gyri, lateral occipitotemporal cortex, posterior and anterior middle temporal gyrus or superior temporal gyrus, was involved in 2 to 8 stages of visual processing. For example, a sequence of potentials visible around 130 – 240 ms post-stimulus was the largest in the fusiform gyrus, but was also present in several other

structures including V4, posterior superior gyrus and middle temporal gyrus. Finally, studies show that patterns of activity that are thought to be characteristic of higher visual areas can also be found in the early visual regions (Lamme, Super, & Spekreijse, 1998; Lee, Yang, Romero, & Mumford, 2002; Kourtzi, Tolias, Altmann, Augath, & Logothetis, 2003). All this evidence shows that, for most areas beyond V1, V2 and V3, it is impossible to be certain where exactly in the visual hierarchy a given region is located and there is no simple division between "higher" and "lower" visual areas (Juan & Walsh, 2003; Pascual-Leone & Walsh, 2001; Anderson & Martin, 2006; Angelucci & Bressloff, 2006; Bullier, 2003).

Determining the organisation of the visual system is also challenging because cortical areas that support visual processing are interconnected in a sophisticated and not yet fully understood fashion with a network of feed-forward, feedback and horizontal projections (Bullier, 2003; Salin & Bullier, 1995; Gilbert, 1993; Lamme, Super, & Spekreijse, 1998; Felleman & Van Essen, 1991; Markov, et al., 2014). These connections create a network of parallel and highly reciprocal channels, allowing complex interactions within and between different regions of the visual system and beyond it. For instance, V1 sends strong feed-forward signals to V2 and MT (Kuypers, Szwarcbart, Mishkin, & Rosvold, 1965; Van Essen, Newsome, Maunsell, & Bixby, 1986) but also receives feedback information from V2, V4, IT and MT that modifies its responses (Gattass, Sousa, Mishkin, & Ungerleider, 1997; Huang, Wang, & Dreher, 2007; Bullier, Hupé, James, & Girard, 2001; Bullier, 2003). It appears that conduction rates of feedback and feed-forward connections are quite similar, at least between V1 and V2 (Girard, Hupe, & Bullier, 2001). This suggests that visual information may travel up the visual hierarchy as fast as it travels down. The role of different types of cortical connections is unclear, but reports suggest that feed-forward processing mainly determines the receptive field tuning properties of neurons in the visual system, and that the converging feed-forward input from lower-level areas facilitates the selectivity of neurons in the higher areas (Bullier, 2003). Feedback and horizontal connections on the other hand are thought to mediate processes related to visual awareness and attention (Lamme, Super, & Spekreijse, 1998), but they also seem to be involved in bottom-up selectivity. According to the model by Ullman (1995, 2006) feedback projections may carry different hypotheses concerning the interpretation of the viewed stimulus that are sent down to meet the incoming feed-forward activity, giving rise either to extinction or reinforcement of neural activity associated with different interpretations.

All in all, it seems that the visual system does not adhere to the naïve top-to-bottom or simple-to-complex hierarchical organisation, at least beyond the visual areas V1, V2 and V3. The mismatch between the structure of the visual system and the timing of responses throughout it as well as the complexity of connections between the areas suggests that networks supporting visual processing may be organised according to its functional purpose rather than anatomy. The functional roles of neural systems supporting visual processing will be presented next.

1.2.2 FUNCTIONAL SPECIALISATION OF CORTICAL PATHWAYS SUPPORTING VISUAL PROCESSING

Functional specialisation hypothesis suggests the existence of neural pathways specialising in different type of visual information processing. These pathways, although not completely separate, utilise incoming information in different ways depending on outcome requirements (Goodale & Milner, 1992). Examples of such functionally specialised pathways are the dorsal and ventral visual streams. The dorsal stream is mainly involved in visuo-motor control, grasping and object manipulation; hence it is also called the "where" pathway. The ventral stream on the other hand is primarily engaged in recognition of objects; hence it is also called the "what" pathway. The existence of these pathways is mainly supported by the contrasting effects of lesions in monkeys' brain areas involved in the two pathways (Ungerleider & Pasternak, 2003). Both streams originate in the primary visual cortex (V1), and continue via V2 where from the dorsal stream is directed into the dorsal sites of the parietal lobe via MT, whereas the ventral stream is directed into the IT lobe (areas TEO and TE) via V4 (Ungerleider & Mishkin, 1982; Goodale & Milner, 1992). Many areas within the stream share sensitivity to some stimulus properties, such as colour, shape or texture (Ungerleider & Pasternak, 2003). The last stations of both streams project into the perirhinal cortex and the parahippocampal areas TF and TH, from which information is sent via entorhinal cortex to the medial temporal lobe (MTL) regions, such as hippocampus (Mormonne, et al., 2008). Both streams also have heavy connections with the prefrontal areas (Ungerleider, Gaffan, & Pelak, 1989; Webster, Bachevalier, & Ungerleider, 1994; Cavada & Goldman-Rakic, 1989) as well as subcortical structures, including pulvinar, claustrum and basal ganglia (Webster, Bachevalier, & Ungerleider, 1995; Ungerleider, Galkin, & Mishkin, 1983). The ventral stream also has direct projections to the amygdala (Webster, Bachevalier, & Ungerleider, 1993). The two-stream hypothesis is supported by evidence from mice brains showing two sub-networks – one connected to the parietal and motor cortices, and another to the temporal and the parahippocampal structures, resembling dorsal and ventral pathways

(Wang, Sporns, & Burkhalter, 2012). It is noteworthy that the visual processing in the two streams is not completely segregated. For example, there is growing evidence that the dorsal regions carry information about objects in 3D, including shape (Lehky & Sereno, 2007; Sereno, Trinath, Augath, & Logothetis, 2002), size and orientation (Murata, Gallese, Luppino, Kaseda, & Sakata, 2000), contributing to a view-invariant object representation in the cortex.

The response latencies in the regions of dorsal and ventral stream differ considerably. The dorsal stream engages more areas of the *fast* brain, including V1, V2, MT and MST, resulting in shorter response latencies, usually less than 100 ms. The ventral stream relies more on the *slow* brain areas, such as TEO and TE, and has longer latencies, usually above 100 ms (Ungerleider & Pasternak, 2003; Bullier, 2003). Longer response latencies within the ventral stream may be related to lower myelination density in the grey matter areas of the temporal lobe compared to the dorsal stream areas in the parietal lobe and MT. Most connections to the dorsal stream contain higher densities of neurofilament protein, indicating a higher proportion of large, myelinated, rapidly conducting axons, like those connecting V1 and MT (Movshon & Newsome, 1996). Also, bypass connections between regions, such as those from V1 to V4 or from V2 to IT (Nakamura, Gattass, Desimone, & Ungerleider, 1993), seem to be less frequent within the ventral stream. Most neural connections in the ventral pathway appear to be reciprocal in a way that projections from the first area to the second are reciprocated by the projections from the second to the first (Felleman & Van Essen, 1991). Despite the reciprocity, much of the processing appears to be sequential, perhaps contributing to longer response latencies compared to the dorsal stream that engages more parallel channels (Desimone & Ungerleider, 1989). Moving forward through the ventral stream, there is a gradual decrease in the retinotopy of cortical areas (responses of single neurons in the IT cortex become independent on the object's position in the visual field) and the selectivity to increasingly complex stimulus features and combination of features emerges (Tanaka, 1993). Also, a degree of selectivity in object-related responses seems to be present in the areas that the ventral stream projects to – the medial temporal lobe (MTL). Mormann, et al. (2008) found that the level of object selectivity in regions of the MTL was related to their response latencies – the least selective parahippocampal cells responded the earliest with mean latencies of 271 ms, compared to ~400 ms for more selective cells in entorhinal cortex, hippocampus and amygdala. These results hint that hierarchical object processing is present also beyond the ventral stream.

To sum up, visual processing engages a sophisticated network of cortical areas whose organisation seems to have some hierarchical properties, as inferred from anatomy and the neurons' response latencies, but involves also large number of parallel and reciprocal channels. Thus, inferences about the existence of stages in visual processing are difficult to make. Visual areas also appear to belong to largely independent cortical pathways, which are specialised in processing different aspects of visual information. Despite much progress, the understanding of structure and function of the primate visual system is still fragmented and many gaps in knowledge are waiting to be filled. These include detailed characteristics of the neural processes involved in object categorisation which are the subject of this thesis. These processes have already been the subject of a considerable body of prior research, which is reviewed in the following section.

1.3 OBJECT (FACE) PROCESSING IN THE PRIMATE VISUAL SYSTEM

The processing of objects begins in V1 with the analysis of local contours orientation, colour, contrast and brightness in a retinotopic manner – subsets of neurons are responsible for different locations within the visual field (Tootell, Hamilton, Silverman, & Switkes, 1988; Geisler, Albrecht, & Crane, 2007). Information is then sent forward to V2, which mainly examines colour, combinations of orientations, basic form of a stimulus, and border ownership (Ts'o, Roe, & Gilbert, 2001; Zhou, Friedman, & von der Heydt, 2000; Anzai, Peng, & Van Essen, 2007). Moving forward into V4, cells become more jointly tuned to the processing of multiple stimulus dimensions and conjunctions of features, such as width, length or disparity (Desimone & Schein, 1987; Pasupathy & Connor, 2002) and about a third of the V4 cells are sensitive to stimulus curves and angles (Gallant, Connor, Rakshit, Lewis, & Van Essen, 1996; Pasupathy & Connor, 1999). As the information reaches areas TEO and TE in the IT cortex, critical features needed to activate neurons tend to be moderately complex (Tanaka, 1997), and some cells exhibit strong preferential responses towards particular object categories, for example faces (Tsao, et al., 2003; 2006, 2008; Freiwald, et al, 2009, 2010). Cells in the IT cortex also encode configural relationships between object parts, supporting three-dimensional complex shapes representation (Yamane, Carlson, Bowman, Wang, & Connor, 2008). However, it is still uncertain where and when exactly the first object- and face-sensitive neural responses appear in the cortex and what visual information the brain uses to create object representations. Some aspects of when and what questions will be answered in the

experimental work presented in this thesis, but first research developments to date that have also addressed these, and related, questions will be reviewed.

1.3.1 THE WHERE AND WHEN OF OBJECT (FACE) PROCESSING

Accumulating research evidence coming from single cells, intracranial and scalp recordings, optical intrinsic signal imaging (OISI), and functional magnetic resonance imaging (fMRI) studies in monkeys and humans suggests that object processing is supported by both distributed and localised cortical activity, appearing within the first 200 ms after stimulus onset. Most object representations seem to rely on distributed patterns of excitatory and inhibitory neuronal responses of different parts of the cortex, which process various visual features and/or their combinations (Haxby, Gobbini, Furey, Ishai, Schouten, & Pietrini, 2001; Tsunoda, Yamane, Nishizaki, & Tanifuji, 2001; Cukur, Huth, Nishimoto, & Gallant, 2013; Sato, Uchida, Lescroart, Kitazono, Okada, & Tanifuji, 2013; Tanaka, 1997; Wang, Tanaka, & Tanifuji, 1996; Wang, Tanifuji, & Tanaka, 1998). However, both human and monkey IT cortex seem to also possess localised patches of clustered neurons specialised in processing of particular object categories, such as faces, body-parts or places (Kanwisher, McDermott, & Chun, 1997; Reddy & Kanwisher, 2006; Bell, Hadj-Bouziane, Frihauf, Tootell, & Ungerleider, 2009; Bell, et al., 2011; Tsao, Freiwald, Knutsen, Mandeville, & Tootell, 2003; Tsao, et al., 2006; Hung, et al., 2005; Kiani, et al., 2005; Matsumoto, et al., 2005; Efiuku, et al., 2004). Whether these patches are truly category-selective or rather display strong preferences towards one category, while still processing other stimuli, remains uncertain. However, there is considerable evidence that processing of at least one category of objects – faces – may be particularly privileged in both monkey and human cortex, and since face images were the primary stimuli used in the experiments for this thesis, the literature concerning face processing in both species will be presented next.

FACE PROCESSING IN MONKEYS

Various studies suggest that the processing of faces has preference over other objects in parts of IT cortex – it seems to be faster and associated with a unique neural circuitry (Wang, et al., 1996, 1998; Freiwald, Tsao & Livingstone, 2009; Freiwald & Tsao, 2010; Tsao, et al., 2003, 2006). There is also evidence suggesting innate nature of face processing ability that is independent of experience (Sugita, 2008). Several interconnected cortical patches specialised in face processing have been identified in monkeys' areas TE and TEO, but their exact number and location varies across studies, due to methodological differences in defining category-selective regions (Bell, et al., 2009). Typically, 2-6

regions per hemisphere have been reported and these include: posterior lateral (PL), middle fundus (MF), middle lateral (ML), anterior fundus (AF), anterior lateral (AL), and anterior medial (AM) (Pinsk, et al., 2005; 2009; Bell, et al., 2009; 2011; Freiwald & Tsao, 2010; Tsao, et al., 2003; 2006; 2008; Issa & DiCarlo, 2012; Moeller, Freiwald, & Tsao, 2008). The recent monkey studies indicate that more than 80% (and even up to 97%) of visually responsive cells in these patches exhibit high selectivity for faces, with responses being significantly stronger and earlier than responses to non-face categories (Issa & DiCarlo, 2012; Freiwald & Tsao, 2010; Freiwald, Tsao & Livingstone, 2009). This proportion is much higher compared to older studies, which reported only 10-30% of cells in a studied region to be face-selective (Perret, et al., 1982; Desimone, et al., 1984). The difference most likely stems from the methodological advances – most current studies use fMRI-guided single-cell recordings that facilitate the targeting of a highly face-selective area, whereas most earlier studies recorded from regions that were less precisely localised. Regardless of number and location of face patches, most studies seem to agree that the properties of individual neurons' tuning to face stimuli seem to vary across and within patches.

Recent evidence suggests that there is a build-up in the level of selectivity and timing of responses from posterior, via middle to anterior face patches (Freiwald & Tsao, 2010; Tsao, et al., 2008; Issa & Dicarlo, 2012; Bell, et al., 2009). For example, Freiwald & Tsao (2010) found that neurons in ML/MF patches responded to faces viewed from specific angles, while neurons in AL and AM achieved partial and almost full view invariance, respectively. There was also an increase in number of cells significantly modulated by face identity – from 19% of cells in ML/MF, 45% in AL to 73% in AM patch. Similar build-up across face patches was visible with regards to response latencies. Peak latencies of the local field potentials (LFP) evoked by faces increased from ML/MF (126 ms), through AL (133 ms), and further to AM (145 ms) patch. Bell, et al. (2011) also found neuronal response latencies to faces versus other objects to appear earlier in MF/ML than in AL/AM patches: ~110 versus ~120 ms, respectively. Considerably earlier overall neuronal latencies across all the patches were reported by Issa & DiCarlo (2012) – the median peak latencies across all object categories in the PL, ML and AM/AL patches were 74, 79 and 80 ms, respectively. For faces, the earliest responses in the PL patch were observed already ~60 ms and peaked ~80 ms post-stimulus. Overall, the temporal dynamics and the increase in selectivity of neuronal responses from posterior to anterior face patches seem to support hierarchical models of face processing in the IT cortex

(Tamura and Tanaka, 2001). What is puzzling is the considerable inter-studies variability in the timing of face-sensitive responses in the visual system.

Multiple studies that recorded face-related single-cell activity in monkey IT or the superior temporal sulcus (STS) reported response latencies larger than 100 ms (Bell, et al., 2009; Tsao, et al., 2006; Freiwald & Tsao, 2010; Freiwald, Tsao & Livingstone, 2009). Moreover, Efiuku, et al. (2004) demonstrated that out of a wide range of neuronal response latencies to faces, from 117 to 350 ms, only the late neurons (with responses >200 ms) correlated with monkeys' behavioural performance in a face identification task. Along similar lines, Tsao, et al. (2006) showed that only the later (~130 ms post-stimulus), but not the early LFP activity (~100 ms) in the middle face patch of monkeys' IT cortex was face-specific and corresponded to neurons' peak firing rate. On the other hand, several studies have observed cells responding selectively to face stimuli already around 60 – 100 ms in anterior middle temporal sulcus (Kiani, et al., 2005), the STS (Edwards, et al., 2003; Keysers, et al., 2001; Sugase, et al., 1999), the PL face patch of the IT cortex (Issa & DiCarlo, 2012), as well as other IT regions of the cortex (Matsumoto, et al., 2005). Also, microstimulation of sites in the lower bank of the STS and in area TE between 50-100 ms post-stimulus can bias monkeys' classification of noise stimuli towards faces (Afraz, et al., 2006). The timing differences across monkey studies could reflect real timing differences among neurons, but they could also be related to methodological differences: first, the many different locations the recordings have been made from (Yovel & Freiwald, 2013) and second, the problem with clearly defining what constitutes a face-selective region (Issa & DiCarlo, 2012; Tanaka, 2003). Thus, the evidence is mixed, but it seems that at least some of the face-selective sites in monkey IT cortex can respond already before 100 ms.

FACE PROCESSING IN HUMAN BRAINS

In humans, the object processing network involves areas in lateral occipital and ventral temporal lobe. In particular, strong preferential responses towards faces versus other object categories have been found in the midfusiform gyrus (the fusiform face area - FFA), the inferior occipital gyrus (the occipital face area - OFA) and the posterior superior temporal sulcus (pSTS) (Hoffman & Haxby, 2000; Kanwisher & Yovel, 2006; Sergent, et al., 1992; Kanwisher, McDermott & Chun, 1997). These regions have been associated with processing of invariant face characteristics, such as gender and identity, but also changeable face features, such as eye gaze or emotional expression (Hoffman & Haxby, 2000; Smith, et al., 2007; Andrews & Ewbank, 2004; Engell & Haxby, 2007). The importance of these regions in face processing is highlighted by neurological studies of

patients suffering from prosopagnosia – inability to recognise faces. Prosopagnosic patients suffer from lesions in various regions of the face-related network, such as the OFA, the FFA or the pSTS. Despite considerable heterogeneity in lesions locations and the extent of the recognition impairment between individual cases, data from these patients indicate that the OFA and the FFA are necessary for normal face identity processing (Rossion, Caldara, Seghier, Schuller, Lazeyras, & Mayer, 2003; Barton, Press, Keenan, & O'Connor, 2002). However, there has been growing evidence that FFA is also involved in the processing of objects other than faces (Hanson & Schmidt, 2011; Haxby, et al., 2001; Gauthier, 2000; Mur, et al., 2011; Huth, et al., 2012). It appears that FFA contains spatially segregated subdivisions whose activity is selectively enhanced and suppressed by categories other than faces, such as animals or vehicles (Cukur, Huth, Nishimoto, & Gallant, 2013; Grill-Spector, Sayres, & Ress, 2006). Broad tuning to processing of different object categories has been observed throughout the human ventral temporal cortex. For example, Haxby, et al., (2001) showed that fMRI response patterns in the object-selective areas that discriminated between faces, cats, man-made objects and scrambled texture images could also be found in the areas activated maximally only to one category. However, most support for the existence of face-selective regions in humans comes from fMRI data, which measures blood oxygenation levels in the cortex (BOLD response), and hence is not a direct measure of functional specialisation of cells. Moreover, demonstrating that a given area strongly responds to particular object categories is necessary, but not sufficient, to conclude that this area performs object recognition.

To measure how fast category-sensitive responses appear in the human brain, the vast majority of studies use non-invasive electrophysiological scalp recordings (EEG and MEG). There is a considerable debate regarding what cognitive processes are reflected in the shape (amplitude, latency) of the ERP waveforms in response to visual stimulation. Particularly widely debated is categorical sensitivity of the so called N170 component – a negative deflection of the waveform visible ~170 ms post-stimulus (ranging typically from 130 – 200 ms). The N170 tends to be larger in response to faces compared to a variety of other stimulus categories (Rossion, Joyce, Cottrell, & Tarr, 2003; Itier & Taylor, 2004; Rousselet, Macé, & Fabre-Thorpe, 2004; Bentin, McCarthy, Perez, Puce, & Allison, 1996), although some studies question its sensitivity to faces (Thierry, 2007). The N170 has been linked with activity in the OFA, FFA and the STS (Deffke, et al., 2007; Shibata, et al., 2002; Herrmann, Ehlis, Muehlberger, & Fallgatter, 2005; Itier & Taylor, 2004; Nguyen & Cunnington, 2014; Nguyen, Breakspear, & Cunnington, 2013), although recently the face-

related activity in the OFA and the FFA/STS have been dissociated and linked with the P1 and the N170, respectively (Desjardins & Segalowitz, 2013; Sadeh, Podlipsky, Zhdanov, & Yovel, 2010). It has not been determined yet what kind of neural processes the N170 is driven by and some studies have pointed out its link to task-related processes (Rousselet, et al., 2011) and expertise (Tanaka & Curran, 2001). It has also been suggested that the N170 deflection may reflect the accumulation of diagnostic face information useful for decision making, that concludes when the N170 peaks (Schyns, Gosselin, & Smith, 2009; Smith, et al., 2007).

However, the notion that the N170 is the first marker of face-related processes has been challenged by a number of studies. A considerable number of other studies have found ERP face-sensitivity before the N170 time window, in particular around the first positive ERP peak called P1, typically visible between 80 - 120 ms post-stimulus. Studies report delayed P1 latencies for inverted versus upright faces (Itier & Taylor, 2002, Linkenkaer-Hansen, et al., 1998) or amplitude alterations when intact face images are compared to their pixel scrambled versions (Linkenkear-Hansen, et al., 1998; Herrmann et al., 2005), images of buildings (Halit, et al., 2000) or places (Rivolta, et al., 2012). These early (~100 ms) face-related responses usually appear around medial and inferior occipital brain/scalp regions, around the location of striate and extra-striate visual areas, including the OFA (Linkenkear-Hansen, et al., 1998; Halit, et al., 2000; Rivolta, et al., 2012). It is uncertain if such early face-sensitive responses are also present in the FFA. Several studies using depth recordings from the fusiform gyrus have reported local field potentials (LFPs) in response to faces peaking at various times after 100 ms (Allison, Puce, Spencer, & McCarthy, 1999; Halgren, Baudena, Heit, Clarke, & Marinkovic, 1994; McCarthy, Puce, Belger, & Allison, 1999; Puce, Allison, & McCarthy, 1999; Barbeau, et al., 2008). However, none of these studies have reported the onsets of the responses. There are also few reports of face-sensitive responses, visible as early as 50 – 80 ms after stimulus presentation, captured using intracranial depth electrodes in medial occipital lobe (Halgren, et al., 1994), or using scalp ERPs (Seeck, et al., 1997; Mouchetant-Rostaing, et al., 2000; George, et al., 1997). However, the latter group of findings has been linked to habituation and priming processes based on perceptual similarity of visual stimuli rather than category-specific processing (Debruille, Guillem, & Renault, 1998).

Further support for the early category-sensitive processes comes from studies that applied pattern classifiers trained on electrophysiological data to discriminate responses associated with different object categories. The classifiers were able to decode stimulus

category (faces, natural scenes, tools, bodies) with above chance accuracy from the activity in occipital lobe and the inferior occipital gyrus (where the OFA is located) already from 60 – 95 ms onwards (van den Nieuwenhuijzen, et al., 2013; Carlson, et al., 2013; Cauchoix,et al., 2014; Isik, et al., 2013), and in the fusiform gyrus from 100 ms onwards (Liu, et al., 2009). In the latter study however, the large high-pass filter cutoff of 1Hz applied to the data might have smeared the onset effects back in time (Acunzo, MacKenzie, & van Rossum, 2012; Rousselet, 2012; Widman & Schroger, 2012). Pattern classifiers are informative tools, useful to study multivariate patterns of activation in high dimensional space, such as the brain. However, one concern with the classifier studies is that demonstrating that a classifier is able to detect response patterns useful for discrimination between object categories does not mean that these response patterns produced object representation that are available to the brain or used by the brain in explicit object categorisation. Still, a lot of uncertainty remains concerning the amount of diversity and overlap in response tuning of individual neurons within face-selective patches, which can support robust yet precise face recognition mechanisms.

All in all, it seems that in both monkey and human brains, sensitivity to object category may appear already around or before 100 ms after stimulus presentation, but the overall evidence is inconclusive. To appropriately study ERP onsets of face processing in humans, advancements in methodology are necessary. Research reported in this thesis (Section 4) uses causal filtering of EEG data which does not distort onsets, robust statistics with spatial-temporal cluster-based multiple comparisons correction, and analyses of single-subject data in a sample of 120 subjects, to quantify the onsets of face-sensitive ERP responses in the human visual system.

COMPARISON BETWEEN MONKEY AND HUMAN FACE PROCESSING SYSTEMS

The visual systems in monkey and human brains have important homologies as well as noticeable and important differences. The primary visual cortex occupies only about 3% of total cortical volume in humans, in comparison to 6% of the cortex in chimpanzees and 11-12% in macaques (Sereno & Tootell, 2005). However, the arrangement of many retinotopically organised visual areas in human occipital cortex strongly corresponds to the pattern found in macaques. These areas include: V1, V2, V3 (V3d), VP (V3v), V3A, and V4v (DeYoe, et al., 1996; Orban, Van Essen, & Vanduffel, 2004; Tootell, Tsao, & Vanduffel, 2003). Beyond these regions, the correspondence between human and monkey visual systems is less obvious, and the similarities and

dissimilarities between species in terms of the areas that support object and face processing are still debated.

In both human and macaque monkeys, multiple face-sensitive areas have been found, located primarily in the temporal lobes, in regions associated with object processing. However, the exact number and locations of face areas seem to differ between the two species; in macaques face patches seem to be more numerous than in humans and located mostly inside or close to the STS, while the majority of human face areas are situated more ventrally (Figure 1.5). Recently though, a face patch located in the ventral TE has been identified in monkeys (Ku, Tolias, Logothetis, & Goense, 2011), and it has been shown that more face-responsive areas may exist in humans, as an additional one has been identified in human anterior ventral temporal cortex (Pinsk, et al., 2009; Tsao, Moeller, & Freiwald, 2008). This suggests that the anatomical correspondence between macaque and human face processing systems might be higher than previously thought.

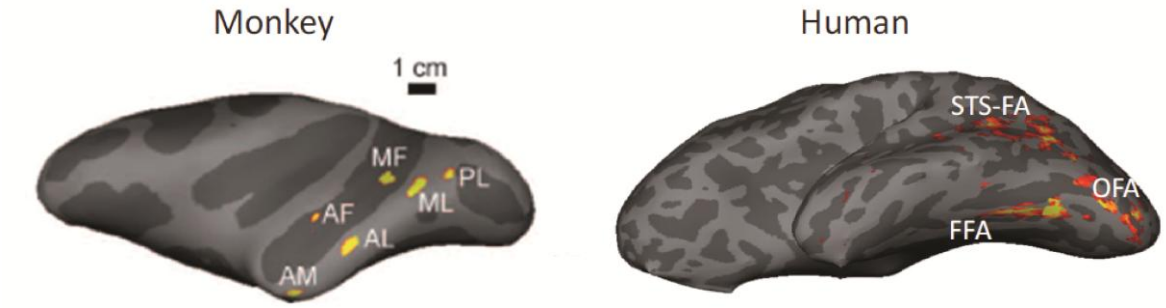

Figure 1.5. *Face areas in monkey (left) and human (right) brains. Face patches in monkeys: PL – posterior lateral; MF – middle fundus; ML – middle lateral; AF – anterior fundus; AL – anterior lateral; AM – anterior medial. Face areas in humans: OFA – the Occipital Face Area; FFA – the Fusiform Face Area; STS-FA – the superior temporal sulcus-face area. (Adapted from Yovel & Freiwald (2013), Fig. 1A).*

In both monkey and human brains, face areas seem to form a network. However, while in macaques face processing regions are tightly interconnected (Moeller, Freiwald, & Tsao, 2008), it seems that in humans structural and functional connectivity between the OFA and the FFA is stronger than between the OFA/FFA and the STS (Gschwind, Pourtois, Schwartz, Van De Ville, & Vuilleumier, 2012; Davies-Thompson & Andrews, 2012.). In both species, though, there seems to be an increase in response latencies, face selectivity, and receptive field size from posterior to anterior face regions, suggesting that hierarchical organisation of the face recognition system might be one of the common features of macaques and humans (Freiwald & Tsao, 2010; Hemond, Kanwisher, & Op de Beeck, 2007; Sadeh, Podlipsky, Zhdanov, & Yovel, 2010). Thus, it has been proposed that the PL patch in monkeys might be an equivalent of the OFA in humans, supporting

intermediate stages of face processing (Issa & DiCarlo, 2012), while the ML/MF and AL/AF/AM patches might correspond to different parts of the STS and the FFA (Yovel & Freiwald, 2013; Tsao, Moeller, & Freiwald, 2008; Pinsk, et al., 2009; Rajimehr, Young, & Tootell, 2009). Finally, the absolute response latencies are longer in humans than in monkeys and this is mainly due to differences in brain size across species (Sereno & Tootell, 2005). When extrapolating from monkey to human latencies, the 3/5 ratio rule seems to provide a good fit with the data (Schroeder, et al., 1995; 2004).

All in all, the correspondence between macaque and human face processing systems is evident, but still many dissimilarities exist. Establishing homologies between species has proven difficult, as multiple criteria need to be considered, such as structural and functional similarities (e.g. number of synapses per neuron is 2000-6000 in monkeys and 7000-10000 in humans), cytoarchitecture, gene expression and connectivity links to behaviour (Orban, Van Essen, & Vanduffel, 2004; Yovel & Freiwald, 2013; Tsao, Moeller, & Freiwald, 2008). Nonetheless, studying the monkey brain can inspire important insights about the neural correlates of face recognition in humans.

The description of the locations and timing of neuronal object and face processing is only part of the story; it is also necessary to ask what information the brain uses to categorise incoming visual input and how this information is used to achieve it.

1.3.2 THE WHAT AND HOW OF OBJECT (FACE) PROCESSING

What visual information is used by the brain to categorise objects, including faces? How is this information integrated in the cortex to arrive at complex object representations? Based on electrophysiological data and animal and human brain imaging various theoretical and computational models of visual object processing in the brain have been put forward. Most models consist of stages, resembling hierarchical organisation of the visual system (Hmax hierarchical model (Serre, et al., 2007), Textsynth (Portilla & Simoncelli, 2000), SpatialPyr (Lazebnik, Schmid, & Ponce, 2006), with the number of computational steps often limited by the rapidness of object categorisation. Other models are based on measuring certain characteristic of the visual input, such as contrast distributions (Ghebreab, Scholte, Lamme, & Smeulders, 2009; Scholte, Ghebreab, Waldorp, Smeulders, & Lamme, 2009). Object classification accuracy of several popular models have been tested by Crouzet and Serre (2011) who found that the Hmax and Textsnyth hierarchical models, that are based on processing of intermediate complexity features performed best and reached level of performance similar to an average observer.

The Weibull model measuring contrast statistics of the visual input performed poorly. However, because of the high complexity of the models as well as non-linearity and high-dimensionality of the inputs, it is difficult to determine what exactly drives classification accuracy in these models. The important findings are that highest performing models had a hierarchical nature, resembling organisation of the visual system, and were mostly utilising features of intermediate complexity, which is consistent with empirical data (Tanaka, 1997; Sato, et al., 2013) and theoretical models, like the one put forward by Ullman (2006).

In his fragment-based hierarchy model Ullman (2006) proposed that object categorisation (distinguishing between object classes) and object recognition (individual identification) relies on a limited number of informative object features that are extracted during learning from observed examples of a given object class. An object feature is considered informative if it reduces the ambiguity about the class this object belongs to. In other words, an informative feature will frequently appear in objects within one class but not in those from outside this class. Importantly, the features are considered in the order of the amount of information they deliver – from most to the least informative. In Ullman's (2006) model the most informative features for object categorisation are usually of intermediate complexity, such as eyes for face, wheels for cars or paws for animals (Ullman, Vidal-Naquet, & Sali, 2002). However, recognition of individual exemplars within a class relies on increasingly finer, local features, all the way to the basic edges and lines. Therefore, an extraction of informative features takes place on multiple levels, suggesting a hierarchical nature of object processing. Also, via observational learning the brain creates an abstract representation of object that deals with robustness of categorisation process under different viewing conditions. These internal representations are later used to facilitate the speed of object recognition by serving as potential interpretations for the incoming visual input. Ullman's (2006) model predicts preferential activation in object processing regions in a presence of highly informative visual features versus less informative ones. However, it remains unclear to what extent object categorisation utilises high-level feature processing (shapes of different complexity) and low-level visual input (contrast, luminance, spatial frequency, edges or contours) (Rousselet & Pernet, 2011; Schyns, Gosselin, & Smith, 2009; VanRullen, 2011).

THE ROLE OF HIGH-LEVEL VISUAL FEATURES IN FACE CATEGORISATION

Theoretically the number of potential shapes and objects that the visual system can encounter is infinite. Thus, shape processing needs to be robust and high-dimensional, but the exact nature of the dimensions remains elusive. Brincat & Connor (2004) presented ~ 1000 different 2D silhouette shapes to macaques and found that 80% cells in TEO and TE areas showed significant selectivity to shapes, regardless of their retinotopic position and size. This suggests that neurons in these areas integrate information about multiple (usually 2-4) contour fragments, such as straight and curved edges, using linear and nonlinear summation of contours signals. Linearity and nonlinearity was correlated with responsiveness – cells with linear responses were selective to broad range of shapes, cells with nonlinear responses were selective to only a few shapes or part combinations. These results support theories of IT selectivity to critical features, explicit coding of structural relations between parts, and part-based representation of objects, at least in the posterior IT.

Due to its high social and evolutional importance faces are thought to be "special" among other stimulus categories, and multiple studies have identified cells in parts of monkey IT cortex that appear to be sensitive to certain face fragments and/or their combinations. For example, Issa & DiCarlo (2012) discovered that in monkeys neuronal spike activity around 60 – 100 ms in 108 out of 111 sites of the posterior IT face patch (PL) was primarily driven by the contralateral eye-like features surrounded by the face outline. The other eye, nose and mouth have contributed mainly to the activity after 100 ms? The activity between 60 – 100 ms was also independent on retinal position of the eye-like feature and was much weaker when the eye was absent from the image. Another study of Freiwald, Tsao & Livingstone (2009) found that cells in the middle face patch in macaques signalled the presence or absence of face fragments and were tuned to the geometry of facial features. The most popular parameter was face aspect ratio - more than half the cells (59%) were tuned to it, followed by iris size (46%), height of feature assembly (39%), inter-eye distance (31%) and face direction (27%) with little representation for mouth and nose. 90% of the studied neurons responded to one or more critical face features (on average 2.8 per cell), but there were no cells that were tuned to all aspects of the face. The latter piece of evidence suggests that face detection does not rely on holistic processing, although facial layout geometry and eye geometry seem to be very important, and cells seem to encode axes, rather than individual faces. Moreover, most cells showed a one-to-one mapping of their firing rate to the feature value suggesting that

cells indeed measure feature dimensions, such as iris size or distance between eyes. The existence of one-to-one mapping between firing amplitude and feature value, varying degrees of cell feature selectivity and a considerable amount of face-related suppression of cell activity suggest that all levels of response, including minimal ones, may carry information important for object categorisation. This proposal is supported by the evidence from single cell recordings in macaques showing that cells in anterior IT cortex were most often tuned to an average face and deciphering identity of the input may rely on signals of varying strengths resolving individual features in a comparative process against the internal representation (Leopold, Bondar, & Giese, 2006).

In humans, some studies have managed to link the processing of the contralateral eye with early evoked potentials, namely the N170 (Schyns, et al., 2003; Smith, et al., 2004; 2007; 2009). Using EEG Schyns, Petro & Smith (2007) discovered that integration of facial features started at the contralateral eye about 50 ms before the peak of the N170 and proceeded down the face, stopping when the information diagnostic for a particular expression has been integrated (and N170 peaks). The important finding was that different information was diagnostic for different facial expression: the eyes for fear or the mouth for happiness. Additionally, the further down a face the diagnostic feature was located, the longer it took to integrate the information and the longer the latency of the N170, meaning the N170 for "happy" peaked later than for "fear". Along the same vein, McCarthy & Puce (1999) found that the latency of a negative ERP peak ~200 ms post-stimulus was the earliest for full faces and was progressively delayed for face fragments in the order: eyes, lips and noses. Thus, face (an object) processing may rely on accumulation of perceptual evidence that resolves in time and utilises certain critical dimensions or features that are highly informative (diagnostic) for a given category (Philiastides & Sajda, 2006; Ullman, 2006; Smith, et al., 2004; Issa & DiCarlo, 2012).

Indeed, recent evidence from monkeys shows that patches of face-selective neurons in the anterior IT cortex not only have common functional properties – display similar patterns of activity to the preferred object – but also consist of finer functional columns responsive to individual features of the stimulus and their configurations (Sato, et al., 2013). Columnar organisation of monkey area TE where cells with overlapping but slightly different selectivity cluster together was also found by Tanaka (1993). These findings indicate that object representation is distributed across many cells in multiple columns, not by simple summation of feature columns, but rather based on combinations of active and inactive columns representing individual features (Tsunoda, Yamane, Nishizaki, &

Tanifuji, 2001). Such distributed and hierarchical representation of objects in the cortex allows responses to remain robust to subtle changes in visual input, while at the same time facilitates precision of the representation (Tanaka, 1993; 1997).

It remains to be determined if different face patches support different and complementary aspects of face representations and to what extent they overlap. It is possible that processing of different face fragments is supported by different face patches, embedded in a wider object representation network (Sato, et al., 2013), or by cortical areas outside of those currently associated with face or object categorisation (Tsao & Livingstone, 2008). Additionally, because IT cells do seem to display preferences towards one or more visual features, the challenge would be to constrain the stimulus space taking into consideration these preferences. Finally, it is possible that for specific categories or particular tasks, the brain might make use short-cuts and rely more on global, low-level input, instead of high-level visual information.

LOW-LEVEL FEATURES IN OBJECT CATEGORISATION - THE ROLE OF IMAGE FOURIER PHASE AND AMPLITUDE SPECTRA

There is evidence that object and face recognition processes rely not only on the high-level features and their combinations, but also on low-level properties of the visual input, such as contrast, spatial frequency, edges and contours. It has been suggested that particularly the early (~100 ms) neuronal activity associated with object categorisation is sensitive to low-level cues (Rossion & Caharel, 2011). Particularly debated is the contribution of Fourier amplitude (power) and phase spectra to object-related brain activity. Amplitude spectrum carries information about orientations and spatial frequency content of an image, whereas the phase spectrum contains information about local image structures, such as edges and contours, because edges require the alignment of phase across different spatial frequency components (Morrone & Burr, 1988; Kovesi, 1999; Hansen, Farivar, Thompson, & Hess, 2008). The importance of phase for object recognition has been demonstrated in studies conducted by Piotrowski and Campbell (1982) and Oppenheim and Lim (1981) who showed that, when mixing the Fourier amplitude of one image with Fourier phase of another image, the outcome resembles its phase contributor much more than its amplitude contributor. Since then, studies using well-controlled stimuli with amplitude spectra equated between images have demonstrated that early visual processing appears to rely mostly on phase information by detecting edges and lines of the object starting at about 130-150 ms after stimulus onset (e.g. Loschky & Larson, 2008; Wichmann, Braun, & Gegenfurtner, 2006; Rousselet, Pernet, Bennet & Sekuler, 2008;

Rousselet, Husk, Bennett, & Sekuler, 2005; Wichmann, Drewes, Rosas, & Gegenfurtner, 2010; Jaques & Rossion, 2006; Allison, Puce, Spencer, & McCarthy, 1999; Rousselet, et al., 2007).

Moreover, animal data indicate that complex cells in V1 are more sensitive to their preferred visual features when they are present in non-random phase natural scenes compared to random phase images (Felsen, Touryan, Han, & Dan, 2005). Interestingly, this increased sensitivity is present for images of natural phase but random power spectrum and absent for images of random phase and natural power spectrum. This suggest that complex cells rely more on the phase regularities when detecting visual features, than on amplitude spectrum which is consistent with studies highlighting the importance of phase congruence in visual processing (Morrone & Burr, 1988; Kovesi, 1999). Furthermore, Phillips & Todd (2010) showed than even when dealing with macrostructures of contrasting luminances, the visual system does not need amplitude spectrum for discrimination between them, as all the necessary information can be completely extracted from short- and long – distance spatial alignments of features contained in a phase domain. These findings emphasise how essential phase information is for object recognition, although they do not answer what is the role (if any) of amplitude spectrum in this process.

Many natural images have similar spatial frequency amplitude spectra, and phase is thus essential to discriminate among them. However, when images have substantially different Fourier amplitudes, the role of phase may be no longer essential (Juvells, Vallmitjana, Carnicer, & Campos, 1991). This idea is supported by the existence of computational algorithms that can efficiently classify images of natural scenes using non-localized or coarsely localized amplitude spectrum information (Oliva & Torralba, 2001; Crouzet & Serre, 2011). Furthermore, human observers can detect degradation in amplitude spectra in meaningless synthetic textures (Clarke, Green, & Chantler, 2012), or discriminate between wavelet textures using higher order statistics (Kingdom, Hayes, & Field, 2001). Hence, provided that amplitude spectrum information is available for the task at hand, human observers might be able to use it when categorising objects and natural scenes. In particular, some studies suggest that when a stimulus is presented rapidly, the amplitude spectrum may provide a type of abstract information not obviously related to the semantic content of an image, but sufficient for its broad categorisation (Oliva & Torralba, 2006; Joubert, Rousselet, Fabre-Thorpe, & Fize, 2009; Honey, Kirchner, & VanRullen, 2008; Crouzet & Thorpe, 2010; VanRullen, 2006).

Alternatively to the two previous accounts, it is also plausible that object and scene categorization do not depend on phase or on amplitude alone, but on an interaction between them. For instance, categorisation accuracy decreases when the amplitude of each stimulus is replaced by the average amplitude across stimuli, while retaining the original phase (Drewes, Wichmann, & Gegenfurtner, 2006). Accuracy is also affected when the amplitude is swapped within image category in an animal detection task - e.g. the amplitude spectrum of a fish is mixed with the phase spectrum of a tiger (Gaspar & Rousselet, 2009). Because swapping amplitude spectra within category should preserve their diagnostic properties in an animal detection task, this result suggests the existence of a specific relationship between phase and amplitude spectra, which, when disturbed, hampers image classification.

Some neuroimaging studies have also claimed that neural processes underlying object recognition are at least partially driven by global image information contained in the amplitude spectrum. Rossion & Caharel (2011) reported ERP differences between two categories of colour images: faces and cars. The differences were visible as early as 80 – 100 ms post-stimulus onset for both intact and phase scrambled versions of faces and cars. The authors concluded that the differences observed between the intact picture categories were due to low-level image properties (amplitude spectrum), and not to high-level categorical information. Another study using fMRI showed larger BOLD (Blood Oxygenation Level Dependent) responses to faces compared to places in face-preferential brain regions (FFA) for intact images and for their phase-scrambled versions, although the responses were weaker in the latter case. Based on these results, the authors concluded that at least part of the categorical BOLD differences to intact images could be due to uncontrolled low-level image properties Andrews, Clarke, Pell, & Hartley (2009). However interpretations proposed in both of these studies seems questionable. In the case of Rossion and Caharel (2011) study, the early ERP responses could have been driven by differences in contrast or colour between the two image categories – a potential confound the authors acknowledged. Moreover, both studies used only intact and phase-scrambled images of faces and places and did not include necessary control conditions in which amplitude spectra were equated across categories or swapped between categories. One of the purposes of the work outlined in this thesis (Section 2) was to resolve the debate concerning the relative contribution of Fourier phase and amplitude spectra to ERP responses associated with object categorisation by employing parametric manipulation of phase and amplitude along the continuum from 0 to 100% in 10% steps intervals.

To sum up, it seems that both human and monkey brains contain a number of distributed regions that are especially tuned to processing of faces and can respond to them remarkably fast – even before 100 ms post-stimulus. However, the exact number, organisation and response latencies of these regions as well as the role each of them plays in face recognition, remains the subject of continuous investigation. It is also unclear what visual information the brain uses to categorise images, and when this information modulates the ERP responses. Further, there are factors than can influence the processing speed of complex objects in the brain, such as aging. Accumulating experimental evidence points out that visual processing speed decreases with age and this slowdown is related to a variety of physiological changes occurring in the aging brain which will be reviewed below.

1.4 THE AGE-RELATED SLOWDOWN IN VISUAL PROCESSING SPEED

Aging has been associated with a decline in cognitive abilities and one of the indicators of this decline is a decrease in processing speed. Many older people often require more time to perform even simple cognitive tasks such as detection, discrimination or recognition of visual targets (Salthouse & Ferrer-Caja, 2003; Verhaeghen & Salthouse, 1997). Most commonly, the age-related slowdown is visible in the increase in reaction times when performing a task requiring a speeded response with a key-press upon making a decision (Salthouse, 2000). However, it is still unclear whether effects of aging on processing speed are independent from its effects on other cognitive variables, including memory or reasoning, but models that assume independence seem to fit quite poorly into the data (Salthouse, 1998; Salthouse & Czaja, 2000). Instead, evidence from research seems to support a shared model in which age has a broad effect on many variables related to cognitive and non-cognitive functioning (e.g. visual acuity or auditory sensitivity). Moreover, the shared and unique magnitude of aging effects on these variables, translated into behavioural changes, can be measured (Lindenberger & Potter, 1998; Lindenberger, Mayr, & Kliegl, 1993; Verhaeghen & Salthouse, 1997). Thus, it seems that aging influences what is common between different cognitive abilities, for example memory and processing speed – a notion supported by evidence that most cognitive variables are typically positively correlated (Deary, 2000).

It appears that alterations in processing speed are a major factor underlying age-related impairments in cognitive deficits because about 75% of variance is shared between

age-related slowing and multiple other measures of cognitive performance (Salthouse, 1996). Based on this data, a theory has been put forward in which slow processing impairs cognitive performance in two ways: via limited time and simultaneity mechanisms. First, if early operations take longer with age, the amount of time available for later operations is reduced – an issue primarily relevant in the presence of external time limits or concurrent task demands. Second, products of early processing may be lost or become obsolete by the time later processing is completed, meaning that some information might not be available when needed. Thus, a slowdown in processing speed with age may have a variety of influences on cognitive processes, which could be reflected in altered brain activity and behavioural patterns. However, there are several concerns in aging research that limit the inferences one can make with regards to the properties of the age-related decline in cognition. These include the correlational nature of age-related effects, the potential for spurious correlations and the commonness of cross-sectional studies.

Because age cannot be randomly assigned or manipulated, the effects of age on any variable cannot be interpreted in causal terms, but only in correlational. Despite this limitation, age can be conceptualized as a continuum along which causal factors operate, thus may remain an informative index of cumulative causal influences (Salthouse & Ferrer-Caja, 2003). Another issue concerns the potential for spurious correlations if a relationship between two variables, that both change with age, is found to be significant. Partialling out the influence of age from both of these variables before correlating them is a robust way to validate this existence of a true relationship. Finally, the prevalence of cross-sectional comparisons with relatively small sample sizes and the limited number of longitudinal studies restricts the scope for inferences about the process of aging. However, both longitudinal and cross-sectional studies converge on the finding of nearly linear age-related decline in cognitive abilities, including speed (Salthouse, 2011).

Many behavioural markers of changes in cognitive processing speed with age exist. These changes may stem from cumulative age-related declines across multiple neuronal systems that support fast object categorisation and the unique pattern of these declines may vary between individuals. Various changes in brain physiology and in patterns of neural activity may be related to reduction in speed of visual object categorisation with age and these will be reviewed next.

A variety of structural and functional changes occur in the healthy aging brain (Raz & Rodrigue, 2006) that might contribute to the age-related cognitive decline, including a

decrease in processing speed. These changes include alterations in grey and white matter volumes, changes in myelination of axons, hyperactivity of neurons and a decrease in the selectivity of neuronal responses. These will be discussed in the following sections.

1.4.1 AGE-RELATED CHANGES IN GREY AND WHITE MATTER

First, studies show that with age there is a decrease in overall brain tissue volume by about 0.4 – 0.5% / year (Resnick, Pham, Kraut, Zonderman, & Davatzikos, 2003; Tang et al., 2001; Chee et al., 2009) manifesting itself in surface area shrinkage and cortical thinning. The rate of brain volume decrease seems to accelerate from the mid-fifties to about 1 – 1.5% / year, with considerable variation across individuals (Raz, et al., 2005). The estimates of grey matter volume shrinkage vary between studies and range between 0.2 – 0.4 % / year (Good, et al., 2001; Resnick, Pham, Kraut, Zonderman, & Davatzikos, 2003; Chee, et al., 2009). The majority of volumetric studies show that some grey matter regions undergo especially severe volume loss with age, in particular prefrontal areas, but also anterior insula, cerebellum and the hippocampus. Significant but more moderate age-related changes appear in medial temporal (entorhinal cortex), inferior temporal, parietal and occipital association areas, while sensory cortices, including primary visual cortex, seem to be largely spared (Raz, Ghisletta, Rodrigue, Kennedy, & Lindenberger, 2010; Raz, et al., 2005; Good, et al., 2001; Resnick, Pham, Kraut, Zonderman, & Davatzikos, 2003; Raz, Rodrigue, & Haacke, 2007; Raz, et al., 2013). Studies using voxel-based morphometry (VBM) to access local tissue density confirm, to a large extent, the findings obtained using volumetric approaches, with an exception of additional striate cortex atrophy (Tisserand, et al., 2004).

Significant individual differences exist in the level of age-related atrophy in total and regional brain tissue volume. Individual variability in volume decline is visible in majority of brain regions, but it is especially pronounced in the visual cortex, fusiform gyrus, inferior temporal cortex, cerebellum and prefrontal white matter and seems to correlate across regions, suggesting a common cause (Raz, et al., 2005). Variety of moderators can contribute to variation in brain volume shrinkage with age. These include factors related to vascular health, such as hypertension (Strassburger, et al., 1997), glucose homeostasis (Moran, et al., 2013), a person's genotype (Moffat, Szekely, Zonderman, Kabani, & Resnick, 2000) and the presence of pathological changes, such as Alzheimer's disease (Thompson, et al., 2001). For example, Raz et al. (2005) discovered the age-related acceleration of shrinkage of the hippocampus was limited to older adults that were diagnosed with hypertension. Also, regions that are normally preserved in the healthy

aging, such as striate cortex show deterioration in persons with hypertension and other vascular disease factors (Raz, et al., 2007). Because individual differences in brain shrinkage may potentially contribute to individual variability in cognitive abilities, sampling a wide range of ages for experimental investigations becomes particularly important in aging research.

A link between age-related regional grey matter volume shrinkage and change in cognitive abilities, measured with variety of behavioural tests, is unclear (Raz & Rodrigue, 2006). Some data suggest that a loss in frontal grey matter and hippocampus volume in older adults is linked to a drop in performance in fluid intelligence and memory tests (Raz, et al., 2008; Taki, et al., 2010). Reduced processing speed in elderly, expressed in reaction time prolongations, has been associated with a decline in total grey matter volume in a sample of ~250 participants (Chee, et al. 2009). Some studies have found that a decrease in processing speed was related to changes in cerebellar morphology with age, in particular grey matter volume loss in the vermis (MacLullich, et al., 2004; Paul, et al., 2009; Eckert, Keren, Roberts, Calhoun, & Harris, 2010), linking processing speed declines with sensory-motor problems (Hogan, 2004). Regions involved in object processing network, including occipital associative areas, inferior temporal lobe and fusiform gyrus seem to undergo moderate volume shrinkage with aging (Raz, et al., 2005; Chee, et al., 2009; Kennedy, et al., 2009) but how this relates to age-related deficits in face perception observed for example by Salthouse (2004) remains a mystery. Minimal atrophy of the primary visual cortex suggests the basic perceptual processes are largely preserved in healthy aging, although factors other than volume shrinkage may negatively impact striate and other cortices' performance, such as myelin degeneration and cells' response selectivity which will be discussed next.

Post-mortem and *in vivo* examinations indicate that with age there is a considerable and widespread decline of white matter volume, even in very healthy individuals (Piguet, et al., 2009; Resnick, Pham, Kraut, Zonderman, & Davatzikos, 2003). Over a lifetime, white matter volume appears to decrease by 20-30% and the overall length of myelinated nerve fibers drops by nearly 30%, or even up to 45% in some samples (Marner, Nyengaard, Tang, & Pakkenberg, 2003; Tang, Nyengaard, Pakkenberg, & Gundersen, 1997; Pakkenberg & Gundersen, 1997). This decline seems to accelerate in advanced aging (Salat, et al., 2009) and is associated with age-related drop in a number of myelinated fibers (Marner, Nyengaard, Tang & Pakkenberg, 2003), and a loss and deformation of myelin sheaths (Peters, 2002; Peters, Moss & Sethares, 2000), despite overall preservation

in number of neurons (Freeman, et al., 2008). The axons that lost their myelin are continually remyelinated by oligodendrocytes whose number do not decline with age. However, axons' new sheaths are significantly thinner and contain additional nodes of Ranvier prolonging the conduction rates along nerve fibres (Peters, 2009). Additionally, myelin sheaths can become deformed, for example by developing local splittings or additional myelin layer making the overall sheath too large for an axon. Both types of alterations in myelination were observed in V1 in monkeys, despite no observed loss in the number of myelinated nerve fibers in their visual cortex (Nielsen & Peters, 2000). These breakdowns of myelin correlated significantly with cognitive deficits in individual monkeys. The correlation was related to how breakdowns of myelin lead to changes in axonal conduction velocities across the brain (Peters, Moss, & Sethares, 2000). Thus, age-related myelin degeneration can contribute to the gradual slowing of the transmission rates across neuronal populations and may lead to slower processing in aging.

Studies accessing white matter microstructure using diffusion tensor imaging (DTI) and tractography indicate that aging does not have an uniform effect on white matter density in different brain regions (Good, Johnsrude, Ashburner, Henson, Friston, & Frackowiak, 2001; Deary, Bastin, Pattie, Clayden, & Whalley, 2006; Salat, et al., 2005). It seems that regions myelinated late in the course of brain development (e.g. prefrontal cortex) tend to undergo stronger age-related shrinkage (Raz, 2000). The deterioration seems to increase gradually starting from posterior to anterior brain areas with frontal cortex being most strongly affected (Salat, et al., 2009; Davis, et al., 2009). Only few studies have looked at the age-related changes in white matter in areas associated with object processing. Salat, et al. (2009) discovered a loss in white matter volume in the inferior temporal cortex in older adults, in particular the fusiform gyrus, and Thomas, et al. (2008) found an age-related reduction in diffusion metrics in one of the fiber tracts passing through the fusiform regions (inferior fronto-occipito fasciculus – IFOF). However, no statistical tests that access links between white matter integrity and cognitive abilities were reported in these studies. A drop in number of myelinated nerve fibers in anterior commissure, which supports the transfer of visual information between hemispheres, has been linked to cognitive decline in elderly (Sandell & Peters, 2003). Further, a disruption in white matter connectivity in the ventral occipito-temporal cortex has been found to correlate with face recognition impairments in patients with congenital prosopagnosia (Thomas, et al., 2009). Given that object and face processing is supported by a distributed network of brain areas, including the ventral pathway, it is possible that a breakdown in

connectivity between these areas caused by age-related white matter deterioration may lead to deficits in face perception found for example by Salthouse (2004).

Multiple studies have reported links between age-related changes in density of white matter and modulations in behavioural markers of processing speed, mostly reaction times. Longer processing in the elderly seems to correlate with frontoparietal (Kennedy & Raz, 2009) and global indices of white matter integrity loss (Deary, et al., 2006), although some studies do not find this link (Charlton, et al., 2006; Charlton, et al., 2008). An association between white matter density loss in the anterior limb of the internal capsule and longer processing in visual detection task has also been reported (Madden, et al., 2004). What also tends to affect speed-dependent performance are ischemic lesions expressed as white matter hyperintensities (WMH) which are common in normal healthy elderly (Gunning-Dixon & Raz, 2000; Prins, et al., 2005; van den Heuvel, et al., 2006). Rabbit et al. (2007) found that WMH prevalence accounted for all of the age-related variance between individuals 65 – 84 years old in psychometric tests of speed. Thus, it seems that breakdowns in integrity and transmission between fiber bundles of white matter white matter can disrupt or slowdown cognitive processing abilities in older adults, including object categorisation.

Finally, there are considerable individual variations in white matter volume and these are significantly related to grey matter volume, especially in the frontal brain regions (Raz, Rodrigue, & Acker, 2003). Accumulating evidence indicates that both grey and white matter undergo a number of changes leading to a general slowing in neural information processing, although their exact contributions are not clear.

1.4.2 AGE-RELATED DEGRADATION OF RESPONSE SELECTIVITY OF NEURONS AND DECREASE IN SPECIALISATION OF NEURONAL NETWORKS

Another possible cause of aging related slowdown in neural visual information processing is the degradation in response selectivity of neurons in striate and extrastriate visual cortices. With senescence, receptive filed properties, such as orientation and direction selectivity of cells in V1 and V2, decrease in rhesus monkeys (Schmolesky M. , Wang, Pu, & Leventhal, 2000; Yu, Wang, Li, Zhou, & Leventhal, 2006). This is accompanied by neural hyperactivity – an increase in cells' spontaneous activity, visual responsiveness and a decrease in signal-to-noise ratio (Schmolesky, et al., 2000; Yu, et al., 2006; Hua, Li, He, Zhou, Wang, & Leventhal, 2006). Wang et al. (2005) have found that in old monkeys' V1 and V2 neural hyperactivity was accompanied by delays in the latency of intracortical (within V1 and V2) as well as intercortical (between V1 and V2) transfer of information and the effect was much more severe in V2 compared to V1 (Figure 1.6). Interestingly, there were no age-related delays in cell responses in layer 4 of V1 (both 4Cα and 4Cβ layers) that receives a direct input from the magnocellular and parvocellular pathways layers of lateral geniculate nucleus (LGN) and projects to the remaining layers of V1 and from there to V2. The response latencies of cells in V1, outside of layer 4, were 70 ms (young) and 84 ms (old) and in V2, 82 ms (young) and ~114 ms (old)[1]. There was also a significant age-related increase in the range of responses between short and long latency cells, from 15 ms (young) to 30 ms (old) in V1 and from 30 (young) to 60 ms (old) in V2. This suggests that intracortical information processing speed declines with age and this effect is more pronounced in V2 than in V1. Moreover, the information transfer between V1 and V2 took on average longer in old monkeys: ~30 ms compared to ~10 ms (median = ~20 ms) in the young ones. Varying aging effects on cells' response latencies in V1 and V2 suggest that different delays might be induced on inputs coming to the higher visual areas from V1 and V2 in a way that is difficult to predict.

[1] The reported latencies come from Table 1 in Wang et al. (2005). Note the discrepancy between old monkeys' V2 latencies reported in Table 1 (114 +- 24 ms), and their median V2 onset latencies presented in Figure 2 (~105 ms). The reason for this discrepancy is uncertain since there is not enough details in the method section and in the Table 1 caption with regards how the latencies in Table 1 were computed.

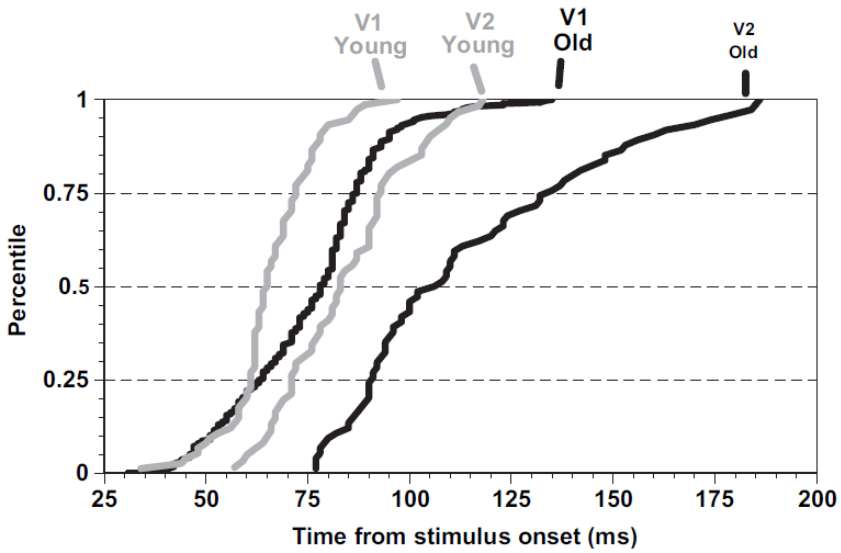

***Figure 1.6.**. Onset latencies of V1 and V2 cells in young and old monkeys. The percentage of cells with any given onset latency in areas V1 [including layer 4 – author's ed.] and V2 are shown in cumulative distribution plots, where solid grey and black lines represent the combined data of young and old monkeys, respectively [0.5 percentile indicates median latency – author's ed.]. The difference in latency between cells in areas V1 and V2 is greater in old animals indicating that signal transfer between these areas takes longer in old monkeys. Also, the range of latencies within both areas V1 and V2 is significantly greater in old than in young monkeys. Thus, intracortical signal transfer takes longer in both areas V1 and V2 of old monkeys and area V2 is affected more than area V1. (Reprinted from Wang et al., 2005, Fig.2).*

The observed delays can have several potential underlying correlates. One of them is previously discussed alterations in axon myelination leading to a slowdown in conduction along nerve fibres. Another hypothesis was proposed by Wang, et al. (2005) who suggested that cell hyperactivity in the older brain may induce early failures in excitatory transmission that in turn is reflected in increased latencies of information transfer, but no correlation between excitatory transmission and age-related delays was reported in this study. An increase in visually driven spontaneous responses in monkeys' V1 and V2 also implies a possible degradation of inhibitory mechanisms within cortical circuits. Studies investigating the role of GABA inhibitory transmitter and its agonists show that in a healthy brain GABA mediated inhibition is prevalent across the neocortex (Letinic, Zoncu, & Rakic, 2002) and that level of GABA declines with age (McGeer & McGeer, 1976). Moreover, administration of GABA into V1 cells of old monkeys led to improvement of previously deteriorated orientation and motion direction selectivity of these cells, decreased cells' spontaneous activity and increased their ability to signal visual stimuli (Leventhal, Wang, Pu, Zhou, & Ma, 2003). GABA mediated inhibition also contributes to the generation of receptive fields' structures and stimulus selectivity of

neurons in area TE of IT cortex in monkeys (Wang, Fujita, & Murayama, 2000; Wang, FujitaI., Tamura, & Murayama, 2002). In particular, the blockade of GABA mediated inhibition changed stimulus selectivity of more than 80% of recorded TE neurons, for example making them responsive to stimuli that were originally ineffective, including faces. 37% of neurons showed changes in luminance contrast and spatial frequency selectivity after the release from inhibition (Wang, et al., 2000). This provides direct evidence for the importance of inhibitory processes mediated by GABA in responsiveness of cells and preventing age-related degradation of cortical functions. Because deficits in GABA inhibition influence response selectivity and timing both at the beginning and towards the end of the ventral pathway, it is not unreasonable to assume that the entire visual system might be at least partially affected, leading to accumulating delays in processing speed along the visual stream.

Finally, some research has suggested that age-related effects in visual processing speed may be associated with dedifferentiation – an age-related reduction in specialisation of cortical networks. It has been suggested that measures of various cognitive functions are more intercorrelated in older than in younger adults (Babcock, Laguna, & Roesch, 1997; Lindenberger & Baltes, 1997). Looking at brain data, voxels sensitive to different object categories overlap more in old than in young subjects suggesting that patterns of brain activity become more generalised with age (Park, et al., 2004). Moreover, older adults tend to exhibit bilateral frontal activity in various memory or semantic tasks for which young people show lateralized activity (Cabeza, McIntosh, Tulving, Nyberg, & Grady, 1997; Reuter-Lorenz, et al., 2000; Cabeza, Anderson, Locantore, & McIntosh, 2002). The functional significance of this effect is difficult to interpret, but it suggests that older people may recruit different, and perhaps less efficient, cortical circuits when performing the same task as young adults. The reasons for that may vary. For instance, it can be due to an increase in the amount of neural resources necessary to perform the task, which nonetheless remains specialized. It may also reflect the involvement of areas that are specialized in young people, while playing a more general role in older people (Park, et al., 2004). It has been also proposed that older individuals may rely more on the pre-frontal cortex to compensate for ineffective perceptual processes (Grady, 2000), perhaps by sending additional feedback from frontal to occipitotemporal regions (Horwitz, et al., 1995), which may introduce a delay. However, the evidence for the compensation theory and the age-related over-recruitment of frontal brain regions in elderly may as well be a cross-sectional fallacy. Nyberg, et al. (2010) contrasted cross-sectional and longitudinal

analyses approaches using fMRI data from the same subjects scanned in two sessions 6 years apart. While frontal over-recruitment was present in the former case, frontal under-recruitment emerged in the latter. This discrepancy stemmed from inclusion in the follow up study participants with higher frontal activations and better memory performance already in the first session, relatively to participants who dropped out before the second scan. This suggests that cross-sectional studies may be subject to sampling biases that include relatively highly performing older individuals, motivated to take part in research. The compensation theory was further challenged by results indicating that age-related decrease in response selectivity in ventral visual regions could not be compensated by encoding information across larger numbers of voxels or by engaging additional resources within and outside the ventral visual cortex (Carp, Park, Polk, & Park, 2011). Both, under- and over-recruitment can result in decreased processing speed whether due to atrophy and diminished cortical resources or due to necessity of engaging additional brain regions to support less effective cognitive processes. However, the exact link between dynamic resource allocation in the brain and speed of visual processing remains unclear.

The age-related dedifferentiation in cortical responses has also been observed in object processing regions of the ventral pathway (Voss, et al., 2008; Carp, Park, Polk, & Park, 2011; Park, et al., 2012). Carp, et al. (2011) found that age-related decrease in distinctiveness of multivariate neuronal activation patterns in response to visual stimuli not only in the ventral visual pathway, but also in the inferior parietal, and medial and lateral prefrontal cortices. On the other hand, in an fMRI study with a sample of 200 adults 20 to 89 years old Park, et al. (2012) found a decrease in face-selective activity in the fusiform face area (FFA), but not in the occipital face area (OFA), nor in the STS. This suggests that dedifferentiation might not be a ubiquitous cortical phenomenon. The effect in the FFA was driven by increased activity to houses which supports the hypothesis that dedifferentiation may stem from broadening of tuning curves in cortical areas, supported by the evidence from animal studies showing widening of the range of stimuli cells in the aged monkey visual cortex respond to (Schmolesky, et al., 2000; Leventhal, et al., 2003). High specialisation of cells in processing particular stimuli, such as face depends on the amount of exposure and is achieved with experience (Logothetis, Pauls, & Poggiot, 1995). It is also reflected in the rate of accumulation of information useful for object categorisation - the more specialised the cells the faster the process (Perrett, Oram, & Ashbridge, 1998). Thus, with aging, cortical dedifferentiation reflected in reduction in neural specialisation may lead to categorical evidence growing slowly in populations of

cells broadly tuned to stimulus type. This can contribute to slowdown in the visual processing speed observed in the elderly on a behavioural and neuronal level. Moreover, more broadly tuned cells might need more signal in a noisy input for the categorisation to occur, compared to young people who may have more noise-resistant responses. Indeed, increased sensitivity to noise in the elderly has been found in Rousselet, et al. (2009) suggesting that older people may require more information to achieve the same level of performance as young people.

Most indices of dedifferentiation rely on qualitative measures of spatial overlaps between regions of brain activity in young and old adults and introducing more quantitative measures of thereof is needed. A shift towards quantitative measures would facilitate studying individual differences and their relation to cognitive functioning. Lately, such measures have been proposed based, for example, on the ability of a mutlivoxel pattern classifier to accurately predict stimulus category based on patterns of neural activity (Park, Carp, Hebrank, Park, & Polk, 2010) or on magnitude and variance in brain activity (Voss, et al., 2008). Using the former method, Park , et al. (2010) showed that variability in neural specificity was significantly related to individual differences in tests scores. Understanding the factors underlying individual variability in brain activity is of great importance in aging research, because it allows us to relate structural and functional changes in the cortex to cognitive functioning across the lifespan. A larger number of longitudinal studies involving a full age range of participants, including middle age ones, is needed to track the variety of complex changes occurring in the aging brain that underlie slow-down in processing speed.

To sum up, a variety of changes in brain morphology appear with age, including alterations in grey and white matter, and reduction in response selectivity and inhibitory mechanisms of neurons. All of them can negatively impact the speed of visual processing. Because aging does not have a uniform effect on cognition and its neural correlates, it is possible that various stages of visual object processing will also be affected differently. Due to its excellent temporal resolution, non-invasiveness and ease of application, EEG is a particularly suitable method to study changes in visual processing speed in healthy adults across the lifespan. Many studies made use of EEG to investigate age-related slowdown in processing using simple (e.g. checkerboards) and complex (e.g. faces) and these will be reviewed next.

1.4.3 AGING EFFECTS IN EEG AND VEP STUDIES USING SIMPLE STIMULI

Studies employing gratings or checkerboard stimuli to study visual evoked potentials (VEPs) typically consider several major components: N1 (or N75 – negative deflection ~75ms post-stimulus), P1 (or P100 – positive peak ~100ms), N2 (or N140 – negative deflection ~140ms) and P3 (or P300 – positive peak between 300 – 600 ms). Most studies showed age-related decreases in amplitude and increases in latency of VEPs around P1 (Celesia, Kaufmann, & Cone, 1987; Allison, Hume, Wood, & Goff, 1984; Tobimatsu, Kurita-Tashima, Nakayama-Hiromatsu, Akazawa, & Kato, 1993). However, less consistent results were observed for the N2 component – its latency does not seem to increase with age in one study using checkerboards (Celesia & Daly, 1977), but increased in another (Allison, Wood, & Goff, 1983). Another study using checks found age-related prolongation in the latency of visually evoked responses only after 300 ms (component P3) in a sample of 120 subjects age 20 to 80+ (Figure 1.7 A&B) (Polich, 1997). Finally, Kügler (1997) reported relatively small latency increases in later components N250 and P300 that accelerated from age 60 onwards in a sample of 344 healthy individuals age 18 – 98 years old (Figure 1.7 C).

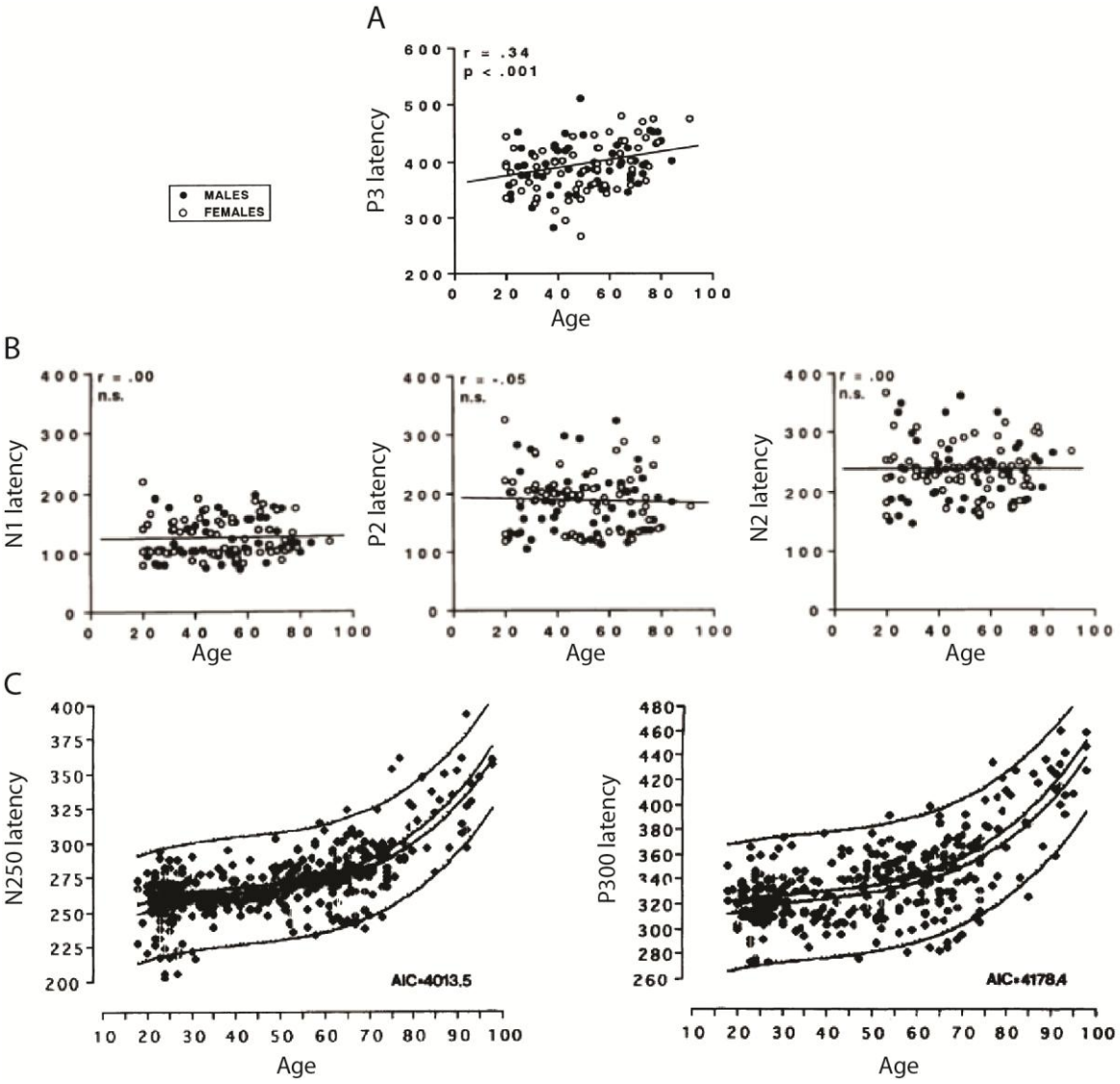

Figure 1.7. *Latencies of ERP responses to checkerboards as a function of age* ***(A)*** *P3 latency (ms) for each subject at the Cz electrode position (Adapted from Polich, et al., 1997, Fig.8, p. 251).* ***(B)*** *N1, P2, and N2 latency (ms) for each subject at Cz electrode (Adapted from Polich, et al., 1997, Fig.9, p. 252. Note that N1, P2 and N2 seem to cover different time windows that typically reported for these components. However, Polich, et al. (1997) did not provide the time windows that were assigned to N1, P2, N2 in the article).* ***(C)*** *Third-order polynomial regression functions for both the N250 and P300 latencies (ms) of 344 healthy subjects between 18 and 98 years of age. The 95%-confidence and prediction intervals are shown (Adapted from Kügler, et al., 1997, Fig. 1, p. 18-19).*

It is plausible that the observed differences in aging effects found in visual evoked potentials partially reflect the co-appearing age-related changes in sensitivity to such parameters as stimulus' spatial and temporal frequency, luminance and contrast. Celesia, et al. (1987) and Sokol, Moskowitz & Towle (1981) pointed out that VEPs depend on the check size used during the experiment - VEPs latencies vary for age-matched visually normal subjects as a function of stimulus spatial frequency. Patterns of high spatial frequency (small checks) induce longer latency VEPs compared to patterns of lower spatial

frequency (large checks). Age-related effects in VEPs also seem to differ as a function of spatial frequency of the stimulus. Sokol, et al. (1981) have found that with aging latency increase occurs more rapidly for small checks (12 min of arc) than to large checks (48 min of arc). Significant aging effect for 15 min of arc checks but not for 51 min of arc checks were also found by Celesia, et al. (1987). This indicates that different spatial frequency channels within the human visual system may be affected differently by senescence.

Prolongations in early ERP latencies might also be related to changes in luminance and contrast sensitivity with age. There is a well-documented link between luminance and the latencies of neuronal responses in various parts of the visual system documented in animals using multi-focal ERG (Raz, Seeliger, Geva, & Percicot, 2002). Research applying neutral density filters to manipulate retinal illumination in young subjects showed that pattern ERG and P100 latencies are delayed by decreased illumination (Froelich & Kaufman, 1991). Shaw and Cant (1980) pointed out that the effect of age on the P100 latency depends on stimulus' luminance – at lower (5 cd/m^2) luminance levels there was a considerable increase in P100 latency for subjects older than 50, while only a little latency increase has been observed at high luminance (50 cd/m^2). However, this finding was challenged by a report of similar ERP aging effects at 11 cd/m^2 and 180 cd/m^2 luminance levels (Tobimatsu, Kurita-Tashima, Nakayama-Hiromatsu, Akazawa, & Kato, 1993). Interestingly, it seems that age-related delays in retinal and cortical activity can be abolished after equating retinal illuminance between age groups by using neutral density filters (Trick, Trickl, & Haywood, 1986). All in all, it remains unclear to what extent aging effects on the ERPs are dependent on luminance of the visual input.

Age effects observed at P100 seem to be also mediated by changes in contrast sensitivity with age. Tobimatsu, et al. (1995) found that a reduction in contrast of checkerboard pattern leads to significant differences in the latency of P100 between young and middle age group, contrary to high contrast checks where no difference was observed. For older participants both low and high contrasts patterns have elicited significant P100 latency increase compared to middle age group. Comparing alterations in pattern reversal ERG and visual evoked potentials with age-related decline in psychophysical performance suggests that some neural changes may take place between retina and the striate cortex but the exact locus is difficult to identify (Tobimatsu, Kurita-Tashima, Nakayama-Hiromatsu, Akazawa, & Kato, 1993). Additionally, Morrison and Reilly (1989) have showed that incrementing the stimulus contrast makes VEP's of older observers resembling those of the young ones. It appears therefore, that age-related reduction in contrast sensitivity may

partially contribute to the observed increase in ERP latencies around 100 ms post-stimulus in older and middle age participants.

1.4.4 AGING EFFECTS IN EEG STUDIES USING COMPLEX STIMULI.

EEG studies that use more complex stimuli, such as images of faces or houses show that in humans 200 ms is sufficient for the visual system to elicit responses reflecting sensitivity to the higher-order content of the image, such as object category (Rousselet, Husk, Bennett, & Sekuler, 2008; VanRullen & Thorpe, 2001). A variety of studies have investigated age-related changes in latencies of the early (<200 ms) and late (>200 ms) ERP responses to complex objects, yielding ambiguous results.

Several studies did not find aging effects in the early ERPs to complex stimuli, such as faces (Pfutze, Sommer, & Schweinberger, 2002; Chaby, George, Renault, & Fiori, 2003; Gao, et al., 2009; Chaby, Jemel, George, Renault, & Fiori, 2001). These studies observed age-related delays only at later stages of visual processing (>200 ms). For example, Chaby, et al. (2001) have found that older subjects had behaviourally more difficulties in discriminating between congruent famous and incongruent famous faces and this effect was accompanied by a significant latency increase in the later stages of visual processing >400ms post-stimulus. Contrary to these negative results, several studies reported age-related latency increases or amplitude modulations of early ERPs to faces (Nakamura, et al., 2001; Wiese, Schweinberger, & Hansen, 2008; Gazzaley, et al., 2008; DeFockert, Ramchurn, Velzen, Bergstrom, & Bunce, 2009; Daniel & Bentin, 2010), letters (Falkenstein, Yordanova, & Kolev, 2006; Kolev, Falkenstein, & Yordanova, 2006), and letter-number pairs (De Sanctis, et al., 2008). Four studies using faces found that the latency of the face-sensitive negative ERP peak around 170 ms post-stimulus was delayed in the older group compared to the young group, but this effect was not visible around 100 ms post-stimulus (Nakamura, et al., 2001; Wiese, Schweinberger, & Hansen, 2008; Daniel & Bentin, 2010; Gazzaley, et al., 2008). De Fockert, et al. (2009) reported ERP amplitude modulations around 170 ms in the elderly, but did not carry out latency analyses. However, many of ERP aging studies suffer from methodological shortcomings. The most common limitation is restricting analyses to easily identifiable EEG peaks on selected electrodes, thus discarding the potentially valuable information in regarding cortical processes between the peaks.

Recent studies by Rousselet, et al. (2009, 2010) overcame these drawbacks and demonstrated a reduction in visual processing speed of about 1 ms/year staring from about

age 20 onward in a sample of 62 healthy adults age 19 to 98 years old (Rousselet, et al., 2010). This delay has been computed using 50% integration time – a measure based on the shape of the whole EEG waveform between 0-500 ms post-stimulus. This measure takes into consideration both, latencies and amplitudes of the ERPs, providing a cumulative index of the speed of visual processing (Figure 1.8 A & B). Age-related effects reflected in the ERPs started at about 120 ms after stimulus onset and reached a maximum at around 190 ms, when the young group was about 50 ms ahead of the old group. Additionally, a qualitative change in the time-course of brain activity occurring at around 47 years of age was observed (Figure 1.8 C). Single subject data analyses revealed considerable individual differences in the speed of visual processing (indexed with 50% integration time) among subjects (Rousselet, et al., 2010). Some 60-70 old subjects were as fast as the 20-30 year-olds (or some 20-30 year-olds were as slow as the 60-70 year-olds (Figure 1.8 A). The reasons for this variability are difficult to reconcile with other EEG aging studies because most of them do not provide individual subject data, but only group averaged ERPs.

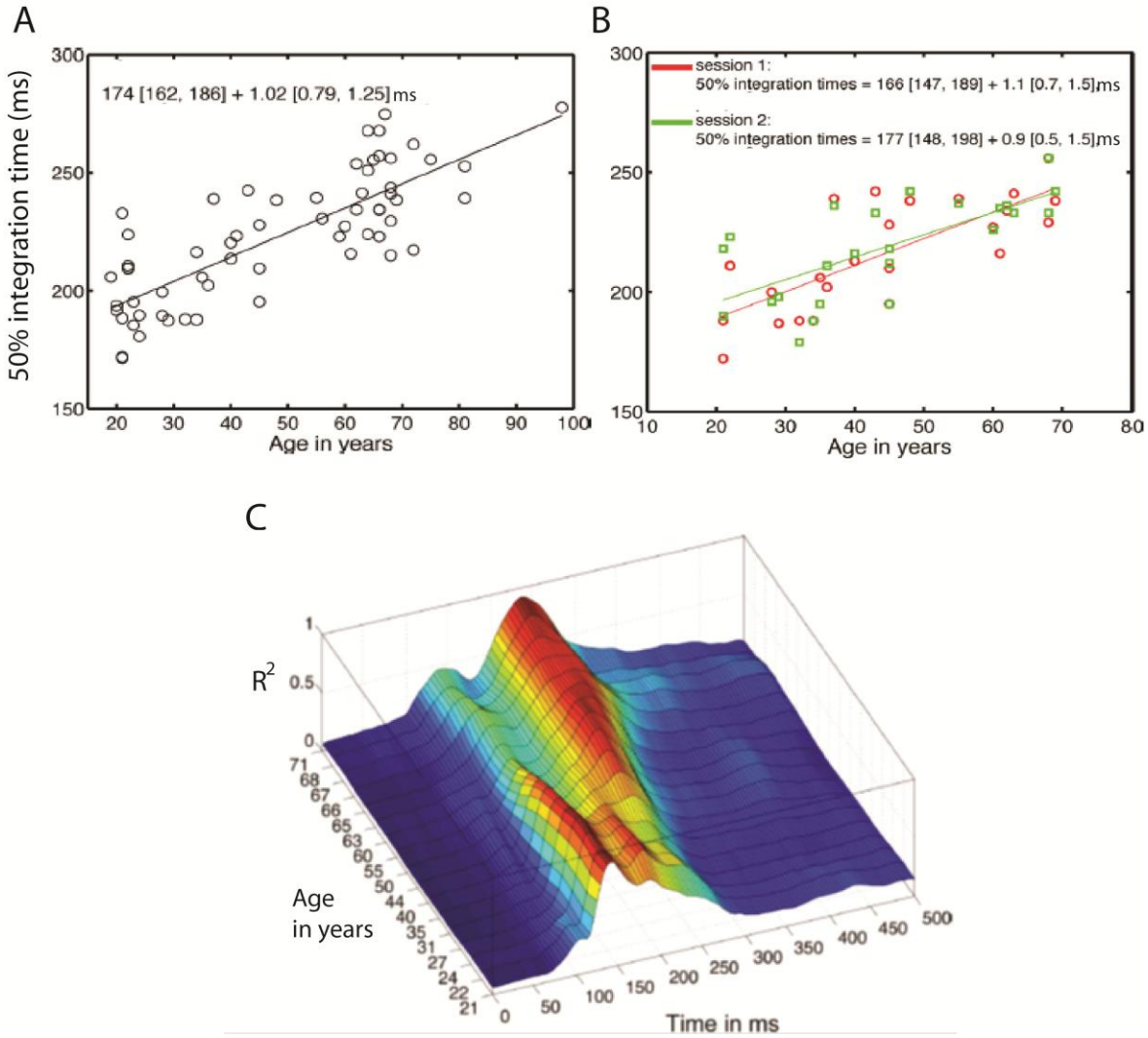

Figure 1.8. *Changes in ERP processing speed and in the shape of ERP waveforms as a function of age* ***(A)*** *Processing speed expressed in the 50% integration time (50IT), for 62 subjects (one dot per subject). Equation for the regression of 50IT against age is provided inside the plot.* ***(B)*** *Processing speed expressed in 50IT for two experimental sessions [for the 24 retested subjects – authors' ed.] – red circles are for session 1 and green squares are for session 2 (two symbols per subject). For each session regression equation (50IT against age) is given inside the plot.* ***(C)*** *The graph shows changes in the ERP sensitivity to manipulation of image properties (phase coherence) over time (0-500 ms post-stimulus) for different age groups. ERP modulations are expressed in* R^2 *functions reflecting general linear model (GLM) fit into EEG data. The GLM model contained two face identities, global phase coherence and local phase coherence of images as predictors.* R^2 *(model fit) ranges from 0 (dark blue) to 1 (dark red) (A, B and C are adapted from Rousselet, et al., 2010. A - Fig.9C p. 10; B - Fig 12B, p.11; C - Fig. 8, p.9).*

EEG aging effects may be also confounded with modulations related to task demands. Different types of tasks might require different attentional resources and top-down control and this can be reflected in varying ERP patterns. In young adults, task requirements have been found to alter early EEG activity ~150 or even as early as 100 ms after stimulus onset in experiments in which the same complex category images (faces, natural scenes, animals, vehicles) were either to be attended or to-be-ignored in different

blocks (VanRullen & Thorpe, 2001; Gazzaley, Clapp, Kelley, McEvoy, Knight, & D'Esposito, 2008). However, the very early (~100 ms) task effects may be due to uncontrolled perceptual differences between stimulus categories. Rousselet, Macé, Thorpe, & Fabre-Thorpe (2007) have shown that very early tasks effects that were initially visible ~100 ms for faces were abolished after controlling for variability in physical properties of images, while the later effects ~150 ms persisted. On the other hand, no task-related or top-down modulations in EEG activity before 200 ms were observed in several other studies using faces (Puce, Allison, & McCarthy, 1999; Carmel & Bentin, 2002; Se´verac-Cauquil, Edmonds, & Taylor, 2000). Despite these conflicting results, it is possible that task effects that are absent in young subjects may be present in old subjects and task difficulty may affect brain activity of older adults' differently than in younger adults.

Furthermore, it appears that the amount of perceptual evidence needed to accurately perform an object categorisation/recognition task increases with age, which can be related to changes in visual system's sensitivity to noise. Manipulation of evidence is often done by increasing the amount of visual noise, for example by scrambling Fourier phase spectra of images which carries most information about the category (Gaspar & Rousselet, 2009). Noteworthy, the level of noise should not be equated with the level of task difficulty. Although some practical correspondence can be drawn between them, cortical processes that underpin them might be quite different and translate into distinct ERP patterns. Indeed, Banko, et al. (2011) discovered that only the presence of noise and not the overall task difficulty had an effect on the first 300 ms of EEG activity in response to faces. The presence of noise has been found to affect EEG activity around 100 – 300 ms post-stimulus in both young and old adults (Philiastides & Sajda, 2006; Rousselet, et al., 2009; Rousselet, et al., 2010; Rousselet, Gaspar, Wieczorek, & Pernet, 2011a). It also seems that older subjects might be more sensitive to noise than young people. Rousselet, et al. (2010) found that older participants needed more information (stimuli with less noise) to achieve the same level of behavioural performance as young participants. The age-related changes in sensitivity to image structure were reflected in ERP delays starting ~120 ms post-stimulus, with the strongest effects at 208 ms. These delays might have several underlying phenomena, including decreasing processing speed with age, reduced neural specialisation in resolving signal from noise in the stimuli or deficits in inhibitory control. If the first interpretation is correct, then it is possible that later ERP activity in older adults may become functionally equivalent to earlier ERP activity in young adults (Rousselet, et al., 2010). The presence of noise increases processing demands and while dedifferentiation

seem to take place in the aging brain, it is plausible that reduced response tuning introduces a delay. Finally, older subjects may have more difficulties with supressing irrelevant or distracting information (noise) and the link between inhibitory deficits and modulations in early (<200 ms) ERPs has been suggested in several studies (Gazzaley, et al., 2008; Gazzaley, Cooney, McEvoy, Knight, & D'Esposito, 2005; Zanto & Gazzaley, 2009).

Other methodological variables, such as sample characteristics, may also contribute to the considerable amount of variability in age-effects on visual ERPs between various studies. All aging studies differ in their sample size, age range coverage, and density within age decade. This is not trivial issue because substantial amount of variability in visual processing speed within young, middle aged old age groups has been observed in aging research (Rousselet, et al., 2010). Thus, simple difference in the number of subjects in their, 40', 50' or 60' included in sample can potentially have an impact on a direction of the results. Moreover, lack of replications and reliability studies does not allow us to infer about how much of the observed effects could have depended on the day of testing. Finally, averaging data within age groups may lead to results that do not resemble any of the individual subjects (Gaspar, Rousselet, & Pernet, 2011), especially taking into consideration large individual differences in the speed of processing visible on both a neuronal and behavioural level. Experimental work reported in this thesis overcomes these issues by employing large sample of participants age 18-79, with roughly equal spread across decades. Moreover, all the subjects were tested twice to assess the reliability of the results and data were analysed on a single subject basis (Section 3).

To sum up, despite strong evidence that visual object processing slows down with age, the exact origins of the aging effects, as well as the origin of the inter-individual differences within age groups (Rousselet, et al., 2010), are still unclear. Apart from physiological changes occurring in the aging brain, it is possible that part of the age-related delays is due to factors affecting speed of processing before visual information arrives the cortex, in particular reduced retinal illumination that appears in the aging eye.

1.5 THE AGING EYE

1.5.1 OPTICAL PARAMETERS

Processing of visual information does not start at the cortex. After entering the eye, visual information travels from the retina, through the lateral geniculate nucleus (LGN) in the thalamus, via striate cortex to finally arrive to higher-order visual areas. Each of these areas may have its own contribution to the decrease in processing speed because age-related neural loss occurs from retina to cortex, suggesting that the decline in visual cognition is due to a combination of degenerative neural changes occurring at different stages within visual stream (Marshall, 1987; Devaney, 1980). This could account for the progressively increasing delay after stimulus onset found in (Rousselet, et al., 2009). Because visual processing starts at the retina, age- related alterations in processing speed may already begin there, for instance due to changes in pupil's response properties.

In healthy eyes, the size of the pupil controls to a large extent the amount of light that reaches the retina. An increase in the level of illumination results in a decrease in pupil size, and vice versa. The response to changing light conditions (pupil light reflex) is usually completed in a few seconds for increase in light, and up to a minute for withdrawal of light (Reeves, 1920; Crawford, 1936). A complete pupil adaptation to brightness occurs quite rapidly, however darkness adaptation is slower and may take even up to 30 minutes. In healthy eyes, both pupils respond equally to stimulation of only one eye – this phenomenon is known as the consensual light reflex (Szczepanowska-Nowak, Hachol, & Kasprzak, 2004). Pupil reaction is more extensive if both eyes receive stimulation compared to only one-eye stimulation. The diameter of the pupil may vary between 2 mm in high illumination to about 8 mm in darkness. Thus, the amount of light entering the pupil changes by the factor of 16 (Atchison & Smith, 2002). This variation is not sufficient to maintain a constant level of retinal illuminance, considering that humans operate comfortably over a 10^5 times luminance range from bright light (~1000 cd/m^2) to full moonlight (~0.01 cd/m^2). According to Campbell and Gregory (1960) the purpose of pupillary light response is to optimize visual acuity for various light levels. At various levels of photopic illumination (moderate to high light levels) the pupil also fluctuates in size with approximate frequency of 1.4 Hz – a phenomenon known as hippus.

Importantly, pupil diameter decreases with increasing age which leads to a reduced amount of light that reaches the retina in elderly eyes. This phenomenon, known as senile miosis, is present at all illuminance levels, although the rate of pupil change with age

decreases for higher luminance levels (Winn, Whitaker, Elliott, & Phillips, 1994). There is high variability in pupil diameters within an age group which decreases when luminance level increases (Figure 1.9) (Winn, et al., 1994). The size of the pupil reaches its maximum during teenage life and declines since then. For instance, Kadlecova, et al. (1958) have found pupil size varied from about 7.5 mm at the age of 10 years and decreased to 5mm at the age of 80 years. Also, the speed and the range of pupillary reaction, including the pupil's responsiveness to changes in luminance level, declines with age (Kumnick, 1954). Interestingly, the reduction in pupil size with age can also be beneficial for vision – it diminishes changes in higher-order aberrations (comatic and spherical aberrations or trefoil) (Applegate, Donnelly, Marsack, Koenig, & Pesudovs, 2007) and the eye's optical transfer function at lower light levels (Guirao, et al., 1999). Additionally, it reduces the diameter of retinal blur circle, boosting the depth of focus by about 0.5 D between 30 and 70 years of age (Weale, 1992). Nonetheless, because senile miosis reduces retinal illuminance, it could contribute to the delays and the considerable within age-group individual differences in cortical processing speed found in previous studies.

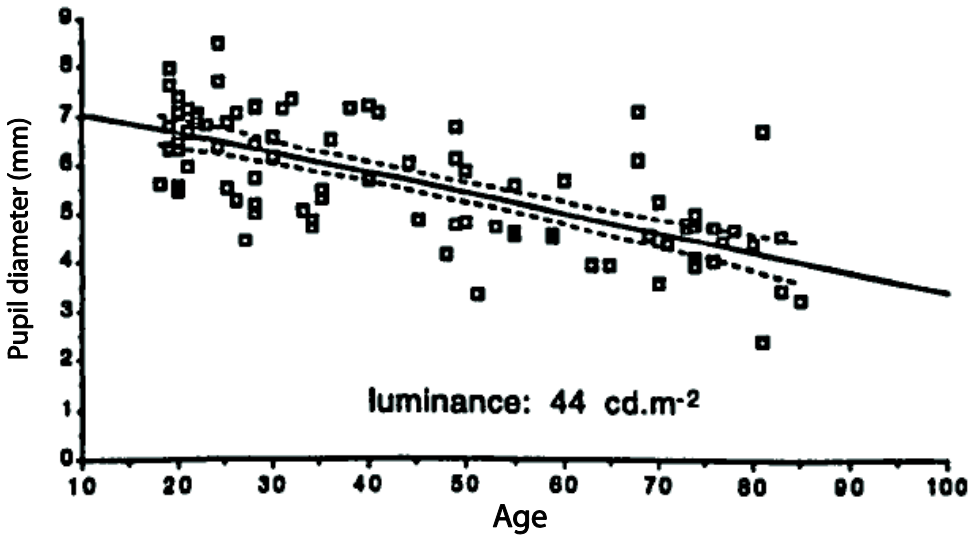

Figure 1.9. *Pupil diameter as a function of age for luminance = 44 cd/m^2. Data are fitted by linear regression with the 95% confidence limits indicated by the dotted line. (Reprinted from Winn et al. (1994), Fig. 2, p.1135).*

Other optical properties of the eye also change with age, leading to a decline in visual performance. Most dramatic changes are observed in the lens. With age, the lens increases in volume and mass (Cook, Koretz, Pfahnl, Hyun, & Kaufman, 1994), while the maximum possible change in lens shape decreases, reducing the amplitude of accommodation – the reflexive autofocus of the eye that allows objects to be well focused

on the retina (Koretz, Cook, & Kaufman, 2002). The eye's ability of accommodation decreases from the fifth decade of life onwards and seems to disappear altogether in the sixth (Birren & Schaie, 2001). Alterations in corneal thickness, shape and transmittance have also been found (Birren & Schaie, 2001). Light transmittance of both ultraviolet (wavelength 10 – 400 nm) and visible wavelengths (400 – 780 nm) goes down with age, while light absorption goes up, due to decrease in lens transparency (Artigas, Felipe, Navea, Fandino, & Artigas, 2012). Additionally, after the age of 40 (Fujisawa & Sasaki, 1995) there is a growth in the amount of optical backward and forward scatter (variations in the refractive index). Unlike for the absorption and backward scatter, increasing the light level does not compensate for the forward scatter. Forward scatter produces a veiling glare over the retina and reduces the contrast of the retinal image. This may cause low-contrast images to become invisible.

All in all, combining the reduction in pupil size, scatter and the drop in ocular transmittance leads to approximately 60% of light loss at the retina at lower light levels, between the ages of 20 and 60 years. This corresponds to more than 43 % of light loss at the retina of an older person at low light levels. Thus, there is a considerable difference between retinal illumination of younger and older adults which can affect the information transfer through the visual system and in turn be reflected in changes in processing speed in the cortex.

1.5.2 AGING EFFECTS ON LOW-LEVEL VISION

All the above optical factors contribute to age-related changes in such aspects of vision as visual acuity and contrast sensitivity. Visual acuity (the ability to resolve fine detail) diminishes year by year starting at about 50 years of age (Sekuler & Sekuler, 2000). Part of this deficit can be explained by changes in optical properties of the eye, such as decreased transparency, increased scatter and pupil miosis that lead to reduced retinal illuminance. However, the optical contribution can be challenged by first, the fact that when the crystalline lens is replaced with an artificial intraocular one, the acuity decline persists (Jay, Mammo, & Allan, 1987) and second, that acuity deficit becomes larger at lower luminance levels. It seems likely that acuity loss in the elderly is also related to changes occurring in the retina or brain (Owsley & Burton, 1991). The retinal loss in number of photoreceptors, ganglion cells or bipolar cells or a dysfunction in the connections between them can result in acuity decline. Moreover, studies in monkeys indicate that a selective damage to the parvocellular pathway (but not the magnocellular pathway) can lead to visual acuity deficits (Schiller, Logothetis, & Charles, 1990a).

It has been established in the 1980s that with age there is a decrease in spatial contrast sensitivity under photopic conditions, particularly at intermediate and high spatial frequencies in both fovea and periphery (Crassini, Brown, & Bowman, 1988; Owsley, Sekuler, & Siemsen, 1983). For low spatial-frequencies elevation of the contrast sensitivity threshold occurs when older observers view stimuli at high temporal frequency (Habak & Faubert, 2000). Also, the size of spatial contrast sensitivity deficit in aging seems to increase with progressively lower luminance levels (Sloane, Owsley, & Alvarez, 1988). For instance, in daylight older and young adults are equally sensitive to 0.5 cpd grating while under scotopic conditions the older subjects require on average three times as much contrast as younger subjects to discern a target (Schefrin, Tregear, Harvey, & Werner, 1999). There is a controversy regarding the extent to which the decline in contrast sensitivity can be attributed to optical and neural factors. The results of psychophysical studies using laser interferometry to bypass the optics of the eye and generate an image directly on the retina are conflicting: some opt for the former (Burton, Owsley, & Sloane, 1993) some for the latter hypothesis (Morrison & McGrath, 1985). Two further studies using adaptive optics to control for monochromatic higher-order aberrations (Elliot, 1987; Elliott, et al., 2009) support the neural approach. Although contrast sensitivity decline may be partially due to light scatter, it seems unlikely to be due to senile miosis because it persists when pupil diameter is controlled (Elliott, Whitaker, & MacVeigh, 1990) or due to the lens because it is still present when articificial intraocular lens is used (Morrison and McGrath, 1985). Additionally, anatomical observations indicate that age-related loss of retinal ganglion cells is relatively mild (Spear, 1993). The controversy in the origins of contrast sensitivity decline with age might have arisen because of inter-studies differences in inclusion criteria for subjects who differed in terms of their visual acuity that positively correlates with contrast sensitivity (Spear, 1993). To sum up, the data suggest that contrast sensitivity declines with age, in particular for mesopic and scotopic light conditions and for intermediate and high spatial frequency stimuli under photopic conditions. It is probably safe to assume that for most EEG aging studies that apply complex stimuli, age-related contrast sensitivity decline is not a major concern because they largely use monitors that operate in the photopic range. However, the majority of these studies do not report luminance under which subjects were tested and do not control for spatial frequency content of their stimuli, while it has been shown that under photopic conditions: variations in luminances can modulate latencies of ERP responses (Tobimatsu, Kurita-Tashima, Nakayama-Hiromatsu, Akazawa, & Kato, 1993; Shaw & Cant, 1980) and age effects on

contrast sensitivity depend on spatial frequency of the visual input (Owsley, Sekuler, & Siemsen, 1983).

1.6 THESIS RATIONALE

Visual object categorisation in the brain is a widely studied phenomenon but our understanding of it remains fragmented. Research work presented in this thesis addressed several enduring questions in visual neuroscience with regards to complex object processing: what low-level image information the brain is sensitive to when categorising objects and what is the timing of this sensitivity; how does the speed of object processing change with age; what is the contribution of optical factors, such as retinal illuminance, to individual differences and age-related delays in processing speed; and finally when do the first face-sensitive responses occur in the brain. These questions were addressed using EEG and robust data analyses techniques.

First, the question what visual information brain uses to categorise complex objects, such as faces, remains unclear. Studies using single cell recordings show that features of varying complexity are processed in different parts of ventral visual pathway. How this processing is reflected in activity of large populations of neurons recorded using EEG, is uncertain. In particular, the contribution of low-level stimulus characteristics, such as those carrying global (amplitude spectrum) and local (edges and contours) image information, to EEG activity associated with object categorisation is still debated. The debate stems in part from conceptual mistakes in the literature. For example, demonstrating that human observers can detect, or are impaired by amplitude spectrum manipulations, does not mean that observers actually use the amplitude spectrum when both phase and amplitude are available (Gaspar & Rousselet 2009; Wichmann, et al. 2010). Also, to my knowledge, no study has systematically assessed ERP sensitivity to phase and amplitude using systematic, parametric designs. Thus, in my first experiment (Section 2) I went beyond simple categorical designs and employed continues manipulation of phase and amplitude information from 0-100% in 10% intervals. This approach allowed not only to systematically measure the contribution of phase and amplitude to the ERPs, but also to determine the direction of this contribution by applying linear modelling of ERP data. Also, for the first time in the field, I computed the timing and unique contribution of phase and amplitude effects to individual subjects' ERPs and assessed reliability of my results by

testing my subjects twice. I found a major phase contribution but little evidence for amplitude spectrum contribution to early (<200 ms) ERPs to faces and houses.

Second family of questions addressed in this thesis concerns the timing of neural processes underlying object categorisation, how this timing is affected by senescence and whether optical factors can contribute to the age-related and individual differences in visual processing speed. With aging, there is a variety of changes appearing in the cortex, including white and grey matter atrophy, decrease in neuronal response specificity and inhibition and increase in cells' spontaneous activity. All of these can contribute to the age-related slowdown in visual processing speed, as indicated by studies using recordings of single cells activity as well as of populations of neurons (EEG and MEG). However, despite considerable body of ERP aging research, no agreement has been reached concerning what stages of visual object processing are subject to aging effects and how this translates into EEG modulations. Some studies observed age-related alterations in ERPs in response to faces before 200 ms post-stimulus, while other studies found only later effects. Recently, using component-free approach Rousselet, et al. (2009, 2010) demonstrated an age-related 1 ms/year ERP delay in visual processing speed of faces. Age effects on the ERPs started about 120 ms and were the strongest around 160 ms post-stimulus. Large individual differences in ERP processing speed were also observed. However, the origins of the age-related delay and of the individual variability remain elusive. Because visual processing starts at the eye, it is possible that at least part of the variability in processing speed may be of optical, rather than cortical origin. Considerable within-age group individual differences in size of the pupil have been observed. Moreover, pupil size decreases with age (senile miosis). Pupil size largely determines retinal illuminance which has been found to affect response latencies of neurons within the visual stream – the lower the retinal illuminance the later the responses. However, no study have tried to determine if there is a link between age-related and individual variability in visual processing speed observed at the cortex, and age-related decrease and individual variability in pupil size.

Thus, to assess the relationship between pupil size and age-related changes in speed of ERP responses I conducted two experiments (Sections 3 and 4), in which subjects' retinal illuminance was manipulated using neutral density filters (Section 3) and pinholes of varying sizes placed in front of their eyes (Section 4). Both of these methods were used previously to manipulate the amount of light that reaches observers' retinas (Eagan, et al., 1999).While neutral density filters allow to control stimulus luminance, pinholes placed in front of observers' eyes act as artificial pupils altering retinal illuminance without changing

stimulus luminance. Thus, the two methods complement each other and serve as a control to one another. The study involved EEG recordings of 62 healthy adults, age 18-79 years old, in two sessions each. Including participants with roughly even spread across age decades allowed for precise quantification of the rate of slowdown over the lifespan – a result that is largely lacking in ERP aging research dominated by cross-sectional comparisons. Moreover, my study is the first one to assess reliability of the aging effects by retesting all the participants on a separate day. The index of visual processing speed for each individual was computed based on the shape of the whole ERP waveform, was computed. This method leaves behind traditional peak measurements and incorporates both, latency and amplitude alterations along the time-course of EEG activity. In short, my results replicated the age-related 1 ms/year in ERP processing speed and showed that individual differences in pupil size could not account for this delay, nor for the individual variability in speed of processing, indicating that aging effects on the ERPs are largely cortical in origin. Moreover, age started to influence visual ERPs around 125 ms post-stimulus, spearing the earliest ERP responses to faces that were visible around 90 ms.

Building on the latter result of no age effects on the onsets of face-related ERP responses, my final project (Section 5) aimed for precise quantification of onsets in large sample of participants, using state-of-the-art analyses approaches. Research work to date is inconclusive with regards to precise timing of the first ERP responses sensitive to faces. Most studies suffer from methodological shortcomings, such as small sample sizes, using statistics that lack multiple comparisons corrections, focusing on group averaged ERPs, restricting analyses to easily identifiable peaks and, probably most crucially, applying EEG data filters that can potentially disrupt the latencies of the earliest significant ERP responses. The goal of my final project was to quantify the onsets of ERP sensitivity to faces by overcoming methodological shortcomings in the field to date. To this end, I combined data of a total of 120 subjects, collected in the aging experiment reported in Section 3, and in two independent studies using similar stimuli (Rousselet, et al., 2009, 2010). To my knowledge no study has yet quantified ERP face sensitivity onsets in individual subjects belonging to such a large group, with age range 18-89 years old. Further, I used novel and robust statistical analyses, including bootstrap spatial-temporal multiple comparison corrections. The final advantage of my study was the application of causal filtering of EEG data which does not distort onsets of the effects. The main findings were that the earliest ERP sensitivity to faces was visible at the median latency of 87 ms

post-stimulus, and the onset distributions did not change when low-pass filtering or 20% trimmed means, instead of means, across ERP trials were applied.

2 ERP SENSITIVITY TO IMAGE PROPERTIES

Evidence from parametric, test-retest, single-subject analyses.

One major challenge in determining how the brain categorises objects is to tease apart the contribution of low-level and high-level visual properties to behavioural and brain imaging data. So far, studies using stimuli with equated amplitude spectra have shown that the visual system relies mostly on localised information, such as edges and contours, carried by phase information. However, some researchers have argued that some event-related potentials (ERP) and blood-oxygen-level-dependent (BOLD) categorical differences could be driven by non-localised information contained in the amplitude spectrum.

The goal of this study was to provide the first systematic quantification of the relative contribution of phase and amplitude spectra to early ERPs to faces and objects. Overall, a major contribution of phase information to face- and object-related ERPs was observed, with little evidence for a contribution of the amplitude spectrum.

2.1 METHODS

2.1.1 SUBJECTS

Eight subjects took part in the experiment (six males, two females; median age = 28, min = 20, max = 32). Six of them completed a second experimental session between 5-8 months after the first one. Session 2 had the same experimental settings as session 1, except the sequence of stimuli, which was randomised for each session. Three subjects were members of the lab, including two of the authors, and the remaining five subjects were naive regarding the purpose of the experiment. Two subjects were left-handed, six were right-handed. We tested subjects' visual acuity using a Colenbrander mixed contrast card set. All subjects had normal or corrected to normal visual acuity in the range of 20/25 to 20/10 dec, at 40 cm, 63 cm and 6 m distances. Subjects' contrast sensitivity was measured using Pelli-Robson Contrast Sensitivity Chart, yielding results of 1.95 and above (normal range). All participants also filled in a general health and life style questionnaire.

The median number of education years was 21.5 (min = 19, max = 24). All reported good to excellent vision and hearing, and at least weekly exercise. One person reported smoking. All subjects read a study information sheet explaining the behavioural and EEG experimental procedures and provided written informed consent.

2.1.2 STIMULI

Two object categories were used in the experiment: faces and houses (one exemplar image per category, chosen from a set of 10; see details in Rousselet, Husk, Bennett, & Sekuler, 2008b; Husk, Bennett, & Sekuler, 2007). The same house and face were used for all the subjects. All images had the same mean pixel intensity and RMS contrast of 0.1. Phase and amplitude spectra were manipulated of face and house images parametrically and independently using Matlab 2007b (Figure 2.1A). Global phase coherence was altered in 10% intervals, resulting in images containing from 70% to 0% phase coherence (Philiastides & Sajda, 2006; Rousselet, et al., 2008a). Amplitude spectra were manipulated by replacing the original image's amplitude spectrum with composite amplitude spectra, ranging from 100% face amplitude (0% house amplitude), through 50% face amplitude (50% house amplitude), to 0% face amplitude (100% house amplitude), in 10% steps. These manipulations resulted in 88 face and 88 house conditions, with 8 phase (0-70%) and 11 amplitude levels (0-100%). A maximum phase coherence level of 70% was used to reduce the length of the experiment and because increasing phase coherence beyond 70% does not lead to significant behavioral and ERP changes in most subjects (Rousselet, Husk, Pernet, Gaspar, Bennett, & Sekuler, 2009; Rousselet, et al., 2008a).

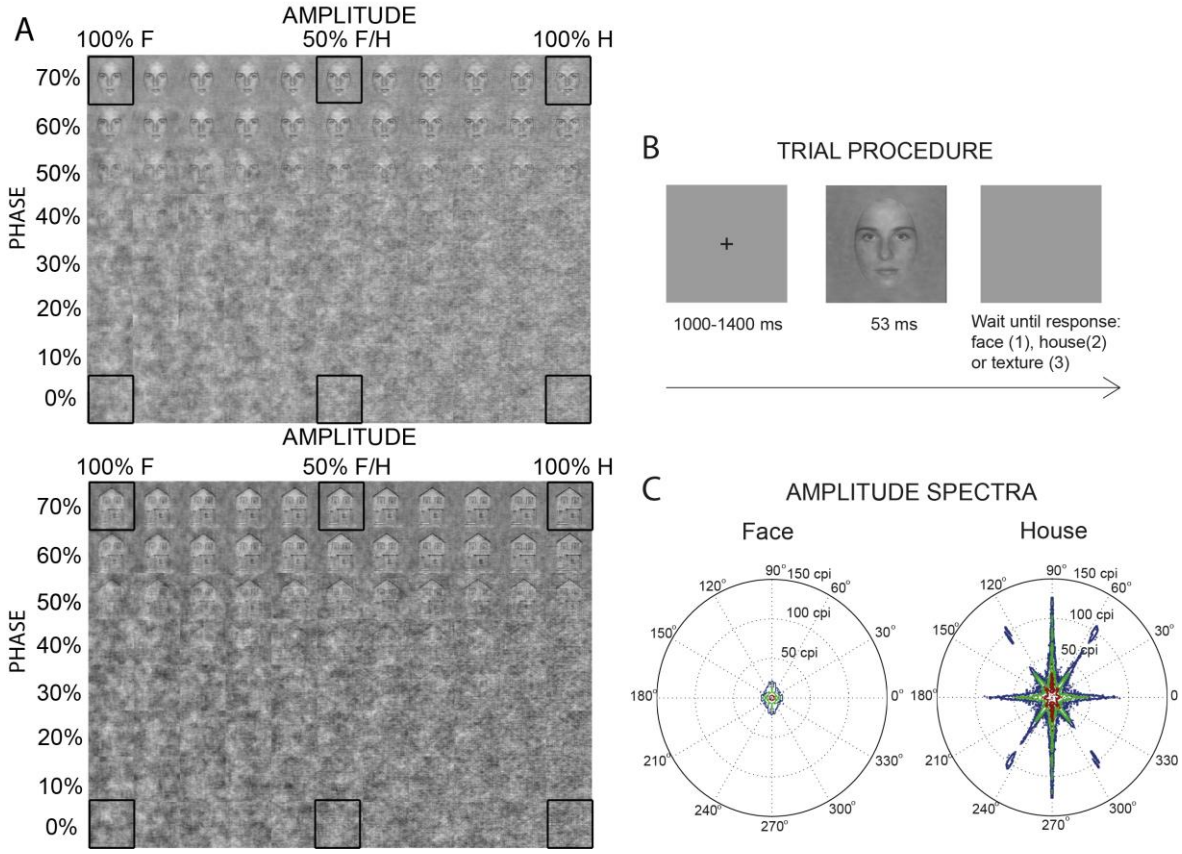

Figure 2.1. *Stimuli.* ***(A)*** *There were a total of 88 face conditions (top) and 88 house conditions (bottom). For the two categories, amplitude is expressed along the X-axis, from 100% face amplitude (0% house amplitude) on the left, to 0% face amplitude (100% house amplitude) on the right, in 10% intervals. Phase is expressed along the Y-axis from 0% phase coherence at the bottom to 70% phase at the top, in 10% intervals.* ***(B)*** *Trial timeline. For presentation purposes the face image is not to scale.* ***(C)*** *Amplitude spectrum contours of face (left) and house (right) images. Spectral energy contours were computed by averaging the amplitude spectra of all images within one object category. The red, green and blue contours indicate the boundaries of 60%, 80% and 90% of the total power contained below the relevant spatial frequencies (50, 100, 150 cycles per image) indicated by the radius of each circle.*

2.1.3 EXPERIMENTAL PROCEDURE

EEG electrode application lasted about 30 min. Subjects sat in a sound attenuated booth. They were asked to position their heads on a chin-rest to maintain a viewing distance of 80 cm and then were given experimental instructions. Subjects were asked to categorise images as faces, houses or textures by pressing a corresponding key on a computer keyboard (1, 2, or 3 on the numerical pad), using three fingers of their dominant hand. The order of the response keys was randomly assigned. Stimuli were presented on a Samsung SyncMaster 1100Mb monitor (600 x 800 pixels, height and width: 30 x 40 cm, 21º x 27º of visual angle). All images were 256 x 256 pixels (9º x 9º of visual angle) and were displayed on a grey background (RGB 128, 128, 128) with luminance 33 cd/m^2. In each trial, first a fixation cross appeared for a random interval between 1000 and 1400 ms,

followed by a stimulus presented for 5 frames (i.e. a maximum of 53 ms), and then by a blank screen which remained displayed until subjects' response (Figure 2.1B). There were 10 blocks, each with 176 trials: 88 images of faces and 88 images of houses. Each of the 88 images represented one of the 88 conditions. There were thus a total of 10 trials per image category and condition. The whole experiment contained 1760 trials and lasted about 75 minutes, excluding electrode application.

2.1.4 BEHAVIOURAL DATA ANALYSIS

Generalized Estimating Equations (GEE, IBM SPSS Statistics 19) were used to build binary logistic models of the occurrence of "face" and "house" responses in all subjects. The occurrence of "face" responses within the face stimuli matrix (Figure 2.1 A, top panel) was separately modeled from the occurrence of "house" responses within the house stimuli matrix (Figure 2.1 A, bottom panel), for each session separately. In the first case, "face" responses were coded as "1" and all the other responses were coded as 0, whereas in the second case all "house" responses were coded as "1" and the remaining responses were coded as "0". Both models contained phase and amplitude as within-subject continuous predictors (covariates). The within-subject dependencies were assumed to be homogenous (exchangeable correlation matrix option in SPSS). Model effects were computed using Wald chi-square statistics. Because subjects responded "house" to face stimuli or "face" to house stimuli in only 1-5% of trials, depending on the session, we did not model this behavior. Statistical analysis of rare events (appearing on less than 10% of the trials) may lead to spurious results.

2.1.5 EEG RECORDING

EEG was recorded at 512 Hz using the Active Electrode Amplifier System (BIOSEMI) with 128 electrodes mounted on an elastic cap. Two additional electrodes were placed at the outer canthi of the eyes and two below the eyes. During analog to digital conversion, a 5th order Bessel filter was applied to prevent aliasing. The filter had a -3 dB point at 1/5th of the sample rate, i.e. 102.4 Hz. DC coupled data were saved to file.

2.1.6 EEG DATA PRE-PROCESSING

EEG data were pre-processed using Matlab and the open-source toolbox EEGLAB (Delorme & Makeig, 2004; Delorme, et al., 2011). Data were first re-referenced off-line to an average reference, band-pass filtered between 0.5 Hz and 40 Hz using a two-way least square FIR filter (pop_eegfilt function in EEGLAB) and then epoched from -300 to 1200 ms. The use of a non-causal high-pass filter means that the true onsets of some of the

effects could be later than the onsets reported in this paper (VanRullen, 2011; Rousselet, 2012; Widman & Schroeger, 2012; Acunzo, MacKenzieb, & van Rossum, 2012). Noisy electrodes were then detected by visual inspection and rejected on a subject-by-subject basis (number of rejected electrodes: median = 3, min = 0, max = 18). Baseline correction was performed using the average activity between -300 ms until stimulus onset. Subsequently, we used Independent Component Analysis (ICA), as implemented in the infomax algorithm from EEGLAB. If ICA decomposition yielded components representing noisy electrodes (IC with a very focal, non-dipole activity restricted to one electrode while the rest of the map around the electrode is flat), the noisy channels were removed and the ICA was repeated. Components representing blinks, lateral eye-movements or muscle contraction were rejected individually for each subject (number of rejected components: median=2, min=1, max=6). After rejection of artifactual components, data were re-epoched between -300 and 500 ms and baseline correction was performed again. Finally, data epochs were removed based on an absolute threshold value larger than 100 μV and the presence of a linear trend with an absolute slope larger than 75 μV per epoch and R^2 larger than 0.3. The median number of trials accepted for analysis was 1729 out of 1760 (min = 1572, max = 1757).

2.1.7 EEG DATA ANALYSIS

Data from individual subjects were analyzed using the LIMO EEG toolbox, a plug-in to the EEGLAB environment (Pernet, et al. 2011). Independently at each time point and at each electrode, single-trial ERPs were modeled as:

$$ERP = \beta_1 F + \beta_2 H + \beta_3 F\,amp + \beta_4 F\,\varphi + \beta_5 F\,int + \beta_6 H\,amp + \beta_7 H\,\varphi + \beta_8 H\,int + \beta_0 + \varepsilon \qquad (1)$$

In this model, images of faces (F) and houses (H) were two categorical predictors, whereas global phase coherence (φ), amplitude spectrum (amp) and the phase x amplitude interaction (int) were continuous predictors. Amplitude was coded as the proportion of face amplitude (Figure 2.2). β_0 was a constant term and ε was the error. The design matrix for the main model is presented in Figure 2.2 (left panel).

Subsequently, for each subject individually the electrode with maximum model fit, termed the max R^2 electrode, was determined. This electrode captured the maximum ERP sensitivity to our image structure manipulation. The max R^2 electrodes for all subjects for the main regression model and for the categorical interaction model are provided in top left

plots of Figures 2.6 and 2.10, respectively and in the Appendix A – Supplementary Figures 7, 8, 9 & 10.

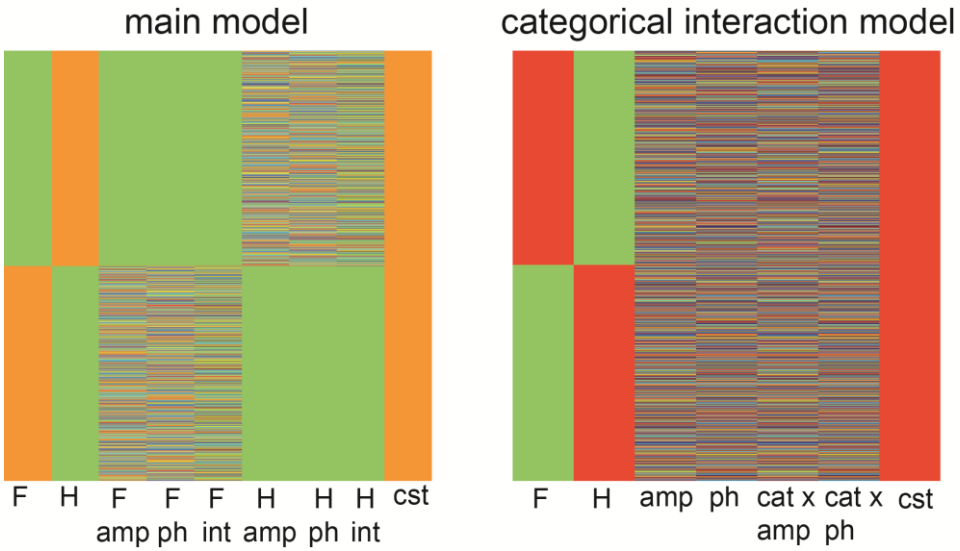

Figure 2.2. *Design matrices. Left – main model (equation 1); right – categorical interaction model (equation 2). Rows represent single-trials; columns represent the predictors of the GLM. Both models contained two categorical predictors – faces and houses (F and H), and continuous predictors – there were 6 regressors in the main model: amplitude, phase and their interaction for faces, and for houses, and 4 regressors in the categorical interaction model: amplitude, phase, category x amplitude interaction and category x phase interaction. The last column in both designs represents a constant term.*

2.1.8 UNIQUE VARIANCE ANALYSIS

The amount of unique variance each predictor explained at the max R^2 electrode in each subject was determined by computing semi-partial correlation coefficients. Separately for each session and each subject, the maximum unique variance for each predictor in three time windows: P1 (80-120 ms), N1 (130-200 ms) and P2 (200-300 ms) was measured. These time windows were defined based on conventions in the ERP literature as well as visual inspection of the data. A percentile bootstrap test was used to determine if, across subjects, the medians of the unique variances differed significantly between phase and amplitude for faces and houses. Medians were estimated using the Harrell-Davis estimator of the 0.5 quantile (Wilcox, 2005).

2.1.9 CATEGORICAL INTERACTION ANALYSIS

If the amplitude spectrum carries categorical information, categorical effects should be modulated by amplitude – in other words, we should observe a category x amplitude interaction. A second model was designed to test this interaction (Figure 2.2, right panel):

$$ERP = \beta_0 + \beta_1 F + \beta_2 H + \beta_3 amp + \beta_4 \varphi + \beta_5 cat\ x\ amp + \beta_6 cat\ x\ \varphi + \varepsilon \quad (2)$$

In this model there were two categorical variables: faces (F) and houses (H), and four continues variables: amplitude (amp), phase (φ), category x amplitude interaction (cat x amp) and category x phase (cat x φ) interaction. Interaction terms were computed by multiplying the categorical predictor (F=1 or H=-1) by z-scored continues predictors (amp or φ).

2.1.10 CROSS-SESSION RELIABILITY ANALYSIS

We assessed the reliability of phase and amplitude effects across two experimental sessions by calculating the difference between beta-coefficients obtained from each session at the max R^2 electrode. We tested the significance of the beta differences using a max temporal cluster bootstrap statistics. First, we pooled together single-trial data from the two sessions. Then we drew two bootstrap samples, with replacement, from the pooled data. The number of trials in each bootstrap sample was the same as the number of trials originally recorded in each session. The bootstrapped samples for each session were then analysed using the corresponding GLM. Bootstrap sampling and model fitting was performed 1000 times. Using these 1000 iterations, we calculated percentile bootstrap univariate 95% confidence intervals for the beta coefficient differences across sessions. Next, the confidence intervals were used to define temporal clusters of absolute beta differences in the bootstrapped and the original data. Original cluster sums of absolute differences were considered significant if they were larger than the 95^{th} percentile of the corresponding bootstrap distribution of maximum cluster sums (i.e. $p<0.05$ corrected for multiple comparisons).

2.2 RESULTS

2.2.1 BEHAVIOUR

The behavioural data indicated that subjects relied more on phase than on amplitude spectrum to categorise images (Figure 2.3). There was a significant effect of phase on the number of subjects' face responses to face stimuli and on the number of house responses to house stimuli in both sessions (faces session 1: Wald Chi-Square (WCS) = 12.160, p = 0.0001; faces session 2: WCS = 268.622, p = 0.0001; houses session 1: WCS = 24.044, p = 0.0001; session 2: WCS = 11.148, p = 0.0001). Participants' accuracy significantly improved as global phase coherence of images increased from 0 to 70% (faces session 1: β= 11.300, 95% Wald Confidence Interval = [4.9, 17.6]; faces session 2: β

= 18.438 [16.2, 20.6]; houses session 1: β = 9.581 [5.752, 13.411]; houses session2: β = 12.148 [5.017, 19.279]). Significant effects of amplitude on subjects' face responses to face stimuli or house responses to house stimuli were present only in session 2 (faces: WCS = 8.446, p = 0.004; houses: WCS = 4.289, p = 0.038), but not in session 1 (faces: WCS = 3.219, p = .073; houses: WCS = 1.715, p = 0.190). In session 2, the beta coefficient associated with a significant amplitude effect for face stimuli was positive (β = 1.514 [0.493, 2.536]), indicating that participants responded "face" more often when the amplitude changed from 0 to 100% face. In the same session, the beta coefficient for house stimuli was negative (β = -3.989 [-7.763, -.214]) suggesting that subjects pressed "house" less often when the amplitude increased from 0 to 100% face. There was no interaction between phase and amplitude in any of the sessions. In sum, the behavioural results suggest that phase is the main contributor to subjects' categorisation decision. However, participants' responses appear to be influenced also by the congruency between phase and amplitude spectra – if a stimulus contained amplitude and phase information of a face, the number of "face" responses increased; if a stimulus had house phase spectrum and face amplitude, the number of "house" responses decreased. However, this result was not consistent across sessions; hence it is difficult to interpret.

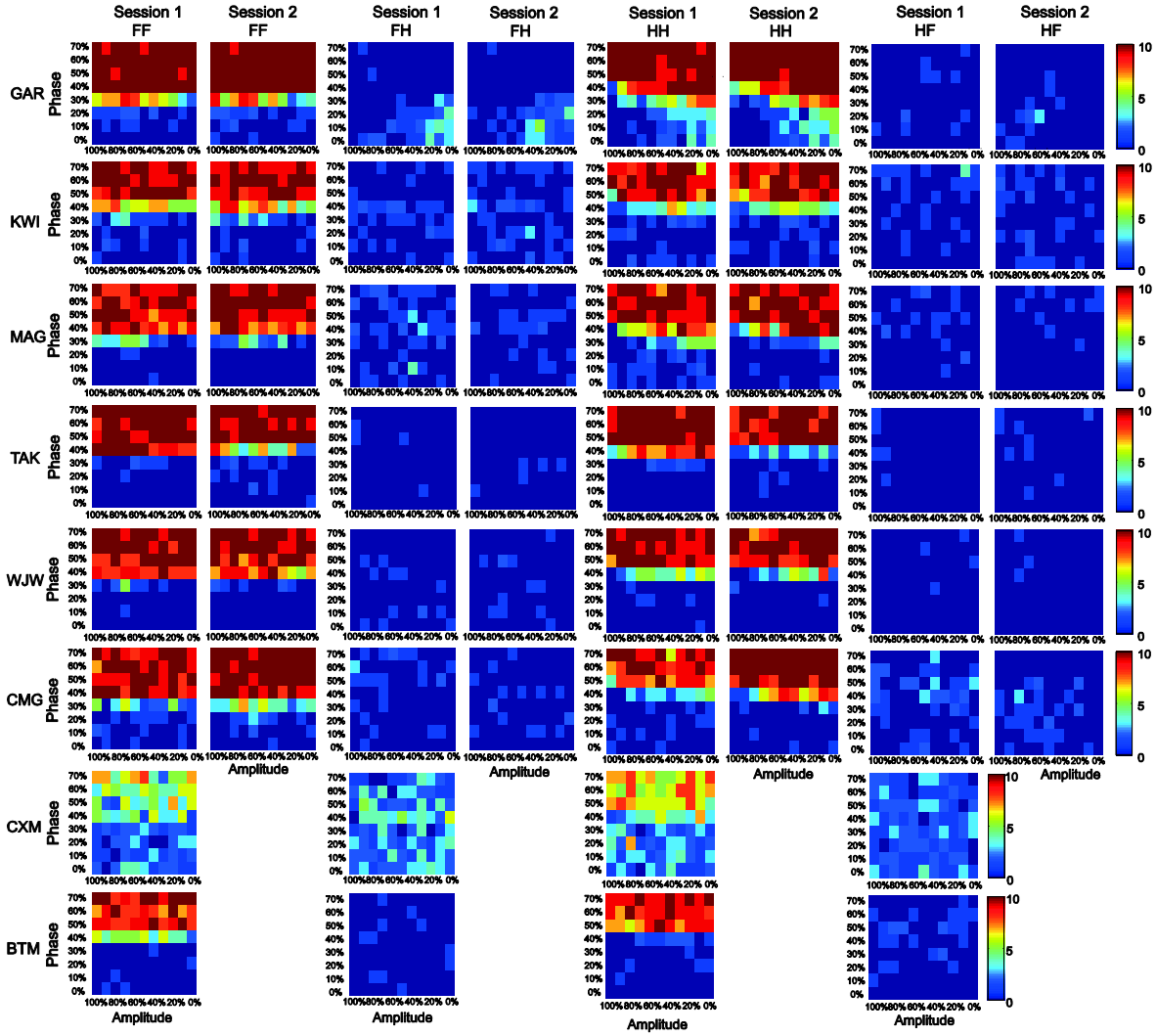

Figure 2.3. *Behavioural results. Matrices showing how many times in each session subjects categorized an image from the face stimuli matrix either a "face" (columns FF) or a "house" (columns FH). Each matrix contains colour-coded numbers of answers (from 0 - dark blue, to 10 - dark red) for the 88 conditions (one condition per cell). The Y axis represents global phase coherence (0-70%).The X axis represents amplitude spectrum coded from 100% face amplitude (= 0% house amplitude) in the left column to 0% face amplitude (100% house amplitude) in the right column.*

2.2.2 EEG

The results suggest that phase is the main contributor to early categorical ERPs in humans. The max R^2 electrode in each participant was also the electrode showing maximum phase sensitivity. Phase effects peaked at around 170 ms after stimulus onset for faces, and slightly later, at 185 ms, for houses (Table 2.1); at these latencies, amplitude spectrum and phase x amplitude spectrum interaction effects were negligible (Figure 2.4, row 1; Appendix A – Supplementary Figures 1-6). Phase effects before 200 ms post-stimulus were visible at lateral-occipital electrodes in all subjects (Figure 2.5, Appendix A – Supplementary Figures 1 & 2). In the 6 subjects tested twice, the time-courses of the beta coefficients associated with phase effects were also reliable across sessions, although

significant differences in latency, magnitude or both were observed in 3 subjects (MAG, GAR and KWI; Appendix A – Supplementary Figures 11 & 12).

	Peak latency Session 1		Peak latency Session 2		Peak latency S1 – S2 difference	
	Faces	Houses	Faces	Houses	Faces	Houses
Phase	170 [160, 182]	185 [174, 195]	168 [154, 185]	185 [170, 196]	2 [-6, 11] ms	2 [-13, 13] ms
Amplitude	160 [144, 186]	144 [131, 159]	179 [138, 200]	176 [141, 193]	-9 [-23, 16] ms	-20 [-54, 13] ms

Table 2.1. *Median latencies (ms) of peak sensitivities to phase and amplitude spectra. The two right-hand columns contain differences between sessions for each effect. Square brackets contain 95% percentile bootstrap confidence intervals.*

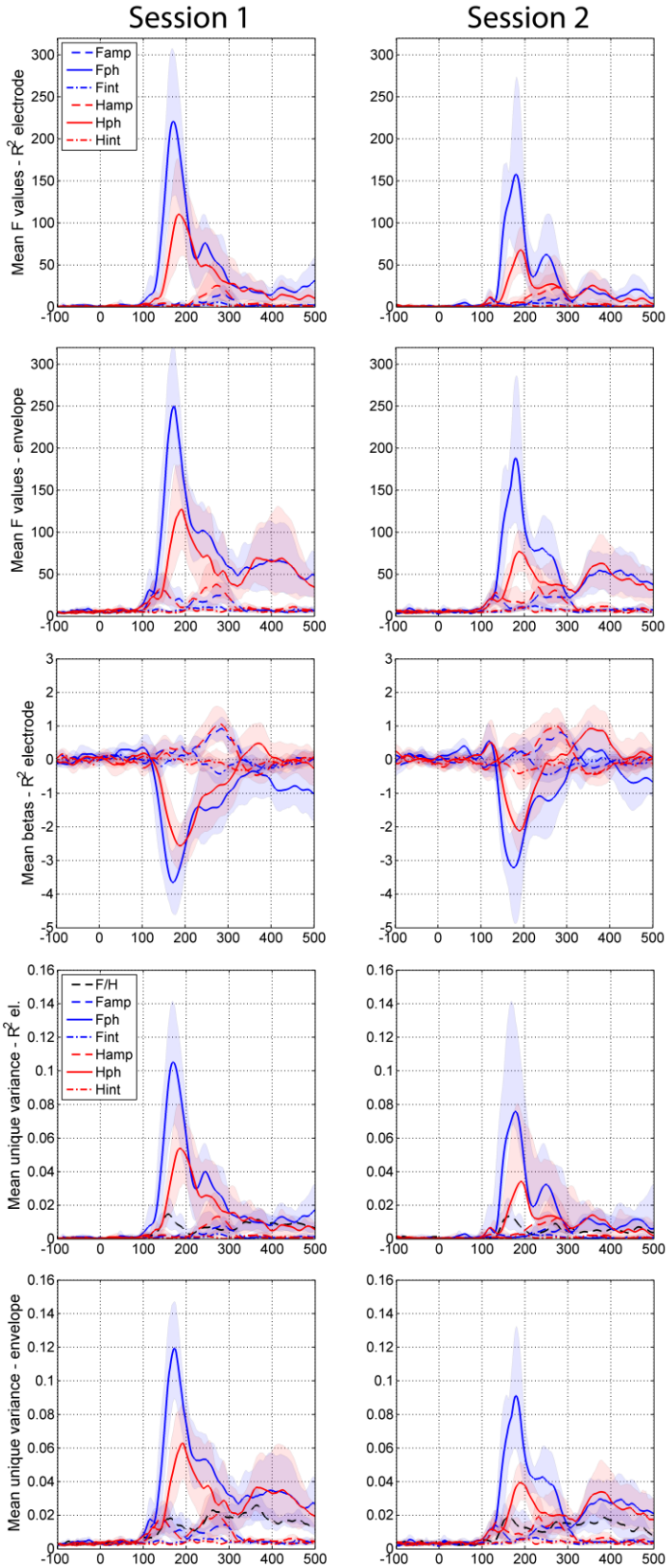

Figure 2.4. *Time course of effects associated with each predictor in the main regression model. Row 1: mean F values at max R^2 electrode; row 2: mean of max F values across all electrodes (envelope); row 3: mean beta coefficients at max R^2 electrode; row 4: mean unique variance at max R^2 electrode; row 5: mean of the max unique variance across electrodes. Shading represents 95% confidence intervals around the means.*

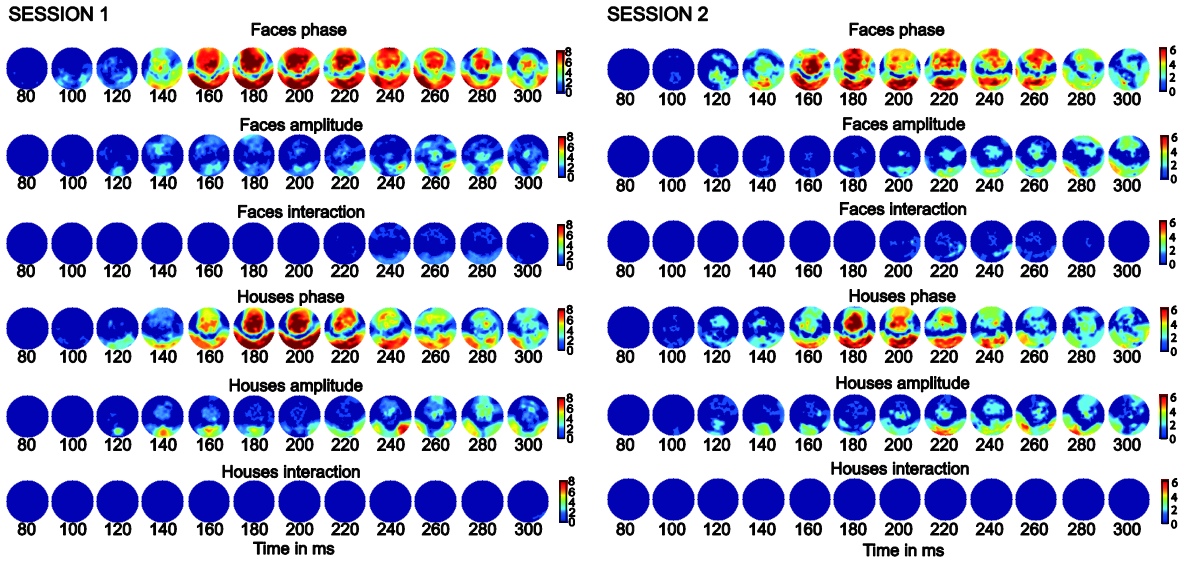

Figure 2.5. *Topographic maps of the frequencies of the effects from the main regression model. Maps are colour-coded according to the number of subjects showing the effects, from 0 subjects (dark blue) to the maximum number of subjects for that session (dark red). Each row shows the scalp distributions between 80 and 300 ms post stimulus.*

Large amplitude spectrum effects occurred before 200 ms after stimulus onset at medial occipital electrodes in 3 out of 8 subjects for faces and in 6 out of 8 subjects for houses (Figure 2.5). The medial occipital amplitude sensitivity peaked at the median latency of 160 ms (session 1) and 179 ms (session 2) for faces, and at 144 ms (session 1) and 176 ms (session 2) for houses (Table 2.1) with no significant differences between sessions (Table 2.1).

The latencies of maximum early sensitivities to phase and amplitude differed only for houses in session 1 (Table 2.2) – the strongest amplitude effects occurred significantly earlier than phase effects. Additionally, some subjects showed also amplitude effects after 200 ms post-stimulus, at lateral-occipital electrodes.

Finally, only three subjects had significant interaction effects, and they occurred after 200 ms post-stimulus: one subject (KWI) showed a significant interaction for faces in both sessions and in one session for houses (Appendix A – Supplementary Figures 5 & 6); two subjects had an interaction effect in one session for face stimuli.

	Phase vs. amplitude Session 1		Phase vs. amplitude Session 2	
	Faces	Houses	Faces	Houses
Peak	8 [-6, 15]	40 [21, 54]	-12 [-21, 22]	9 [-21, 50]

Table 2.2. *Differences between median latencies (ms) of maximum sensitivity to phase and amplitude: phase vs. amplitude, separately in faces and houses. A negative difference means an earlier effect for phase compared to amplitude. Square brackets contain 95% percentile bootstrap confidence intervals.*

	Faces vs. houses Session 1		Faces vs. houses Session 2	
	Phase	Amplitude	Phase	Amplitude
Peak	-15 [-25, -7]	16 [8, 41]	-16 [-23, -5]	3 [-43, 51]

Table 2.3. *Differences between median latencies (ms) of maximum sensitivity to phase and amplitude: faces vs. houses, separately for phase and amplitude. A negative difference means an earlier effect for faces compared to houses.*

DIRECTION OF THE EFFECTS

Beyond the mere presence or absence of phase and amplitude effects, it is also important to consider the direction of the effects, as indicated by the sign of the beta coefficients. At the max R^2 electrode, between about 130 and 200 ms, the phase beta coefficients were negative in all participants which means that ERPs to faces and houses (i.e. the N170) became more negative as phase changed from 0% (stimuli perceived as textures) to 70% (stimuli perceived as faces or houses – Figure 2.4, row 3; Figure 2.6; Appendix A – Supplementary Table 1; Supplementary Figures 7 – 10). In most subjects and most sessions, amplitude spectrum effects had the opposite direction: a positive beta coefficient indicated that as the amplitude spectrum changed from 0% to 100% face amplitude, ERPs to faces and houses became more positive. The same pattern of amplitude effect was observed at the max R^2 electrode (Figure 2.6; Appendix A – Supplementary Figures 7 – 10, columns 2 & 5), and at the electrodes where maximum sensitivity to amplitude was found (Appendix A – Supplementary Figures 7 – 10, columns 3 & 6). The only cases where beta coefficients for phase and amplitude went in the same direction appeared in subject WJW (faces in session1; houses in both sessions) and TAK (houses in session 2) but the similarities were short-lived and mostly present beyond 200 ms post-stimulus.

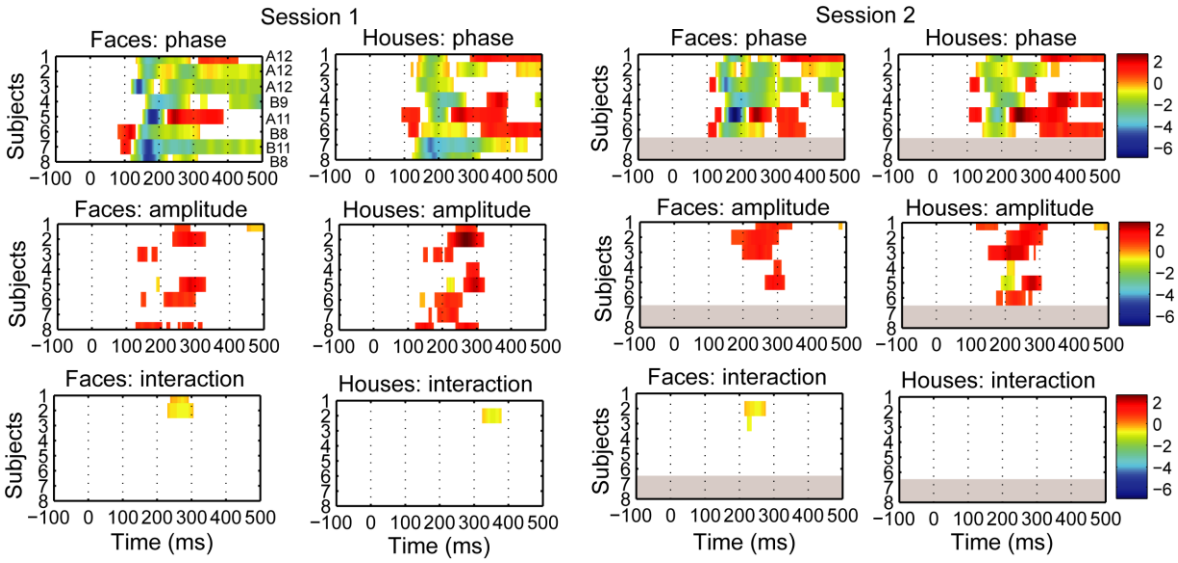

Figure 2.6. *Time-courses of beta coefficients associated with each predictor of the first regression model. The betas are from the electrode of the max R^2 for each subject (provided on the right hand side of the top left plot). Rows shaded in grey indicate missing subjects in Session 2.*

UNIQUE VARIANCE

The phase spectrum had significantly larger unique explained variance than the amplitude spectrum for both faces and houses, in the N1 and P2 time windows, but not in the P1 time window (Figures 2.7 & 2.8). This was the case at the max R^2 electrode and at the maximum across all electrodes (envelope; Appendix A – Supplementary Table 2). In contrast to phase, the amplitude spectrum explained close to zero unique variance in the N1 time window, at the max R^2 electrode (Figures 2.7 & 2.8, Appendix A – Supplementary Table 3). However, amplitude did explain small amount of unique variance at medial occipital electrodes in the P1 and N1 time windows and at lateral-occipital sites in the P2 time window (Figure 2.9, Appendix A – Supplementary Table 3). The phase x amplitude interaction explained nearly no unique variance in any time window. Overall, within the first 200 ms post-stimulus, phase accounted for the largest part of the ERP variance with a lateral-occipital scalp distribution, whereas amplitude had a weak contribution at medial occipital electrodes.

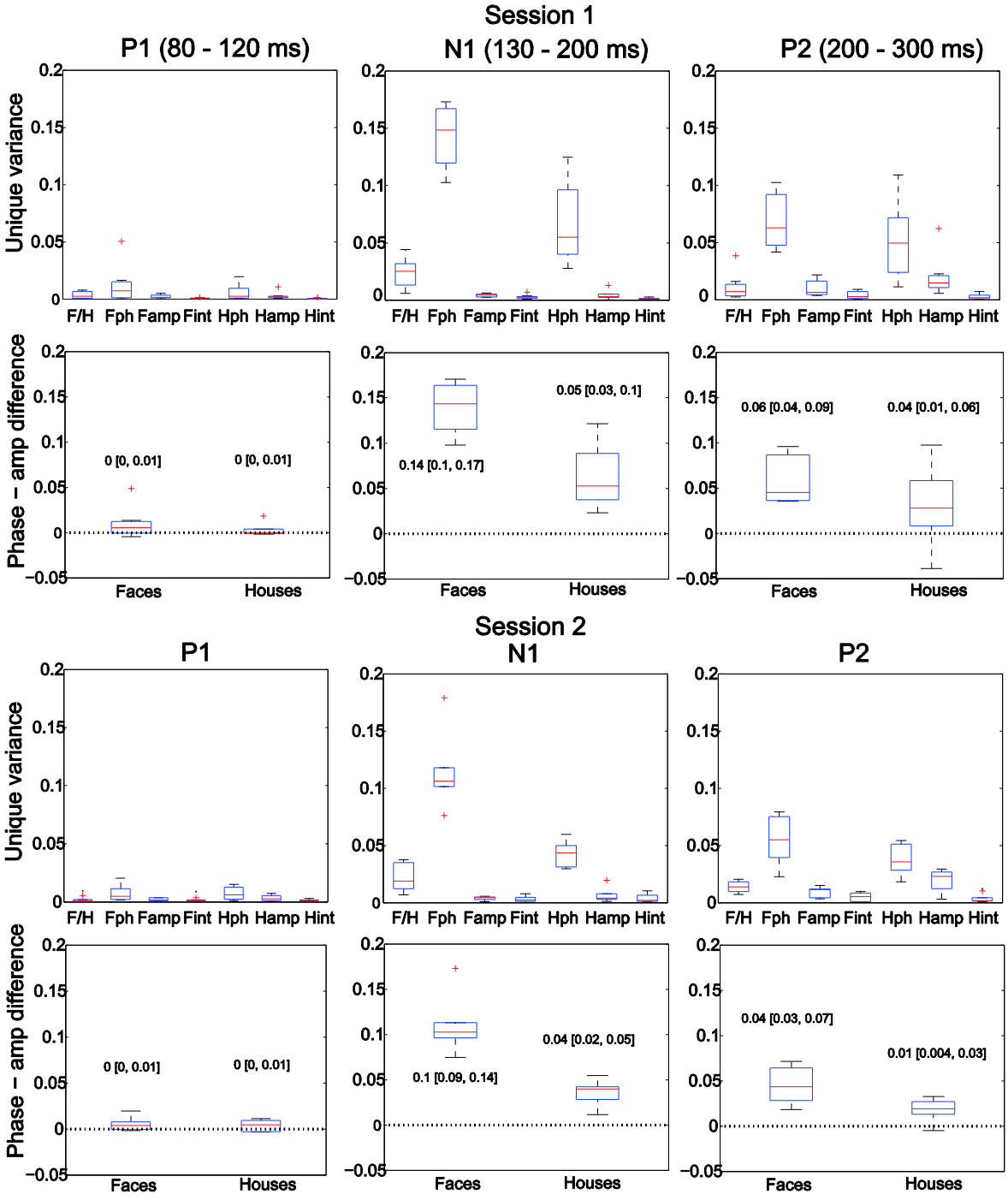

Figure 2.7. *Boxplots of maximum unique variance explained by each predictor at the max R^2 electrode, in three time windows: P1 (80-120ms), N1 (130-200ms) and P2 (200-300ms). The boxplots show distributions across subjects. Session 1 is shown in row 1 and session 2 in row 3. Rows 2 and 4 depict distributions of differences of unique explained variance between phase and amplitude. Near each boxplot, the median difference is given with its 95% percentile bootstrap confidence interval.*

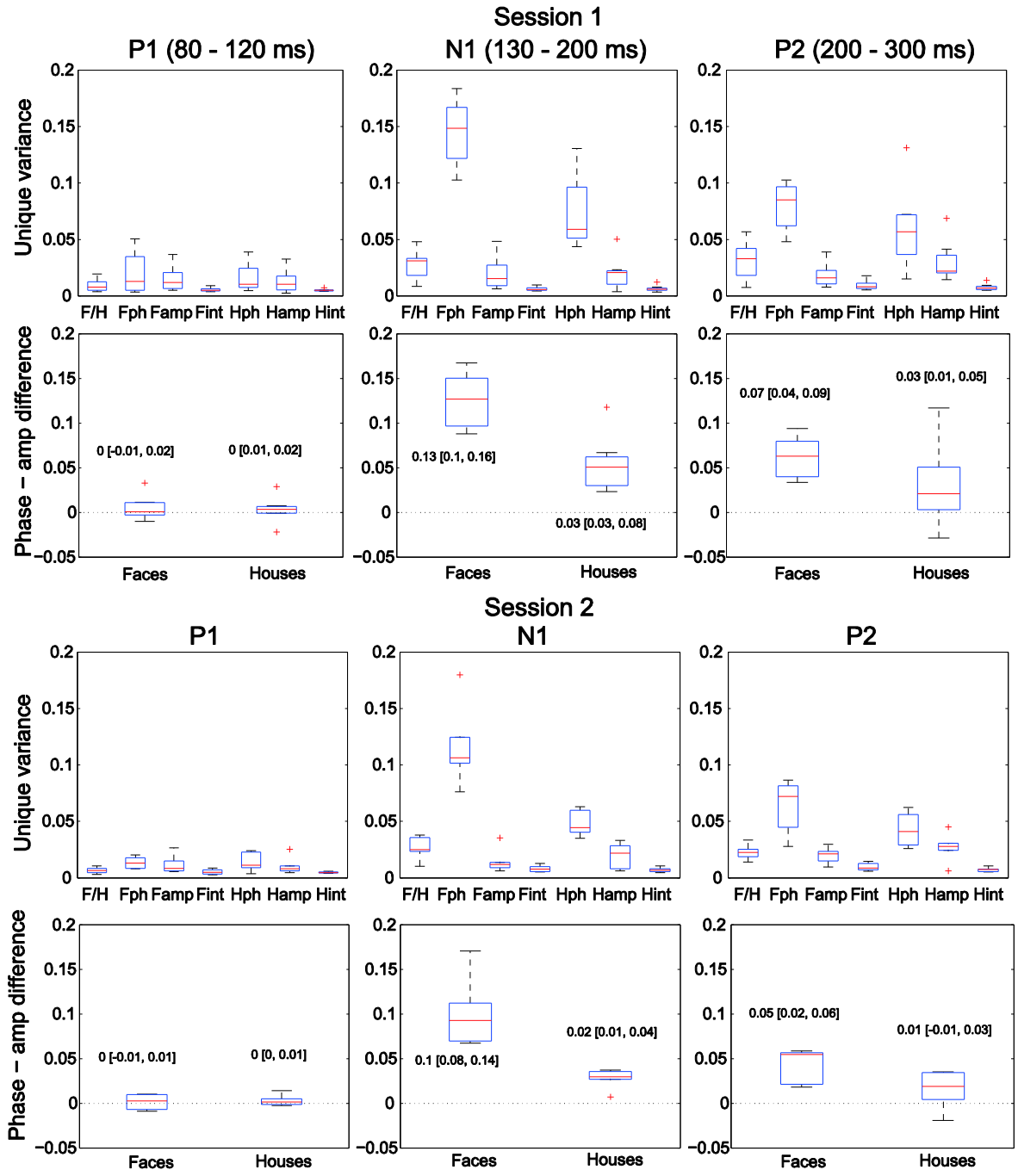

Figure 2.8. *Maximum unique explained variance across all electrodes (envelope). See Figure 2.7 caption for details.*

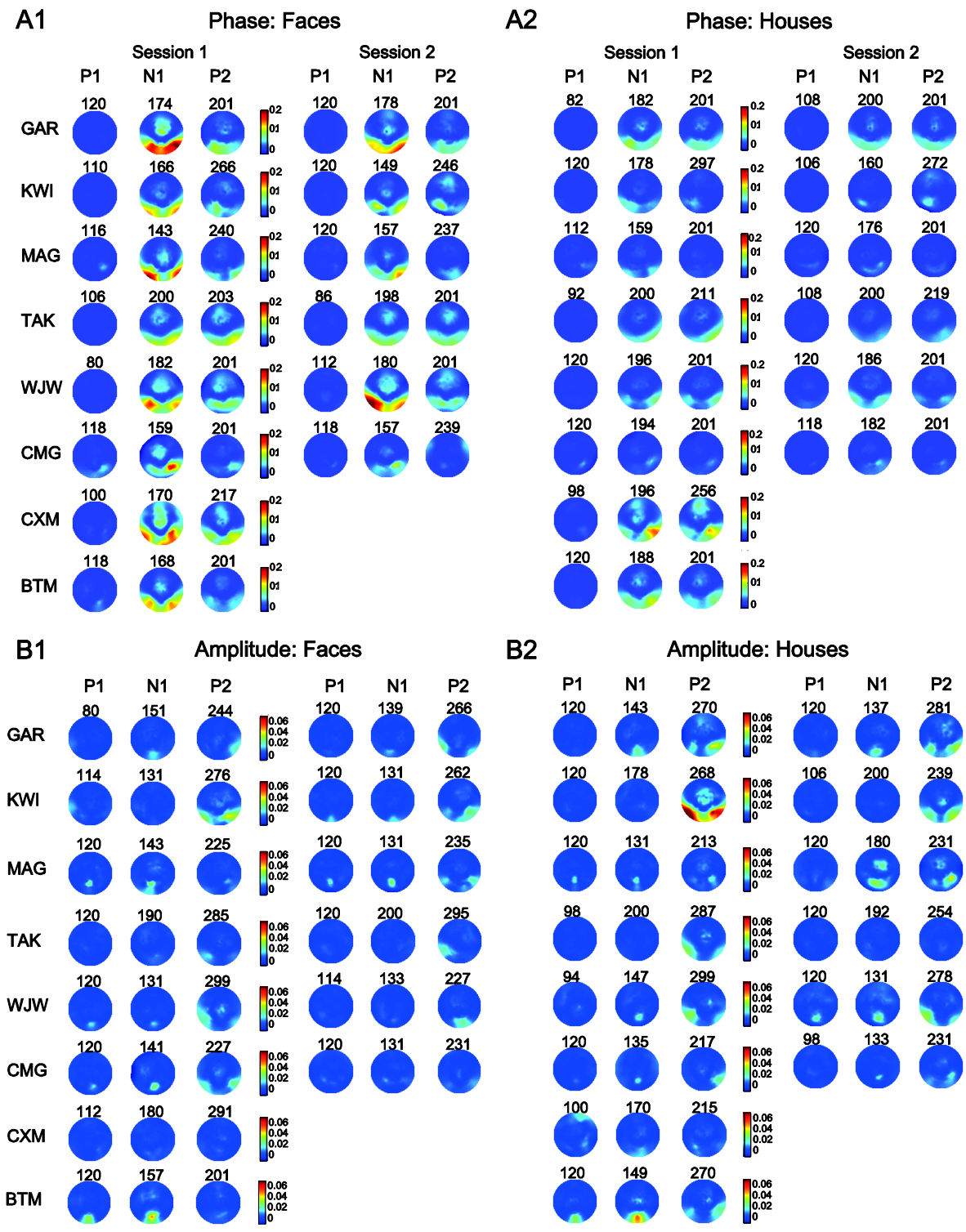

Figure 2.9. *Topographic maps of unique explained variance for each predictor: face phase (panel A1), house phase (A2), face amplitude (B1) and house amplitude (B2). Each row shows colour-coded maps for one subject at the time point of maximum unique variance in three time windows: 80-120 ms (P1), 130-200ms (N1) and 200-300 ms (P2). The time point (ms) at which each map is plotted is shown above the map. Different scales for phase and amplitude were used, because the amount of unique explained variance for amplitude was small compared to phase.*

PHASE AND AMPLITUDE INTERACTIONS WITH IMAGE CATEGORY

Results of the second model analysis revealed that only phase, but not amplitude, interacted significantly with image category (Figure 2.10; Appendix A – Supplementary Table 4; Supplementary Figures 13 & 14) indicating that categorical differences are modulated by phase, but not by amplitude. This effect was significant in all participants and sessions, and had a lateral-occipital scalp distribution in both sessions (Figure 2.11). Despite the presence of main amplitude effects in all subjects (apart from TAK, session 2), the category x amplitude interaction was not significant in any of the 8 subjects in session 1 and in 7 out of 8 subjects in session 2. Subject TAK, who did not show any main amplitude effect, showed sensitivity to category x amplitude interaction in session 2 at left frontal electrodes.

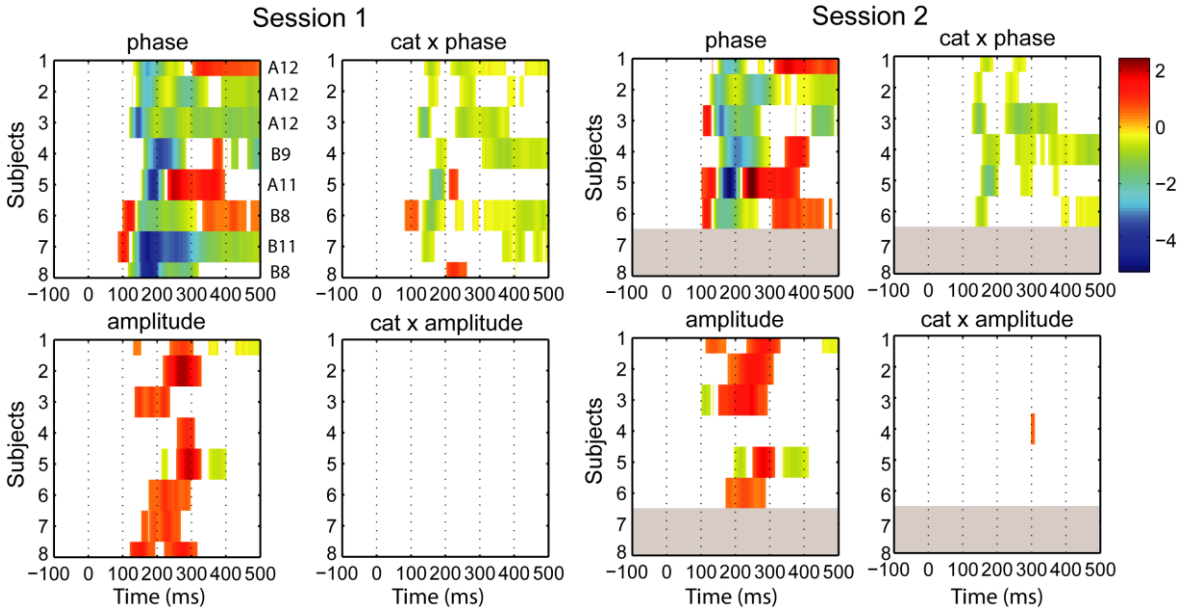

Figure 2.10. *Time-courses of beta coefficients associated with each predictor of the second regression (categorical interaction) model ("cat" states for image category). The betas are from the max R^2 electrode from each subject (provided on the right hand side of the top left plot). Rows shaded in grey indicate missing subjects in Session 2.*

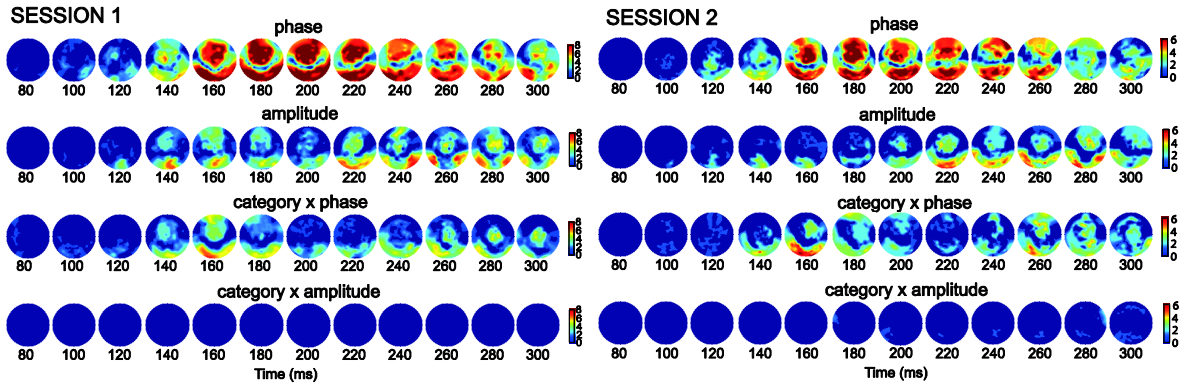

Figure 2.11. *Topographic maps of the frequency of effects from the second regression model. Maps are colour-coded according to the number of subjects showing the effects at a given electrode, from 0 subjects (dark blue) to the maximum number of subjects for that session (dark red). Each row shows one effect between 80 and 300 ms post stimulus.*

In sum, the results show that phase information is the major contributor to the early categorical ERPs observed at lateral-occipital electrodes. As the amount of phase information in the image increases, this image is perceived more as a face or a house and the corresponding N1 becomes more negative. In contrast, amplitude spectrum sensitivity is mostly observed at medial-occipital electrodes in the P1-N1 window and as amplitude information becomes more face-like, the corresponding ERPs become increasingly positive. Furthermore, phase spectrum explains significantly more unique ERP variance in the N1 and P2 time windows than amplitude and only phase interacts significantly with image category.

2.3 DISCUSSION

Overall, the results suggest that early ERPs to faces and objects are mostly modulated by the phase spectrum, not by the amplitude spectrum. First, in contrast to phase effects, amplitude effects were very weak, inconsistent across sessions and across subjects. Second, amplitude sensitivity before 200 ms post-stimulus occurred at medial-occipital electrodes, rather than at the lateral-occipital electrodes that showed the strongest phase effects and categorical ERP differences. Third, as expected, the early ERPs over lateral-occipital sites were becoming increasingly negative as phase coherence of images increased from 0% (noise) to 70%. In contrast, Fourier amplitude modulated ERPs in the opposite direction: ERPs became increasingly positive as images contained increasing amount of face Fourier amplitude. Fourth, the amplitude spectrum accounted for little unique ERP variance compared to phase. Finally, only phase but not amplitude interacted with categorical differences. Overall, these results suggest that the phase spectrum is the

main contributor to early categorical ERP differences, whereas amplitude's contribution is much weaker and present mostly beyond 200 ms post-stimulus. This conclusion seems to be a fair interpretation of my results, and could well apply to a larger range of stimuli. However, because I used a simplified set of cropped faces and houses, future studies will have to investigate if the present results hold for more realistic stimuli too. At least, the present study provides a systematic approach to tackle this sort of empirical problems.

My findings question the claims of Rossion & Caharel (2011) and Andrews, et al. (2010) that the amplitude spectrum can be responsible for visual categorical differences similar to those observed with intact images. It seems likely that the effects observed in Rossion & Caharel (2011) were not due to amplitude spectrum differences, but instead due to differences in color between their two image categories. In keeping with this idea, it has been shown that the presence of color that is diagnostic for a given category (e.g. green for forest) can speed up early categorization processes reflected in ERPs (Goffaux, Jacques, Mouraux, Oliva, Schyns, & Rossion, 2005).

An alternative, simpler explanation might also account for the results of the fMRI study by Andrews, et al. (2010). In that study, they found BOLD differences between phase scrambled images of faces and houses. Instead of being driven by amplitude spectrum differences, their BOLD differences could have been due to differences in image orientation. Indeed, in their study, intact and scrambled images were both vertical for faces and horizontal for places. Image orientation could have created expectations sufficient to influence BOLD responses in FFA and PPA, as suggested by recent studies that have shown that expecting a face can boost neural responses to noise stimuli in the lateral-occipital-temporal cortex (Smith, Gosselin, & Schyns, 2012; Hansen, Farivar, Thompson, & Hess, 2008).

Additionally, Rossion & Caharel (2011) and Andrews, et al. (2010) failed to include important control conditions, making it even more difficult to validate their claims. In the present study, I attempted to overcome the above shortcomings by either adding control conditions or using a parametric experimental design that provides a more sensitive way of capturing ERP variability associated with changes in physical image properties. Using a general linear model approach, I was able to show that despite the presence of main amplitude effects in almost all subjects, these effects could be dissociated from phase effects: they differed in timing, strength, scalp distribution, reliability, and they did not interact with image category. My results converge with the explanation proposed by

Clarke, et al. (2012), who suggested that cortical sensitivity to amplitude spectrum arises not because amplitude carries information about image category but because the visual system detects and responds to changes in spatial frequency content of the visual input, regardless of its category. In keeping with this idea, a recent study by Hansen, Johnson and Ellemberg (2012) shows relatively strong modulations of early ERPs by the spatial frequency content of pictures of natural scenes. This implies that the mere presence of ERP differences between images with different amplitude spectra is not sufficient to conclude that image categorisation can be achieved by relying purely on the amplitude spectrum (Rousselet, Pernet, Caldara, & Schyns, 2011b; VanRullen, 2011). Moreover, VanRullen & Thorpe (2001) have demonstrated that even though ERPs at about 100 ms post-stimulus can differentiate between visually distinct image categories, only later neural activity, beyond 150 ms, correlates with subjects' decision (see also: Philiastides & Sajda, 2006; Philiastides, Ratcliff, & Sajda, 2006).

Instead of explicit categorical processing, the early (<200 ms) main amplitude effects could reflect the visual system's sensitivity to distributions of local contrast energy. ERP sensitivity to contrast statistics of images of natural textures has been reported recently: it reached a maximum at the medial occipital electrode Oz in the time-window 100-200 ms (Groen, Ghebreab, Lamme, & Scholte , 2012a; Groen, Ghebreab, Lamme, & Scholte, 2012b; Hansen, Johnson, & Ellemberg, 2012). This scalp distribution and timing fits very well with the amplitude effects found in the present study.

Finally, I would like to stress that my results should not be used to justify not controlling low-level stimulus parameters. To the contrary, tight control over physical properties of visual stimuli is absolutely crucial to study higher-level object categorisation (Rousselet & Pernet, 2011). As it was already mentioned, the present results might be limited to the simplified cropped faces and houses that were used as stimuli. Further, task constraints were not manipulated; therefore a contribution of amplitude spectrum information in different tasks cannot be ruled out (Rousselet, Pernet, Caldara, & Schyns, 2011). Also, the amplitude spectrum did have an effect at some electrodes and in some subjects: in different experimental contexts, these ERP differences could be misinterpreted as high-level categorical responses. Thus, careful control over image properties is necessary to systematically study object categorisation.

3 ERP AGING EFFECTS – OPTICAL FACTORS AND INDIVIDUAL DIFFERENCES

This section, and the next, focus on the effects of aging on ERP visual processing speed and the contribution of optical factors (retinal illuminance and pupil size) to individual variability in the age-related ERP delays. This section presents an ERP experiment in which subjects age 18-79 had their retinal illuminance manipulated using neutral density filters that alter the stimulus' luminance.

The first goal of this study was to replicate the previous finding of Rousselet, et al. (2010) that aging slows down visual processing at the rate of 1ms/year, which was successfully achieved. Further, it was aimed to determine whether retinal illuminance modulates age-related delays in ERP measures of processing speed. The hypothesis was that if ERP aging delays depend on senile miosis and retinal illuminance, there should be no difference in processing speed if differences in retinal illuminance are abolished. However, it was found that age-related changes in processing speed are not due to senile miosis, as they were independent of luminance. Another aim was to answer whether individual differences in visual processing speed can be accounted for by variability in retinal illuminance, which they could not. The results strongly suggest that age-related face ERP delays are not due to optical factors.

3.1 METHODS

3.1.1 SUBJECTS

The study involved 59 subjects (31 females, 28 males, age range of 18-79, Table 3.1). To assess the test-retest reliability of the results and to control for luminance manipulation order, all but eight subjects took part in a second experimental session. Prior to the experiment, all subjects read a study information sheet and signed an informed consent form. The experiment was approved by the School of Psychology Ethics Committee (approval no. FIMS00740). Persons who reported any eye condition (i.e. lazy eye, glaucoma, macular degeneration, cataract), had a history of mental illness, were taking

psychotropic medications (e.g. antidepressants, beta-blockers) at the moment of testing or use to take them, suffered from any neurological condition (i.e. Parkinson's, Alzheimer's, dementia), had diabetes, had suffered a stroke or a serious head or eye injury and who had their vision tested more than two years ago (for people under 60 year old) or more than one year ago (for people aged 60 and above) were excluded from taking part in the experiment. Subjects' visual acuity and contrast sensitivity were assessed in the lab on the day of the first session using a Colenbrander mixed contrast card set and a Pelli-Robson contrast sensitivity chart. All subjects had normal or corrected-to-normal vision (Table 3.1) and contrast sensitivity in the range of 1.95 and above (normal score). One older subject reported the start of a monocular cataract that did not require medical treatment at the moment of testing. All subjects filled in a general health and life style questionnaire. All reported very good or excellent hearing and most reported at least weekly exercise. All subjects in the older group (>60) were in good cognitive health as indicated by their scores (>26 out of 30) at the MOCA test during the first experimental session. Subjects were compensated £6/hour for their participation.

Age bracket	**Age (median [min, max])**	**Number of subjects (females, males)**	**Visual acuity**		**MOCA Scores (median, [min, max])**	**Years of education (median, [min, max])**
			High contrast 63 cm (median [min, max])	**Low contrast 63 cm (median [min, max])**		
18-19	19 [18, 19]	5 (4,1)	105 [100, 110]	95 [90, 100]	n/a	15 [15, 16]
20-29	22 [21, 29]	12 (6,6)	105 [95, 108]	94.5 [90, 102]	n/a	18 [17, 25]
30-39	32 [30, 38]	9 (2,7)	107 [99, 109]	97 [90, 102]	n/a	18 [14, 23]
40-49	43.5 [41, 49]	8 (4,4)	106 [95, 112]	98.5 [88, 103]	n/a	18 [12, 23]
50-59	54 [50, 59]	6 (2,4)	105 [95, 105]	94 [90, 95]	n/a	17 [13, 19]
60-69	64.5 [60, 67]	10 (7,3)	94 [80, 106]	85.5 [75, 95]	29 [27, 30]	15.5 [5, 21.5]
70-79	72 [70, 79]	9 (6,3)	98 [78, 105]	88 [63, 94]	28 [26, 30]	14 [11, 21]

Table 3.1. *Subjects' information.*

3.1.2 STIMULI

The stimuli were pictures of faces and textures (Figure 3.1A). There were 10 identities of faces (Rousselet, Pernet, Bennett, & Sekuler, 2008). Faces were grey-scaled front view photographs oval-cropped to remove hair and pasted on a uniform grey background. A unique image was presented on each trial by introducing noise into the face images. Faces had 70% phase coherence (see details in Rousselet, Pernet, Bennett, & Sekuler, 2008). Textures had random phase (0% phase coherence). All stimuli had an amplitude spectrum set to the mean amplitude of all faces. All stimuli also had the same mean pixel intensity, RMS contrast = 0.1, and occupied 9˚ x 9˚ of visual angle.

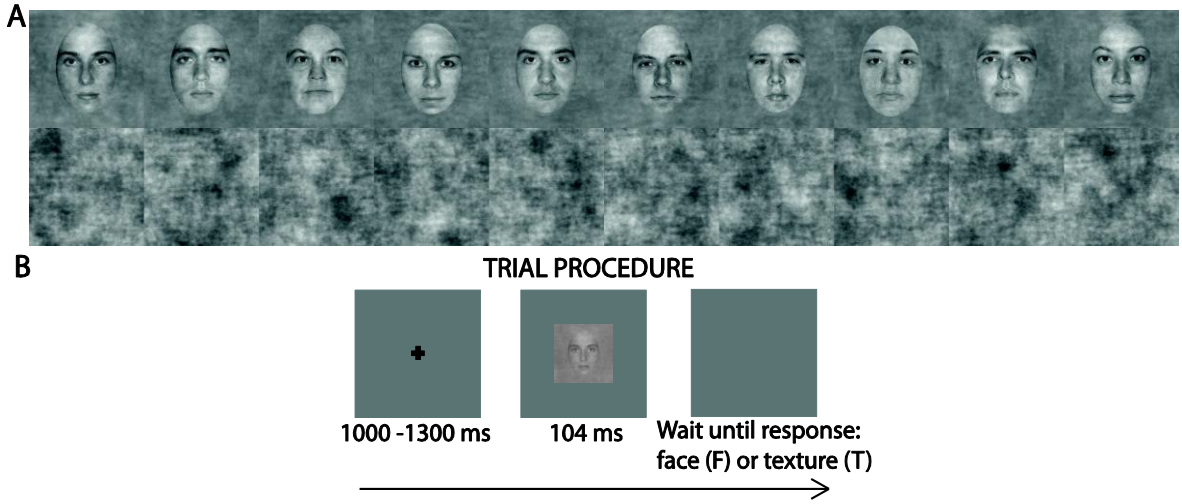

Figure 3.1. (A) *10 face identities at 70% phase coherence and 10 examples noise textures used in the luminance experiment.* ***(B)*** Single trial procedure. For presentation purposes the fixation cross and the face image are not to scale.

3.1.3 EXPERIMENTAL PROCEDURE AND DESIGN

Most subjects participated in two experimental sessions. The screen luminance progressively decreased in bright to dark (b2d) sessions, and increased in dark to bright (d2b) sessions. The order of the sessions was randomly assigned on the first day of testing. We altered screen luminance by placing neutral density filters in front of the computer screen. The filters were attached to thin wooden frames, which were pierced at the top, so that they could hang from pegs attached to the wall above the screen. The filters covered the screen completely. Each filter had 0.3 optical density (f-stop reduction = 2). This is equivalent to a 50% reduction in optical power transmitted through the filter. In other words, adding one filter in front of the screen reduced the screen's luminance by 50%, adding another filter reduced it by another 50% and so on.

The luminance levels from the brightest to the darkest were: 60.8, 31, 16, 8.16, 4.19, 2.17, 1.12, and 0.59 cd/m^2. Both sessions commenced with the highest luminance block (60.8 cd/m^2). In the b2d session, starting from block 2, the luminance was progressively reduced by adding one filter in each block to reach seven filters in block 8 (0.59 cd/m^2). In the d2b session, in block 2 we used the maximum number of filters, seven. Then in each block we removed one filter, to reach one filter in block 8. Block 9 in each session was again conducted without any filters, as in block one (60.8 cd/m^2). The luminance of the screen with and without filters was measured using a Minolta CS-100 colorimeter. The measurements were done at the center of the monitor about one hour after switching it on and before running each participant.

During the experiment, subjects sat in a sound attenuated booth and rested their head on a chin rest. Stimuli were displayed on a Samsung SyncMaster 1100Mb monitor (600 x 800 pixels, height and width: 30 x 40 cm, 21˚ x 27˚ of visual angle; refresh rate – 85 Hz, bits per pixel – 32). Viewing distance measured from the chin rest to the monitor screen was 80 cm. Subjects were given experimental instructions including a request to minimise blinking and movement. Subjects were asked to categorise images of faces and textures by pressing '1' for face and '2' for texture, on the numerical pad of a keyboard, using the index and middle fingers of their dominant hand. Before the main experiment, subjects performed a 40 trial practice block containing 20 trials with auditory feedback, followed by another 20 trials without feedback. After the practice block, the dim lights in the booth were switched off and an adaptation screen with grey uniform background (RGB 128,128,128) was turned on. A 60 sec light adaptation was performed at the beginning of all blocks, except in block 2 of d2b sessions, in which the adaptation lasted for 5 min. This longer duration was necessary due to the large luminance difference between zero and seven filters. After the adaptation and before each experimental block, pupil size in participant's right eye was measured three consecutive times (the mean of these three measurements was later used for the analyses). For the first 22 subjects we used a Colvard (Oasis Mediacla Inc.) pupillometer; for the remaining subjects we used a NeurOptics VIP™-200 pupillometer. When pupil measurement was completed, subjects were ready to proceed with the experiment.

The experiment had a mixed design with image category and luminance as within-subject factors and age as between-subject factor. There were 9 experimental blocks, each consisting of 150 trials: 70 faces (10 face identities, each repeated 7 times, each time with a unique noise field) and 70 unique noise textures. Additionally, there were 10 practice trials

(5 faces and 5 textures) at the beginning of each block with auditory feedback signalling to subjects whether their response was correct or not. The whole experiment consisted of 1350 trials, including 90 practice trials. Each trial began with a small fixation cross (size: 12 x 12 pixels; 0.4º x 0.4º of visual angle) displayed at the centre of the monitor screen for a random time interval of about 1000 – 1300 ms, followed by an image of a face or a texture presented for about 9 frames (~104 ms) (Figure 3.1B). These durations are multiples of refresh screen durations and do not necessarily reflect the actual duration during which image pixels were active (Elze, 2010). After the stimulus, a blank screen was displayed until subject's response. The fixation cross, the stimulus and the blank response screen were all displayed on a grey uniform background (RGB 128, 128, 128). The importance of accuracy over speed was stressed to subjects. Subjects performed the task very well: in all the luminance levels, most subjects had accuracy above 95% and all exceeded 90%. One experimental block lasted for approximately 4 minutes and the whole experiment (with breaks but excluding electrode application) lasted for about 1 hour 30 min.

3.1.4 EEG RECORDING

EEG data were recorded at 512 Hz using an Active Electrode Amplifier System (BIOSEMI) with 128 electrodes mounted on an elastic cap. Four additional electrodes were placed at the outer canthi and below the eyes.

3.1.5 EEG DATA PRE-PROCESSING

EEG data were pre-processed using Matlab 2011a and the open-source toolbox EEGLAB 11.0.2.1b (Delorme & Makeig, EEGLAB: an open source toolbox for analysis of single-trial EEG dynamics including independent component analysis, 2004). Data were first re-referenced off-line to an average reference and an individual channel mean was removed from each channel. Data were then band-pass filtered between 0.3 Hz and 40 Hz using a non-causal two-way least square FIR filter (pop_eegfilt function in EEGLAB). Non-causal filtering can potentially distort onsets (Acunzo, MacKenzieb, & van Rossum, 2012; VanRullen, 2011; Widman & Schroeger, 2012; Rousselet, 2012). Therefore, onsets of ERP differences were analysed by creating a second dataset in which data were pre-processed with 4th order Butterworth filters: high-pass causal filter at 2 Hz and low-pass non-causal filter at 40 Hz. Data from the two datasets were then epoched between -300 and 1200 ms around stimulus onset. Noisy electrodes were detected by visual inspection of the non-causal dataset and rejected on a subject-by-subject basis (the same electrodes were rejected in the two datasets). Baseline correction was performed using the average activity

between time 0 and -300 ms. The reduction of artifacts, such as eye-movements or blinks was performed using Independent Component Analysis (ICA), as implemented in the infomax algorithm from EEGLAB. If ICA yielded components representing noisy electrodes (e.g. IC with a very focal, non-dipole activity restricted to one electrode whereas the rest of the map was flat), the noisy channels were removed and the ICA was repeated. ICA was performed on the non-causal FIR-filtered datasets and the ICA weights were then applied to the causal Butterworth-filtered datasets (on a subject by subject basis) in order to ensure removal of the same components from both datasets. After rejection of artifactual components, data were re-epoched between -300 and 500 ms and baseline correction was performed again. Finally, artifactual data epochs were removed based on an absolute threshold value larger than 100 µV and the presence of a linear trend with an absolute slope larger than 75 µV per epoch and R2 larger than 0.3. The median number of trials accepted for analysis was 1313 out of 1350 [min: 1163, max: 1345] in bright to dark sessions and 1318 [min: 1166, max: 1344] in dark to bright sessions.

3.1.6 ERP STATISTICAL ANALYSES

Statistical analyses were conducted in single subjects and at the group level using Matlab 2011a and the LIMO EEG toolbox (Pernet, Chauveau, Gaspar, & Rousselet, 2011). To model EEG data we used a general linear model (GLM) across trials, at all time points and all electrodes. Multiple comparisons correction was performed using a bootstrap spatial-temporal clustering technique (Rousselet, Gaspar, Wieczorek, & Pernet, 2011; Pernet, et al., 2011; Bieniek, Pernet & Rousselet, 2012).

3.1.7 AGING EFFECTS ON VISUAL PROCESSING SPEED

SINGLE SUBJECT DATA ANALYSES

Several measures of visual processing speed we extracted based on the timing and the amplitude of the difference between face and texture ERPs. To that end, a general linear model (GLM) was used with faces and textures at each luminance level as categorical predictors. Subsequently, linear contrasts (t-tests) between beta coefficients for faces and textures for each luminance level were computed. This model was applied separately to the causal-filtered and non-causal filtered datasets of each subject. Thus, for each subject and for every electrode the time course of model fit and of t statistics associated with each linear contrast were obtained. Then, for each subject, the electrode with the highest squared t statistics in the block with the brightest luminance (60.8 cd/m^2) was determined. It is a data-driven approach that does not make assumptions about the

localisation of the effects, and allows us to identify the electrode with the maximum sensitivity to our experimental manipulation, independently in each subject. We refer to this electrode as the max t^2 electrode and report it according to the electrode numbering in Biosemi format (see Appendix A, Supplementary Figure 15 for the Biosemi electrode map with corresponding electrodes from the 10/10 system).

From the outputs of our single-subject GLMs, three estimates of processing speed were derived. The first measure was the onset of the earliest significant differences between face and texture ERPs at each luminance level. The onsets were obtained from the GLM applied to all the electrodes of the causal-filtered dataset of each subject. The second measure was the time it takes to integrate 50% of the cumulative t^2 function, which we refer to as the 50% integration time (50IT) (Rousselet, Gaspar, Pernet, Husk, Bennet, & Sekuler, 2010). This measure incorporates potential changes in the shape of the ERP difference waveform that may occur with age. The integration was done over time, from 0 to 500 ms, and across all electrodes. The last measure was the latency of the maximum ERP difference (peak latency) between faces and textures recorded at the max t^2 electrode for each subject. Although ERP latency is not a direct index of processing speed, it could reflect the accumulation of information in neuronal population that ceases when an ERP peaks (Schyns, Gosselin, & Smith, 2009). In that sense, it can potentially carry an indication of timing of neuronal processes. Both, 50IT and peak latency were obtained from the non-causal filtered data, for each luminance level and for each subject.

GROUP DATA ANALYSES

To visualise age-related changes in the shape of the t^2 functions (that reflects changes in the ERP difference waveform) the quantiles of the age distribution of my sample were calculated using the Harrell-Davis estimator, which is based on a weighted sum of sorted values (Wilcox, Introduction to Robust Estimation and Hypothesis Testing, 2005). The same weights were then applied to the t^2 functions for each luminance level individually (Rousselet, et al. 2010).

To calculate descriptive statistics (median 50ITs with 95% confidence intervals (CI, reported in square brackets)) percentile bootstrap procedure was used with 1000 samples and with Harrel-Davis estimator of the median. Comparisons between 50IT for the 60.8 cd/m^2 luminance condition and all the other luminance conditions were done using a two-tailed percentile bootstrap test for dependent groups; comparisons between young 50ITs in each pinhole condition and the 50ITs of old adults obtained in the luminance

experiment (in 60.8 cd/m^2 condition) were done using two-tailed percentile bootstrap test for independent groups.

To determine if pupil size, retinal illuminance, the measures of processing speed (50IT, onsets, peak latencies) and peak amplitudes of ERP differences varied with age, group level regressions for each luminance level were computed using Matlab's *robustfit* function, with the default parameters. Then, percentile bootstrap confidence intervals around the slopes and intercepts were calculated in the following way. First, subjects were sampled with replacement, keeping their corresponding age, 50ITs, onsets, peak latencies and amplitudes of ERP differences. Second, regressions between each measure of processing speed and age, at each luminance level were performed. These two steps were performed 1000 times, and each time all the slopes and intercepts were saved. Then, the bootstrapped slopes and intercepts were sorted, and the 2.5 and 97.5 percentiles were used to form the boundaries of 95% bootstrap confidence intervals. To calculate whether the regression slopes and intercepts for the brightest condition differed from the other luminance conditions, the bootstrapped slopes and intercepts of pairs of conditions were subtracted to derive 95% bootstrap confidence intervals of the differences.

The next aim was to find out if, after accounting for age, we could explain individual variability in 50ITs and peak latencies of ERP differences by the variability in subjects' pupil sizes. To address that question the 50IT/age residuals and the peak latencies/age residuals were regressed against the pupil/age residuals. Again, the percentile bootstrap procedure was used to build confidence intervals of the slopes and intercepts.

Finally, the onset and the maximum latency of the aging effects were determined by calculating how much of the cumulative t^2 function of each subject has been integrated up to each time point between 0 and 500 ms. Then, at each time point, and for each luminance level separately, regressions between the integrated t^2 and age across subjects were calculated. To determine when the regression slopes became significantly different from zero a bootstrap procedure was used (see Rousselet, et al., (2010) for description).

3.1.8 LUMINANCE EFFECT ON FACE-TEXTURE ERP DIFFERENCES

SINGLE SUBJECT DATA ANALYSES

In the second part of the analyses, the time course of luminance effects on face and texture ERPs was quantified using a single-trial ANCOVA model. The model had two categorical predictors – faces and textures, one continuous predictor – luminance, and an

interaction term between luminance and category. Luminance was entered into the model as the z-score of the log luminance levels. This model was applied to causal and non-causal filtered datasets of individual subjects. From the analyses of the causal-filtered datasets we obtained onsets of luminance and luminance x category interactions. From the analyses of the non-causal filtered data the latency of the strongest luminance and interaction F values was obtained.

GROUP DATA ANALYSES

To determine if the ERP onsets and the latencies of maximum sensitivity to luminance and luminance x category change with age, regressions for the onsets and maximum latencies of each effect against age were performed. Then, the 95% bootstrap confidence intervals around the slopes and intercepts as well as around the difference between the slopes and intercepts of the two effects were calculated. Similar procedure as described in section 3.1.7 (group data analyses) was used.

3.1.9 OVERLAP BETWEEN THE ERPS OF YOUNG AND OLD OBSERVERS

In the third part of the analysis, it was determined if the ERPs of old observers in the brightest condition could be matched to that of young observers at lower luminance levels. To this end, the overlap between the t^2 functions of older (>60, n=18) observers in the brightest luminance condition and young observers (<30, n=15) at each luminance level was quantified. First, the t^2 functions were normalised within participant by dividing their t^2 functions by the maximum t^2 across all luminance levels and time points. Then, the t^2 functions were averaged across subjects, separately for young and old subjects. To calculate the percentage of t^2 overlap between young and old, the area under the mean t^2 functions for young and old observers was computed using trapezoidal numerical integration (*trapz* function in Matlab) and expressed as a proportion of the overall area under the two functions. The overlaps were calculated between the mean t^2 function of young subjects at each luminance level and the mean t^2 function of old subjects in the two conditions with the highest luminance (60.8 cd/m^2 - conditions 1 and 9).

The 95% confidence intervals around the overlaps as well as around mean t^2 functions of young and old adults were computed using a bootstrap procedure. First, separately for the young and old group, subjects were sampled with replacement. Subsequently, mean t^2 functions for young and old samples were computed and the overlap between the two functions for each luminance level was calculated. Also, within group overlap for old subjects was computed by sampling two different samples from the old

group and calculating the overlap between their means. This procedure was performed 1000 times, each time saving the mean t^2 functions for young and old groups in each condition, the overlaps and the difference in overlaps between the two brightest conditions (the first and the last block). Then, each of the bootstrap estimates was sorted and used the 2.5 and 97.5 percentiles to form the boundaries of 95% bootstrap confidence intervals.

3.2 RESULTS

The first goal of this study was to replicate the ERP aging effects reported in Rousselet, et al. (2010). Second goal was to determine if age-related delays in ERP measures of visual processing speed are luminance dependent. Third goal was to answer whether individual differences in processing speed can be explained by the variability in observers' retinal illuminance. The final aim was to determine if the ERPs of old observers can be matched to the ERPs of young observers tested at lower retinal illuminance levels.

First, the results replicated previous findings of Rousselet, et al. (2010): aging slows down visual processing, expressed in the 50IT, at the rate of 1 ms/year. This delay was observed in the present study at all luminance levels, which suggests that age effects are not luminance dependent. It was also found that aging prolongs peak latencies of the face-texture ERP differences at the average rate of 1.5 ms/year. However, no effects of age on the onset of ERP differences were observed. The early ERPs to faces and textures were delayed with decreasing luminance, an effect visible in individual subjects in both sessions (Figure 3.2). Finally, individual differences in visual processing speed could not be explained by inter-subject variability in retinal illuminance. Finally, the ERPs of old observers could not be matched to those of young adults at lower luminances. These findings suggest that the age-related slowdown in visual processing is not due to optical factors.

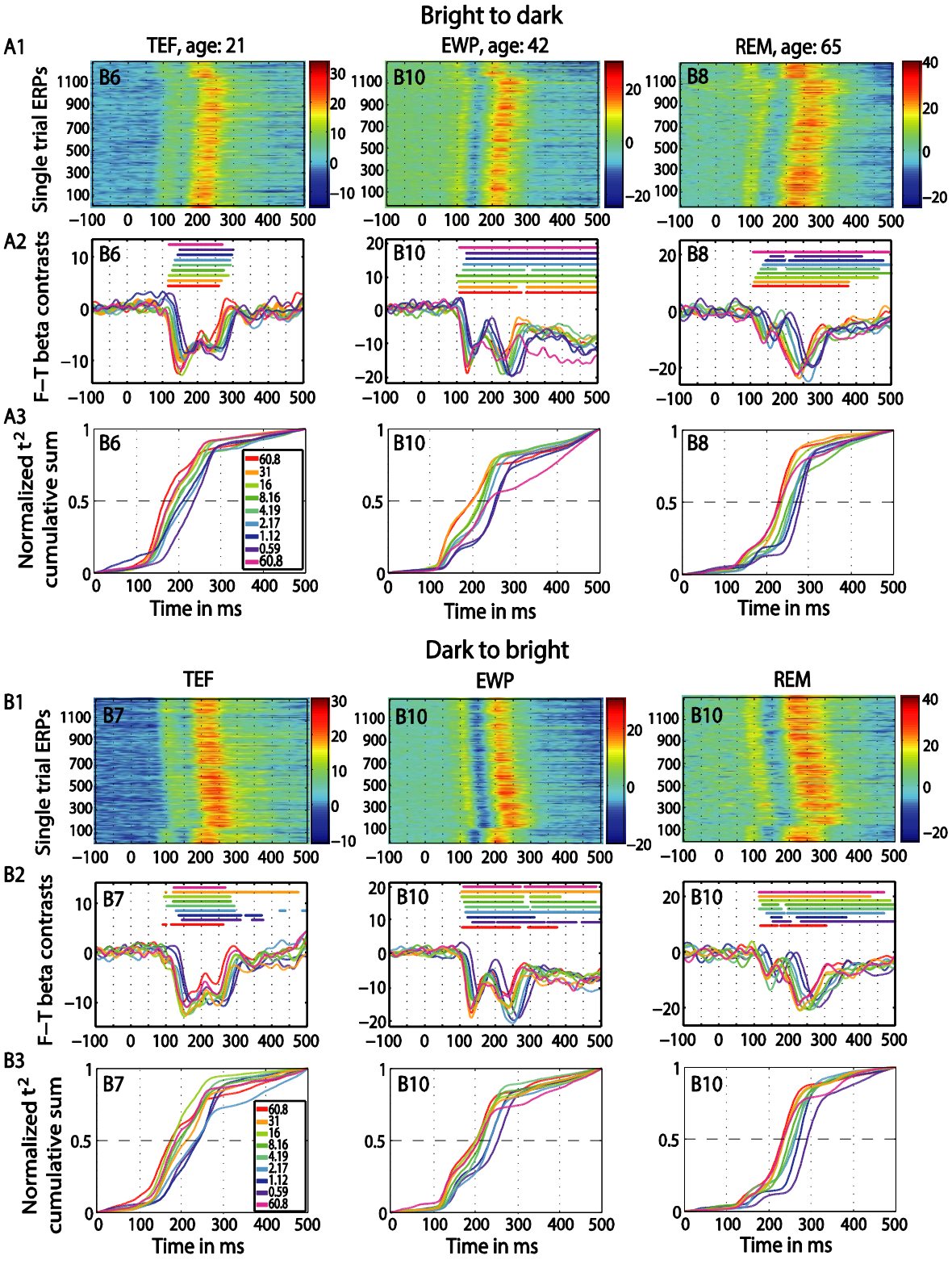

Figure 3.2. *ERP results in individual subjects. Data of three representative subjects: one young (TEF, age 21), one middle-age (EWP, age 42) and one old (REM, age 65) for b2d session (panel A) and d2b session (panel B) at the max t^2 electrode (indicated in the top left corner of plots A2 and B2). Electrode map is provided in the Supplementary Figure 4.* ***(A1 & B1)*** *Single trial ERPs, in μV.* ***(A2 & B2)*** *Time-courses of contrasts between face and texture beta-coefficients for each luminance level; horizontal lines indicate significant differences.* ***(A3 & B3)*** *Normalised t^2 cumulative sums at each luminance level.*

3.2.1 AGE EFFECTS ON 50% INTEGRATION TIMES, PEAK LATENCIES, ONSETS AND AMPLITUDES OF FACE-TEXTURE ERP DIFFERENCES

First, a qualitative age-related change in the overall shape of the t^2 functions for all luminance levels was observed (Appendix B – Supplementary Figure 1). This qualitative change was captured by the measure of processing speed (50IT), showing a significant age-related delay of ~1 ms/year (Figure 3.3 A, Appendix B – Supplementary Tables 1 & 2). This effect was present at all luminance levels, and in both experimental sessions. There was no significant difference between the 50IT/age regression slope at the brightest luminance level (60.8 cd/m^2) and all the other luminance conditions, suggesting that the 1 ms/year slope is similar across luminance levels (Appendix B – Supplementary Tables 1-4). The peak latencies of face-texture ERP differences were also delayed by age at all luminance levels and in both sessions, with an average slope of 1.5 ms/year (Figure 3.3 B, Appendix B – Supplementary Tables 1 & 2).

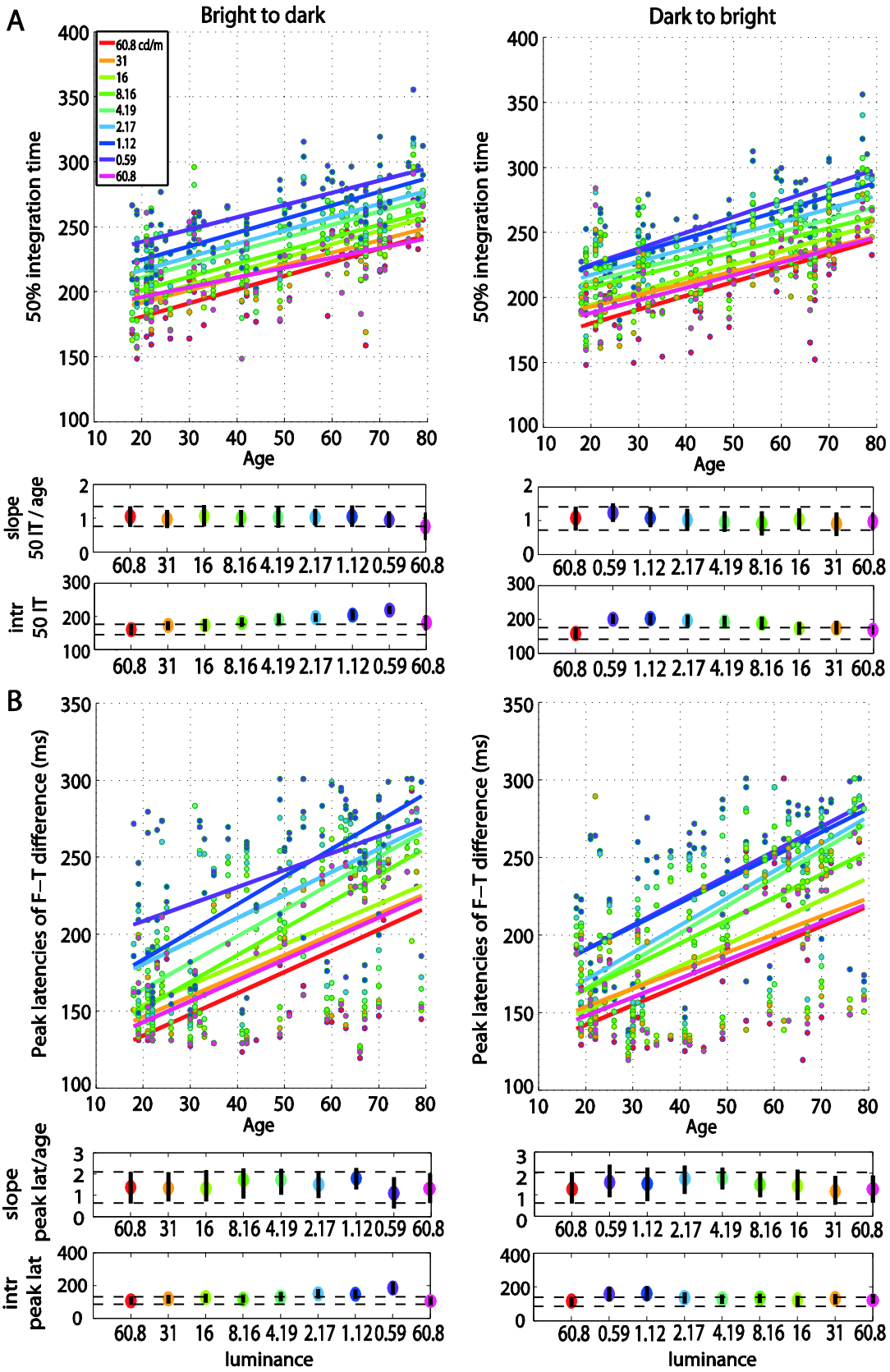

Figure 3.3. *Regressions of 50IT and peak latencies of face-texture ERP differences against age. Regression fits between* ***(A)*** *50IT and age and* ***(B)*** *latencies of maximum face-texture ERP differences and age, for all luminance levels. B2d sessions are shown in column 1, d2b sessions in column 2. The two horizontal plots below each regression plot contain slopes and intercepts (intr) as colored dots, with confidence intervals as vertical black lines. Horizontal dashed black lines show the boundaries of the confidence intervals of the slopes and intercepts in the first brightest condition (60.8 cd/m^2).*

The analyses revealed no age effect on the onsets of face-texture ERP differences, except for some small effects that were inconsistent across sessions, present at 0.59 cd/m^2 in the bright to dark session only, and at the 60.8, 1.12 and 2.17 cd/m^2 in the dark to bright session only (Figure 3.4 A, Appendix B – Supplementary Tables 1 & 2). There was also no aging effect on the amplitude of face-texture ERP differences at all luminance levels and in the two experimental sessions (Figure 3.4 B, Supplementary Tables 1 & 2).

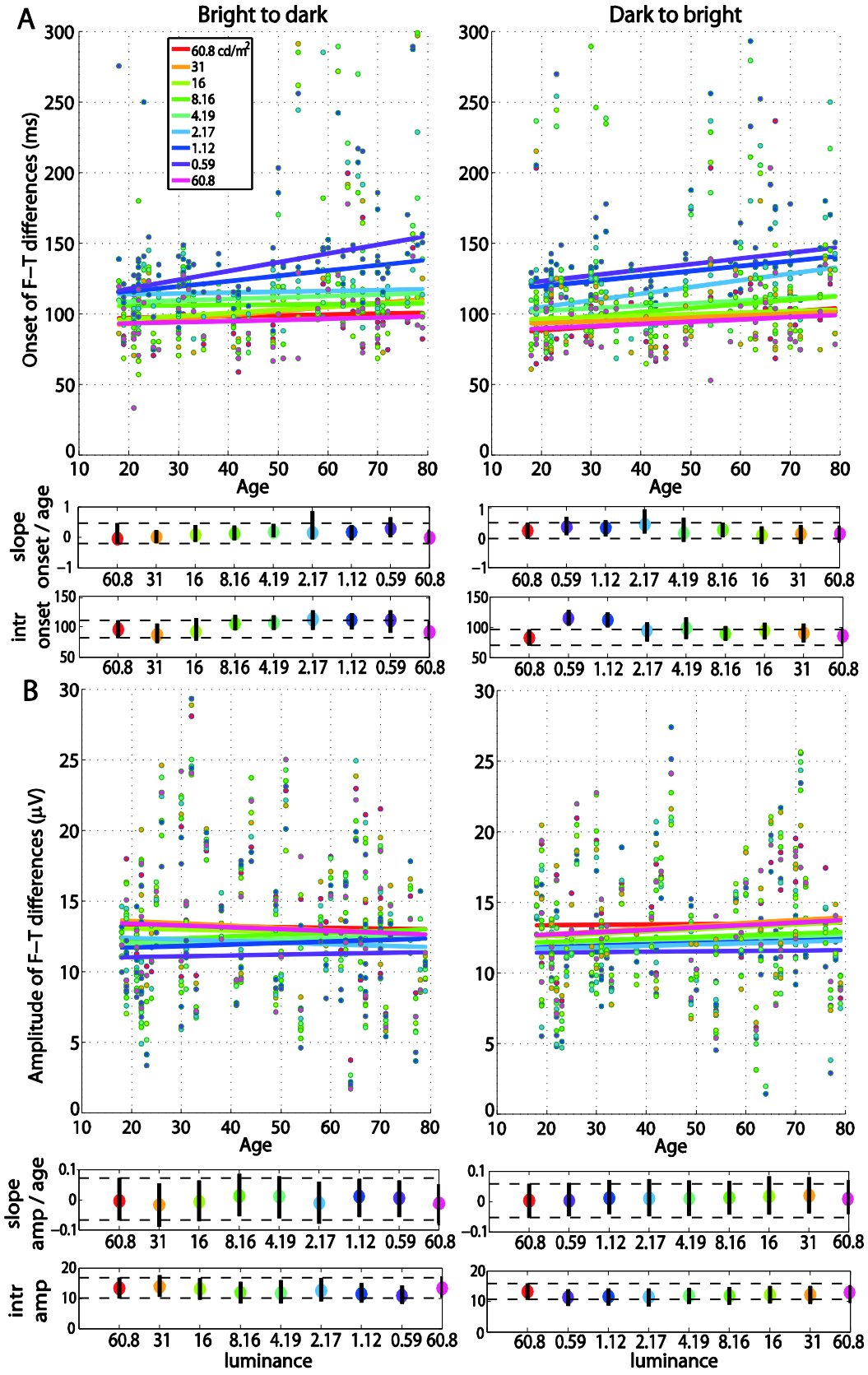

Figure 3.4. *Regressions of onset and amplitude ERP differences against age. (A) Regression fits between the onset of significant face-texture ERP differences and age and (B) between maximum amplitude of face-texture ERP differences and age, for all luminance levels. See Figure 4 caption for details.*

Finally, aging started to affect processing speed at 131 ms (b2d) and at 125 ms (d2b) post-stimulus at 60.8 cd/m^2, except in blocks 7 (8.16 cd/m^2) and 9 (60.8 cd/m^2) of the d2b session, where aging effects commenced already at 94 and 106 ms, respectively. Aging effects were the strongest around 201 ms (b2d) and 203 ms (d2b) at the highest luminance and were delayed up to ~260 ms at 0.59 cd/m^2. Reduced luminance also prolonged the onset of aging effects from ~125 ms at 60.8 cd/m^2 up to 162 ms at 0.59 cd/m^2 (Figure 3.5 A & B).

A

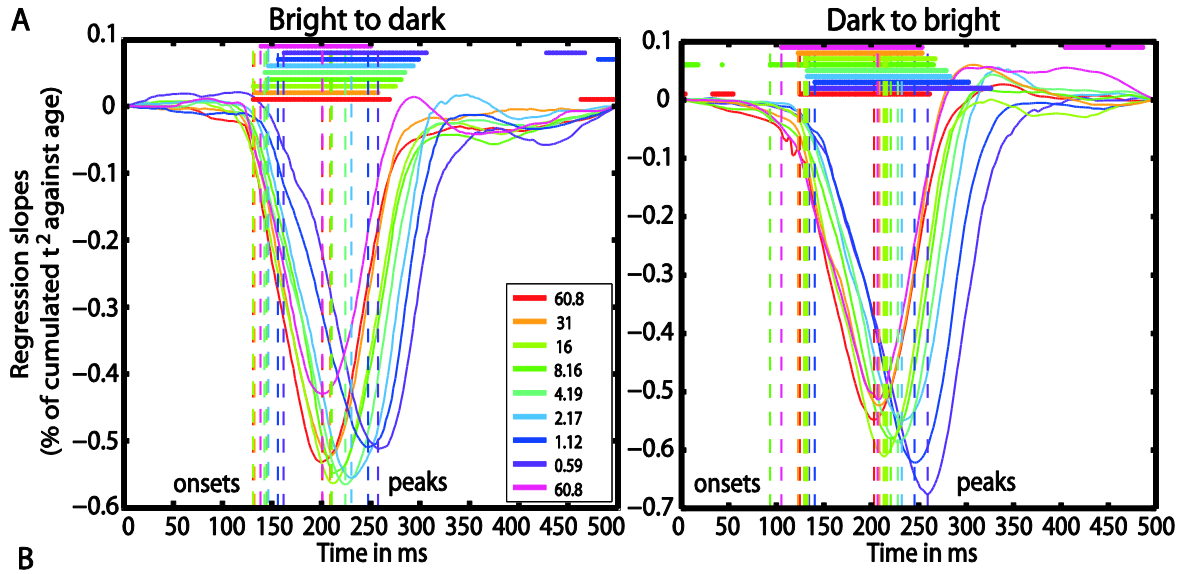

B

b2d	**Luminance**	**60.8**	**31**	**16**	**8.16**	**4.19**	**2.17**	**1.12**	**0.59**	**60.8**
	Onset	131	133	131	145	143	147	156	162	139
	Peak latency	201	209	211	211	225	231	248	259	201
d2b	**Luminance**	**60.8**	**0.59**	**1.12**	**2.17**	**4.19**	**8.16**	**16**	**31**	**60.8**
	Onset	125	135	141	133	133	94	131	123	106
	Peak latency	203	260	246	232	229	221	215	209	207

Figure 3.5. *(A) Time-courses of % of cumulated t2/age regression slopes. Each curve shows the time-course at one luminance level. Horizontal lines indicate significant regression slopes. Vertical dashed lines mark the onsets and the peak latencies of significant aging effects.* ***(B)*** *Table of onsets (ms) and peak latencies (ms) of the aging effects on the processing speed for all luminance levels (cd/m^2) for b2d and d2b experimental sessions.*

3.2.2 AGE EFFECTS ON PUPIL SIZE AND RETINAL ILLUMINANCE

The regressions between pupil size and age revealed senile miosis - a significant reduction of pupil size with age that was present at all luminance levels in both sessions (Figure 3.6 A). The slope of the pupil/age regression was in the range of -0.03 mm (60.8 cd/m^2) to -0.05 mm (0.59 cd/m^2) per year (Appendix B – Supplementary Tables 1 & 2). This is equivalent to about 0.6 – 1 mm decrease in pupil size every 20 years – from ~5 mm at 20 years old to ~3.5 mm at 80 years old at 60.8 cd/m^2 and from ~7 mm to 20 years old to ~4.5 mm at 80 years old at 0.59 cd/m^2. The pupil/age regression slope at the brightest

luminance did not differ from the slopes at the lower luminance levels (Appendix B – Supplementary Tables 1& 2). The intercepts of the pupil/age regressions differed between the brightest luminance and all the other conditions and increased from 5 mm at 60.8 cd/m^2 to 7 mm at 0.59 cd/m^2.

As expected, retinal illuminance decreased with increasing age (Figure 3.6 B) and both the slope and the intercept of the retinal illuminance/age regression differed significantly between 60.8 cd/m^2 and all the other luminance conditions (Appendix B – Supplementary Tables 1 & 2). The slope ranged from about -12 at 60.8 cd/m^2 to -0.2 at 0.59 cd/m^2 in both sessions. The intercept was 1400 Td at 60.8 cd/m^2 and dropped to 24 Td at 0.59 cd/m^2.

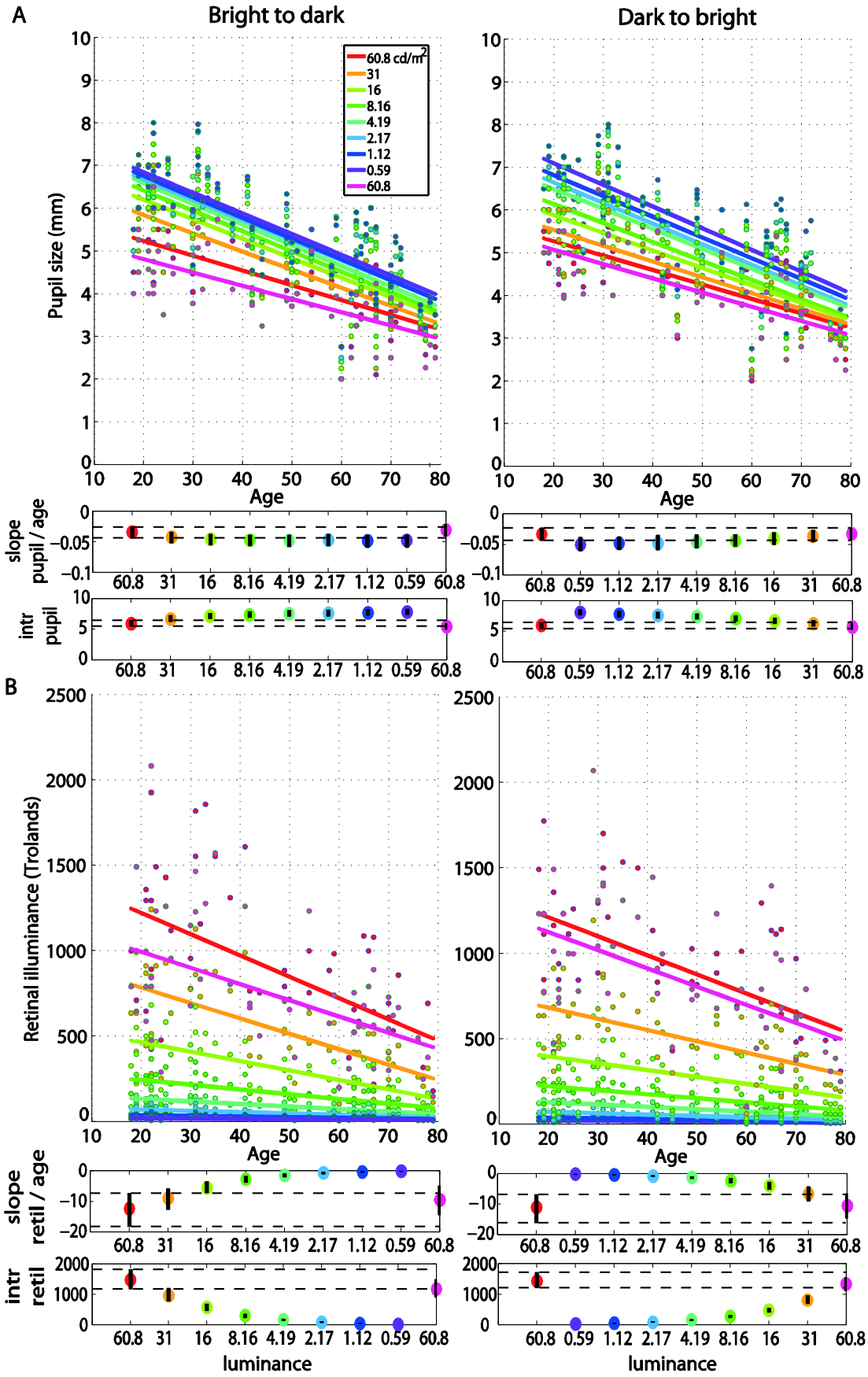

Figure 3.6. *Regressions of pupil size and retinal illuminance against age.* ***(A)*** *Regression fits between pupil size and age and* ***(B)*** *between retinal illuminance and age, for all luminance levels. See Figure 3.4 caption for details.*

After partialling out the effect of age from 50IT, from peak latencies of face-texture ERP differences and from pupil size, individual differences in 50IT (Figure 3.7 A) and in peak latencies (Figure 3.7 B) could not be accounted for by variability in pupil size across subjects (Appendix B – Supplementary Table 5). Regression slopes between 50IT/age residuals and pupil size/age residuals were not significant at any luminance level.

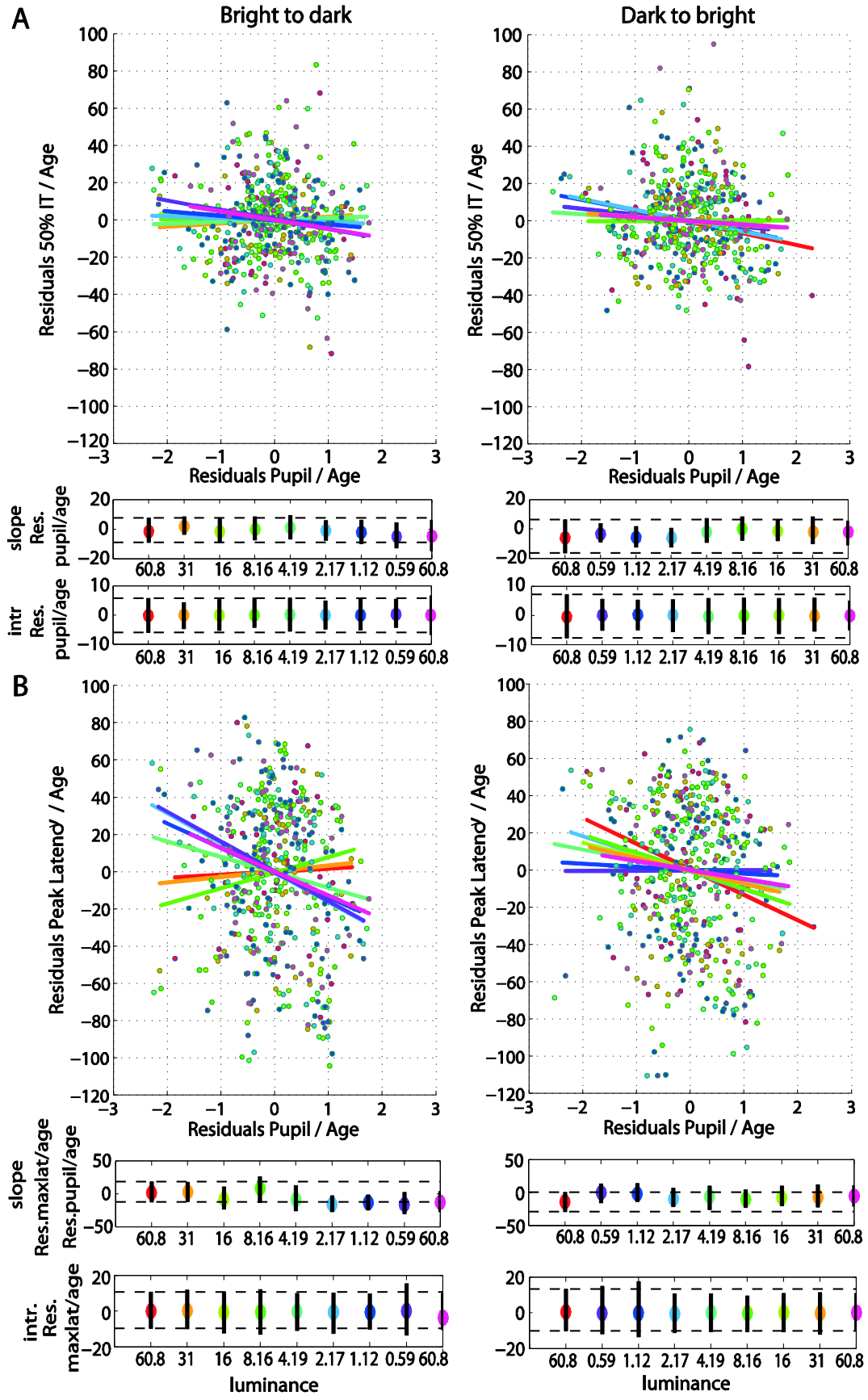

Figure 3.7. (A) *Regressions of residuals of 50IT/age against residuals of pupil size/age for all luminance levels.* ***(B)*** *Regressions of residuals of peak latency of face-texture ERP differences/age against residuals of pupil size/age for all luminance levels. See Figure 3.4 caption for details.*

3.2.3 AGE EFFECTS ON ERP SENSITIVITY TO LUMINANCE AND CATEGORY X LUMINANCE INTERACTION

The onsets of ERP sensitivity to luminance and to category x luminance interaction did not change with age (Figure 3.8 A) and the age regression slopes for the two effects did not differ (b2d: diff = -0.19 [-0.51, 0.10]; d2b: diff = -0.13 [-0.42, 0.15]). Luminance started to affect the ERPs at about 66 ms [60, 72] in the b2d session and 60 ms [52, 71] in d2b session (Figure 3.8 A). This is about 20 ms before (b2d: diff = -20 ms [-36 -3]; d2b: diff = -19 ms [-34, -4]) luminance began to interact with stimulus category at 86 ms [68, 103] (b2d) or 80 ms [66, 97] (d2b) (Figure 3.8 A & B). The ERP sensitivity to luminance was the strongest around 152 ms in b2d session and 129 ms in d2b session, whereas the category x luminance interactions peaked at about 118 ms (b2d) and 104 ms (d2b) post-stimulus (Figure 3.8 B & C). However, the latencies of the two effects did not differ significantly (differences between regression intercepts, b2d: diff = 34 [-9, 84]; d2b: diff = 25 [-32, 91]). There was also no age effect on the timing of maximum sensitivity to luminance in any of the sessions (Figure 3.8 C). However, aging delayed the latency of maximum interaction between stimulus category and luminance at the rate of 1.03 ms [0.05, 1.93] per year in b2d and 1.69 ms [0.79, 2.59] per year in d2b. The difference between the regression slopes of luminance and category x luminance effects was not significant (b2d: diff = -0.64 [-1.83, 0.69]; d2b: diff = -0.89 [-2.17, 0.26]).

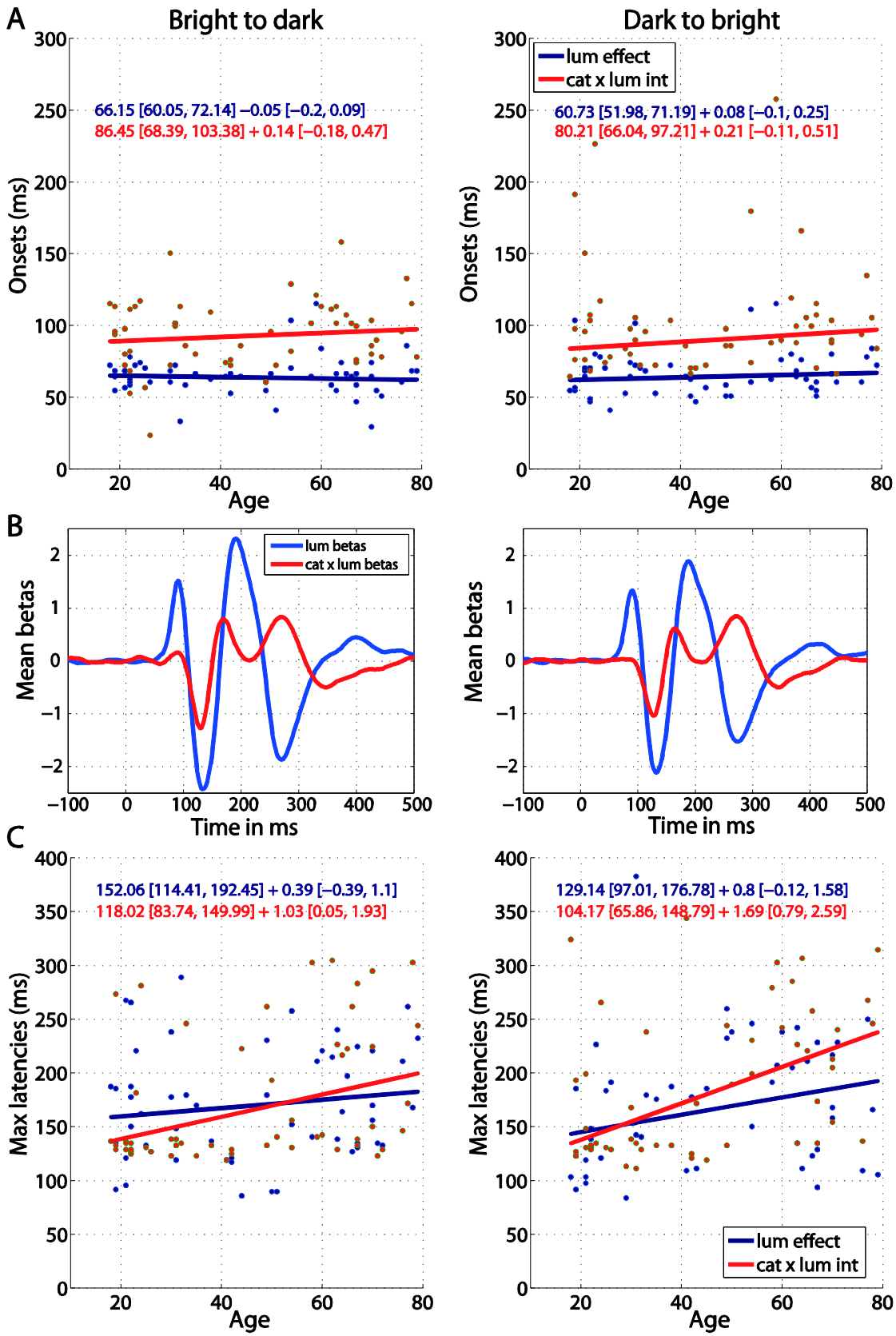

Figure 3.8. *Regressions of luminance effect and category x luminance interaction against age.* ***(A)*** *Onsets of the two effects against age for b2d (left column) and d2b sessions (right column).* ***(B)*** *Mean (across all subjects) beta coefficients associated with two predictors: luminance and category x luminance interaction.* ***(C)*** *Latencies of the maximum effects against age. Each subplot contains regression equations in the format intercept + slope with their confidence intervals in square brackets. The colour of each equation corresponds to the regression line for each effect.*

3.2.4 OVERLAP BETWEEN YOUNG AND OLD SUBJECTS

The median 50IT of young adults (<30) at the highest luminance (60.8 cd/m^2) was 181 ms (95% bootstrap CI = [169, 196] in b2d) and 183 ms [168, 199] in d2b (Figure 3.9 A tables). At the same luminance, the median 50IT of older subjects (>60) was 232 ms [225, 238] (b2d) and 237 ms [222, 247] (d2b), which is ~50 ms slower than the processing speed of young subjects in both experimental sessions (b2d: diff = -50 ms [-64, -34]; d2b: diff = -53 ms [-72, -33]). Indeed, visual processing of young adults was significantly faster than that of old adults in all but the two darkest conditions (1.12 and 0.59 cd/m^2) in both sessions, and the 2.17 cd/m^2 condition in d2b session (Appendix B – Supplementary Table 6).

The latencies of peak face-texture ERP differences were also delayed by age in both sessions. ERP differences in young adults at the luminance of 60.8 cd/m^2 peaked at the median latency of 139 ms [133, 154] (b2d) and at 143 ms [133, 169] (d2b), whereas for old adults the differences peaked at 224 ms [162, 238] (b2d) and at 224 ms [175, 242] (d2b) (Figure 3.9 B tables). This is an ~80 ms difference between peak ERP latencies of young and old subjects at the highest luminance (b2d: diff = -84 ms [-100, -33]; d2b: diff = -80 ms [-100, -27]). The latencies of the peak ERP differences of old adults (at 60.8 cd/m^2) were significantly longer than those of young adults for all luminance levels, apart from 1.12 and 0.59 cd/m^2 conditions in both sessions and 2.17 cd/m^2 in b2d session only (Appendix B – Supplementary Table 6).

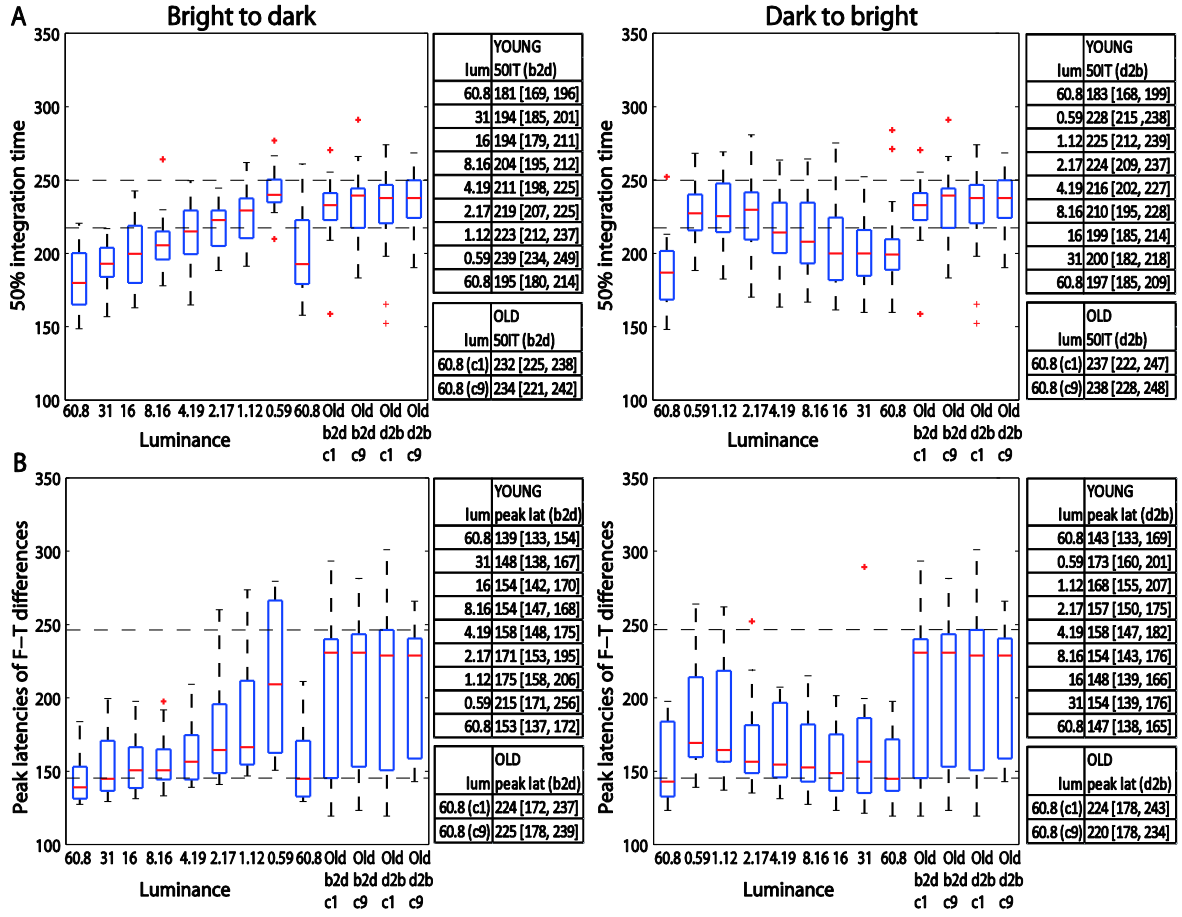

Figure 3.9. (A) *Boxplots of 50% integration times and* ***(B)*** *peak latencies of face-texture ERP differences for young (<30 years old) and old (>60 years old) adults. The median (across subjects) 50ITs and peak latencies along with confidence intervals are provided in the tables to the right of the subplots. For young subjects median 50IT and peak latencies for all conditions are given; for old subject, they are given for the two brightest conditions (condition 1 (c1) and 9 (c9)).*

A qualitative age-related change in the shape of t^2 functions was shown in Figure 3.2; Figure 3.10 A shows the mean t^2 functions for young (<30 years old) and old (>60 years old) adults. The percentage of overlap between normalised t^2 functions of these two age groups was computed to determine if the brain responses of old adults could be matched to that of young adults experiencing reduced retinal illuminance. The overlap increased with decreasing luminance, starting from about 69-74% at 60.8 cd/m^2 to about 83-86% at 0.59 cd/m^2 in both sessions (Figures 3.10 B & 3.11A). The overlap within the old group exceeded 90% indicating that old subjects are more similar to each other than to young subjects at any luminance level (Figure 3.11 A). In addition, even in the two conditions where the overlap was the highest - 86% at 0.59 cd/m^2 and 85% at 1.12 cd/m^2, the retinal illuminance of young subjects was only about 5% of that of old subjects (Figure 3.11 B), thus suggesting that retinal illuminance cannot account for young vs. old differences in processing speed.

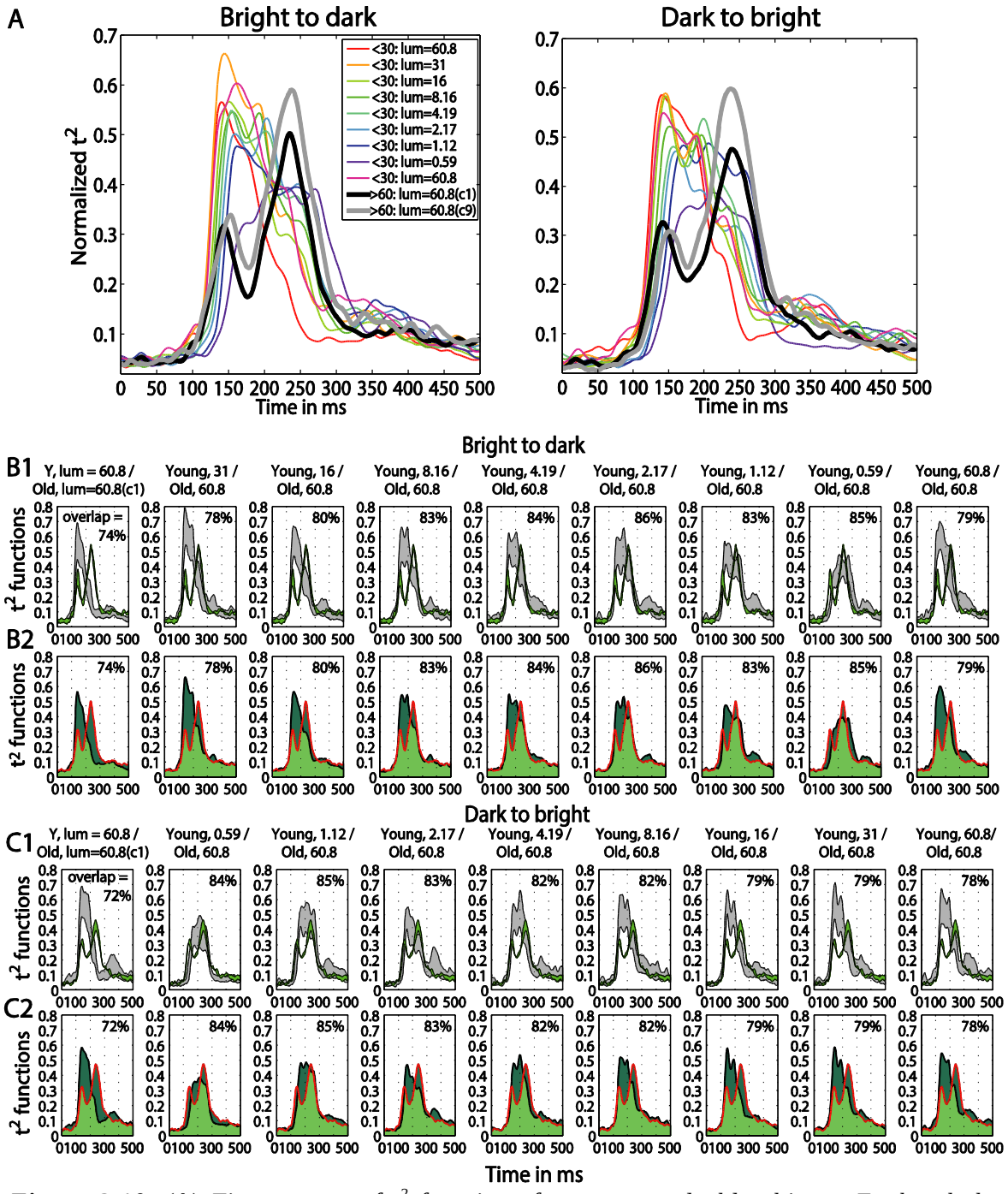

Figure 3.10. (A) *Time-course of t^2 functions for young and old subjects. Each subplot shows mean time-courses, across young subjects (<30 years old), at each luminance level, and across old subjects (>60 years old) in the two conditions with the highest luminance: condition 1 (c1) plotted in black and condition 9 (c9) plotted in grey.* ***(B1, C1)*** *Confidence intervals of young and old t^2 functions. Each subplot shows the time-course of 95% confidence intervals of the mean t^2 functions of young subjects (in grey) at each luminance level and of old subjects (in green) in the first brightest condition (luminance = 60.8 cd/m^2).* ***(B2, C2)*** *Overlaps between young and old t^2 functions. Each subplot depicts the area under the t^2 function of young (<30) and old (>60) subjects shaded in dark green. The edges of the young t^2 functions are black, those of old t^2 functions are red. The overlap between t^2 functions for young and old subjects is shaded in light green. The proportion of overlap is given inside each subplot and the luminances are given in the title of each subplot.*

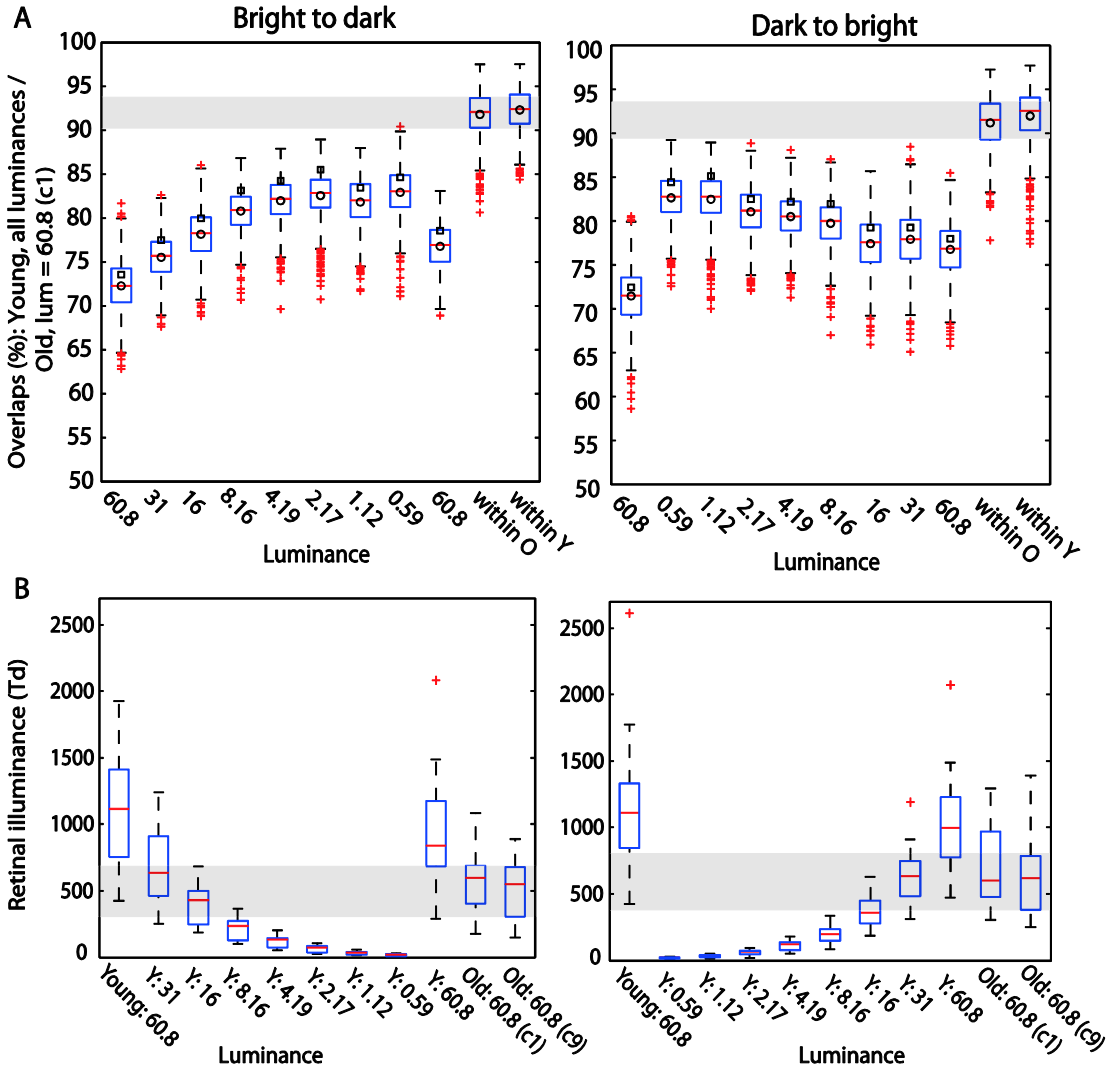

Figure 3.11. (A) *Boxplots of t^2 function overlaps between young and old adults. In each subplot, the first 9 boxplots show overlaps for young subjects at each luminance. The last two boxplots show the within group overlaps for old and young subjects, in the first brightest condition (60.8 cd/m^2), for b2d and d2b session. In each boxplot the square indicates the percentage of overlap between young and old yielded by our calculation; the circle is the mean of the bootstrapped overlaps – thus, the difference between the values for circle and square suggests that our estimation of the overlap is positively biased.* ***(B)*** *Retinal illuminance of young and old subjects. The first nine boxplots in each subplot depict the distributions of retinal illuminances in young subjects, at nine luminances; the two last boxplots in each subplot show results in old subjects in the two brightest conditions (luminance = 60.8 cd/m^2).*

4 ERP AGING EFFECTS – PINHOLE EXPERIMENT

The luminance experiment presented in the previous section showed that individual variability in retinal illuminance and pupil size could not account for individual differences in visual processing speed in a sample of subjects age 18-79. A second experiment presented in this section complements these findings by investigating if there is a causal relationship between pupil size and processing speed. Young subjects' pupil sizes were directly manipulated by placing pinholes of varying sizes in front of their eyes. Pinholes act as artificial pupils altering retinal illuminance without changing stimulus luminance. The aim was to establish if old subjects' ERP processing speed at high luminance (60.8 cd/m^2) could be matched match to that of young subjects wearing pinholes. The results show that this match was unsuccessful corroborating the results from the previous section of aging effects on ERP processing speed being due to neural, rather than optical factors.

4.1 METHODS

4.1.1 SUBJECTS

10 subjects (median age = 28.5, min = 22, max = 34, 6 males, 10 right handed) took part in two experimental sessions conducted one week apart. Seven of them also participated in the luminance experiment 5 to 6 months earlier. Each subject's visual acuity was measured using Collenbrander mixed contrast card set and contrast sensitivity was measured using Pelli-Robson chart. The measurements were taken for both eyes separately (monocular testing), on the day of the first session. All subjects had normal or corrected-to-normal vision and contrast sensitivity (Table 4.1), and all reported very good hearing, at least weekly exercise and none reported smoking. None of the subjects reported suffering from an eye disease, or a mental condition and none was taking psychotropic medications. All subjects gave written informed consent and were compensated for their participation at the rate of £6/hour.

Visual acuity				**Contrast sensitivity**		**Years of education**
High contrast 63 cm (median [min, max])		**Low contrast 63 cm (median [min, max])**		**(median [min max])**		**(median [min max])**
Right eye	Left eye	Right eye	Left eye	Right eye	Left eye	
107	105.5	95	93	1.95 [1.95, 2.10]	1.95 [1.95, 2.10]	19 [15, 25]

Table 4.1. *Pinhole experiment subjects' information.*

4.1.2 STIMULI

The stimuli were faces and textures generated as in the luminance experiment.

4.1.3 EXPERIMENTAL DESIGN

The experiment consisted of 7 blocks in each session. The two experimental sessions differed in terms of pinhole order employed: in the "small to big" (s2b) session pinhole size of 1 mm was applied in block 2. The pinhole size then increased by 1mm in each subsequent block to reach 5 mm in block 6. In the "big to small" (b2s) session, a 5 mm pinhole was used in the 2nd block and then pinhole size decreased by 1 mm in each block, up to 1mm in block 6. The first and the last blocks in both sessions were conducted without pinhole. All subjects participated in one s2b and one b2s session that were randomly assigned.

Each block contained 210 trials: 100 faces (10 face identities repeated 10 times, each time with unique noise field), 100 unique noise textures, and 10 practice trials at the beginning of every block (5 faces and 5 textures). The whole experiment had a total of 1470 trials. The task and trial procedure were the same as in the luminance experiment.

4.1.4 PROCEDURE

The experiment was conducted in the same lab booth as the luminance experiment. The stimuli were displayed on the same monitor with a luminance of 60.8 cd/m^2, which was constant across blocks. The viewing distance was also 80 cm. Subjects performed the experiment monocularly using the eye with best visual acuity – 4 subjects used their left eye and 6 subjects used their right eye. The other eye was occluded with an optician eye patch. For the purpose of light adaptation, before each experimental block, subjects were instructed to look at the monitor screen with uniform grey background (128 128 128) and luminance of 60.8 cd/m^2 for 60 seconds. After adaptation, subjects' pupil size in the non-occluded eye was measured using a NeurOptics pupillometer, following the same

procedure as in the luminance experiment. After pupil measurement, an optical trial lens frame (model TF-1002, Danyang Huasu Optical Co., Ltd.) was put on subjects' head. The pinholes were black circular plates 4 cm in diameter with a circular aperture of 1, 2, 3, 4 or 5 mm located in the middle of the plate. To determine the optimal position of the pinhole in front of the non-occluded eye, the smallest (1 mm) pinhole plate was inserted into the trial frame. Subsequently, the experimenter adjusted the pinhole position until a rectangular frame displaying the message "Press any key to start… (Block 1 of 7)" (size: 256 x 256 pixels, 9° x 9° of visual angle, displayed in the centre of the screen) was centred in the subjects' visual field (the message was not displayed during light adaptation). Each subject's visual field extent, while looking through the pinhole, was computed by taking into consideration the distance between the eye and the pinhole plate and the pinhole size. The median visual angle across subjects for pinholes of 1, 2, 3, 4 or 5 mm was 15˚, 17˚, 18˚, 20˚, and 22˚, respectively, in the s2b and 14˚, 16˚, 18˚, 20˚, and 22˚ in the b2s procedure. Thus, the 9˚ x 9˚ stimuli were visible even through the smallest pinhole. Once the trial frame with 1 mm pinhole was optimally installed, subjects conducted a 40 trial practice block, which was similar to the practice block in the luminance experiment. After the practice block and a small break, subjects proceeded with the experiment.

4.1.5 EEG DATA ACQUISITION AND PRE-PROCESSING

Data were acquired and pre-processed in the same way as in the luminance experiment, except that causal-filtered datasets were not created. All analyses were done on the non-causal filtered data (band-pass filtered between 0.3 Hz – 40 Hz using a two-way least square FIR filter (*pop_eegfilt* function in EEGLAB).

4.1.6 EEG DATA ANALYSIS

EEG data were analysed using Matlab 2011a and the LIMO EEG toolbox (Pernet, Chauveau, Gaspar, & Rousselet, 2011). General linear modelling of single-trial EEG data was used and the procedure was similar to the one used in the luminance experiment, except there were seven face-texture contrasts, instead of nine – one for each of the seven pinhole conditions. As in the luminance experiment, the results were corrected for multiple comparisons using a spatial-temporal clustering approach. For descriptive statistics and all comparisons, a similar percentile bootstrap procedure was used as in the luminance experiment.

4.2 RESULTS

The goal of the second experiment was to determine if, by decreasing young subjects' pupil size, their processing speed could be slowed and their ERPs could match to those of old subjects. The results show that the ERPs of young subjects were delayed for all pinhole sizes compared to the no pinhole condition. This effect was the strongest with the 1 mm pinhole and was visible at the level of single trial ERPs (Figure 4.1 A), face-texture ERP differences (Figure 4.1 B), and cumulative sums of t2 functions (Figure 4.1 C). Also, contrary to our hypothesis that the smaller the pinhole, the bigger the overlap between young and old subjects' ERPs, the overlap was higher for 4 and 5 mm pinholes compared to 1 and 2 mm pinholes (Figure 4.4). However, even at 4 or 5 mm, we were unable to match the ERPs of young observers to those of old observers.

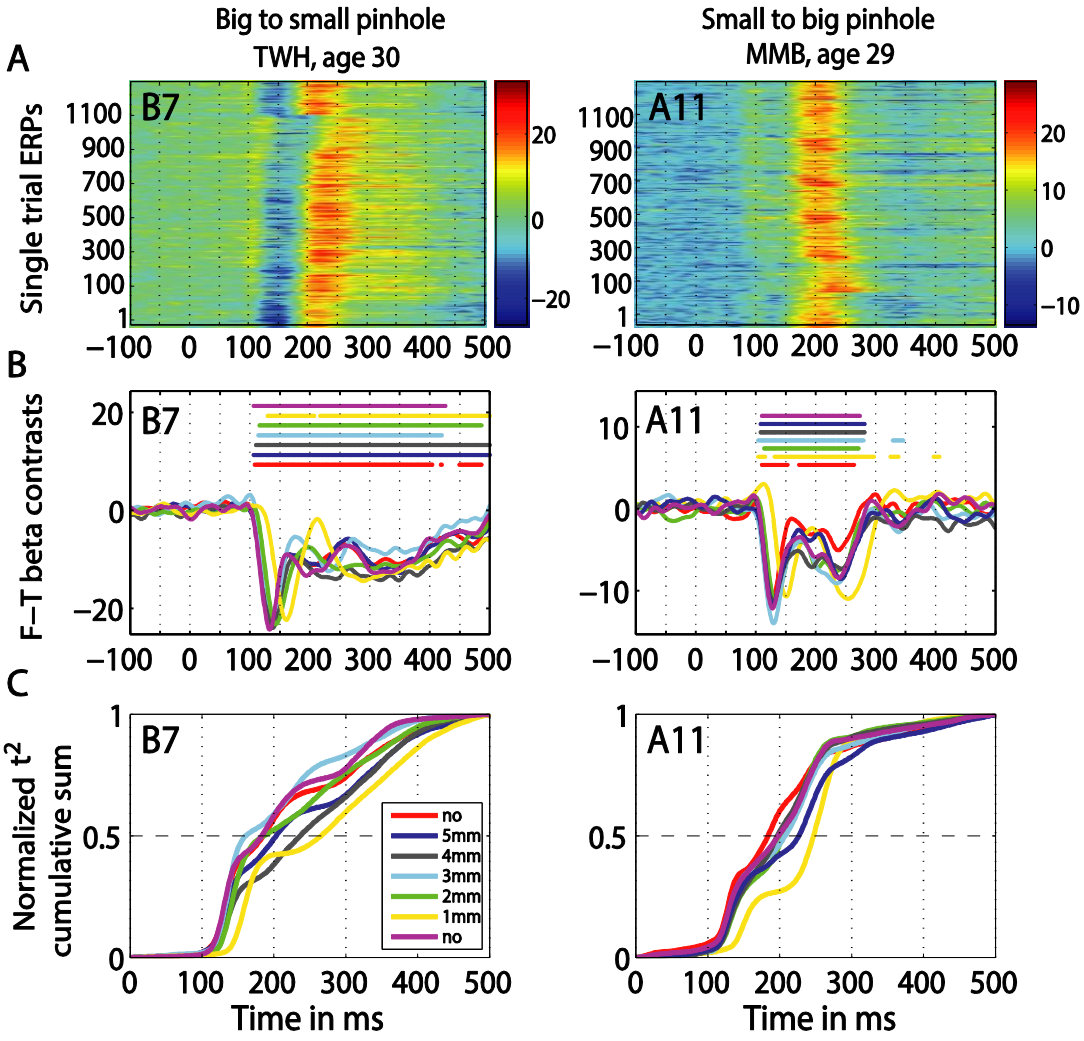

Figure 4.1. *Individual subjects data. Data of two representative subjects: TWH (age 30), and MMB (age 29) in b2s (column 1) and s2b (column 2) sessions at the max t^2 electrode for that subject, indicated in the top left corner of each plot.* ***(A)*** *Single-trial ERPs.* ***(B)*** *Time-courses of contrasts between face and texture beta-coefficients for each pinhole condition. Horizontal lines indicate significant differences.* ***(C)*** *Cumulative sums of t^2 functions for each pinhole condition.*

4.2.1 EFFECT OF PINHOLES ON ERP PROCESSING SPEED

Young subjects' 50ITs increased from 189 ms in the first no pinhole condition to 265 ms (b2s) and 251 ms (s2b) with a 1 mm pinhole (Figure 4.2, Table 4.2). We found significant differences in 50ITs between the no pinhole condition and 1, 2 and 3 mm pinhole sizes in both sessions; for 4 mm the difference was significant only in the b2s session, and for 5 mm pinhole in the s2b session. There was no significant difference between the two no pinhole conditions within the same session.

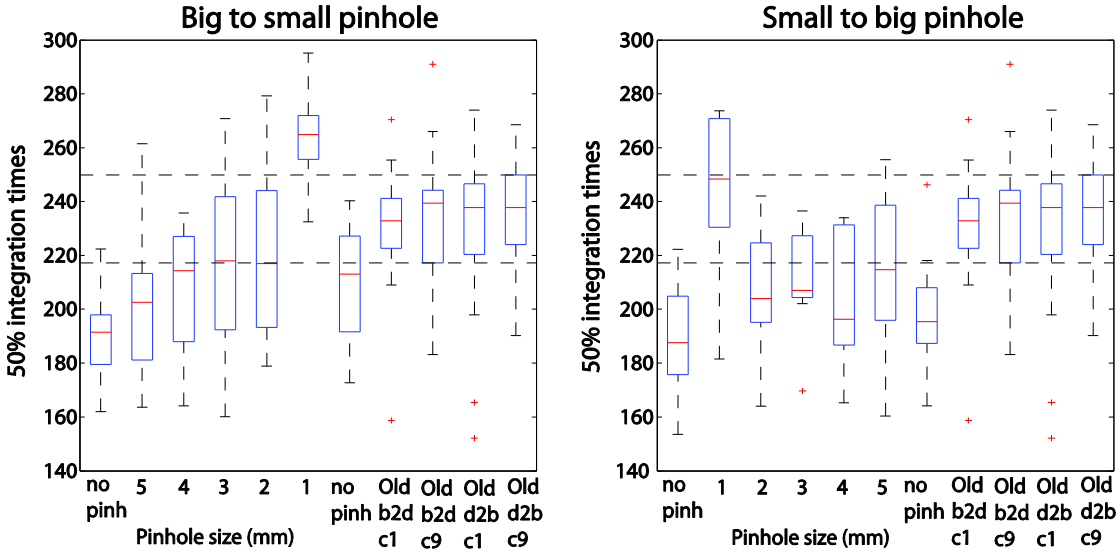

Figure 4.2. *Boxplots of 50% integration times. Boxplots 1-7 show 50ITs across all pinhole subjects, in each pinhole condition. Boxplots 8-11 show old subjects' 50ITs from the two brightest conditions of the luminance experiment (60.8 cd/m^2 – c1 and c9), for the b2d and d2b sessions. Horizontal dashed lines indicate the lowest 25th and the highest 75th quantile across the old subjects' 4 conditions.*

	no pinhole (first)	1 mm pinhole	2 mm pinhole	3 mm pinhole	4 mm pinhole	5 mm pinhole	no pinhole (last)
b2s	189 [177, 204]	265 [251, 277]	219 [194, 248]	219 [191, 243]	211 [187, 227]	198 [180, 216]	211 [190, 226]
	Difference	-75 [-88, -62]	-29 [-57, -10]	-29 [-54, -4]	-22 [-38, -3]	-9 [-24, 5]	-22 [-40, 2]
s2b	189 [174, 205]	251 [216, 267]	205 [193, 228]	210 [200, 225]	204 [186, 226]	217 [195, 237]	196 [180, 212]
	Difference	-62 [-73, -42]	-16 [-28, -5]	-20 [-30, -13]	-15 [-35, 1]	-27 [-47, -5]	-7 [-27, 15]

Table 4.2. *50% integration times for all pinhole conditions. The median 50IT (ms) and its 95% CI (in square brackets) is given for each pinhole condition and each session. Differences between the first "no pinhole" condition and each of the remaining pinhole conditions (1-5 mm and the last condition with "no pinhole") are also provided along with the 95% CIs.*

4.2.2 MATCHING OF PROCESSING SPEED BETWEEN YOUNG AND OLD SUBJECTS.

Young subjects' 50ITs for 2 and 3 mm pinholes in the b2s session matched those of old subjects from both b2d or d2b luminance sessions (b2d: 2 mm – diff = -14 [-39, 16]; 3 mm – diff = -14 [-41, 11]). However, in the s2b session, 50IT matched between young and old subjects (from both luminance sessions) for 1 and 5 mm pinhole sizes (b2d: 1 mm – diff = 19 [-15, 36]; 5 mm – diff = -16 [-38, 5]; d2b: 1 mm – diff = 14 [-16, 37]; 5 mm – diff = -20 [-43, 1]). 50ITs for all the remaining pinhole sizes differed significantly from those of old subjects (Figure 4.2, Appendix B – Supplementary Table 6).

Furthermore, a qualitative difference in the shape of the t^2 functions of young adults with no pinhole (and luminance level = 60.8 cd/m^2) and old subjects tested at 60.8 cd/m^2 was observed (Figure 4.3). This shape difference was visible for all pinhole conditions. Additionally, in the 1mm pinhole condition, the onsets of the face-texture ERP differences in young subjects were delayed compared to the onsets of the old adults in the luminance experiment (Figure 4.3). The calculation of the overlap between t^2 functions of young and old adults revealed that in both pinhole sessions, the overlap was 5-14% higher when young subjects wore pinholes compared to the no pinhole condition (Figure 4.4). For the b2s session the overlap was the highest for 2 and 3 mm pinholes ~81-82% (Figure 4.4 A), whereas for the s2b session it was the highest for the 5 mm pinhole ~73-74% (Figure 4.4 B). This result converges with the finding that 50ITs of young and old adults matched for 2 and 3 mm pinholes in b2s session and for the 5 mm pinhole in s2b session. Finally, the overlaps were 3-8% higher for the 5 mm pinhole size compared to 1 mm, which goes against the hypothesis that the smaller the pinhole in young subjects the bigger the overlap between young and old ERPs. Thus, although pinholes delay visual processing, they are not sufficient to make young subjects' ERPs look old.

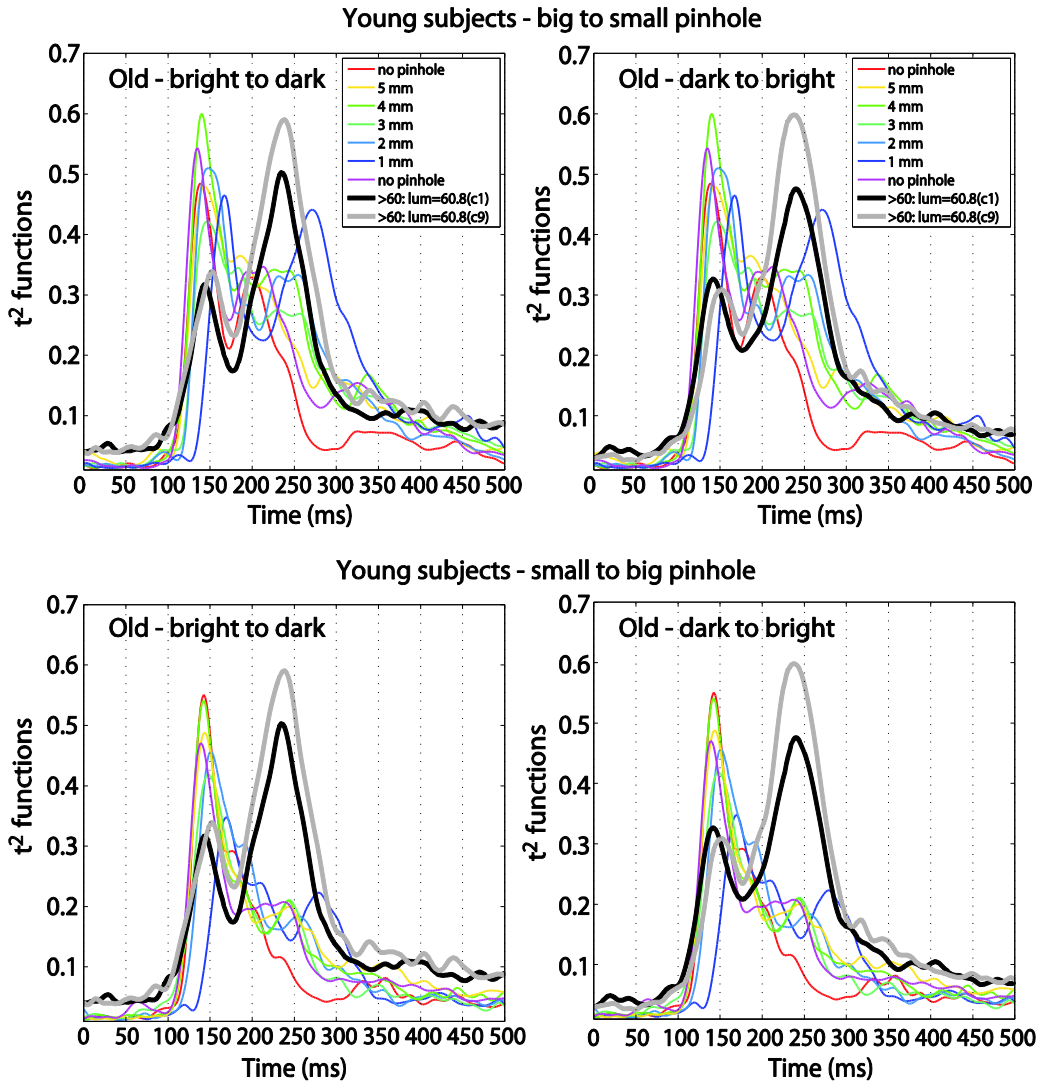

Figure 4.3. *Time-course of normalized t^2 functions for young and old subjects. Each subplot shows the time-courses of mean normalized t^2 functions of young subjects, in all conditions of the pinhole experiment, and of old subjects from the luminance experiment, in the two conditions with the highest luminance 60.8 cd/m^2: condition 1(c1) plotted in black, and condition 9 (c9) plotted in grey.*

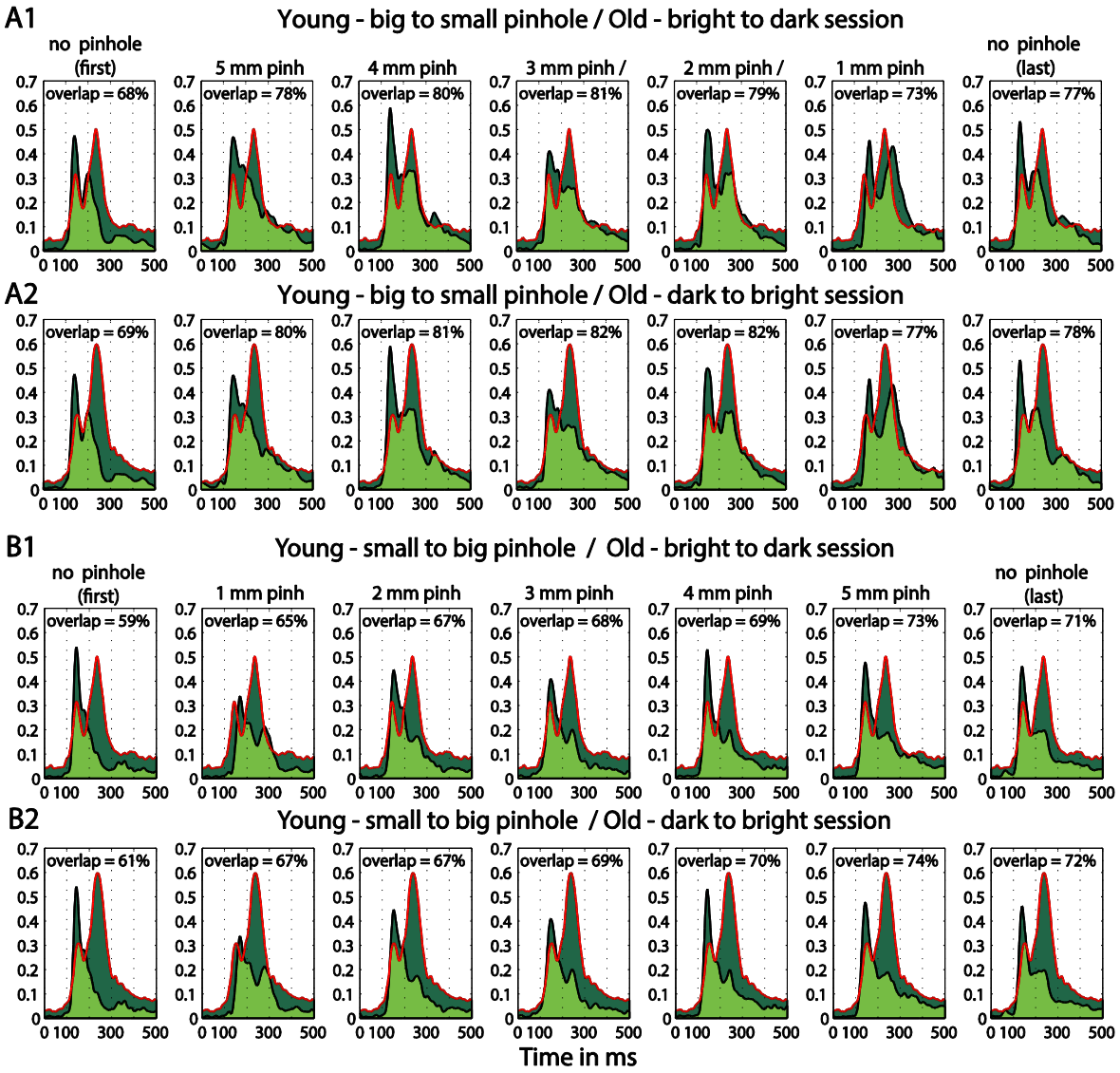

Figure 4.4. *Overlaps between t^2 functions of young subjects tested in the pinhole experiment and old subjects tested in the luminance experiment.* ***(A)*** *Overlap between old (>60) adults in the first brightest (60.8 cd/m^2) condition from the b2d* ***(A1)*** *and d2b* ***(A2)*** *session of the luminance experiment and young subjects in all the pinhole conditions of the pinhole experiment's b2s session.* ***(B)*** *Overlap between old subjects in the brightest (60.8 cd/m^2) condition from the b2d* ***(B1)*** *and d2b* ***(B2)*** *session of the luminance experiment and young subjects in all the pinhole conditions of the pinhole experiment's s2b session. Each subplot depicts the area under the t^2 functions of young and old subjects, shaded in dark green. The edges of the t^2 functions for young and old subjects are highlighted in black and in red, respectively. The overlap between t^2 functions for young and old subjects is shaded in light green. The proportion of overlap is given inside each subplot.*

4.3 DISCUSSION

The study presented in this section addressed several enduring questions about aging effects on visual processing speed, as reflected in ERPs. It was measured by how much the visual processing of faces slows down throughout adulthood; the onset of the slowdown; and the contribution of luminance and pupil size to the age-related delay.

4.3.1 AGE-RELATED ERP DELAYS

First, the data confirms previous findings of Rousselet, et al. (2010), suggesting that aging slows down visual processing speed by 1 ms/year. This result was extended by showing that this rate of slowdown is constant across luminance levels, from 60.8 to 0.59 cd/m^2. At the highest luminance (60.8 cd/m^2), the processing speed of older (>60) subjects was ~230 ms, about 50 ms slower than that of younger (<30) subjects (~180 ms). Aging also prolonged the latencies of maximum face-texture ERP differences, but at a sharper rate: on average by ~1.5 ms/year; the strongest face-texture ERP differences were observed ~140 ms post-stimulus in young adults, but only after 220 ms in older adults – about 80 ms later. Aging effects started around ~125 ms post-stimulus at 60.8 cd/m^2 and, because of a main effect of luminance, were delayed up to 162 ms at 0.59 cd/m^2; maximum aging effects appeared at ~200 ms at 60.8 cd/m^2 and were delayed to ~260 ms at 0.59 cd/m^2.

Previous research yielded inconclusive results regarding the dependency of aging effects on luminance: some research showed similar ERP aging delays regardless of the luminance level (Tobimatsu, et al., 1993), whereas others suggested that ERP aging effects were stronger at low luminances (e.g. Shaw & Cant, 1980). The findings of Shaw and Cant (1980) do not contradict our observations – the luminance level beyond which their aging effect became weaker (~72 cd/ m^2) is higher than our maximum luminance (60.8 cd/m^2). Unfortunately, we are unable to relate the dependency between luminance and aging effects found in our study to other face ERP aging studies, because only one of them reported the mean luminance of their stimuli: 64 cd/m^2 (Pfutze, Sommer, & Schweinberger, 2002). In this study, Pfutze, et al. (2002) reported no changes in P1 and N170 peak latencies with age. However, their results cannot be directly compared to our results because they did not consider the entire time-course of the effects, as is done in our approach. Nevertheless, it is possible that at luminances higher than the ones used in the present study, ERP aging effects may decrease and future studies should address this question. Including information about luminance and contrast of the stimuli into method sections would also facilitate the comparison of age-related effects across studies.

In the current study, and the previous ones (Rousselet, et al., 2009; Rousselet, et al., 2010), my lab found ERP aging effects starting at about ~125 ms post-stimulus, and lasting for about 200 ms, with the strongest effects in the N170 time window. Aging effects in the N170 time window have been reported in several studies (Gazzaley, et al., 2008, Nakamura, et al., 2001; Wiese, et al., 2008). However, present results confirm that aging effects start earlier than the N170 peak, in keeping with the idea that peak analyses should be abandoned in favour of systematic time-point by time-point analyses (Rousselet & Pernet, 2012). Noteworthy, ERP studies using checkerboards have reported age-related latency increases already around 100 – 110 ms post-stimulus (Tobimatsu, et al., 1995; Shaw & Cant 1980; Sokol, Moskowitz, & Towle, 1981). However, checkerboards and faces differ in spatial frequency content, and it is thus difficult to compare the absolute latencies of the ERPs elicited by these two types of stimuli.

Among studies using faces (Pfutze, Sommer, & Schweinberger, 2002; Chaby, George, Renault, & Fiori, 2003; Daniel & Bentin, 2010; Gao, XU, ZhangG, Zhao, Harel, & Bentin, 2009; Chaby, Jemel, George, Renault, & Fiori, 2001; Gazzaley, et al., 2008, Nakamura, et al., 2001; Wiese, et al., 2008; Wiese, Komes, & Schweinberger, 2012) discrepancies in N170 aging effects could be due to variability in stimulus parameters (e.g. whether or not external features were preserved, size, color, contrast, luminance), or ERP analysis approach (focused on peak amplitude and latency or peak-independent analyses), or both. It seems unlikely that particular stimuli could explain the presence of early aging effects because very different stimuli were used also among studies that did find delays in early ERPs, as well as among those that did not. Nevertheless, future work could determine how the aging effects observed in the present work are linked to potential differences in ERP information content, for instance using reverse correlation techniques (Schyns, Gosselin & Smith, 2009; Smith, Gosselin & Schyns, 2012). This would allow determining if age-related changes in ERP shape are due to changes in diagnostic information, which might reflect, for instance, differences in task related strategies.

At present, it seems more plausible that the differences in ERP aging effects between the current study and the existing literature stem from the application of different measures of age-related delays. Most studies focus on component peak latencies in pre-defined time windows, whereas our analyses take into consideration changes in the overall shape of the ERP, and is independent of ERP peaks and regions of interests. Thus, it is entirely possible that similar aging effects would be obtained by applying data analyses approach used in this work to data from other studies. Moreover, the 1 ms/year age-related

delay in processing speed, obtained with the present analysis approach, has been replicated both within studies (testing our subjects twice), and across studies in independent samples of subjects from two countries (Rousselet, et al., 2009, Rousselet, et al., 2010).

4.3.2 LUMINANCE EFFECT ON THE ERPS

The results indicate that, independently of age, luminance strongly modulated ERPs. Previous research has shown that decreasing luminance increases the latencies of neuronal responses in cortical areas including V1 (Rousselet G. A., Husk, Bennett, & Sekuler, Time course and robustness of ERP object and face differences, 2008b), superior colliculus (Marino, et al., 2012) and in the LIP - lateral intraparietal area (Tanaka, Nishida, Aso, & Ogawa, 2013). Early ERPs (~100 ms) are also delayed by changes in luminance (Cant, Hume, & Shaw, 1978; Tobimatsu, et al., 1993; Johannes, Munte, Heinze, & Mangun, 1995; Wicke, Donchin, & Lindlsey, 1964). The present study extends this finding by showing that luminance affects most of the ERP time-course, within 500 ms post-stimulus, starting about 60 ms post-stimulus, with maximum modulations occurring between 130 – 150 ms. These strongest luminance effects occurred after the P100 time-window, a period of activity commonly thought to be most sensitive to changes in low-level visual factors, such as luminance (Shaw & Cant, 1980), contrast (MacKay & Jeffreys, 1973), size (Yiannikas & Walsh, 1983) or color (Anllo-Vento & Hillyard, 1996). My results suggest that it is not the P100 but the 130 – 150 ms period that is most strongly modulated by luminance – the period usually associated with higher-order cognitive processes, such as object and face categorization (Itier & Taylor, 2004), expertise (Tanaka & Curran, 2001), or task-related processes (Rousselet, Gaspar, Wieczorek, & Pernet, 2011a). Stronger sensitivity to changes in luminance around 130-200 ms, rather than around 100 ms, has also been observed in a study using short flashes of vertical bars (Johannes, et al., 1995). Thus, visual ERP studies should not underestimate the effects of low-level factors beyond the P1 time window. Reporting the screen luminance is also essential to be able to compare ERP latencies across studies.

4.3.3 CONTRIBUTION OF PUPIL SIZE AND SENILE MIOSIS TO AGE-RELATED ERP DELAYS

The results show that pupil size decreases with aging at the rate of ~0.03 mm/year at 60.8 cd/m^2, ~0.04 mm/year at intermediate luminances, and ~0.05 mm/year at 0.59 cd/m^2. This is equivalent to about 0.6 – 1 mm reduction every 20 years. These estimates match quite well those obtained in previous studies – for instance Winn (1994) found a decrease in pupil size of about 0.03 mm/year at 220 cd/m^2 and ~0.04 mm/year at 44 and 9

cd/m^2. Birren, Casperson and Botwinick (1950) reported a 2.5 mm difference in pupil size between subjects in their twenties and subjects in their eighties (~0.04 mm/year) at 3.18 cd/m^2. Between the same age groups, Sokol et al. (1981) observed a slightly smaller reduction in pupil size of 1.5 mm (0.025 mm/year) at 1.9 cd/m^2. Finally, our senile miosis measurements fit well with a recent model that estimates pupil size based on age, luminance, size of adaptive field and whether one or two eyes have been adapted (Watson & Yellott, 2012).

Contrary to the expectations, senile miosis is unlikely to be a factor explaining age-related delays in visual ERPs. Moreover, individual variability in pupil size within age groups cannot account for individual differences in visual processing speed. First, after partialling out the effect of age from our processing speed measurements and from pupil size, we failed to find a relationship between processing speed and pupil size. Second, at 31 and 16 cd/m^2, the luminance conditions providing the best retinal illuminance match between young and old subjects, the overlap between their ERPs was the second smallest (after 60.8 cd/m^2). Additionally, in the conditions where young-old ERP overlap was the highest (0.59, 1.14, 2.17 cd/m^2), the retinal illuminance of young subjects was only about 5-10% of that of old adults. Furthermore, in experiment 2, the ERPs of old subjects tested at high luminance could not be matched to those of young subjects wearing pinholes. In fact, a counterintuitive result was observed: the young-old ERP overlap was 3-8% higher in the 5 mm pinhole size condition compared to the 1 mm condition. Overall, the results demonstrate that ERPs to faces are delayed by aging at the early stages of visual processing (< 200 ms) and strongly suggest that these delays are of cortical, rather than optical origin.

4.3.4 CONTRIBUTION OF OTHER OPTICAL FACTORS AND CONTRAST SENSITIVITY TO ERP AGING DELAYS

Ruling out senile miosis as possible contributor to age-related visual processing delays does not necessarily mean that no other optical factors are involved. With age, there is a reduction in lens light transmittance (Boettner & Wolter, 1960), as well as in the eye's ability to accommodate, which decreases from the fifth decade of life onwards and seems to disappear altogether in the sixth decade (Birren & Schaie, 2001). Additionally, after the age of 40, the amount of intraocular light scatter increases, leading to a reduction in retinal image contrast (Fujisawa & Sasaki, 1995). Under these circumstances, senile miosis is actually beneficial because it diminishes optical aberrations (Applegate, Donnelly, Marsack, Koenig, & Pesudovs, 2007); it also boosts depth of focus, improving contrast and

the overall quality of the retinal image (Weale, 1992). Despite the positive effects of senile miosis, overall, reduction in pupil diameter, increase scatter and a decrease in ocular transmittance lead to approximately 60% of light loss at the retina, at lower light levels, between the ages of 20 and 60 years. However, this reduced retinal illuminance in old subjects is unlikely to account for the ERP aging delays found in this study because even when retinal illuminances of young and old subjects matched, their ERPs did not.

Another factor that could potentially contribute to our ERP aging delays is a decline in spatial contrast sensitivity with age. The effects of diminished contrast sensitivity in the elderly have been primarily studied at the early stages of visual processing, especially around the P100 (Tobimatsu, 1995; Tobimatsu, Kurita-Tashima, Nakayama-Hiromatsu, Akazawa, & Kato, 1993; Morrison & Reilly, 1989). Morrison & Reilly (1989) showed that incrementing stimulus contrast makes ERPs of older observers resemble those of young observers. Tobimatsu, et al., (1993) found that a reduction in contrast of checkerboard patterns leads to significant differences in P100 latency between young and middle age groups, contrary to high contrast checks for which no difference was observed. In the older group, P100 latencies were delayed compared to the middle age group for both low and high contrast checks. My stimuli had RMS contrast of 0.1, which is similar to the low contrast stimuli used by Tobimatsu, et al. (1993). It is therefore possible that for higher contrast stimuli, our aging effects would be less pronounced; to my knowledge no face ERP study has yet addressed the link between stimulus contrast and aging delays.

However, it is unlikely that reduction in contrast sensitivity could fully explain the ERP aging delays found here. Contrast sensitivity loss under photopic light conditions has been observed in particular for intermediate and high spatial frequencies – above 2 cycles/degree of visual angle (Owsley, Sekuler, & Siemsen, 1983). In my stimuli, 90% of the total power was contained within the low to intermediate spatial frequency range (Bieniek, Pernet, & Rousselet, 2012, Figure 1) – below 20 cycles/image, which for our image size of 9º of visual angle is equivalent to ~2.2 cycles/degree. This suggests that most of the spatial frequency content of our images is below the range that is typically affected by aging. Also, age-related differences in contrast sensitivity are larger under mesopic and scotopic light conditions than in photopic conditions (Sloane, Owsley, & Alvarez, 1988; Owsley, 2011). In my study, only the 0.59 cd/m^2 luminance condition falls within the mesopic range. However, the aging effect for that luminance level did not differ from the

one observed at the highest luminance level. Thus, a link between our aging effects and contrast sensitivity loss is unlikely.

4.3.5 POSSIBLE ACCOUNTS FOR THE ERP AGING EFFECTS

Finally, in this last section, I speculate about the main factors that could account for age-related processing speed slowdown, including: alteration in axons' myelination, reduced synaptic and network efficiency, decrease in neuronal response selectivity, inhibitory deficits, and neuronal network reorganisation.

First, slowdown of visual processing speed with age may be due to myelin alteration: aging is associated with degeneration of myelin sheaths of cortical neurons that subsequently get remyelinated, but with shorter internodes, leading to slower conduction along nerve fibres (Peters, 2009; Peters, 2002). Changes in myelin sheaths are distributed across grey matter and white matter, suggesting that communication both within and between cortical regions might be disturbed (Peters, 2002). In keeping with these anatomical observations, there is direct evidence for age-related slowing in the visual system: Wang, et al. (2005) reported delays in the latency of inter-cortical spiking activity, between V1 and V2, as well as intra-cortical activity, within V1 and V2, and this effect was more pronounced in V2 compared to V1.

In humans, post-mortem analysis reveals stronger changes in white-matter density than in grey-matter density with healthy aging (Piguet, et al., 2009). Using in-vivo techniques, several studies have suggested a relationship between age-related decline in white matter and cognitive function including speed of processing (Eckert, 2011; Eckert, Keren, Roberts, Calhoun, & Harris, 2010; Salami, Eriksson, Nilsson, & Nyberg, 2012; Bucur, Madden, Spaniol, & Provenzale, 2008). However, some of these studies potentially suffer from a statistical problem arising from the artificial correlation between time-dependent variables (Hofer & Sliwinski, 2001; Lazic, 2010). These studies also use composite behavioural measures of processing speed that do not have the specificity and the temporal resolution potentially afforded by EEG and MEG.

Additionally, animal studies suggest that aging is associated with a decrease in spine numbers and spine density (Duan, et al., 2003), as well as with alterations in the strength and efficiency of synaptic connections (Mostany, et al., 2013). Although at a different scale, reduced efficiency of cortical networks in older individuals has also been suggested in humans (Achard & Bullmore, 2007). This loss in efficiency may be linked to

the degradation of neuronal response selectivity, which in turn could translates into slower processing times. Indeed, animal research shows that aging is associated with an increase in spontaneous activity of neurons, a reduction in signal to noise ratio, and a deterioration of orientation and direction selectivity in V1 and V2 (Schmolesky M. , Wang, Pu, & Leventhal, 2000; Yu, Wang, Li, Zhou, & Leventhal, 2006; Hua, et al., 2006). This increase in noise and decrease in selectivity of neuronal responses may lead to broader tuning of neuronal populations and impair face-specialised processing. This notion is supported by fMRI findings of reduced differentiation of BOLD signal between faces and pink noise textures (Park, et al., 2004) accompanied by an increase in BOLD response to all categories in regions normally preferentially active for certain categories only (Park, et al., 2004; Voss, et al., 2008; Payer, Marshuetz, Sutton, Hebrank, Welsh, & Park, 2006). If populations of cells become less tuned to a specific stimulus, the rate of accumulation of evidence supporting its recognition would slow down, leading to longer processing times (Perrett & Ashbridge, 1998).

The deterioration of visually driven neuronal responses has also been linked to an age-related reduction in GABA concentration. The administration of GABA to V1 cells of senescent monkeys' improved selectivity of visual responses, demonstrating a direct link between inhibitory processes and healthy visual function (Leventhal, Wang, Pu, Zhou, & Ma, 2003). In humans, inhibitory deficits in elderly subjects have been captured at the level of populations of neurons using EEG. For instance, Gazzaley, et al. (2008) found that older adults have more difficulties with suppressing task-irrelevant information, which manifests itself in longer N170 latencies (but unaffected P1 latencies). It is unclear whether the present results of the most prominent aging effects occurring in the N170 time window can be linked to inhibitory deficits or decreased specialisation of face-selective processes: further research should address this question.

Although they cannot yet be linked to particular processes, it seems plausible that the earliest aging effects (~125) involve activity from higher-order visual areas. Intracranial recordings showed face-sensitive responses in extrastriate areas (Halgren, et al., 1994), occipital and temporal structures (Liu, et al., 2009), and in the fusiform gyrus (Barbeau, et al., 2008) as early as ~100 ms. Strikingly, one small cortical patch can generate the whole P1-N170-P2 complex (Sehatpour, et al., 2008; Rosburg, et al., 2010; Allison, Puce, Spencer, & McCarthy, 1999). Studies using scalp recordings have also reported responses differentiating between faces and other objects already ~100 ms post stimulus (Liu, Harris, & Kanwisher, 2002; Herrmann M. J., Ehlis, Ellgring, & Fallgatter,

2005; Itier & Taylor, 2002; Linkenkaer-Hansen, et al., 1998; Pizzagalli, Regard, & Lehmann, 1999; Halit, de Haan, & Johnson, 2000; Yamamoto & Kashikura, 1999). However, some of these studies used non-causal filters with relatively large high-pass cut-offs between 0.8 Hz and 1.5 Hz, which could have shortened onsets by smearing effects back in time (Rousselet, 2012; Acunzo, MacKenzie, & van Rossum, 2012; Widman & Schroeger, 2012). In the present study a causal Butterworth high-pass filter was used, which does not distort onsets, and it was found that face-texture ERP differences started around 90 ms post-stimulus. This suggests that the visual system detects faces very rapidly, and that aging starts to affect visual processes within 35 to 40 ms after face detection.

However, if degeneration of myelin and increased noise of neuronal responses are visible already in V1 (Peters, Sethares, & Killiany, 2001; Schmolesky, et al., 2000), we would expect to see ERP aging differences earlier than ~125 ms post-stimulus. This is assuming serial processing from V1 onward, and our capacity to measure evoked responses from all successive stages, which is a rather unrealistic model (Foxe & Simpson, 2002). Additionally, face stimuli are not optimal to capture very early brain activity, and different strategies have been suggested to measure the earliest cortical onsets, as reflected in the C1 component, starting around 60 ms post-stimulus (Kelly, Gomez_Ramirez, & Foxe, 2008). Whether age-related differences in activity from striate and early extra-striate areas might occur in the absence of differences in the onset of face related areas remain to be investigated.

Reduced selectivity of neuronal responses and deficits in inhibition of irrelevant information may lead to slower accumulation of evidence useful for decision making. It has been suggested that subjects' behavioural choices can be predicted from the activity in two EEG time windows associated with the accumulation of evidence useful for decision making: one early (~N170) and one late (>300 ms) (Philiastides, Ratcliff, & Sajda, 2006; Philiastides & Sajda, 2006). In my study, aging effects started 35 – 40 ms after the onsets of face/texture differences. Moreover, subjects' behavioural performance did not change with age and was close to 100%. Thus, it seems plausible that, for all age groups, stimulus processing starts at the same time, but when the aging effects appear, the whole cascade of information accumulation necessary for a behavioural decision is disturbed, leading to longer processing times, without necessarily hampering subjects' performance - at least in an easy task such as ours. The task used in our study was designed to be very easy in order to measure age-related ERP differences in processing speed in the absence of behavioural differences.

Age-related neuronal changes might also lead to the involvement of additional or different neuronal circuits – reorganisations that could potentially explain aging results found in the present study. Indeed, age-related reorganisation of neuronal networks during face processing has been observed by Grady, McIntosh, Horwitz & Rapoport (2000). They discovered that in young adults better recognition of degraded face images was positively correlated with the activity in the fusiform gyrus, in contrast to old adults for whom behavioural performance correlated with activity in the posterior occipital cortex. Other studies found that when task difficulty increases (for instance because faces are degraded), older observers rely more on prefrontal areas, suggesting that, with age, there is an over recruitment of frontal activity to compensate for poorer performance of the sensory systems (Grady, 2008). In the current study, the behavioural task was very simple, most likely not requiring the involvement of compensatory brain circuits. However, the exact task conditions that promote frontal compensation in old adults are still poorly understood. Also, evidence for over-recruitment and compensation have been obtained from cross-sectional designs, and have been challenged by a recent longitudinal study (Nyberg, Lovden, Rilund, Lindenberger, & Backman, 2012; Nyberg, et al., 2010).

Finally, the aging effects observed in this study could be related to a decline in perceptual grouping abilities (Kurylo, 2006) and contour integration (Roudaia, Bennett, & Sekuler, 2008; Roudaia, Farber, Bennett, & Sekuler, 2011). Because face and object recognition rely to a large extent on contours and edges carried by image phase information (Bieniek, Pernet, & Rousselet, 2012; Gaspar & Rousselet, 2009), any deficit in a mechanism responsible for contour integration is likely to affect face and object processing. An important research question would thus be to determine the relationship between ERP aging delays and age-related contour integration deficits, which might themselves be due to inhibitory deficits and other neuronal changes.

5 THE ONSET OF ERP SENSITIVITY TO FACES IN THE HUMAN BRAIN

Building on the result presented in the previous section of no age effects on the onsets of face-related ERP responses, my final project (Section 5) aimed for precise quantification of onsets in a large sample of participants. The time needed by the visual system to detect faces has been the subject of considerable debate in electrophysiological literature (Section 1.2 & 1.3). Although the evidence is mixed, it seems plausible that face-sensitive responses might occur already before 100 ms in both human and monkey brains. To address this controversy, the onset of ERP face responses in humans was estimated using an approach that overcomes some of the major limitations of previous ERP research. ERPs of 120 subjects were recorded; 74 of them were tested twice to assess the test-retest reliability of the results. To quantify individual differences data were analysed on individual subject basis. Causal filters were applied to the EEG data, so as to avoid potential onset distortions introduced by non-causal filters commonly used in ERP research (Acunzo, et al., 2012, Rousselet, 2012, Luck, et al., 2005, Widmann & Schroder, 2012). Analyses were performed systematically at all electrodes and time frames and controlled for multiple comparisons using a bootstrap spatial-temporal cluster technique.

5.1 METHODS

5.1.1 SUBJECTS

In this study data from 120 healthy subjects (60 females) age 18-81, recruited and tested in Canada (group 1: n=30) and in the UK (group 2: n=31, group 3: n=59) were pooled together. Basic information about the subjects is given in Table 5.1 and detailed descriptions are provided in Rousselet, et al. (2009) for group 1, Rousselet, et al. (2010) for group 2 and Section 3 for group 3. A total of 73 subjects took part in a second experimental session to assess the reliability of their results (24 subjects from group 2 and 49 subjects from group 3).

Age bracket	Age	Number of subjects (females, males)	Years of education	Visual Acuity	Contrast Sensitivity
18-19	19 [18, 19]	6 (4, 2)	15.5 [15, 18.5]	1.25 [1, 1.6]	1.95 [1.95, 1.95]
20-29	22 [20, 29]	29 (14, 15)	18 [15, 25]	1.25 [0.8, 1.68]	1.95 [1.8, 2.25]
30-39	33 [30, 38]	15 (5, 10)	19 [14,25]	1.25 [0.8, 1.6]	1.95 [1.95, 2.1]
40-49	43.5 [40, 49]	16 (10, 6)	18 [12, 27]	1.25 [0.8, 1.6]	1.95 [1.95, 2.25]
50-59	55 [50, 59]	9 (3, 6)	19 [13, 19]	1.25 [0.63, 1.6]	1.95 [1.95, 1.95]
60-69	66 [60, 69]	31 (16, 15)	16 [5, 21.5]	0.96 [0.4, 1.39]	1.95 [1.95, 1.95]
70-81	73.5 [70, 81]	14 (8, 6)	13.5 [10, 21]	1 [0.4, 1.25]	1.95 [1.65, 1.95]

Table 5.1. *Subjects' information. For each age bracket the median age, years of education, visual acuity (measured using Colenbrander mixed contrast card set at 63 cm and high contrast), and Pelli-Robson contrast sensitivity are, given with minimum and maximum values in square brackets.*

5.1.2 DESIGN AND PROCEDURE

Subjects from all three groups viewed images of faces (F) and textures (T). The same set of 10 faces was used across the three experiments and is described in more detail in Rousselet, Husk, Bennett, & Sekuler (2008), Rousselet, et al., (2010), Rousselet, et al., (2009) and Section 3. In short, all faces were front view grey-scale images, cropped into an oval shape to remove external features (hair, ears). Textures were images with random Fourier phase spectra. All faces and textures had their Fourier amplitude spectra set to the average across faces. Fourier transform of images was computed using *fft2* function in Matlab. All images were 256 x 256 pixels (visual angle: 8° x 8° for group 1 and 9° x 9° for groups 2 and 3) with contrast variance = 0.1. In the original studies, Fourier phase coherence or screen luminance was manipulated to affect the amount of stimulus evidence. Thus, from each study, we chose trials from the conditions in which subjects viewed stimuli with comparable Fourier phase coherence and screen luminance: group 1 – phase coherence = 70% & 0%, luminance = 33cd/m^2 (120 trials/condition); group 2 – phase coherence = 70%, 75% (pooled) & 0%, 5% (pooled), luminance = 33 cd/m^2 (128 trials/condition); group 3 – phase coherence = 70% & 0%, luminance = 60.8 cd/m^2 (150 trials/condition). For group 3, the blocks with luminance = 60.8 cd/m^2 were chosen because the 31 cd/m^2 block had only 75 trials/condition and no difference in processing speed between 60.8 and 31 cd/m^2 was found (Section 3). Also, no ERP difference between 70% and 75% phase coherence, or between 0% and 5% was found (Rousselet, et al. 2009; 2010). Groups 1 and 2 performed a forced choice discrimination task between two pictures of female or male faces that included varying amount of phase noise. Group 3 performed a categorisation task between faces and textures. These task differences among studies

should not affect onsets because task effects on face ERPs are very weak or absent before the N170 time window (Rousselet, Gaspar, Wieczorek, & Pernet, 2011a; Philiastides, Ratcliff, & Sajda, 2006; VanRullen & Thorpe, 2001; Séverac-Cauquil, et al., 2000; Carmel & Bentin, 2002; Lueschow, et al., 2004; Furey, et al., 2006; Okazaki, et al., 2008). Also, as shown in the result section, there was no onset difference among the three groups. Detailed descriptions of experimental procedures and equipment are given in Rousselet, et al. (2009), Rousselet, et al (2010) and in Section 3.

5.1.3 EEG DATA PRE-PROCESSING:

EEG data were obtained in Canada using a 256-channel Geodesic Sensor Net (Electrical Geodesics Inc., Eugene, Oregon), and in the UK using a Biosemi Active Electrode Amplifier System with 128 electrodes. Data were pre-processed using Matlab 2012a and EEGLAB 11.0.2.1b (Delorme & Makeig, 2004; Delorme, et al., 2011). Data were first re-referenced off-line to an average reference. Subsequently, data were filtered independently in two different ways. First, to measure onsets, a 2 Hz causal 4^{th} order Butterworth high-pass filter was used to avoid onset distortion associated with non-causal filtering (Acunzo, MacKenzieb, & van Rossum, 2012; Widmann & Schroger, 2012; Rousselet, 2012). Second, a 1 Hz non-causal 4^{th} order Butterworth high-pass filter was upplied to perform independent component analysis (ICA). Due to high levels of power line noise, the Canadian datasets (group 1) were also low-pass filtered using a 30 Hz non-causal 4^{th} order Butterworth filter. Subsequently, all datasets were re-sampled at 500 Hz and epoched between -300 and 1000 ms around stimulus onset. In the causal filtered dataset, baseline correction was performed using the average activity between time 0 and -300 ms, whereas in the non-causal filtered dataset, individual channel mean was removed from each channel, which increases ICA reliability (Groppe, Makeig, & Kutas, 2009). Noisy electrodes were identified by visual inspection of the non-causal filtered data and rejected from causal and non-causal datasets. ICA was performed on the non-causal filtered data using the infomax algorithm as implemented in EEGLAB. Components representing blinks were then identified and removed from both causal and non-causal filtered datasets (number of ICs removed: median = 2, min = 0, max = 10). Subsequently, data were re-epoched between -300 and 600 ms and baseline correction was performed again. Finally, data epochs were removed based on an absolute threshold value larger than 100 µV and the presence of a linear trend with an absolute slope larger than 75 µV per epoch and R^2 larger than 0.3. Across subjects, the median number of trials available for

analyses was, for faces (session 1/session 2): 127/146; min = 27/92; max = 150/150; for textures: 127.5/146; min = 25/91; max = 150/150.

5.1.4 EEG DATA ANALYSIS:

Statistical analyses were conducted using Matlab 2012a and the LIMO EEG toolbox (Pernet, Chauveau, Gaspar, & Rousselet, 2011).

SINGLE SUBJECT DATA ANALYSES

To determine the onset of face ERP sensitivity, in every subject we computed t-tests between face and texture ERPs, independently at each electrode and each time point. Multiple comparisons correction was performed using a bootstrap spatial-temporal clustering approach (Rousselet, Gaspar, Wieczorek, & Pernet, 2011; Pernet, et al., 2011; Bieniek, Pernet & Rousselet, 2012).

Onsets obtained using t-tests with standard means were compared against those obtained with 20% trimmed means. T-tests on 20% trimmed means can help increase power and might reveal earlier onsets in noisier subjects (Wilcox, 2012; Rousselet, et al. 2008; Desjardins & Segalowitz, 2013). For t-tests on means the *limo_ttest* function was used and for t-tests on trimmed means the *limo_yuen_ttest* function (both functions are part of the LIMO EEG toolbox) was used. This comparison was performed on data without low-pass filtering (*mean* versus *tmean*), and after application of a 40 Hz low-pass 4th order Butterworth filter (*mean lp* versus *tmean lp*). This was done to check if low-pass filtering, as commonly applied in ERP research, produces signal distortions leading to artificially earlier onsets (VanRullen, 2011). This comparison was performed in 90 subjects only, because 30 subjects from the Canadian dataset had to be low-passed filtered during the pre-processing stage to reduce line-noise.

Onsets of ERP face sensitivity were defined as the first significant t-test at any electrode, after removing any significant cluster that started before stimulus onset, which happened in three subjects.

Effect Sizes

Measures of effect size typically used in psychology and neuroscience suffer from two major problems: they are not robust, and they are not intuitive (Cliff, 1996; Wilcox, 2006; Wilcox & Tian, 2011). Here, two powerful measures of effect sizes were used: *delta* (Cliff, 1996) and *Q* (Wilcox & Muska, 1999), which hopefully will gain in popularity.

Cliff's *delta* estimates the probability that a randomly selected observation from one group is larger than a randomly selected observation from another group, minus the reverse probability (Cliff, 1996). This statistic ranges from 1 when all values from one group are higher than the values from the other group, to -1 when the reverse is true. Completely overlapping distributions have a Cliff's *delta* of 0. Cliff's *deltas* of 0.15, 0.33 and 0.47 indicate 15%, 33% and 47% of non-overlap between distributions and correspond approximately to Cohen's d of 0.2, 0.5 and 0.8 – small, medium and large effects sizes (Cohen, 1988) - computed using the *delta2cohd* function from the *orrdom* package for R (Rogmann, 2013). Because *delta* is a statistic based on ordinal, rather than interval properties of the data, it is unaffected by rank preserving data transformations. Its non-parametric nature reduces the impact of extreme values or distribution shape (Hess & Kromrey, 2004). It is related to the Wilcoxon-Mann-Whitney *U* statistic (Birnbaum, 1956). However, the estimate of the standard error of *delta* makes it, in some situations, more robust and more powerful than *U* (Cliff, 1996). Also, contrary to *U*, *delta* is a direct measure of effect size, with an intuitive interpretation.

The *Q* statistic is also a non-parametric measure of effect size and ranges from 0 to 1, with chance level at 0.5. It is the probability of correctly deciding whether a randomly selected observation belongs to the first of two groups and it reflects the degree of separation between two groups (Wilcox & Muska, 1999). *Q* outperforms *d* in some situations. For instance, if two symmetric distributions do not differ in mean, but do differ in variance, large differences can occur in the tails of the distributions. In that case *d* will be close to zero, suggesting wrongly that the two distributions overlap. However, *Q* will be larger than 0.5, suggesting that the two distributions do not overlap. Delta and Q complement each other - the former incorporates the ordinal properties of data, whereas the latter looks at the overlap between two distributions.

The *delta* and *Q* statistics were calculated in Matlab R2012b, using code adapted from the WRS package (Wilcox and Schönbrodt, 2012) in R (R Core Team, 2012). In particular, the WRS function *cid* computes the *d* statistic. The WRS function *qhat* computes *Q*, using the adaptive version of the kernel density estimate (Silverman, 1986).

GROUP DATA ANALYSES

Distributions of results were quantified using the Harrell-Davis estimate of the deciles (Wilcox 2005, p. 71). 95% confidence intervals (CI) are reported in square brackets

throughout Section 4. These CIs were obtained using a percentile bootstrap procedure with 1000 samples (Rousselet, et al., 2010; Section 3).

Onset distributions

Adaptive kernel density estimates (KDE) of onset distributions were computed for each condition using the *akerd* function adapted from R (Wilcox, 2012, p. 51). Adaptive KDE uses the expected frequency as the initial density estimate (Silverman, 1986).

Shift Function

To quantify differences between deciles of onset distributions, the *shift function* for dependent groups (Doksum, 1974; Doksum, 1977) was used. The Matlab implementation presented here was based on Wilcox's R code and includes a correction for multiple comparisons (Wilcox, 2012). The following contrasts were considered: 1) *mean* vs. *mean lp*, 2) *mean* vs. *tmean*, 3) *tmean* vs. *tmean lp*, and 4) *mean lp* vs. *tmean lp*. Because there were no differences between onset distributions in any of these comparisons (Figure 4.2), all further analyses were only performed on the *mean lp* data.

Regression Analyses

Regression analyses were performed to determine if there is a relation between: ERP onsets and age; ERP onsets and effect sizes at onset times; effect sizes and age. To this end group level regressions were computed using Matlab's *robustfit* function, with default parameters. I report slopes and intercepts along with percentile bootstrap confidence intervals (CIs) calculated in the following way. Subjects were sampled with replacement, and this bootstrap sample was used to estimate the regression slopes and intercepts. This sampling with replacement was performed 1000 times, and each time the slopes and the intercepts were saved. Then, the 2.5 and 97.5 percentiles were used to form the boundaries of 95% bootstrap confidence intervals, reported in square brackets.

Test-retest Comparison

To determine the reliability of onset estimates, the distribution of onset differences between two experimental sessions (n=74) was quantified using a shift function, KDEs, and Harrell-Davis estimates of the deciles of this distribution.

Onset differences among groups

To test if onsets of face sensitivity differed across the three groups of subjects a one-way ANOVA (*anova1* function in Matlab) was calculated. There were no onset differences among the three groups of subjects in session 1 ($F(2, 117) = 0.26$, $p = 0.77$),

and between the two groups of subjects in session 2 ($F(1, 72) = 0.21$, $p = 0.65$). Regression analysis was also performed (using *glmfit* function in Matlab, with default parameters) to test if onset variability could be explained by subjects' age, visual acuity, contrast sensitivity years of education or sex (Equation 3). None of these variables significantly predicted onset times (Table 5.2).

$$ONSET = \beta_1 Age + \beta_2 VA + \beta_3 CS + \beta_4 YE + \beta_5 SEX + \beta_0 + \varepsilon \quad (3)$$

	Age	Visual acuity	Contrast sensitivity	Years of education	Sex
Beta coefficient	0.01	1.1	5.7	-0.3	8.4
T statistic	-0.1	0.1	0.2	-0.4	1.8
p-value	0.9	0.9	0.9	0.7	0.1

Table 5.2. *GLM regression of age, visual acuity, contrast sensitivity, years of education and sex as predictors for onset times.*

Monte-Carlo simulations

Monte-Carlo simulations were used to estimate how group median onsets and median test-retest differences changed as a function of the number of subjects. To this end, samples of subjects were drawn from a total pool of 120 subjects: from 5 to 70 subjects, in steps of 5 (fourteen levels). For each sample size, subjects were sampled with replacement 10,000 times, and every time the median onset and the between session median onset differences were computed. The variability among Monte-Carlo estimates was quantified using the inter-quartile range (IQR), which was measured using the *idealf* function adapted from R (Wilcox, 2012). Confidence intervals around the IQRs were calculated using the standard percentile bootstrap procedure.

Control Experiment Methods

So far, parametric analyses of univariate differences in means and trimmed means between distributions of face and noise ERPs were described. But single-trial ERP distributions could in principle differ not only in location, but also in dispersion, skewness, and kurtosis. Differences between ERP conditions could also be distributed across electrodes. So, in order to check if the univariate tests did not miss earlier onsets and if the face onsets measured in the main experiment were comparable to onsets involving other image categories, ERP data from my recent publication (Bieniek, et al., 2012; Experiment 1) was re-analysed using variety of tools. In short, experimental procedure involved eight observers who categorised pictures of faces, houses, and noise textures, presented for 53 ms. Seven observers were tested twice. There were up to 1000 trials per observer in total:

300 face trials, 300 house trials, 300 trials of phase noise textures with the same amplitude spectra as faces and houses, and 100 white noise trials. EEG pre-processing was as described in Section 2, except that the causal filtered data, used to measure onsets, were not low-pass filtered at all, and were transformed into single-trial spherical spline current source density waveforms using the CSD toolbox (Kayser and Tenke, 2006; Tenke and Kayser, 2012). This transformation facilitates more focal locating of neural signal generators. CSD waveforms were computed using parameters 50 iterations, m=4, lambda=10^{-5}. The head radius was arbitrarily set to 10 cm, so that the ERP units in all the figures are $\mu V/cm^2$.

Several statistical tests were used to check if the univariate tests that look for differences between face and noise ERPs using means of ERP distributions did not miss earlier onsets. Onsets were defined by differences among all conditions (one-way ANOVA or equivalent), and differences between pairs of conditions. One-way ANOVA and linear contrasts (t-tests) on means were performed with the LIMO EEG toolbox (Pernet, Chauveau, Gaspar, & Rousselet, 2011). Linear contrasts on 20% trimmed means were computed using a Matlab version of Wilcox's *lincon* R function (Wilcox, 2012). 2-sample Kolmogorov-Smirnoff tests were performed using Matlab's *kstest2* function. Kolmogorov-Smirnoff test is a non-parametric test useful in comparing the distance between two distributions and is sensitive to both, the location and the shape of the cumulative funsions of the two distributions. Also, two types of mutual information (MI) were calculated: between ERP amplitudes and image categories (MI_{cat}), and between ERP amplitudes and image pixels (MI_{pix}). Mutual information measures a mutual dependence between two variables and has been recently gaining in popularity due to its usefulness to quantify how information about external correlate is coded in neural response on a single trial basis. For MI_{pix}, the maximum across pixels was used as summary statistics. MI was calculated using an open access Matlab toolbox (Ince, Mazzoni, Petersen, & Panzeri, 2010; Magri, Whittingstall, Singh, Logothetis, & Panzeri, 2009) with the direct method, quadratic extrapolation bias correction, and four equipopulated bins for image pixels and ERP amplitudes. To look for multivariate effects across electrodes multivariate logistic regression was used, independently at each time point, a one time-frame training window, and a leave-one-out cross validation (Parra, Spence, Gerson, & Sajda, 2005; Philiastides & Sajda, 2006) Finally, variance, skewness and kurtosis were compared between pairs of conditions.

Onsets were measured using bootstrap clustering techniques with 1000 bootstrap samples (Pernet, et al., 2011; Rousselet, et al., 2011) except for logistic regression, for which 200 bootstraps were used because it was extremely time-consuming. In the result section, I report, for every statistical test, the minimum onset across the two sessions for the seven subjects tested twice, and the single onset for the 8th subject.

5.2 RESULTS

Using t-tests with means on low-pass filtered data revealed a median onset of 87 ms [81, 94] in session 1, and a mode of 74 ms (Figure 5.1). The 1st decile of the distribution was 68 ms [64, 73], and the 9th decile was 119 ms [113, 125]. These estimates were reliable across testing sessions, and they did not change for data that were not low-pass filtered, or when 20% trimmed means were used instead of means.

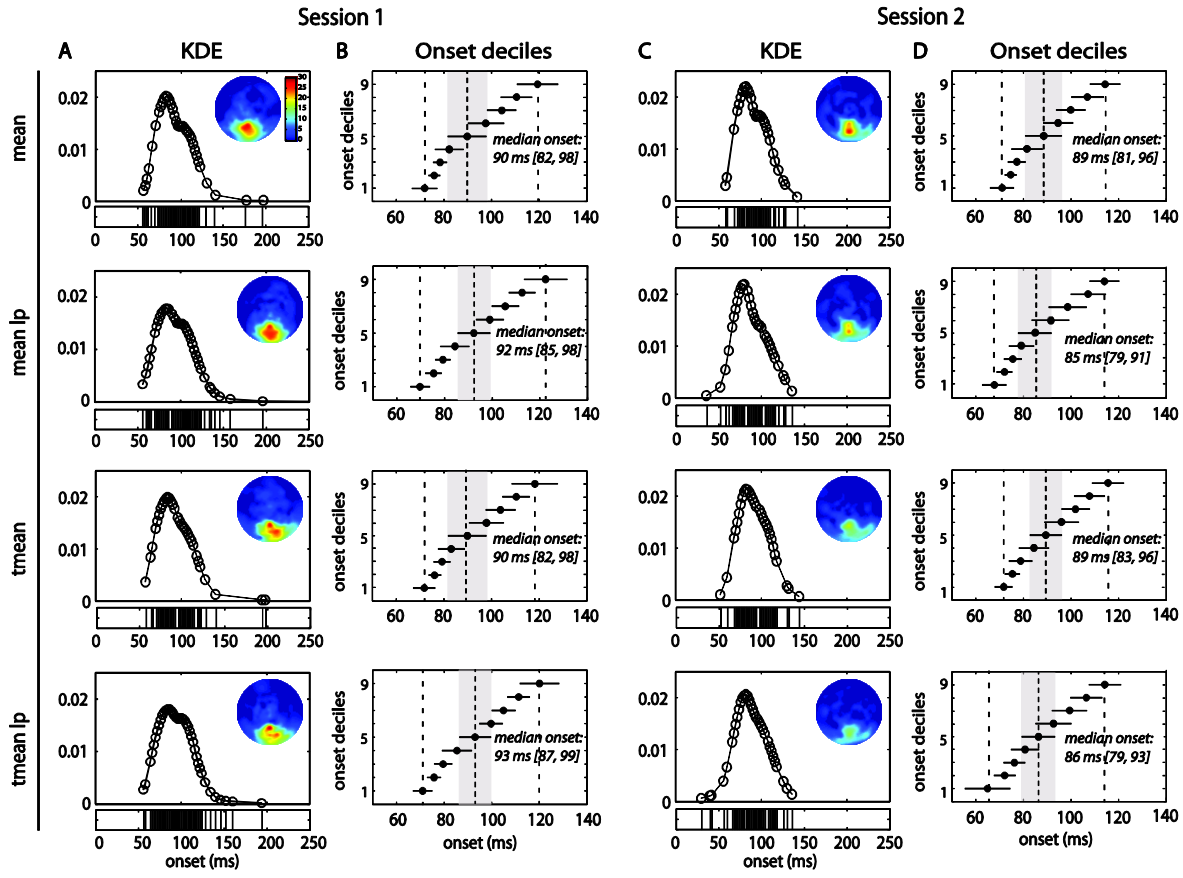

Figure 5.1. *Onset distributions* ***(A, C)*** *Kernel density estimates of onset distributions for each of the 4 conditions (mean, tmean, mean lp and tmean lp). The circles on each plot indicate the estimated frequencies of onsets. Horizontal plots underneath the KDEs depict onsets from individual subjects (one tick per subject). Topographic maps show how many subjects had onsets on each electrode* ***(B, D)*** *Deciles of onset distributions with 95% CIs. The vertical middle dashed line in each plot marks the median and the*

shading highlights the boundaries of the median's CI, which is also given in square brackets. The other two vertical dashed lines indicate the 1st and the 9th deciles

No significant differences were found between any deciles of onset distributions for *mean* vs. *tmean*, *mean lp* vs. *tmean lp*, *mean* vs. *mean lp*, *tmean* vs. *tmean lp*. Results for session 1 are illustrated in Figure 5.2, and were similar in session 2. These results indicate that low-pass filtering or using trimmed means instead of means, does not significantly affect any part of the distributions of face ERP onsets.

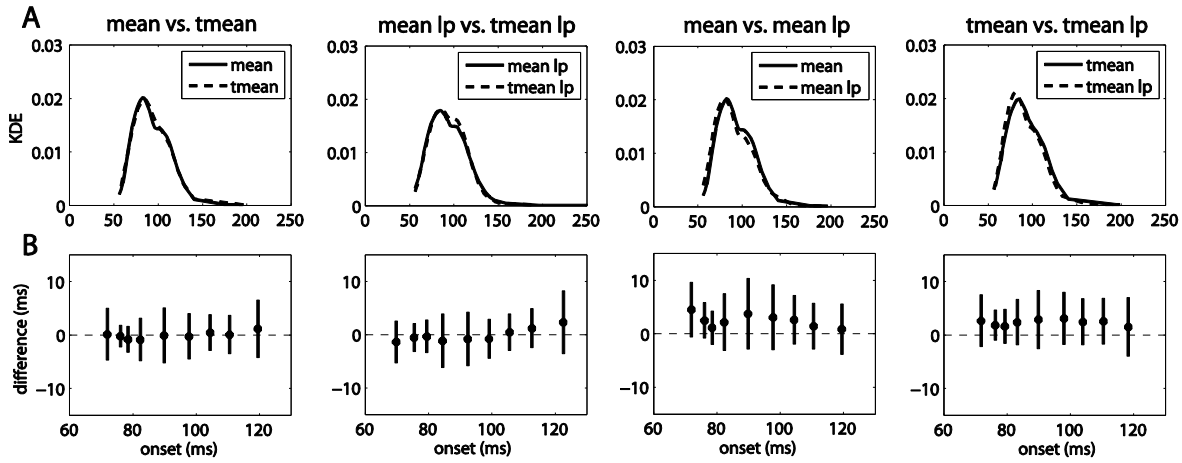

Figure 5.2. *Comparisons of onset distributions.* ***(A)*** *Comparisons of kernel density estimates of onset distributions.* ***(B)*** *Differences between deciles of onset distributions (black dots) with 95% CIs (vertical lines) computed using shift functions for dependent groups. (A) and (B) show data for session 1. Similar results were observed in Session 2.*

Data presented here were from subjects 18 to 81 years old. Thus, I looked at the relationship between ERP face onsets and age, and found no evidence for an aging effect (Figure 5.3), which confirms previous observations (Section 3).

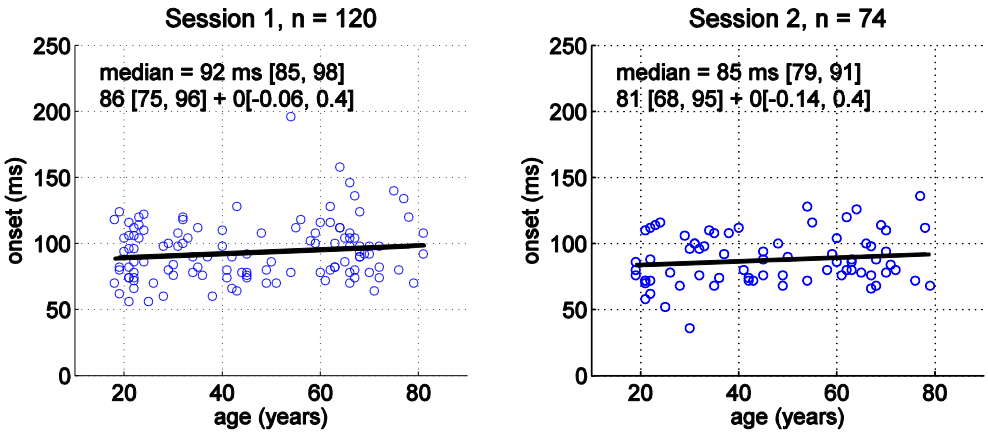

Figure 5.3. *Regressions of onsets against age. Each circle represents the onset from one subject. The regression line appears in black The group median onset and its 95% CI is indicated at the top of each scatterplot. Below the median are regression equations with intercepts and slopes and their corresponding 95% CIs. Both scatterplots contain mean lp data; n = number of subjects.*

The next aim was to look at how big the effects were at onset times (Figure 5.4). In the majority of subjects, *deltas* ranged from 0.1 to 0.3, which corresponds to about 1% to 45% of non-overlap between face and texture ERPs (and to small-medium effect sizes in Cohen's d framework). There was no significant relationship between onset latencies and effect sizes, measured using either *delta* or *Q* (Figure 5.5 A), which means that later onsets were not for instance systematically associated with smaller effect sizes compared to earlier onsets. Effect sizes also did not depend on subjects' age, indicating that aging did not affect the size of earliest face ERP differences (Figure 5.5 B).

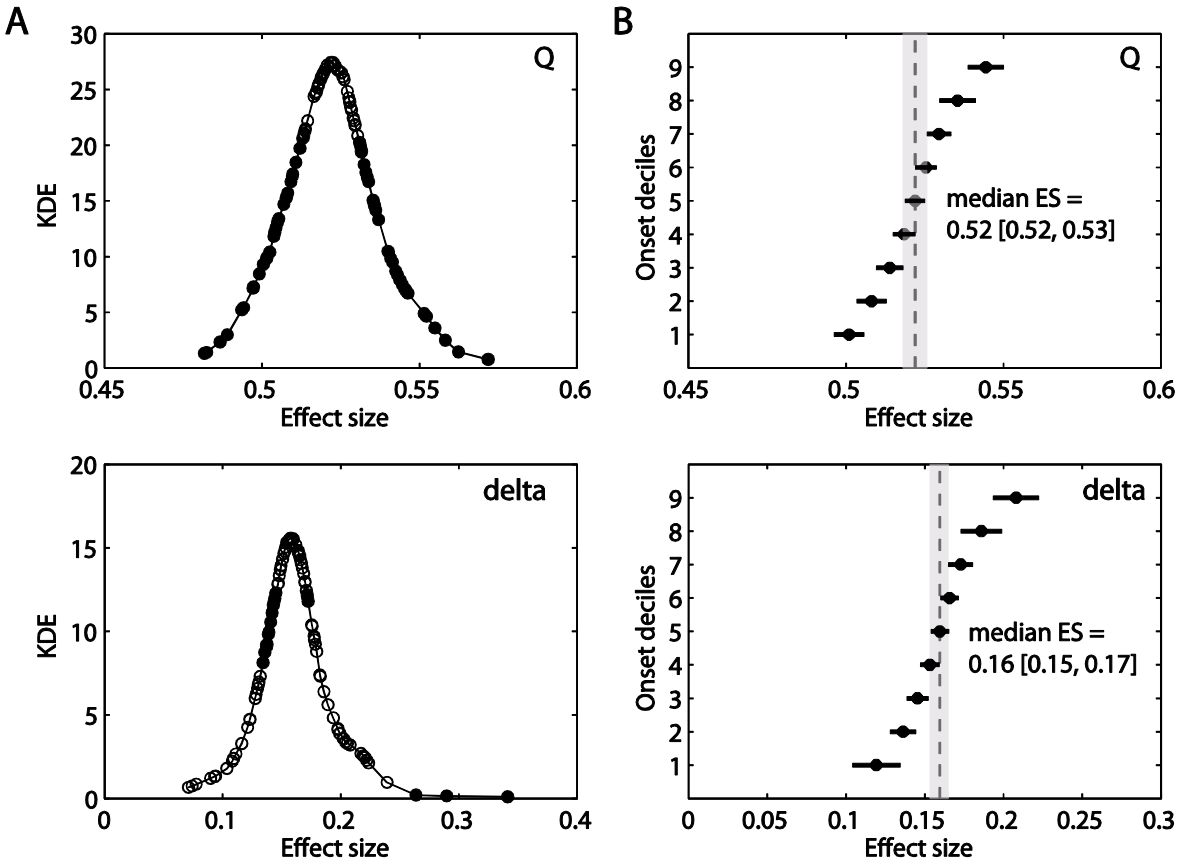

Figure 5.4. *Distributions of effect sizes at onset times.* ***(A)*** *KDEs of effect size distributions.* ***(B)*** *Deciles of effect size distributions with 95% CIs. Both* ***(A)*** *and* ***(B)*** *show data for mean lp condition, session 1. Similar results were observed in session 2.*

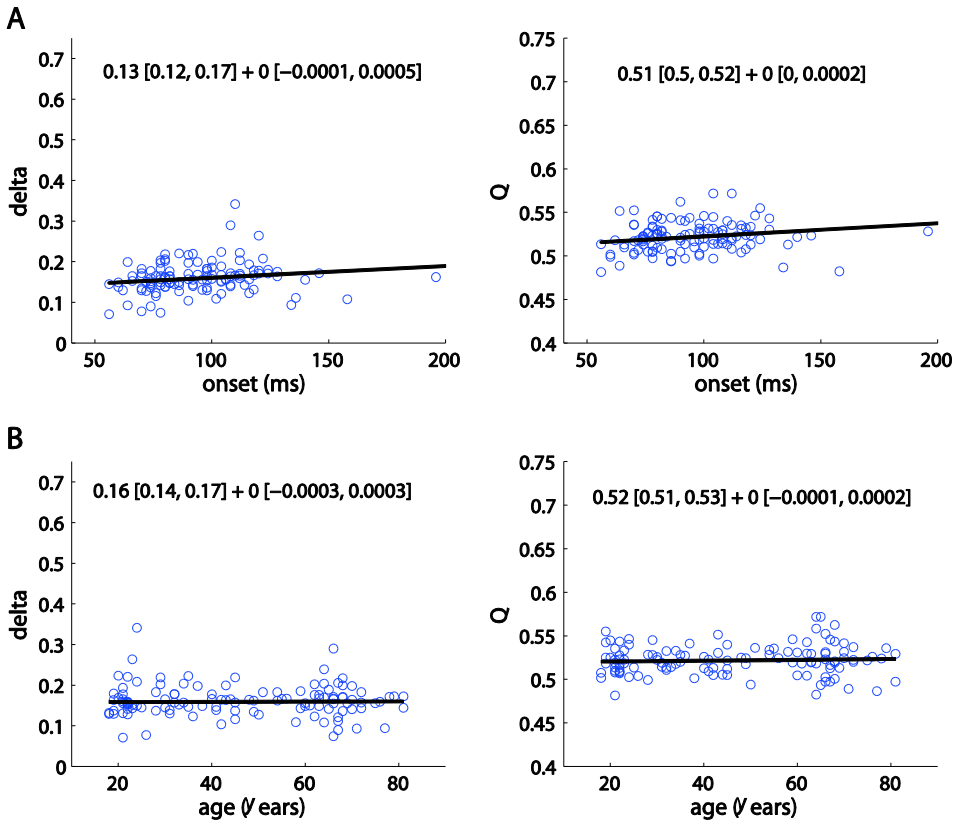

Figure 5.5. *Effect sizes as a function of onset time* ***(A)*** *and age* ***(B)****. The regression equation with intercept and slope and their corresponding 95% CIs is given at the top of each scatterplot. Both (A) and (B) show data for mean lp condition, session 1 (number of subjects, n=120). Similar results were obtained in session 2.*

The analysis of the test-retest differences revealed reliable ERP onsets between experimental sessions. For the 74 subjects tested twice, no significant differences were found between onset deciles obtained in the two sessions (Figure 5.6).

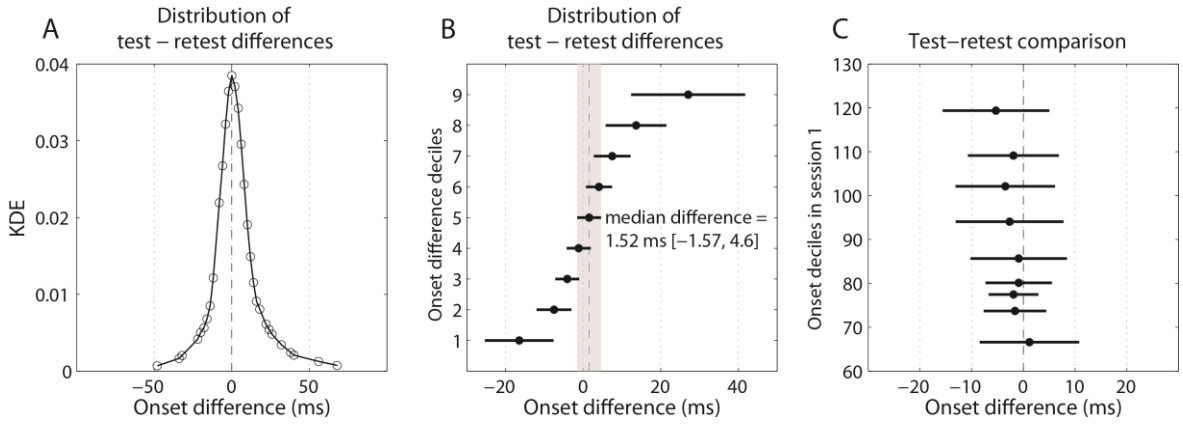

Figure 5.6. *Test-retest differences between experimental sessions.* ***(A)*** *Kernel density estimate of the distribution of onset differences between sessions. Deciles of this distribution, along with their 95% CIs, are shown in panel* ***(B).*** ***(C)*** *shows the results of the shift function analysis comparing onset distributions between sessions in the mean lp condition. Dots represent differences in onset times between sessions at each decile of session 1 onsets; horizontal lines mark the boundaries of the 95% CIs around these differences.*

The variability in median onsets as a function of sample size was estimated using Monte-Carlo (MC) simulations. Medians of MC estimates of onsets and onset differences between sessions changed very little as a function of sample size, but they tended to be larger for smaller samples (Figure 5.7 A). This result indicates that in the long run, smaller sample sizes would tend to over-estimate processing time. The inter-quartile range (IQR) of each MC distribution followed an exponential decay as sample size increased, for both median onset distributions and median onset differences between sessions (Figure 5.7 B). In particular, the right side of the median distributions is much more strongly affected than their left side: this shows that, in the long run, testing at least 20 subjects would help reduce the risk of over estimating onsets and would increase their reliability.

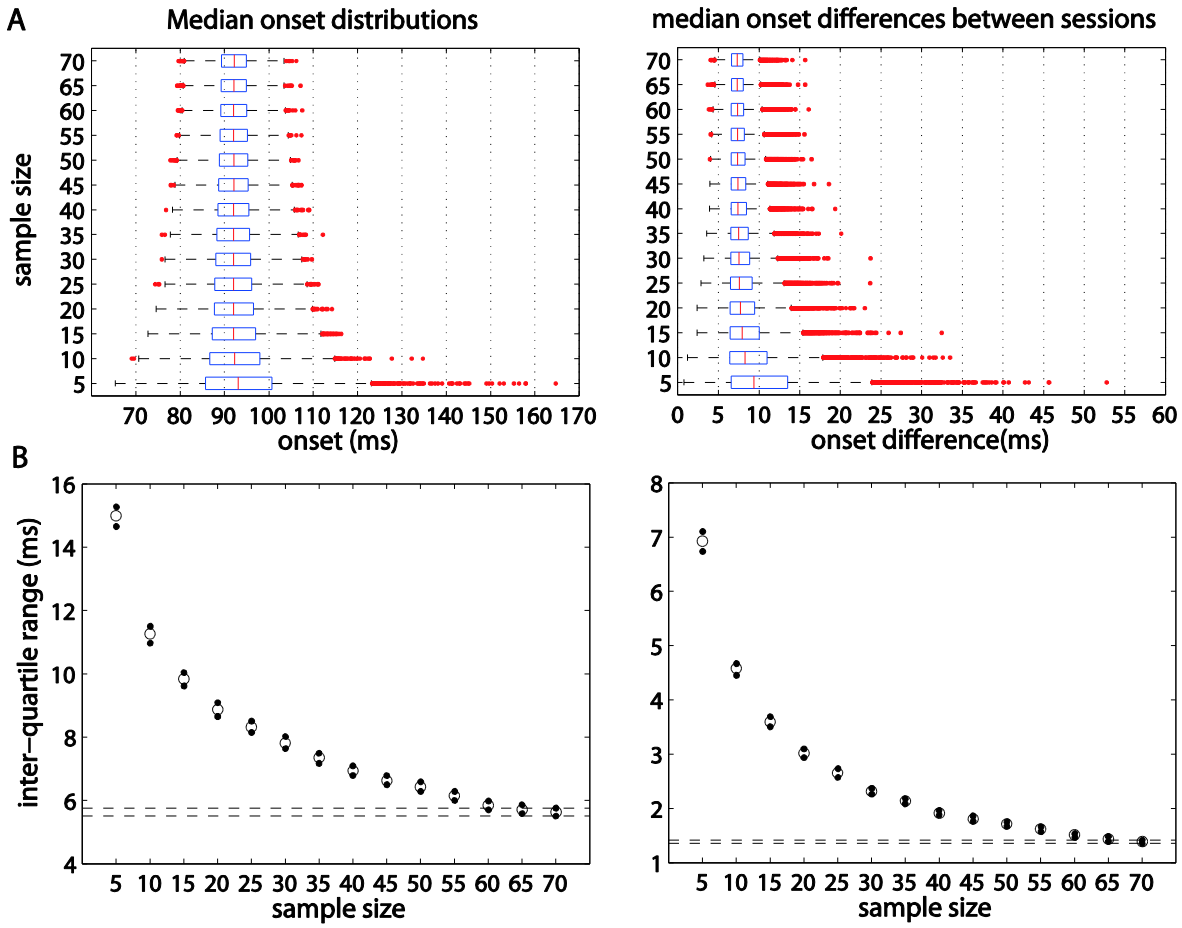

Figure 5.7. *Monte-Carlo estimates of median onsets and median onset differences between sessions as a function of sample size.* ***(A)*** *Boxplots of MC median onset estimates. The red vertical line within each boxplot indicates the median, the extremities of the blue box indicate lower and upper quartiles, and whiskers extend to the most extreme data points, not including outliers, which are marked individually by red dots.* ***(B)*** *IQR of median onsets and median onset differences between sessions. Black dots indicate the boundaries of 95% confidence intervals. The dashed horizontal lines mark the edges of the confidence interval for the IQR obtained with a sample size of 70 subjects.*

Results from the control experiment

The goal of the control experiment was to test in an independent dataset (n = 8) if any earlier onsets have been missed because of differences not captured by parametric comparisons of central tendency. We also tested whether similar onsets would be observed for a control object category (houses) and between our structured textures and a control texture (white noise). For each of the 8 subjects — 7 of which were tested twice (for a total of 15 EEG sessions) — we looked for differences in mean, variance, skewness and kurtosis between four pairs of image categories: textures vs white noise, faces vs. textures, houses vs. textures, and faces vs. houses. Within 200 ms all pairwise comparisons were only significant for means. Differences in skewness and kurtosis were observed beyond 200 ms in a few subjects and only in one of their sessions. Corroborating this result, in every subject and for every contrast, kernel density estimates and shift functions revealed uniform shifts in the single-trial distributions at onset times. We confirmed that categorical ERP differences were essentially due to differences in means by measuring onsets using a range of robust and non-parametric techniques (Figure 5.8). Onsets derived from a one-way ANOVA and t-tests on means were similar to those reported in the main experiment. Results from the other methods were very similar, or led to delayed onsets. Thus, the results from the control experiment suggest that t-tests on the mean, combined with modern control for multiple comparisons, are adequate and sufficient to capture early differences in single-trial ERP distributions. In addition, all pairwise contrasts tended to have the same median onsets, except for t-tests on trimmed means. This goes against the naive hierarchy that would see first emerge differences between textures and white noise, then between textures and objects (with perhaps a face advantage), and finally between faces and houses. Hence, these early ERP differences might correspond to a stage of processing involving the extraction of coarse image statistics (Groen, Ghebreab, Prins, Lamme, & Scholte, 2013).

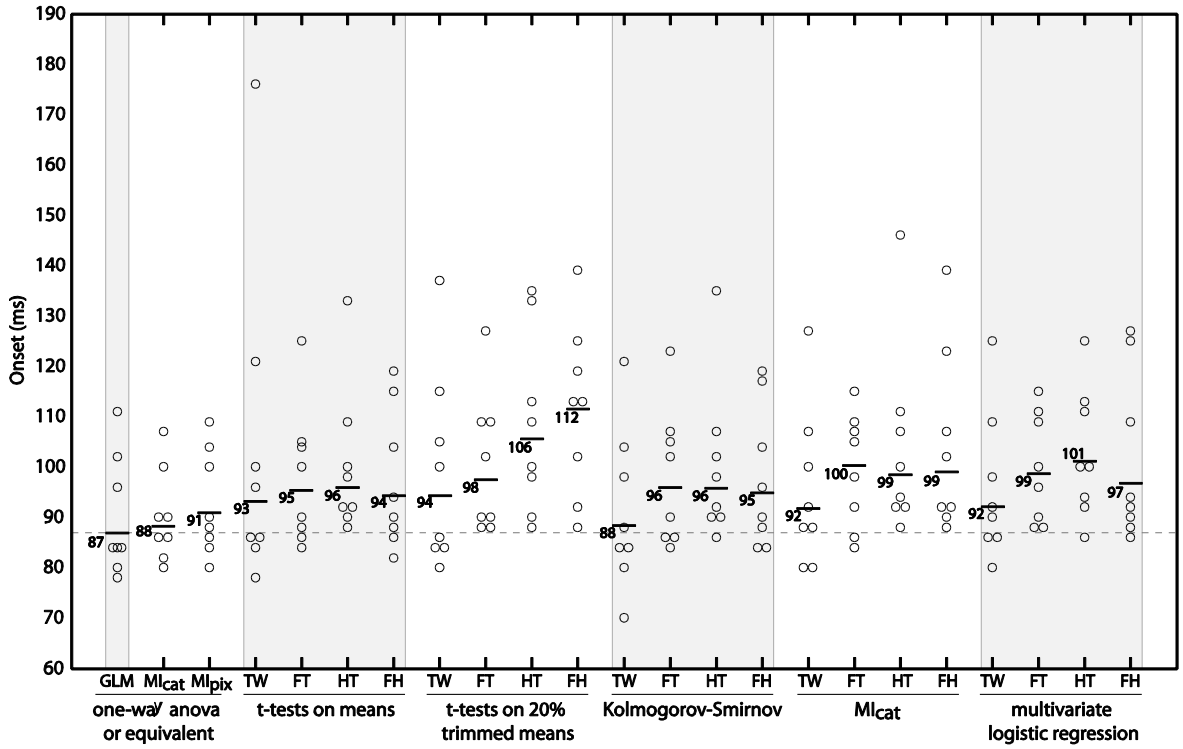

Figure 5.8. *Comparison of onsets from the control experiment. The scatterplots show the onsets of eight subjects, in six families of statistical tests. For the seven subjects that were tested twice, we report their minimum onset (across sessions), for each test. The horizontal bars indicate median onsets (ms). The one-way ANOVA or equivalent tests were performed on the four image categories (W, T, F, H). The other tests involved pairwise comparisons. Abbreviations: GLM=one-way ANOVA on mean; MIcat=mutual information between image categories and ERP amplitudes; MIpix=mutual information between image pixels and ERP amplitudes; W=white noise; T=textures with amplitude spectra matching those faces and houses; F=faces; H=houses.*

5.3 DISCUSSION

ERP face sensitivity onsets were measured in a sample of 120 healthy subjects, aged 18-81 years old. Across subjects, the median onset was 87 ms [81, 94] and this value did not depend on whether EEG data were low-pass filtered or not, or whether we used trimmed means or means across EEG trials. Extending this result, the control experiment suggested that categorical ERP differences at onset time essentially reflect shifts in the means of single-trial distributions, so that statistical tests sensitive to other distributional differences other than the mean did not provide earlier onsets. ERP face onsets also did not change with age, replicating previous observations and suggesting that aging affects face processing beyond the earliest face detection stage (Section 3). Further, no relationship between effect sizes and face ERP onsets was found, suggesting that the large individual differences in onset times (Figure 5.5) were not associated with systematic differences in signal-to-noise ratio across subjects. We also know from the previous Section that

individual differences do not seem to be due to optical factors, such as differences in retinal illuminance. In the present study onset estimates were reliable, with only about 5-10 ms difference between two experimental sessions conducted on separate days, which is consistent with studies showing the stability of scalp and intracranial ERPs across hours and days (Hamerer, Li, Volkle, Muller, & Linderberger, 2013; Bansal, et al., 2012). Finally, Monte-Carlo simulations revealed that small subject sample sizes could lead to under-estimated processing speed and test-retest reliability.

What are the cortical origins and the information content of the face ERP differences around 87 ms? It seems that striate and some extrastriate visual areas could be associated with the onset activity, which in turn might reflect complex shape detection and possibly signal the presence of a face. The present results are compatible with a growing number of studies showing face- and object-sensitive neuronal activity within 100 ms.

5.3.1 CORTICAL ORIGINS OF ERP ONSETS

Face-sensitive M/EEG responses before 100 ms tend to appear around medial and inferior occipital brain/scalp regions, around the location of striate and extra-striate visual areas (Linkenkaer-Hansen, et al., 1998; Halit, et al., 2000; Rivolta, et al., 2012). It is uncertain though if at the time of the 87 ms onset, object and face-associated areas are already active. Activity in the lateral occipital cortex (LOC) that seem to be involved in a general shape processing of all kinds of objects (Grill-Spector, Kourtzi, & Kanwisher, 2001) starts to be visible already before 100 ms post-stimulus (Ales, Appelbaum, Cottereau, & Norcia, 2013). LOC also responds stronger to intact versus scrambled pictures of objects (Malach, et al., 1995). More specifically for face stimuli - recent EEG and concurrent EEG-fMRI studies have suggested dissociation between cortical contributors to face-related activity around 100 ms and around 170 ms (Desjardins & Segalowitz, 2013), linking the former with the OFA, and the latter with the FFA and the STS (Nguyen, et al., 2014; Nguyen, et al., 2013; Sadeh, et al., 2010). Several studies using depth recordings in the fusiform gyrus reported local field potentials (LFPs) in response to faces peaking at various times after 100 ms (Allison, Puce, Spencer, & McCarthy, 1999; Halgren, Baudena, Heit, Clarke, & Marinkovic, 1994; McCarthy, Puce, Belger, & Allison, 1999; Puce, Allison, & McCarthy, 1999; Barbeau, et al., 2008). However, none of these studies have reported the onsets of the responses, thus it is difficult to directly relate them to the results obtained here. In monkeys, single cell recordings suggest that the earliest responses to faces can be present as early as ~60 ms in the anterior middle temporal sulcus (Kiani, et al., 2005), the PL face patch in the IT cortex (Issa & DiCarlo, 2012) and parts of

the STS (Edwards et al., 2003; Sugase, et al., 1999). If one was to apply the 3/5 ratio rule for extrapolating from monkey to human responses latencies (Schroeder, et al., 2004), it seems that we can expect the earliest face-sensitive activity in human IT and STS to occur ~ 100 ms. However, comparisons between monkey and human face processing systems are rendered difficult because of uncertainty in anatomical and functional equivalence (Yovel & Freiwald, 2013; Orban, Van Essen, & Vanduffel, 2004). Therefore, it seems that the 87 ms onset activity might involve visual areas up to and including general shape processing regions (LOC), and perhaps some nodes of the face-related cortical network (OFA). However, this suggestion has to be tested directly in future studies, perhaps by looking again into the collected intracranial data.

5.3.2 INFORMATION CONTENT OF ONSET ACTIVITY

Previous research suggests that our early face ERP onsets could be related to either categorical face detection or non-categorical general shape processing. Studies in monkeys and humans suggest that sensitivity to face features, and in particular the eye area, starts before 100 ms (Issa & DiCarlo, 2012; Smith, et al., 2009). In humans, early face-sensitive activity has been linked with the OFA and it has been suggested that the OFA might be involved in face detection (Schwarzlose, et al., 2008) and processing of face parts (Pitcher, et al., 2011); also, the OFA could be an equivalent to the PL face patch in monkeys, thought to support intermediate stages of face processing (Issa & DiCarlo, 2012; Tsao, et al., 2008; Fairhall & Ishai, 2007; Nguyen, et al., 2013). However, the OFA has also been found to support the processing of non-face objects and 2D shapes (Gilaie-Dotan, et al., 2008; Silvanto, et al., 2010). Also, the OFA seems to be sensitive to changes in face stimuli without subjects being aware of these changes behaviourally, which contradicts the hypothesis of the OFA as a face detector (Fox, et al., 2009; Large, et al., 2008). It is therefore possible that the onset activity observed in the present study did not represent face sensitivity *per se*.

Instead, it is possible that the onset reflects more general shape processing, perhaps involving detection of complex structures in a stimulus, irrespective of their category. Support for this interpretation comes from studies that applied pattern classifiers to M/EEG data. The classifiers were able to decode stimulus category (faces, natural scenes, tools, bodies) with above chance accuracy from the activity in occipital lobe and the inferior occipital gyrus (where the OFA is located) already from 60-95 ms onwards (van den Nieuwenhuijzen, et al., 2013; Carlson, et al., 2013; Cauchoix, et al., 2014; Isik, et al., 2013), and in the fusiform gyrus from 100 ms onwards (Liu, et al., 2009). By looking at the

information content of images, Cauchoix, et al. (2014) discovered that the classifier's performance under 100 ms was largely related to low-level stimulus characteristics, in particular the distribution of image pixel intensities. This distribution reflects image complexity and has been found to explain a large proportion of variance in single-trial ERP distributions (Groen, et al., 2012). In particular, contrast energy modulates ERP responses before 100 ms (Groen, et al., 2013). The latency and mid-line distribution of the effects reported by Groen, et al. (2013) are consistent with our own findings. The results of our control experiment show that the time when ERP responses evoked by distinct images started to diverge was similar, regardless of which image categories were contrasted. This provides further support for the interpretation that the first electrophysiological activity sensitive to differences in visual input is not category specific. In another study, Tanskanen, et al. (2005) demonstrated that mid-occipital MEG activity 70 – 120 ms is not sensitive to the visibility of a face but to manipulations of image spatial frequency. More direct evidence for general complex shape processing around 100 ms comes from LFP recordings from face-selective patches in monkey STS showing that only the activity after 130 ms, but not around 100 ms post-stimulus, is category specific (Tsao, et al., 2006). Further, activity in the fusiform gyrus around 100 ms has also been observed in response to geometric shapes (Barbeau, et al., 2008), and there is growing evidence that FFA is functionally subdivided and involved in processing of objects other than faces (Hanson & Schmidt, 2011; Haxby, et al., 2001; Gauthier, 2000; Mur, et al., 2011; Huth, et al., 2012; Cukur, et al., 2013; Grill-Spector, et al., 2006). It has been also shown that single cells in monkeys' V4 respond better to convex angles and curves than to lines and edges, and that population activity between 70-160 ms represents boundary features and can be used to reconstruct object's shape (Pasupathy, et al., 1999; 2002). Because faces contain many curvatures, they might be particularly effective in driving V4 responses.

Overall, it is possible that the early face onsets observed in the present study reflect some form of face processing, but it could also be associated with general shape detection. Irrespectively of whether the onset activity is face-sensitive or not, this finding establishes a lower benchmark for the earliest ERP responses to complex objects in the human visual system.

6 General Conclusions and Future Directions

Motivated by the inconsistencies and methodological shortcomings in visual neuroscience, this research has been the first to offer a systematic quantification of ERP processing speed of complex objects in the human brain, the ERP sensitivity to stimulus properties as well as the influence of aging and optical factors on processing speed. Instead of relying on categorical experiment designs, ERP peak analyses, small samples, group averages, and p-value-based statistics, I employed parametric designs, analysed the entire ERP time-course on a single subject basis, applied robust statistics, tested large samples of subjects with a broad age range, and assessed the reliability of my results.

The first experimental section of this thesis (Section 2) provided a comprehensive account on the sensitivity of visual ERPs to low-level image characteristics, in particular Fourier phase and amplitude spectra. I have shown that early (< 200 ms) ERPs to faces and objects are driven by edges and contours within an image, contained in the phase spectrum, with almost no contribution from the amplitude spectrum. The amplitude spectrum conveys information about the non-localized spatial frequency content of an image and some researchers have argued that it could be used by the brain to categorise objects, as reflected by the modulation of BOLD and ERP responses. However, no study has actually computed the relative contribution of phase and amplitude information to early ERPs to faces and objects. My work fills this gap by providing the first systematic quantification of ERP sensitivity to phase and amplitude spectra using a range of state-of-the-art analysis techniques, including detailed single-subject general linear modeling of ERP data, test-retest reliability, and unique variance analyses. The results emphasize the need for stimulus control (including the amplitude spectrum), parametric designs, and systematic data analyses, of which we have seen far too little in ERP vision research.

Empirical evidence presented in Section 3 confirmed the previous finding of Rousselet, et al. (2010) that early ERPs to faces are delayed with aging by 1 ms/year, and extended it by demonstrating that these delays are of a cortical, rather than optical, origin. Large inter-subject variability in processing speed within and between age groups has not yet been accounted for in the current research. Experiment 1 showed that individual

differences in processing speed, as reflected in ERP responses collected from 59 subjects, age 18-79, cannot be explained by senile miosis or individual variability in pupil size. Experiment 2 (Section 4) complemented these findings by showing that ERP processing speed of old and young subjects cannot be matched by manipulating their retinal illuminance. Both experiments showed that age-related slowdown in visual processing speed is not related to optical factors. In addition, the study challenged the notion that only activity ~100 ms is affected by stimulus' luminance, and demonstrated that changes in luminance modulate the entire ERP time-course, from 60 – 500 ms. Finally, by analysing the entire ERP time-course 0-500 ms point-by-point I was able to show that the earliest ERP sensitivity to faces was already present ~ 90 ms post-stimulus, while aging effects on the ERPs began around 125-130 ms and were the strongest around 200 ms. This suggests that the visual system detects faces very rapidly, and that aging starts to affect visual processes within 35–40 ms after the detection. Thus, the results confirmed previous findings that aging effects vary in strength across different parts of ERP waveform (Rousselet, et al., 2010) and, for the first time, showed that the onset of ERP face processing is not affected by senescence.

Section 5 presented the extension of previous results – a project that employed the largest to-date sample of 120 subjects, age 18-81, to measure the onsets of ERP sensitivity to faces. Existing studies report conflicting findings with regards to latencies of early face-related ERP responses. This may be due to several reasons: restricting analyses to ERP peaks, group averages, or filtering methods of EEG data that may distort the timings of the effects. In my final study, I used causal filters that preserve onsets, time-point-by-time-point ERP analyses and robust statistical methods to quantify onsets at a single-subject level. I also assessed the reliability of my results by testing subjects on two separate days. The analyses revealed the median ERP face sensitivity onset of ~90 ms, which was not affected by aging and reliable across testing days. This study established a benchmark for the earliest ERP responses to complex objects in the human brain appearing at around 90 ms.

Potential limitation of the projects outlined in this thesis is lack of control over subjects' eye movements. However, subjects were instructed to fixate on the cross in the centre of an image and the stimuli were presented very rapidly (between 53 -104 ms), preventing exploratory eye movements. Moreover, ICA components related to eye movements were rejected from the EEG data during the pre-processing stage.

All in all, the experimental work described in this thesis has furthered the knowledge with regards to the speed of complex objects processing in the visual system, its modulation by aging, optical factors and image properties. I am hopeful that the results of this research will prompt further investigation in this area and encourage a more rigorous approach to neuroimaging and behavioural data analyses in cognitive neuroscience.

Moving forward from this work, there is still much research to be done to fully encapsulate the neural processes underlying object categorisation. We only partially understand how basic visual information such as contrast, luminance or colour is implemented in the human brain, let alone representations of complex objects, such as faces. EEG research has a great potential to provide insights into the temporal dynamics of object processing, but many challenges remain. The biggest of these is probably to understand how exactly cognitive processes are reflected in the shape of ERP waveforms. The relationship between brain activity, behaviour and information available to the visual system on a single-ERP-trial basis is only beginning to be addressed.

An obvious question that could be asked as an extension to this research is which brain areas the ERP aging effects were associated with. Since the effects started ~125-130 ms post-stimulus, it is possible that regions involved in object processing before that time are spared from the adverse impact of advanced age. Some indication that this might be the case comes from fMRI evidence showing age-related dedifferentiation in the fusiform gyrus but not in the OFA or the STS (Park, et al., 2012). On the other hand, age-related slowdown has been observed already before 100 ms in V1 (except layer 4) and V2 in monkeys (Wang, et al., 2005). However, it is uncertain to what extent aging effects reported in non-human primates correspond to those that can be found in humans. Thus, one of the ways forward could be to simultaneously address the age-related slow down in neuronal activity and cortical sources associated with it, for example using MEG. The advantage of this method is both, high spatial and high temporal resolution of the recordings. Another way to investigate which brain areas are spared, and which are subject to aging effects is to use simultaneous EEG, fMRI and DTI recordings. These methods provide complementary information with regards to the timing, locations, and the connectivity between the locations that contribute to object categorisation processes. Finally, analyses based on ICA components can provide information with regards to age-related changes in scalp spectral measures with very little intercorrelation. Because ICA components relate to activity of various brain regions, they could enhance our

understanding about alterations in cortical correlates of aging effects. New developments will hopefully help to create models of the visual system that not only incorporate various levels of neuronal information processing, from activity of single cells to large populations of neurons, but also integrate a dynamic dimension to the models, reflecting changes related to aging.

It would be also interesting to find out if aging effects are also visible in the time-frequency dimension of my EEG data. Research shows that healthy aging is associated with changes in the alpha band activity (8-12 Hz), and this effect might be related to different attention control in the elderly (Deiber, Ibanez, Missonnier, Rodriguez, & Giannakopoulos, 2013; Zanto, Pan, Liu, Bollinger, Nobre, & Gazzaley, 2011). Age-related changes in other frequency bands, such as theta or beta have also been observed (van de Vijver, Cohen, & Ridderinkhof, 2014; Deiber, Ibanez, Missonnier, Rodriguez, & Giannakopoulos, 2013). In general, power topographies specific to certain frequency bands seem to become more uniformly distributed with age (Babiloni, et al., 2004). Thus, it is possible that aging effects observed in my projects were associated with some oscillatory modulations and future studies could address this issue.

Another avenue for potential exploration concerns the relation between the age-related neuronal slowdown of 1ms/year and behavioural indices of cognitive performance. ERPs likely reflect aggregated changes in various cognitive abilities associated with aging. Most cognitive variables, such as processing speed, memory performance or perceptual skills, are correlated with each other, which is consistent with the idea that aging effects on different aspects of cognition are not independent. Thus, it would be of great interest to measure the shared and unique contributions of various behavioural markers of cognitive decline to the ERPs. Moreover, time-point-by-time-point ERP analyses could potentially reveal how age-related changes in different cognitive variables modulate different parts of ERP waveforms, and whether their effects are independent of each other. Regression analyses could also determine if variability in different cognitive variables can explain ERP delays, after accounting for age.

Lastly, multiple neural systems that support functionally different processes might be affected differently by senescence, and the impact of this on changes in neural processing speed is currently difficult to predict. The aim would be to establish a causal, rather than correlational, relationship between aging and reduction in processing speed on behavioural and neural level. Furthermore, it is still uncertain whether different elements of

cognitive processing slow equivalently with age or whether slowing is specific only to certain aspects of processing that may differ between different tasks. All aging studies will also have to deal with the uncertainty whether observed age-related effects indicate that young and old people differ in neural correlates of functionally equivalent processes or that two groups make use of distinct processes perhaps also supported by dissimilar cortical networks. Finally, to account for the role of experience in instructing the organisation of cortical circuitry over life-span, I anticipate an increase in longitudinal, over cross-sectional aging research.

REFERENCES

Achard, S., & Bullmore, E. (2007). Efficiency and cost of economical brain functional networks. *PloS Computational Biology, 3*(2), e17. doi:10.1371/journal.pcbi.0030017.

Acunzo, D. J., MacKenzie, G., & van Rossum, M. C. (2012). Systematic biases in early ERP and ERF components as a result of high-pass filtering. *Journal of Neuroscience Methods, 209*(1), 212-218.

Afraz, S., Kiani, R., & Esteky, H. (2006). Microstimulation of inferotemporal cortex influences face categroization. *Nature, 442*(10), 692-695.

Ales, J. M., Appelbaum, L. G., Cottereau, B. R., & Norcia, A. M. (2013). The time course of shape discrimination in the human brain. *NeuroImage, 67*, 77-88.

Allison, T., Hume, A. L., Wood, C. C., & Goff, W. R. (1984). Developmental and aging changes in somatosensory, auditory and visual evoked potentials. *Electroencephalography Clinical Neurophysiology, 58*, 14–24.

Allison, T., Puce, A., Spencer, D. D., & McCarthy, G. (1999). Electrophysiological studies of human face perception, I: Potentials generated in occipitotemporal cortex by face and non-face stimuli. *Cerebral Cortex, 9*, 415-430.

Allison, T., Wood, C., & Goff, W. (1983). Brain stem auditory, pattern-reversal visual and short-latency somatosensory evoked potentials: latencies in relation to age sex and brain and body siz. *Electroencephalography Clinical Neurophysiology, 55*, 619-636.

Anderson, J. C., & Martin, K. A. (2006). Synaptic connection from cortical area V4 to V2 in macaque monkey. *Journal of Computational Neurology, 495*(6), 709-721.

Andrews, T. J., & Ewbank, M. P. (2004). Distinct representations for facial identity and changeable aspects of faces in the human temporal lobe. *Neuroimage, 23*(3), 905–913.

Andrews, T., Clarke, A., Pell, P., & Hartley, T. (2009). Selectivity for low-level features of objects in the human ventral stream. *NeuroImage, 49*, 703-711.

Angelucci, A., & Bressloff, P. C. (2006). Contribution of feedforward, lateral and feedback connections to the classical receptive field center and extra-classical receptive fieldsurround of primate V1 neurons. *Progress in Brain Research, 154*, 93-120.

Anllo-Vento, L., & Hillyard, S. A. (1996). Selective attention to the color and direction of moving stimuli: Electrophysiological correlates of hierarchical feature selection. *Perception & Psychophysics, 58*(2), 191–206.

Anzai, A., Peng, X., & Van Essen, D. C. (2007). Neurons in monkey visual area V2 encode combinations of oreintations. *Nature Neuroscience, 10*(10), 1313-1321.

Applegate, R. A., Donnelly, I., Marsack, J., Koenig, D. E., & Pesudovs, K. (2007). Three-dimensional relationship between high-order root-mean-square wavefront error, pupil diameter and aging. *Journal of the Optical Society of America, A24*, 578-587.

Artigas, J. M., Felipe, A., Navea, A., Fandino, A., & Artigas, C. (2012). Spectral transmission of the human crystalline lens in adult and elderly persons: Color and total transmission of the visible light. *Investigative Ophtamology and Visual Science, 53*(7), 4076-4084.

Atchison, D., & Smith, G. (2002). *Optics of the human eye*. Edinburgh: Elsevier Science Limited.

Babcock, R. L., Laguna, K. D., & Roesch, S. C. (1997). A Comparison of the Factor Structure of Processing Speed for hunger and Older Adults: Testing the Assumption of Measurement Equivalence Across Age Groups. *Psychology and Aging, 12*(2), 268-276.

Babiloni, C., Babiloni, F., Carducci, F., Cappa, S. F., Cincotti, F., Del Percio, C., et al. (2004). Human cortical rhythms during visual delayed choice reaction time tasks. A high resolutionEEG study on normal aging. *Behavorial Brain Research, 153*, 261-271.

Bakin, J., Nakayama, K., & Gilbert, C. (2000). Visual responses in monkey areas V1 and V2 to three-dimensional surface configurations. *Journal of Neuroscience, 20*, 8188–8198.

Baltes, P., & Linderberger, U. (1997). Emergence of a Powerful Connection Between Sensory and Cognitive Functions Across the Adult Life Span: A New Window to the Study of Cognitive Aging? *Psychology of Aging, 12*(1), 12-21.

Banko, E. M., Gal, V., Kortvelyes, J., Kovacs, G., & Vidnyanszky, Z. (2011). Dissociating the effect of noise on sensory processing and overall decision difficulty. *The Journal of Neuroscience, 31*(7), 2663–2674.

Bansal, A. K., Singer, J. M., Anderson, W. S., Golby, A., Madsen, J. R., & Kreiman, G. (2012). Temporal stability of visually selective responses in intracranial field potentials recorded from human occipital and temporal lobes. *Journal of Neurophysiology, 108*(11), 3073-3086.

Barbeau, E. J., Taylor, M. J., Regis, J., Marquis, P., Chauvel, P., & Liegeois-Chauvel, C. (2008). Spatio temporal dynamics of face recognition. *Cerebral Cortex, 18*, 997--1009.

Barton, J. J., Press, D. Z., Keenan, J. P., & O'Connor, M. (2002). Lesions of the fusiform face area impair perception of facial configuration in prosopagnosia. *Neurology, 58*, 71–78.

Bashore, T. D., Ridderinkhof, K. R., & van der Molen, M. W. (1997). The Decline of Cognitive Processing Speed in Old Age. *Current Directions in Psychological Science, 6*, 163-169.

Bell, A. H., Hadj-Bouziane, F., Frihauf, J. B., Tootell, R. B., & Ungerleider, L. G. (2009). Object representations in the temporal cortex of monkeys and humans as revealed by functional magnetic resonance imaging. *Journal of Neurophysiology, 101*(2), 688–700.

Bentin, S., McCarthy, G., Perez, E., Puce, A., & Allison, T. (1996). Electrophysiological studies of face perception in humans. *Journal of Cognitive Neuroscience, 8*, 551–565.

Bichot, N. P., Shall, J. D., & Thompson, K. G. (1996). Visual feature selectivity in frontal eye fields induced by experience in macaque monkeys. *Nature, 381*, 697-699.

Bieniek, M. M., Pernet, C. R., & Rousselet, G. A. (2012). Early ERPs to faces and objects are driven by phase, not amplitude spectrum information: Evidence from parametric, test-retest, single-subject analyses. *Journal of Vision, 12*(13), 1-24.

Birnbaum, Z. W. (1956). On a Use of the Mann-Whitney Statistic. In J. Neyman, *Proceedings of the Third Berkeley Symposium on Mathematical Statistics and Probability* (Vol. 1, pp. 13–17). Berkeley and Los Angeles, CA: University of California Press.

Birren, J. E., & Schaie, K. W. (2001). *Handbook of psychology of aging.* London: Elsevier.

Boettner, E. A., & Wolter, J. R. (1960). Transmission of the ocular media. *Investigative Ophthalmology, 1*(6), 776-783.

Brickman, A. M., Schupf, N., Manly, J. J., Luchsinger, J. A., Andrews, H., Tang, M. X., et al. (2008). Brain morphology in older African Americans, Caribbean Hispanics, and whites from northern Manhattan. *Archives of Neurology, 65*, 1053-1061.

Brincat, S. L., & Connor, C. E. (2004). Underlying principles of visual shape selectivity in posterior inferotemporal cortex. *Nature Neuroscience, 7*(8), 880-886.

Bucur, B., Madden, D. J., Spaniol, J., & Provenzale, J. M. (2008). Age-related slowing of memory retrieval: Contributions of perceptual speed and cerebral white matter integrity. *Neurobiology of Aging, 29*, 1070–1079.

Bullier, J. (2003). Communications between cortical areas of the visual system. In L. M. Chalupa, & J. S. Werner, *The visual neurosciences* (pp. 522-540). Cambridge: MIT Press.

Bullier, J., Hupé, J. M., James, A. C., & Girard, P. (2001). The role of feedback connections in shaping the responses of visual cortical neurons. *Progress in Brain Research, 134*, 193–204.

Burton, K. B., Owsley, C., & Sloane, M. E. (1993). Aging and neural contrast sensitivity: Photopic vision. *Vision Research, 33*, 939–946.

Cabeza, R., Anderson, N. D., Locantore, J. K., & McIntosh, A. R. (2002). Aging gracefully: compensatory brain activity in high-performing older adults. *Neuroimage, 17*(3), 1394-1402.

Cabeza, R., McIntosh, R., Tulving, E., Nyberg, L., & Grady, C. L. (1997). Age related differences in efective neural connectivity during enconding and recall. *NeuroReport, 8*, 3479–3483.

Cabeza, R., Nyberg, L., & Park, D. (2005). *Cognitive Neuroscience of Aging.* Oxford, New York: Oxford Univeristy Press.

Campbell, F. W., & Gregory, A. H. (1960). Effect of Size of Pupil on Visual Acuity. *Nature, 187*(4743), 1121-1123.

Capalbo, M., Postma, E., & Geobel, r. (2008). Combining structural connectivity and response latencies to model the structure of the visual system. *PLOS Computational Biology, 4*(8), 1-14: e1000159.

Carlson, T., Tovar, D. A., Alink, A., & Kriegeskorte, N. (2013). Representational dynamics of object vision: The first 1000 ms. *Journal of Vision, 13*(10), 1–19.

Carmel, D., & Bentin, S. (2002). Domain specificity versus expertise: factors influencing distinct processing of faces. *Cognition, 83*, 1–29.

Carmel, D., & Bentin, S. (2002). Domain specificity versus expertise: factors influencing distinct processing of faces. *Cognition, 83*, 1–29.

Carp, J., Park, J., Polk, T., & Park, D. C. (2011). Age differences in neural distinctiveness revealed by multi-voxel pattern analysis. *Neuroimage, 56*(2), 736-743.

Cauchoix, M., & Crouzet, A. M. (2013). How plausible is a subcortical account of rapid visual recognition? *Frontiers in Human Neuroscience, 7*(39), doi: 10.3389/fnhum.2013.00039.

Cauchoix, M., Barragan-Jason, G., Serre, T., & Barbeau, E. J. (2014). The neural dynamics of face detection in the wild revealed by MVPA. *The Journal of Neuroscience, 34*(3), 846–854.

Cavada, C., & Goldman-Rakic, P. S. (1989). Posterior parietal cortex in rhesus monkey: II. Evidence for segregated corticocorticalnetworks linking sensory and limbic areas with the frontal lobe. *The Journal of Comparative Neurology, 287*(4), 422-445.

Celesia, G. G., & Daly, R. (1977). Effects of aging on visual evoked responses. *Archives of Neurology, 34*, 403-407.

Celesia, G. G., Kaufmann, D., & Cone, S. (1987). Effects of age and sex on pattern electroretinograms and visual evoked potentials. *Electroencephalography Clinical Neurophysiology, 68*, 161–171.

Chaby, L., George, N., Renault, B., & Fiori, N. (2003). Age realted changes in brain responses to personally known faces: an event-related potential (ERP) study in humans. *Neuroscience Letters, 349*(2), 125-9.

Chaby, L., Jemel, B., George, N., Renault, B., & Fiori, N. (2001). An ERP study of famous face incongruity detection in middle age. *Brain and Cognition, 45*(3), 357-377.

Charlton, R. A., Barrick, T. R., McIntyre, D. J., Shen, Y., O'Sullivan, M., Howe, F. A., et al. (2006). White matter damage on diffusion tensor imaging correlates with age-related cognitive decline. *Neurology, 66*, 217-222.

Charlton, R., Landau, S., Schiavone, F., Barrick, T. R., Clark, C. A., Markus, H. S., et al. (2008). A structural equation modeling investigation of age-related variance in executive function and DTI measured white matter damage. *Neurobiology of Aging, 29*(10), 1547-1555.

Chee, M. W., Chen, K. H., Zheng, H., Chan, K. P., Isaac, V., Sim, S. K., et al. (2009). Cognitive function and brain structure correlations in healthy elderly East Asians. *Neuroimage, 46*, 257–269.

Clarke, A. D., Green, P. R., & Chantler, M. J. (2012). The effects of display time and eccentricity on the detection of amplitude and phase degradations in textured stimuli. *Journal of Vision, 12*(3), doi: 10.1167/12.3.7.

Cliff, N. (1996). *Ordinal methods for behavioral data analysis.* Mahwah, N.J: Erlbaum.

Cohen, J. (1988). *Statistical power analysis for the bahavioral sciences.* Hillsdale, NJ: Lawrence Erlbaum Associates.

Cook, C., Koretz, J., Pfahnl, A., Hyun, J., & Kaufman, P. (1994). Aging of the human crystalline lens and anterior segment. *Vision Research, 34*(22), 2945-2954.

Copenhagen, D. R. (2004). Excitation in Retina: The Flow, Filtering, and Molecules of Visual Signaling in the Glutamatergic Pathways from Photoreceptors to Ganglion Cells. In L. M. Chalupa, & J. S. Werner, *The visual Neurosciences* (pp. 320-333). Cambridge, MA.: The MIT Press.

Crassini, B., Brown, B., & Bowman, K. (1988). Age-related changes in contrast sensitivity in central and peripheral retina. *Perception, 17*, 315-332.

Crawford, B. H. (1936). The dependence of pupil size upon external light stimulus under static and variable conditions. *Proceedings in the Royal Society of London, B, 121*(853), 376-395.

Crouzet, S. M., & Serre, T. (2011). What are the visual features underlying rapid object recognition. *Frontiers in Psychology, 2*(236), 1-15.

Crouzet, S. M., & Thorpe, S. J. (2010). Swap the face! Use of amplitude sepctrum by the visual systemt to drive fast saccades (in preparation).

Crouzet, S. M., Kirchner, H., & Thorpe, S. J. (2010). Fast saccades toward faces: Face detection in just 100 ms. *Journal of Vision, 10*(4), 1–17, doi: 10.1167/10.4.16.

Cukur, T., Huth, A. G., Nishimoto, S., & Gallant, J. L. (2013). Functional Subdomains within Human FFA. *The Journal of Neuroscience, 33*(42), 16748 –16766.

Dacey, D. M. (2004). Origins of perception: retinal ganglion cell diversity and the creation of parallel visual pathways. In M. S. Gazzaniga, *The Cognitive Neurosciences* (pp. 281-301). Cambridge, MA.: MIT Press.

Daniel, S., & Bentin, S. (2010). Age-related changes in processing faces from detection to identification: ERP evidence. *Neurobiology of Aging*.

Davies-Thompson, J., & Andrews, T. J. (2012.). Intra- and interhemispheric connectivity between face-selective regions in the human brain. *Journal of Neurophysiology, 108*(11), 3087–3095.

Davies-Thompson, J., & T., A. (2012). Intra- and interhemispheric connectivity between face-selective regions in the human brain. *Journal of Neurophysiology, 108*(11), 3087-3095.

Davis, S., Dennis, N., Buchler, N., White, L., Madden, D., & Cabeza, R. (2009). Assessing the effects of age on long white matter tracts using diffusion tensor tractography. *Neuroimage, in press*.

De Sanctis, P., Katz, R., Wylie, G. R., Sehatpour, P., Alexopoulos, G. S., & Foxe, J. j. (2008). Enhanced and bilateralized visual sensory processing in the ventral stream may be a feature of normal aging. *Neurobiology of Aging, 29*, 1576–1586.

De Valois, r. L., & De Valois, K. K. (1988). *Spatial Vision.* New York: Oxford University Press.

De Vos, M., Thorne, J. D., Yovel, G., & Debener, S. (2012). Let's face it, from trial to trial: Comparing procedures for N170 single-trial estimation. *NeuroImage, 63*(3), 1196–1202.

Deary, I. J. (2000). *Looking down on human intelligence: from psychometrics to the brain.* Oxford: Oxford University Press.

Deary, I. J., Bastin, M. E., Pattie, A., Clayden, J. D., & Whalley, L. J. (2006). White matter integrity and cognition in childhood and old age. *Neurology, 66*(4), 505-512.

Debruille, J. B., Guillem, F., & Renault, B. (1998). ERPs and chronometry of face recognition: following-up Seeck et al. and George et al. *NeuroReport, 9*(15), 3349–3353.

Deffke, I., Sander, T., Heidenreich, J., Sommer, W., Curio, G., Trahms, L., et al. (2007). MEG/EEG sources of the 170-ms response to faces are co-localized in the fusiform gyrus. *Neuroimage, 35*(4), 1495-1501.

DeFockert, J., Ramchurn, A., Velzen, J., Bergstrom, S., & Bunce, D. (2009). Behavioral and ERP evidence of greater distractor processing in old age. *Brain Research*, 67-73.

Deiber, M.-P., Ibanez, V., Missonnier, P., Rodriguez, C., & Giannakopoulos, G. (2013). Age-associated modulations of cerebral oscillatory patterns related to attention control. *NeuroImage, 82*, 531–546.

Delorme, A., & Makeig, S. (2004). EEGLAB: an open source toolbox for analysis of single-trial EEG dynamics including independent component analysis. *Journal of Neuroscience Methods, 134*, 9–21.

Delorme, A., Mullen, T., Kothe, C., Bigdely-Shamlo, N., Akalin, Z., Vankov, A., et al. (2011). EEGLAB, MPT, NetSIFT, NFT, BCILAB, and ERICA: New tools for advanced EEG/MEG processing. *Computational Intelligence*, article ID 130714.

Desimone, R., & Schein, S. J. (1987). Visual properties of neurons in visual area V4 in macaque: sensititivty to stimulus form. *Journal of Neurophysiology, 57*, 835-67.

Desimone, R., & Ungerleider, L. G. (1989). Neural mechanisms of visual perception in monkeys. In F. B. Grafman, *Handbook of Neuropsychology* (pp. 267–299). Amsterdam: Elsevier.

Desjardins, J. A., & Segalowitz, S. J. (2013). Deconstructing the early visual electrocortical responses to face and house stimuli. *Journal of Vision, 13*(5), 1–18.

Devaney, K. a. (1980). Neuron loss in the aging visual cortex of man. *Journal of Gerontology*, *35*, 836-841.

DeYoe, E. A., Carman, G., Bandettini, P., Glickman, S., Wieser, J., Cox, R., et al. (1996). Mapping striate and extrastriate visual areas in human cerebral cortex. *Procedeeings in National Academy of Science USA*, *93*(6), 2382-2386.

Di Russo, F., Martınez, A., Sereno, M. I., Pitzalis, S., & Hillyard, S. A. (2001). Cortical Sources of the Early Components of the. *Human Brain Mapping*, *15*, 95–111.

Diaz, F., & Amenedo, E. (1998). Ageing effects on flash visual evoked potentials (FVEP) recorded from parietal and occipital electrodes. *Neurophysiology Clinical*, *28*(5), 399–412.

DiCarlo, J. J., & Cox, D. D. (2007). Untangling invariant object recognition. *Trends in Cognitive Sciences*, *11*(8), 333-341.

Doksum, K. A. (1974). Empirical Probability Plots and Statistical Inference for Nonlinear Models in the two-Sample Case. *Annals of Statistics*, *2*(2), 267–277.

Doksum, K. A. (1977). Some graphical methods in statistics. A review and some extensions. *Statistica Neerlandica*, *31*, 53–68.

Drewes, J., Wichmann, F. A., & Gegenfurtner, K. R. (2006). Classification of natural scenes: Critical features revisited. *Journal of Vision*, *6*(6), 10.1167/6.6.561.

Duan, H., Wearne, S. L., Rocher, A. B., Macedo, A., Morrison, J. H., & Hof, P. R. (2003). Age-related dendritic and spine changes in corticocortically projecting neurons in macaque monkeys. *Cerebral Cortex*, *13*, 950-961.

Dubuc, B. (2014, February). *The eye*. Retrieved February 10, 2014, from The brain from top to bottom: http://thebrain.mcgill.ca/flash/a/a_02/a_02_cr/a_02_cr_vis/a_02_cr_vis.html#3

Duncan-Johnson, C. C., & Donchin, E. (1982). The P300 component of the event-related brain potential as an index of information processing. *Biological Psychology*, *14*(1-2), 1-52.

Eckert, M. A. (2011). Slowing down: age-related neurobiological predictors of processing speed. *Frontiers in Neuroscience*, *5*(25), doi: 10.3389/fnins.2011.00025.

Eckert, M. A., Keren, N. I., Roberts, D. R., Calhoun, V. D., & Harris, K. C. (2010). Age-related changes in processing speed: unique contributions of cerebellar and prefrontal cortex. *Frontiers in Human Neuroscience*, *10.3389/neuro.09.010.2010*, 4-10.

Edwards, R., Xiao, D., Keysers, C., Foldiak, P., & Perrett, D. (2003). Color sensitivity of cells responsive to complex stimuli in the temporal cortex. *Journal of Neurophysiology*, *90*, 1245–1256.

Efron, B., & Tibshirani, R. J. (1993). *An introduction to the bootstrap. Monographs on statistics and applied probability (pp. XVI–436 S.).* London: Chapman & Hall.

Eimer, M. (2011). The face-senistivity of the N170 component. *Frontiers in Human Neuroscience*, doi: 10.3389/fnhum.2011.00119.

Eklund, A., Andersson, M., & Knutsson, H. (2011). Fast random permutation tests enable objective evaluation of methods for single-subject fMRI analysis. *International Journal of Biomedical Imaging*, *Jan.*, 627–647, doi:10.1155/2011/627947.

Elliot, D. B. (1987). Contrast sensitivity decline with aging: A neural or optical phenomenon? *Ophthalmic and Physiological Optics*, *7*(4), 415-419.

Elliott, D., Whitaker, D., & MacVeigh, D. (1990). Neural contribution to spatiotemporal contrast senstivity decline in healthy ageing eye. *Vision Research*, *30*, 541-547.

Elliott, S. L., Choi, S. S., Doble, N., Hardy, J. L., Evans, J. W., & Werner, J. S. (2009). Role of high-order aberrations in senescent changes in spatial vision. *Journal of Vision*, *9*, 1-16.

Elze, T. (2010). Misspecifications of stimulus presentation durations in experimental psychology: a systematic review of the psychophysics literature. *PLOS one*, *5*(9), e12792.

Engell, A. D., & Haxby, J. V. (2007). Facial expression and gaze-direction in human superior temporal sulcus. *Neuropsychologia*, *45*, 3234–3241.

Epshtein, B., Lifshitz, I., & Ullman, S. (2008). Image interpretation by a single bottom-up top-down cycle. *Proceedings of The National Academy of Sciences of the USA*, *105*(38), 14298-14303.

Epstein, R., & Kanwisher, N. (1998). A cortical representation of the local visual environment (abstract). *Nature*, *392*(6676), 598.

Fairhall, S. L., & Ishai, A. (2007). Effective connectivity within the distributed cortical network for face perception. *Cerebral Cortex, 17*(10), 2400-6.

Falkenstein, M., Yordanova, J., & Kolev, V. (2006). Effects of aging on slowing of motor-response generation. *International Journal Psychophysiology, 59*(1), 22–29.

Felleman, D. J., & Van Essen, D. C. (1991). Distributed hierarchical processing in the primate cerebral cortex. *Cerebral Cortex, 1*(1), 1-47.

Felsen, G., Touryan, J., Han, F., & Dan, Y. (2005). Cortical Sensitivity to Visual Features in Natural Scenes. *PLoS Biology, 3*(10), 1819 - 1828.

Fox, C. J., Moon, S. Y., Iaria, G., & Barton, J. J. (2009). The correlates of subjective perception of identity and expression in the face network: an fMRI adaptation study. *Neuroimage, 44*(2), 569–580.

Foxe, J. J., & Simpson, G. V. (2002). Flow of activation from V1 to frontal cortex in humans. A framework for defining "early" visual processing. *Experimental Brain Research, 142*, 139–150.

Freeman, S. H., Kandel, R., Cruz, L., Rozkalne, A., Newell, K., Frosch, M. P., et al. (2008). Preservation of neuronal number despite age-related cortical brain atrophy in elderly subjects without Alzheimer disease. *Journal of Neuropathology and Experimental Neurology, 67*(12), 1205-1212.

Freiwald, W. A., & Tsao, D. (2010). Functional compartmentalization and viewpoint generalization within the macaque face-processing system. *Science, 330*(6005), 845-851.

Freiwald, W. A., Tsao, D. Y., & Livingstone, M. S. (2009). A face feature space in the macaque temporal lobe. *Nature Neuroscience, 12*(9), 1187 - 1198.

Friedman, D., Kazmerski, V., & Fabiani, M. (1997). An overview of age-related changes in the scalp distribution of P3b. *Electroencephalography Clinical Neurophysiology, 104*, 498–513.

Froelich, J., & Kaufman, D. I. (1991). Effect of Decreased Retinal Illumination on Simultaneously Recorded Pattern Electroretinograms and Visual-Evoked Potentials. *Investigative Ophthalmology & Visual Science 32,2, 32*(2), 310-318.

Fujisawa, K., & Sasaki, K. (1995). Changes in light scattering intensity of the transparent lenses of subjects selected from population-based surveys depending on age: analysis through Scheimpflug images. *Ophthalmic Research, 27*(2), 89-101.

Furey, M. L., Tanskanen, T., Beauchamp, M. S., Avikainen, S., Uutela, K., Hari, R., et al. (2006). Dissociation of face-selective cortical responses by attention. *Proceedings of the National Academy of Sciences USA, 103*, 1065–1070.

Gallant, J. L., Connor, C. E., Rakshit, S., Lewis, J. W., & Van Essen, D. C. (1996). Neural responses to polar, hyperbolic, and. *Journal of Neurophysiology, 76*, 2718-2739.

Gao, L., XU, J., ZHANG, B., ZHAO, L., HAREL, A., & Bentin, S. (2009). Aging effects on early-stage face perception: an ERP study. *Psychophysiology*, 1–14.

Gaspar, C. M., & Rousselet, G. A. (2009). How do amplitude spectra influence rapid animal detection? *Vision Research*, in press.

Gaspar, C., Rousselet, G., & Pernet, C. R. (2011). Reliability of ERP and single-trial analyses. *Neuroimage, 58*(2), 620-629, ISSN 1053-8119 (doi:10.1016/j.neuroimage.2011.06.052).

Gattass, R., Sousa, A. P., Mishkin, M., & Ungerleider, L. G. (1997). Cortical projections of area V2 in the macaque. *Cerebral Cortex, 7*(2), 110-129.

Gauthier, I. (2000). What constrains the organization of the ventral temporal cortex? *Trends in Cognitive Sciences, 4*(1), 1–2.

Gawne, T. J., Kjaer, T. W., & Richmond, B. J. (1996). Latency: another potential code for feature binding in striate cortex. *Journal of Neuropchysiology, 76*(2), 1356-1360.

Gazzaley, A., Clapp, W., Kelley, J., McEvoy, K., Knight, R., & D'Esposito, M. (2008). Age-related top-down suppression deficit in the early stages of cortical visual memory processing. *Proceedings in National Academy of Sciences USA, 105*(35), 13122-6.

Gazzaley, A., Cooney, J. W., McEvoy, K., Knight, R., & D'Esposito, M. (2005). Top-down enhancement and suppression of the magnitude and speed of neural activity. *Journal of Cognitive Neuroscience, 17*, 507-517.

Geisler, W. S., Albrecht, D. G., & Crane, A. M. (2007). Responses of neurons in primary visual cortex to transient changes in local contrast and luminance. *The Journal of Neuroscience, 27*(19), 5063–5067.

Ghebreab, S., Scholte, h. S., Lamme, V. a., & Smeulders, A. W. (2009). A biologically plausible model for rapid natural scene identification. In Y. Bengio, D. Schuurmans, j. Lafferty, C. K. Williams, & A. Culotta, *Advances in Neural Information Processing Systems* (pp. 629–637).

Gilaie-Dotan, S., Nir, Y., & Malach, R. (2008). Regionally-specific adaptation dynamics in human object areas. *NeuroImage, 39*(4), 1926–1937.

Gilbert, C. D. (1993). Circuitry, architecture, and functional dynamics of visual cortex. *Cerebral Cortex, 3*, 373-386.

Girard, P., Hupe, J. M., & Bullier, J. (2001). Feedforward and Feedback connections between areas V1 and V2 of the monkey have similar rapid conduction velocities. *Journal of Neurophysiology, 85*(3), 1328-1331.

Goffaux, V., Jacques, C., Mouraux, A., Oliva, A., Schyns, P., & Rossion, B. (2005). Diagnostic Colors Contribute to the Early Stages of Scenes Categorization: Behavioral and Neurophysiological Evidence. *Visual Cognition, 12*, 878-892.

Good, C. D., Johnsrude, I. S., Ashburner, J., Henson, R. N., Friston, K. J., & Frackowiak, R. S. (2001). A voxel- based morphometric study of ageing in 465 normal adult human brains. *Neuroimage, 14*, 21–36.

Goodale, M. A., & Milner, D. A. (1992). Separate visual pathways for perception and action. *Trends in neurosciences, 15*(1), 20-25.

Grady, C. (2000). Functional brain imaging and age-related. *Biological Psychology, 54*, 259-281.

Grady, C. L. (2008). Cognitive Neuroscience of Aging. *Annals of the New York Academy of Sciences, 1124*, 127-144, doi: 10.1196/annals.1440.009.

Grill-Spector, K., & Malach, R. (2004). The human visual cortex. *Annual Review Neuroscience, 27*, 649–77.

Grill-Spector, K., Kourtzi, Z., & Kanwisher, N. (2001). The lateral occipital complex and its role in object recognition. *Vision Research, 41*, 1409-1422.

Grill-Spector, K., Sayres, R., & Ress, D. (2006). High-resolution imaging reveals highly selective nonface clusters in the fusiform face area. *Nature Neuroscience, 9*, 1177–1185.

Groen, I. I., Ghebreab, S., Lamme, V. A., & Scholte, H. S. (2012a). Low-level contrast statistics are diagnostic of invariance of natural textures. *Frontiers in Computational Neuroscience, 6*, doi: 10.3389/fncom.2012.00034.

Groen, I. I., Ghebreab, S., Lamme, V. A., & Scholte, H. S. (2012b (in press)). Spatially pooled contrast responses predict neural and perceptual similarity of naturalistic image categories. *PLOS Computational Biology*.

Groen, I. I., Ghebreab, S., Prins, H., Lamme, V. A., & Scholte, H. S. (2013). From image statistics to scene gist: evoked neural activity reveals transition from low-level natural image structure to scene category. *The Journal of Neuroscience, 33*(48), 18814-18824.

Groppe, D. M., Makeig, S., & Kutas, M. (2009). Identifying reliable independent components via split-half comparisons. *NeuroImage, 45*, 1199–1211.

Gschwind, M., Pourtois, G., Schwartz, S., Van De Ville, D., & Vuilleumier, P. (2012). White-matter connectivity between face-responsive regions in the human brain. *Cerebral Cortex, 22*(7), 1564-1576.

Guirao, A., Gonzales, C., Redondo, M., Geraghty, E., N. S., & Artal, P. (1999). Average optical perfomrance of the human eye as a function of age in a normal population. *Investigative Opthamology and Visual Science, 40*, 203-213.

Gunning-Dixon, F. M., & Raz, N. (2000). The cognitive correlates of white matter abnormalities in normal aging: a quantitative review. *Neuropsychology, 14*, 224–232.

Guth, S. K. (1957). Effects of age on visibility. *American Journal of Optometry and Archives of American Academy of Optometry, 41*, 463-477.

Habak, C., & Faubert, J. (2000). Larger effect of aging on the perception of higher- order stimuli. *Vision Research, 40*, 943–950.

Halgren, E., Baudena, P., Heit, G., Clarke, M., & Marinkovic, K. (1994). Spatio-temporal stages in face and word processing. 1. Depth recorded potentials in the human occipital and parietal lobes. *Journal of Physiology, 88*, 1-50.

Halit, H., de Haan, M., & Johnson, M. J. (2000). Modulation of event-related potentials by prototypical and atypical faces. *NeuroReport: Cognitive Neuroscience, 11*(9), 1871-1875.

Hamerer, D., Li, S., Volkle, M., Muller, V., & Linderberger, U. (2013). A lifespan comparison of the reliability, test-retest stability, and signal-to-noise ratio of event-related potentials assessed during performance monitoring. *Psychophysiology, 50*, 111–123.

Hämmerer, D., Li, S. C., Völkle, M., Müller, V., & Lindenberger, U. (2013). A lifespan comparison of the reliability, test-retest stability, and signal-to-noise ratio of event-related potentials assessed during performance monitoring. *Psychophysiology, 50*(1), 111-123.

Hansen, B. C., Farivar, R., Thompson, B., & Hess, R. F. (2008). A critical band of phase alignment for discrimination but not recognition of human faces. *Vision Res, 48*(25), 2523-2536.

Hansen, B. C., Johnson, A. P., & Ellemberg, D. (2012). Different spatial frequency bands selectively signal for natural image statistics in the early visual system. *Journal of Neurophysiology, 108*, 2160–2172.

Hansen, B. C., Thompson, B., Hess, F., R., & Ellemberg, D. (2010). Extracting the internal representation of faces from human brain activity: an analogue to reverse correlation. *NeuroImage, 51*, 373–390.

Hanson, S. J., & Schmidt, A. (2011). High-resolution imaging of the fusiform face area (FFA) using multivariate non-linear classifiers shows diagnosticity for non-face categories. *Neuroimage, 54*(2), 1715–1734.

Haxby, J. V., Gobbini, M. I., Furey, M. L., Ishai, A., Schouten, J. L., & Pietrini, P. (2001). Distributed and overlapping representations of faces and objects in ventral temporal cortex. *Science, 293*, 2425-2428.

Hemond, C. C., Kanwisher, N. G., & Op de Beeck, H. P. (2007). A preference for contralateral stimuli in human object- and face-selective cortex. *PloS One, 2*(6), 1-5.

Herrmann, M. J., Ehlis, A. -C., Ellgring, H., & Fallgatter, A. J. (2005). Early stages (P100) of face perception in humans as measured with event-related potentials (ERPs). *Journal of Neural Transmission, 112*, 1073–1081.

Herrmann, M. J., Ehlis, A. C., Muehlberger, A., & Fallgatter, A. J. (2005). Source localization of early stages of face processing. *Brain Topography, 18*(2), 77-85.

Hess, M. R., & Kromrey, J. D. (2004). Robust confidence intervals for effect sizes: a comparative study of Cohen's d and Cliff's delta under non-normality and heterogeneous variances. *American Educational Research Association*, (pp. 1-30). San Diego.

Hofer, S., & Sliwinski, M. (2001). Understanding Ageing. An evaluation of research designs for assessing the interdependence of ageing-related changes. *Gerontology, 47*(6), 341-352.

Hoffman, E. A., & Haxby, J. V. (2000). Distinct representations of eye gaze and identity in the distributed human neural system for face perception. *Nature Neuroscence, 3*(1), 80-84.

Hogan, M. J. (2004). The cerebellum in thought and action: a fronto-cerebellar aging hypothesis. *New Ideas Psychol., 22*, 97–125.

Honey, C., Kirchner, H., & VanRullen, R. (2008). Faces in the cloud: Fourier power spectrum biases ultrarapid face detection. *Journal of Vision, 8*(12), 1-13.

Horwitz, B., McIntosh, A., Haxby, J., Furey, M., Salerno, J., Schapiro, M., et al. (1995). Network analysis of PET-mapped visual pathways in Alzheimer type demetia. *NeuroReport, 6*, 2287–2292.

Hua, T., Li, X., He, L., Zhou, Y., Wang, & Leventhal, A. (2006). Functional degradation of visual cortical cells in old cats. *Neurobiology of Aging, 27*, 155-162.

Huang, J. Y., Wang, C., & Dreher, B. (2007). The effects of reversible inactivation of postero-temporal visual cortex on neuronal activities in cat's area 17. *Brain Research, 1138*, 111-128.

Hubel, D., & Wiesel, T. N. (1968). Receptive fields and functional architecture of monkey striate cortex. *Journal of Physiology (London), 195*, 215–243.

Hung, C. P., Kreiman, G., Poggio, T., & DiCarlo, J. J. (2005). Fast Readout of Object Identity from Macaque Inferior Temporal cortex. *Science, 310*(863), 863-866.

Husk, J. S., Bennett, P. J., & Sekuler, A. B. (2007). Inverting houses and textures: Investigating the characteristics of learned inversion effects. *Vision Research, 47*(27), 3350-3359.

Huth, A. G., Nishimoto, S., Vu, A. T., & Gallant, J. L. (2012). A continuous semantic space describes the representation of thousands of object and action categories across the human brain. *Neuron, 76*(6), 1210 –1224.

Ince, R. A., Mazzoni, A., Petersen, R. S., & Panzeri, S. (2010). Open source tools for the information theoretic analysis of neural data. *Frontiers Neuroscience, 4*(1), 62-70.

Isik, L., Meyers, E. M., Leibo, J. Z., & Poggio, T. (2014). The dynamics of invariant object recognition in the human visual system. *Journal of Neurophysiology, 111*, 91–102.

Issa, E. B., & DiCarlo, J. J. (2012). Precedence of the eye region in neural processing of faces. *The Journal of Neuroscience, 32*(47), 16666-16682.

Itier, R. J., & Taylor, M. J. (2002). Inversion and contrast polarity reversal affect both encoding and recognition processes of unfamiliar faces: a repetition study using ERPs. *NeuroImage, 15*, 353–372.

Itier, R. j., & Taylor, M. J. (2004). N170 or N1? Spatiotemporal differences between object and face processing using ERPs. *Cerebral Cortex February, 14*(DOI: 10.1093/cercor/bhg111), 132–142.

Jacobs, H., Vissera, P., Van Boxtel, M., aFrisoni, G., Tsolaki, M., Papapostolou, P., et al. (2010). The association between white matter hyperintensities and executive decline in mild cognitive impairment is network dependent. *Neurobiology of Aging, in press*.

Jacques, C., & Rossion, B. (2006). The speed of individual face categorization. *Psychological Science, 17*(6), 485-492.

Jacques, C., Mouraux, A., Oliva, A., S. P., & Rossion, B. (2005). Diagnostic colors contribute to the early stages of scene categorization: Behavioral and neurophysiological evidence. *Visual Cognition, 12*, 878–892.

Jay, J. L., Mammo, R. B., & Allan, D. (1987). Effects of age on visual acuity after cataract extraction. *British Journal of Opthamology, 71*, 112-115.

Johnson, M. H. (2005). Subcortical face processing. *Nature: Neuroscience. Reviews, 6*, 766-774.

Juan, C. H., & Walsh, V. (2003). Feedback to V1: a reverse hierarchy in vision. *Experimental Brain Research, 150*(2), 259-263.

Juvells, I., Vallmitjana, S., Carnicer, A., & Campos, J. (1991). The role of amplitude and phase of the Fourier transform in the digital image processing. *American Journal of Physics, 59*(8), 744-748.

Kadlecova, V., Peleska, M., & Vasko, A. (1958). Dependence on Age of the Diameter of the Pupil in the Dark. *Nature, 182*(1520).

Kanwisher, N., & Yovel, G. (2006). The fusiform face area: a cortical region specialized for the perception of faces. *Philosophical Transactions of the Royal Society B: Biological Sciences, 361*, 2109 –2128.

Kanwisher, N., McDermott, J., & Chun, M. M. (1997). The Fusiform Face Area: A Module in Human Extrastriate Cortex Specialized for Face Perception. *The Journal of Neuroscience, 17*(11), 4302–4311.

Kayser, J. (2009). *Current source density (CSD) interpolation using spherical splines - CSD Toolbox (Version 1.1)*. Retrieved August 16, 2013, from New York State Psychiatric Institute: Division of Cognitive Neuroscience: http://psychophysiology.cpmc.columbia.edu/Software/CSDtoolbox

Kayser, J., & Tenke, C. E. (2006). Principal components analysis of Laplacian waveforms as a generic method for identifying ERP generator patterns: I. Evaluation with auditory oddball tasks. *Clinical Neurophysiology, 117*(2), 348-368, doi:10.1016/j.clinph.20.

Kelly, S. P., Gomez_Ramirez, M., & Foxe, J. J. (2008). Kelly, S. P., Gomez-Ramirez, M., & Foxe, J. J. (2008). Spatial Attention Modulates Initial Afferent Activity in Human Primary Visual Cortex. *Cerebral Cortex, 18*(11), 2629–2636, doi:10.1093/cercor/bhn022.

Kennedy, K. M., & Raz, N. (2009). Aging white matter and cognition: differential effects of regional variations in diffusion properties on memory, executive functions, and speed. *Neuropsychologia, 47*(3), 916–927.

Kennedy, K. M., Erickson, K. I., Rodrigue, K. M., Voss, M. W., Colcombe, S. J., Kramer, A. F., et al. (2009). Age-related differences in regional brain volumes: A comparison of optimized voxel-based morphometry to manual volumetry. *Neurobiology of Aging, 30*, 1657–1676.

Keysers, C., Xiao, D.-K., Foldiak, P., & Perrett, D. I. (2001). The speed of sight. *Journal of Cognitive Neuroscience, 13*(1), 90-101.

Kiani, R., Esteky, H., & Tanaka, H. (2005). Differences in onset latency of macaque inferotemporal neural responses to primate and non-primate faces. *Journal of Neurophysiology, 94*, 1587–1596.

Kietzmann, T., Ehinger, B., Porada, D., Engel, A., & & König, P. (2013). Perceptual Learning Leads to Category Selectivity 100ms after Stimulus Onset. *European Conference on Visual Perception 2013*. 25-29th August, Bremen, Germany.

Kingdom, F. A., Hayes, A., & Field, D. J. (2001). Sensitivity to contrast histogram differences in synthetic wavelet-textures. *Vision Research, 41*(5), 585-598.

Kolev, V., Falkenstein, M., & Yordanova, J. (2006). Motor-response generation as a source of aging-related behavioural slowing in choice-reaction tasks. *Neurobiology Aging, 27*(11), 1719–1730.

Koretz, J., Cook, C., & Kaufman, P. (2002). Aging of the human lens: changes in lens shape upon accommodation and with accommodative loss. *Journal of Optical Society of America, 19*(1), 144-151.

Kourtzi, Z., Tolias, A. S., Altmann, C. F., Augath, M., & Logothetis, N. K. (2003). Integration of local features into global shapes: monkey and human fMRI studies. *Neuron, 37*, 333–346.

Kovesi, P. (1999). Image features from phase congruency. *Videre, 1*, 1–27.

Kovesi, P. (2002). Edges Are Not Just Steps. *ACCV2002: The 5th Asian Conference on Computer Vision*, (pp. 1-6). Melbourne, Australia.

Ku, S., Tolias, A., Logothetis, N., & Goense, J. (2011). fMRI of the face-processing network in the ventral temporal lobe of awake and anesthetized macaques. *Neuron, 70*(2), 352-362.

Kuba, M., Kremlacek, J., Langrova, J., Kubova, Z., Szanyi, J., & Vit, F. (2012). Aging effect in pattern, motion and cognitive visual evoked potentials. *Vision Research, 62*, 9-16.

Kugler, C. (1997). The impact of age-related changes in event-related P300 potentials on detecting early cognitive dysfunction. *Archives of Gerontology and Geriatrics, 25*, 13-26.

Kumnick, L. (1954). Pupillary Psychosensory Restitution and Aging. *Journal of Optical Society of America, 44*(9), 735.

Kurylo, D. D. (2006). Effects of aging on perceptual organization: Efficacy of stimulus features. *Experimental Aging Research, 32*(2), 137–152.

Kuypers, H. G., Szwarcbart, M. K., Mishkin, M., & Rosvold, H. E. (1965). Occipitotemporal corticocortical connections in the rhesus monkey. *Experimental Neurology, 11*, 245–262.

Lamme, V. A., Super, H., & Spekreijse, H. (1998). Feedforward, horizontal, and feedback processing in the visual cortex. *Current Opinion in Neurobiology, 8*, 529–535.

Large, M. E., Cavina-Pratesi, C., Vilis, T., & Culhama, J. C. (2008). The neural correlates of change detection in the face perception network. *Neuropsychologia, 46*(8), 2169–2176.

Lazebnik, S., Schmid, C., & Ponce, J. (2006). Beyondbagsoffeatures: Spatial pyramidmatchingforrec-. *IEEE Computer Society Conference on Computer Vision and Pattern Recognition, 2*, 2169–2178.

Lazic, S. E. (2010). Relating hippocampal neurogenesis to behavior: the dangers of. *Neurobiology of Aging, 31*, 2169–2171.

Lee, J., Williford, W., & Maunsell, J. H. (2007). Spatial Attention and the Latency of Neuronal Responses in macaque area V4. *The Journal of Neuroscience, 27*(36), 9632–9637.

Lee, T. S., Yang, C. F., Romero, R. D., & Mumford, D. (2002). Neural activity in early visual cortexreflects behavioral experience and higher-order perceptual saliency. *Nature Neuroscience, 5*(6), 589-597.

Lehky, S., & Sereno, A. (2007). Comparison of shape encoding in primate dorsal and ventral visual pathways. *Journal of Neurophysiology, 97*(1), 307-319.

Lehmann, D. (1986a). Mapping, spatial analysis and adaptive segmentation of EEG/ERP data. In C. C. Shagass, R. C. Josiasson, & R. A. Roemer, *Brain Electrical Potentials and Psychopathology* (pp. 27-46). Elsevier: Amsterdam.

Lehmann, D. (1986b). Spatial analysis of EEG and evoked potent ial data. In F. H. Duffy, *Topographic Mapping of Brain Electrical Activity* (pp. 29-61). Boston: Butterworths.

Lehmann, D. (1987). Principles of spatial analysis. In A. Gevins, & A. (. Remond, *Handbook of Electroencephalography and Clinical Neurophysiology, Vol. 1: Methods of Analysis of Brain Electrical and Magnetic Signals* (pp. 309-354). Elsevier: Amsterdam.

Leopold, D. A., Bondar, I. V., & Giese, M. A. (2006). Norm-based face encoding by single neurons in the monkey inferotemporal cortex. *Nature Letters, 442*(3).

Letinic, K., Zoncu, R., & Rakic, P. (2002). Origin of GABAergic neurons in the human neocortex. *Nature, 417*(6889), 645-649.

Leventhal, A. G., Wang, Y., Pu, M., Zhou, Y., & Ma, Y. (2003). GABA and its agonists improved visual cortical function in senescent monkeys. *Science, 300*(5620).

Lindenberger, U., & Baltes, P. (1997). Intellectual Functioning in Old and Very Old Age: Cross-Sectional Results From the Berlin Aging Study. *Psychology and Aging, 12*(3), 410-132.

Lindenberger, U., & Potter, U. (1998). The complex nature of unique and shared effects in hierarchical linear regression: Implications for developmental psychology. *Psychological Methods, 3*, 218-230.

Lindenberger, U., Mayr, U., & Kliegl, R. (1993). Speed and intelligence in old age. *Psychology and Aging, 8*, 207–220.

Linkenkaer-Hansen, K., Palva, J. M., Sams, M., Hietanen, J. K., Aronen, H. J., & Ilmoniemi, R. J. (1998). Face-selective processing in human extrastriate cortex around 120 ms after stimulus onset revealed by magneto- and electroencephalography. *Neuroscience Letters, 253*, 147–150.

Litvak, V., Mattout, J., Kiebel, S., Phillips, C., Henson, R. N., Kilner, J., et al. (2011). EEG and MEG data analysis in SPM8. *Computational Intelligence and Neuroscience*, doi:10.1155/2011/852961.

Liu, H., Agam, Y., Madsen, J. R., & Kreiman, G. (2009). Timing, timing, timing: Fast decoding of object information from intracranial field potentials in human visual cortex. *Neuron, 62*, 281–290.

Liu, J., Harris, A., & Kanwisher, N. (2002). Stages of processing in face perception: an MEG study. *Nature Neuroscience, 5*(9), 910-916.

Livingstone, M., & Hubel, D. (1988). Segreagation of from, color, movement and depth: anatomy, physiology and perception. *Science, 240*, 740-749.

Logothetis, N. K., Pauls, J., & Poggiot, T. (1995). Shape representation in the inferior temporal cortex of monkeys. *Current Biology, 5*, 552-563.

Loschky, L. C., & Larson, A. M. (2008). Localised information is necessary for scene categorization, including teh natural/man-made distinction. *Journal of Vision, 8*(1), 4.1-4.9.

Luck, S. J. (2005). *An Introduction to the Event-Related Potential Technique.* Cambridge, MA: MIT Press.

Luck, S. J. (2009). The spatiotemporal dynamics of visual-spatial attention. In F. Aboitiz, & D. (. Cosmelli, *From Attention to Goal-Directed Behavior: Neurodynamical, Methodological, and Clinical Trends* (pp. 51-66). Berlin: Springer.

Lueschow, A., Sander, T., Boehm, S. G., Nolte, G., Trahms, L., & Curio, G. (2004). Looking for faces: attention modulates early occipitotemporal object processing. *Psychophysiology, 41*, 350–360.

MacKay, D. M., & Jeffreys, D. A. (1973). Visually evoked potentials and visual perception in man. In R. Jung, *Handbook of sensory physiology* (pp. 674–678). Berlin: Springer-Verlag.

MacLullich, A. M., Edmond, C. L., Ferguson, K. J., Wardlaw, J. M., Starr, J. M., Seckl, J. R., et al. (2004). Size of the neocerebellar vermis is associated with cognition in healthy elderly men. *Brain and Cognition, 56*(3), 344-348.

Madden, D. J., Bennett, I. J., & Song, W. A. (2009). Cerebral white matter integrity and cognitive aging: contributions from diffusion tensor imaging. *Neuropsychology Reviews, 19*(4), 415-435.

Madden, D. J., Whiting, W. L., Huettel, S. A., White, L. E., MacFall, J. R., & Provenzale, J. M. (2004). Diffusion tensor imaging of adult age differences in cerebral white matter: relation to response time. *NeuroImage, 21*, 1174–1181.

Magri, C., Whittingstall, K., Singh, V., Logothetis, N. K., & Panzeri, S. (2009). A toolbox for the fast information analysis of multiple-site LFP, EEG and spike train recordings. *BMC Neuroscience, 10*(81), doi:10.1186/1471-2202-10-81.

Malach, R. R., Benson, R. R., Kwong, K. K., Jiang, H., Kennedy, W. A., Ledden, P., et al. (1995). Object-related activity revealed by functional magnetic resonance imaging in human occipital cortex. *Proceedings of the National Academy of Sciences USA, 92*, 8135–8139.

Marino, R. A., Levy, R., Boehnke, S., White, B. J., Itti, L., & Munoz, D. P. (2012). Linking visual response properties in the superior colliculus to saccade behavior. *European Journal of Neuroscience, 35*, 1738–1752.

Maris, E., & Oostenveld, R. (2007). Nonparametric statistical testing of EEG- and MEG-data. *Journal of Neuroscience Methods, 164*(1), 177–190.

Markov, N. T., Vezoli, J., Chameau, P., Falchier, A., Quilodran, R., Huissoud, C., et al. (2014). Anatomy of hierarchy: feedforward and feedback pathways in macaque visual cortex. *The Journal of Comparative Neurology. Research in Systems Neuroscience, 522*, 225–259.

Marner, L., Nyengaard, J. R., Tang, Y., & Pakkenberg, B. (2003). Marked loss of myelinated nerve fibers in the human brain with age. *The Journal of Comparative Neurology, 462*(2), 144-152.

Marshall, J. (1987). The ageing retina: physiology or pathology. *Eye, 1*, 282-295.

Matsumoto, N., Okada, M., Sugase-Miyamoto, Y., Yamane, S., & Kawano, K. (2005). Population dynamics offFace-responsive neurons in the inferior temporal cortex. *Cerebral Cortex, 15*(8), 1103-1112.

Maunsell, J. H., & Gibson, J. R. (1992). Visual response latencies in striate cortex of the macaque monkey. *Journal of Neurophysiology, 4*, 1332-1334.

McCarthy, G., Puce, A., Belger, A., & Allison, T. (1999). Electropysiological studies of human face perception. II: Response properties of face-specific potentials generated in occipitotemporal cortex. *Cerebral Cortex, 9*, 431-444.

McGeer, E., & McGeer, P. (1976). In R. Terry, & S. Gershon, *Neurobiology of aging.* New York: Raven.

Milner, A. D., & Goddale, M. A. (2006). *Visual brain in action.* New York: Oxford Univeristy Press.

Milner, A. D., & Goodale, M. A. (2008). Two visual systems re-viewed. *Neuropsychologia, 46*(3), 774–785.

Moeller, S., Freiwald, W. A., & Tsao, D. Y. (2008). Patches with links: a unified system for processing faces in the macaque temporal lobe. *Science, 320*, 1355-1359.

Moffat, S. D., Szekely, C. A., Zonderman, A. B., Kabani, N. J., & Resnick, S. (2000). Longitudinal change in hippocampal volume as a function of apolipoprotein E genotype. *Neurology, 55*(1), 134-136.

Moran, C., Phan, T. G., Chen, J., Blizzard, L., Beare, R., Venn, A., et al. (2013). Brain Atrophy in Type 2 Diabetes: Regional distribution and influence on cognition. *Diabetes Care, 36*(12), 4036-42.

Mormann, F., Kornblith, S., Quiroga, R. Q., Kraskov, A., Cerf, M., Fried, I., et al. (2008). Latency and selectivity of single neurons indicate hierarchical processing in the human medial temporal lobe. *The journal of Neuroscience, 28*(36), 8865-8872.

Morrison, J. D., & McGrath, C. (1985). Assessment of the optical contributions to the age-related deterioration in vision. *Journal of Experimental Physiology, 70*, 249-269.

Morrison, J. D., & Reilly, J. (1989). The pattern visual evoked cortical responses in human ageing. *Quarterly Journal of Experimental Physiology, 74*, 311-328.

Morrone, M. C., & Burr, D. C. (1988). A phase-dependent energy model. *Proceedings of the Royal Society of London Series B-biological Sciences, 235*, 221-245.

Mostany, R., Anstey, J. E., Crump, C. L., Maco, B., Knott, G., & Portera-Cailliau, C. (2013). Altered synaptic dynamics during normal brain aging. *The Journal of Neuroscience, 33*(9), 4094-4104.

Movshon, J., & Newsome, W. (1996). Visual response properties of striate cortical neurons projecting to area MT in macaque monkeys. *Journal of Neuroscience, 16*, 7733–7741.

Mur, M., Ruff, D. A., Bodurka, J., De Weerd, P., Bandettini, P. A., & Kriegeskorte, N. (n.d.). (2012) Categorical, yet graded, single-image activation profiles of human category-selective cortical regions. *The Journal of Neuroscience, 32*, 8649–8662.

Murata, A., Gallese, V., Luppino, G., Kaseda, M., & Sakata, H. (2000). Selectivity for the shape, size, and orientation of objects for grasping in neurons of monkey parietal area AIP. *Journal of Neurophysiology, 83*(5), 2580–2601.

Nakamura, A., Yamada, T., Abe, Y., Nakamura, K., Sato, N., Horibe, K., et al. (2001). Age-related changes in brain neuromagnetic responses to face perception in humans. *Neuroscience Letters, 312*(1), 13-6.

Nakamura, H., Gattass, R., Desimone, R., & Ungerleider, L. G. (1993). The modular organization of projections from areas VI and V2 to areas V4 and TEO in macaques. *The Journal of Neuroscience, September 1993, 13(g):, 13*(9), 3681-3691.

Nguyen, V. T., & Cunnington, R. (2014). The superior temporal sulcus and the N170 during face processing: Single trial analysis of concurrent EEG–fMRI. *NeuroImage, 86*, 492–502.

Nguyen, V., Breakspear, M., & Cunnington, R. (2013). Fusing concurrent EEG-fMRI with dynamic causal modeling: Application to effective connectivity during face perception. *Neuroimage*, doi: 10.1016/j.neuroimage.2013.06.083.

Nichols, T. (2012). Multiple testing corrections, nonparametric methods, and Random Field Theory. *NeuroImage, 62*(2), 811-815.

Nielsen, K., & Peters, A. (2000). The effects of aging on the frequency of nerve fibers in rhesus monkey striate cortex. *Neurobiology of Aging, 21*, 621– 628.

Nowak, L. G., & Bullier, J. (1997). The timing of information transfer in the visual system. In K. S. Rockland, J. H. Kaas, & A. Peters, *Cerebral Cortex* (Vol. 12: Extrastriate Cortex in Primates, pp. 205-241). New York, NY: Plenum Press.

Nyberg, L., Lovden, M., Rilund, K., Lindenberger, U., & Backman, L. (2012). Memory aging and brain maintance. *Trends in Cognitive Sciences, 16*(5), 292-305.

Nyberg, L., Salami, A., Andersson, M., Eriksson, J., Kalpouzos, G., Kauppi, K., et al. (2010). Longitudinal evidence for diminished frontal cortex function in aging. *Procedeeings in the National Academy of Sciences U S A, 107*(52), 22682-22686.

Okazaki, Y., Abrahamyan, A., Stevens, C. J., & Ioannides, A. A. (2008). The timing of face selectivity and attentional modulation in visual processing. *Neuroscience, 152*, 1130–1144.

Oliva, A., & Torralba, A. (2001). Modeling the Shape of the Scene: A Holistic Representationof the Spatial Envelope. *International Journal of Computer Vision, 42*(3), 145–175.

Oliva, A., & Torralba, A. (2006). Building the gist of a scene: The role og global image features in recognition. *Progress in Brain Research, 155*, 23-36.

Oppenheim, A. V., & Lim, J. S. (1981). The importance of phase in signals. *Proceedings of the IEEE, 69*(5).

Orban, G. A., Van Essen, D., & Vanduffel, W. (2004). Comparative mapping of higher visual areas in monkeys and humans. *Trends in Cognitive Sciences, 8*(7), 315-324.

Owsley, C. (2011). Aging and vision. *Vision Research, 51*(13), 1610-1622.

Owsley, C., & Burton, K. B. (1991). Aging and spatial contrast sensitivity: Underlying mechanisms and implications for everyday life. In P. H. Bagnoli, *The changing visual system* (pp. 119-136). New York: Plenum Press.

Owsley, C., Sekuler, R., & Siemsen, D. (1983). Contrast sensitivity throughout adulthood. *Vision Research, 23*, 689-699.

Pakkenberg, B., & Gundersen, H. J. (1997). Neocortical neuron number in humans: effect of sex and age. *The Journal of Comparative Neurology, 384*(2), 312-20.

Park, D. C., Polk, T. A., Park, R., Minear, M., Savage, A., & Smith, M. R. (2004). Aging reduces neural specialization in ventral visual cortex. *Proceedings in Natinal Academy of Science USA, 101*(35), 13091-13095.

Park, J., Carp, J., Hebrank, A., Park, D. C., & Polk, T. A. (2010). Neural specificity predicts fluid processing ability in older adults. *The Journal of Neuroscience, 30*(27), 9253–9259.

Park, J., Carp, J., Kennedy, K. M., Rodrigue, K., Bischof, G., Huang, C., et al. (2012). Neural broadening or neural attenuation? Investigating age-related dedifferentiation in the face network in a large lifespan sample. *The Journal of Neuroscience, 32*(6), 2154-2158.

Parra, L. C., Spence, C. D., Gerson, A. D., & Sajda, P. (2005). Recipes for the linear analysis of EEG. *Neuroimage, 28*(2), 326–341.

Pascual-Leone, A., & Walsh, V. (2001). Fast backprojections from the motion to the primary visualarea necessary for visual awareness. *Science, 292*(5516), 510-512.

Pasupathy, A., & Connor, C. E. (1999). Responses to contour features in macaque area V4. *Journal of Neurophysiology, 82*, 2490-2502.

Pasupathy, A., & Connor, C. E. (2002). Responses to Contour Features in Macaque Area V4. *Nature Neuroscience, 5*(12), 1332-1338.

Paul, R., Grieve, S. M., Chaudary, B., Gordon, N., Lawrence, J., Cooper, N., et al. (2009). Relative contributions of the cerebellar vermis and prefrontal lobe volumes on cognitive function across the adult lifespan. *Neurobiology of Aging, 30*(3), 457–465.

Payer, D., Marshuetz, C., Sutton, B., Hebrank, A., Welsh, R., & Park, D. (2006). Decreased neural specialization in old adults on a working memory task. *Neuroreport, 17*(5), 487-91.

Pernet, C. R., Chauveau, N., Gaspar, C. M., & Rousselet, G. A. (2011). LIMO EEG: A Toolbox for Hierarchical LInearMOdeling of ElectroEncephaloGraphic Data. *Computational Intelligence and Neuroscience*, Article ID 831409.

Perrett, D., Oram, M. W., & Ashbridge, E. (1998). Evidence accumulation in cell populations responsive to faces: an account of generalisation of recognition without mental transformations. *Cognition, 67*(1-2), 111-145.

Perrett, D., Rolls, E. T., & Caan, W. (1982). Visual neurones responsive to faces in the monkey temporal cortex. *Experimental Brain Research, 47*, 329-342.

Peters, A. (2002). The effects of normal aging on myelin and nerve fibers: a review. *Journal of Neurocytology, 31*(8-9), 581-593.

Peters, A. (2009). The effects of normal aging on myelinated nerve fi bers in monkey central nervous system. *Frontiers in Neuroanatomy, doi: 10.3389/neuro.05.011.2009*.

Peters, A., Moss, M. B., & Sethares, C. (2000). Effects of aging on myelinated nerve fibers in monkey primary visual cortex. *Journla of Comparative Neurology, 419*(3), 364-76.

Pfutze, E., Sommer, W., & Schweinberger, S. (2002). Age related slowing in face and name recognition: evidence from event-related brain potentials. *Psychology andl Aging, 17*(1), 140-60.

Philiastides, M. G., & Sajda, P. (2006). Temporal characterization of the neural correlates of perceptual decision making in the human brain. *Cerebral Cortex, 16*(4), 509-18.

Philiastides, M. G., Ratcliff, R., & Sajda, P. (2006). Neural representation of task difficulty and decision making during perceptual categorization: a timing diagram. *The Journal of Neuroscience, 26*(35), 8965– 8975.

Phillips, F., & Todd, J. T. (2010). Texture discrimination based on global feature alignments. *Journal of Vision, 10(6)*(6), 1–14.

Piguet, O., Double, K. L., Kril, J. J., Harasty, J., Macdonald, V., McRitchie, D. A., et al. (2009). White matter loss in healthy ageing: A postmortem analysis. *Neurobiology of Aging, 30*, 1288–1295.

Pinsk, M. A., A. M., Weiner, K. S., Kalkus, J. F., Inati, S. J., Gross, C. G., et al. (2009). Neural representations of faces and body parts in macaque and human cortex: a comparative FMRI study. *Journal of Neurophysiology, 101*(5), 2581-2600.

Piotrowski, L. N., & Campbell, F. W. (1982). A demonstration of the visual importance and flexibility of spatial-frequency amplitude and phase. *Perception, 11*, 337-346.

Pitcher, D., Charles, L., Devlin, J., Walsh, V., & Duchaine, B. (2009). Triple dissociation of faces, bodies, and objects in extrastriate cortex. *Current Biology, 19*(4), 319-24.

Pitcher, D., Garrido, L., Walsh, V., & Duchaine, B. C. (2008). Transcranial Magnetic Stimulation disrupts the perception and embodiment of facial expressions. *The Journal of Neuroscience, 28*(36), 8929-8933.

Pitcher, D., Walsh, V., & Duchaine, B. C. (2011). The role of the occipital face area in the cortical face perception network. *Experimental Brain Research, 209*(4), 481–493.

Pitcher, D., Walsh, V., Yovel, G., & Duchaine, B. (2007). TMS evidence for the involvement of the right occipital face area in early face processing. *Current Biology, 17*(18), 1568-73.

Pizzagalli, D., Regard, M., & Lehmann, D. (1999). Rapid emotional face processing in the human right and left brain hemispheres: an ERP study. *NeuroReport, 10*, 2691-2698.

Polich, J. (1987). Response mode and P300 from auditory stimuli. *Biological Psychology, 25*, 61-71.

Polich, J. (1996). Meta-analysis of P300 normative aging studies. *Psychophysiology, 33*, 334-353.

Polich, J. (1997). EEG and ERP assessment of normal aging. *Electroencephalography and Clinical Neurophysiology, 104*, 244-256.

Portilla, J., & Simoncelli, E. P. (2000). A parametric texture model based on joint statistics. *International Journal of Computer Vision, 40*(1), 49–71.

Prins, N. D., van Dijk, E. J., den Heijer, T., Vermeer, S. E., Jolles, J., & Koudstaal, P. J. (2005). Cerebral small-vessel disease and decline in information processing speed, executive function and memory. *Brain, 128*, 2034–2041.

Puce, A., Allison, T., & McCarthy, G. (1999). Electrophysiological studies of human face perception. III: effects of top-down processing on face-specific potentials. *Cerebral Cortex, 9*, 445–458.

Rabbitt, P., Scott, M., Lunn, M., Thacker, N., Lowe, C., & Pendleton, N. (2007). White matter lesions account for all age-related declines in speed but not in intelligence. *Neuropsychology, 21*, 363-370.

Raiguel, S. E., Lagae, L., Gulyas, B., & Orban, G. A. (1989). Response latencies of visual cells in macaque areas V1, V2 and V5. *Brain Research, 493*, 155-159.

Rajimehr, R., Young, J. C., & Tootell, R. (2009). An anterior temporal face patch in human cortex, predicted by macaque maps. *Proceedings of the National Academy of Sciences of the USA, 106*(6), 1995-2000.

Ratcliff, R., Philiastides, M. G., & Sajda, P. (2009). Quality of evidence for perceptual decision making is indexed by trial-to-trial variability of the EEG. *Proceedings of the National Academy of Sciences of the United States of America, 106*(16), 6539–6544.

Raz, D., Seeliger, M. W., Geva, A. B., & Percicot, C. L. (2002). The effect of contrast and luminance on mfERG responses in a monkey model of glaucoma. *Investigative Ophthalmology & Visual Science, 43*(6), 2027-2035.

Raz, N. (2000). Aging of the brain and its impact on cognitive performance: Integration of structural and fucntional findings. In F. I. Craik, & T. A. Salthouse, *Handbook of Aging and Cognition - II* (pp. 1-90). Mahwah, NJ: Erlbaum.

Raz, N., & Rodrigue, K. M. (2006). Differential aging of the brain: Patterns, cognitive correlates and modifiers. *Neuroscience and Biobehavioral Reviews, 30*, 730–748.

Raz, N., Ghisletta, P., Rodrigue, K. M., Kennedy, K. M., & Lindenberger, U. (2010). Trajectories of brain aging in middle-aged and older adults: regional and individual differences. *Neuroimage, 51*, 501–511.

Raz, N., Gunning-Dixon, F., Head, D., Rodrigue, K., A., W., & Acker, J. (2004). Aging, sexual dimorphism, and hemispheric asymmetry of the cerebral cortex: replicability of regional differences in volume. *Neurobiology of Aging, 25*(3), 377-96.

Raz, N., Lindenberger, U., Ghisletta, P., Rodrigue, K. M., Kennedy, K. M., & Acker, J. D. (2008). Neuroanatomical correlates of fluid intelligence in healthy adults and persons with vascular risk. *Cerebral Cortex, 18*, 718–726.

Raz, N., Lindenberger, U., Rodrigue, K. M., Kennedy, K. M., Head, D., Williamson, A., et al. (2005). Regional brain changes in aging healthy adults: general trends, individual differences and modifiers. *Cerebral Cortex, 15*, 1676-1689.

Raz, N., Rodrigue, K. M., & Acker, J. D. (2003). Hypertension and the brain: vulnerability of the prefrontal regions and executive functions. *Behavioral Neuroscience, 117*, 1169–1180.

Raz, N., Rodrigue, K. M., & Haacke, E. M. (2007). Brain changes and its modifiers: insights from in vivo neuromorphometry and susceptibility weighted imaging. *Annals of the New York Academy of Sciences, 1097*, 84-93.

Raz, N., Schmiedek, F., Rodrigue, K. M., Kennedy, K. M., Lindenberger, U., & Lövdén, M. (2013). Differential brain shrinkage over 6 months shows limited association with cognitive practice. *Brain and Cognintion, 82*(2), 171-180.

Reeves, P. (1920). The response of the average pupil to various intensities of light. *Journal of the Optical Society of America, 4*(2), 35-43.

Resnick, S. M., Pham, D. L., Kraut, M. A., Zonderman, A. B., & Davatzikos, C. (2003). Longitudinal magnetic resonance imaging studies of older adults: a shrinking brain. *Journal of Neuroscience 23,, 23*, 3295–3301.

Reuter-Lorenz, P. A., Jonides, J., Smith, E. E., Hartley, A., Miller, A., Marshuetz, C., et al. (2000). Age differences in the frontal lateralization of verbal and spatial working memory revealed by PET. *Journal of Cognitive Neuroscience, 12*(1), 174–187.

Rivolta, D., Palermo, R., Schmalzl, L., & Williams, M. A. (2012). An early category-specific neural response for the perception of both places and faces. *Cognitive Neuroscience, 3*(1), 45–51.

Rogmann, J. J. (2013). *Package "orddom" - ordinal dominance statistics.* Hamburg, Germany: University of Hamburg, Department of Psychology.

Rosburg, T., Ludowig, E., Dumpelmann, M., Alba-Ferrara, L., Urbach, H., & Elger, C. E. (2010). The effect of face inversion on intracranial and scalp recordings of event-related potentials. *Psychophysiology, 47*, 147–157.

Rossion, B., & Caharel, S. (2011). ERP evidence for the speed of face categorization in the human brain: Disentangling the contribution of low-level visual cues from face perception. *Vision Research, 51*, 1297–1311.

Rossion, B., Caldara, R., Seghier, M., Schuller, A., Lazeyras, M., & Mayer, F. (2003). A network of occipito-temporal face-sensitive areas besides the right middle fusiform gyrus is necessary for normal face processing. *Brain, 126*, 2381–2395.

Rossion, B., Joyce, C., Cottrell, G., & Tarr, M. (2003). Early lateralization and orientation tuning for face, word, and object processing in the visual cortex. *Neuroimage, 20*(3), 1609-1624.

Roudaia, E., Bennett, P. J., & Sekuler, A. B. (2008). The effect of aging on contour integration. *Vision Research, 48*(28), 2767–2774.

Roudaia, E., Farber, L. E., Bennett, P. J., & Sekuler, A. B. (2011). The effects of aging on contour discrimination in clutter. *Vision Research, 51*(9), 1022–1032.

Rousselet, G. A. (2012). Does filtering preclude us from studying ERP time-courses? [General Commentary]. *Frontiers in Psychology, 3*(131), doi: 10.3389/fpsyg.2012.00131.

Rousselet, G. A., & Pernet, C. R. (2011). Quantifying the time course of visual object processing using ERPs: it's time to up the game. *Frontiers in Psychology, 2*(107), doi:10.3389/fpsyg.2011.00107.

Rousselet, G. A., Gaspar, C. M., Pernet, C. R., Husk, J. S., Bennett, P., & Sekuler, A. (2010). Healthy aging delays scalp EEG sensitivity to noise in a face discrimination task. *Frontiers in Psychology, 1*(19), doi: 10.3389/fpsyg.2010.00019.

Rousselet, G. A., Husk, J. S., Bennett, P. J., & Sekuler, A. B. (2005). Spatial scaling factors explain eccentricity effects on face ERPs. *Journal of Vision, 5*(10), 755-763.

Rousselet, G. A., Husk, J. S., Bennett, P. J., & Sekuler, A. B. (2008b). Time course and robustness of ERP object and face differences. *Journal of Vision, 8*(12), 1-18.

Rousselet, G. A., Husk, J. S., Pernet, C. R., Gaspar, C. M., Bennett, P. J., & Sekuler, A. B. (2009). Age-related delay in information accrual for faces: Evidence from a parametric, single-trial EEG approach. *BMC Neuroscience, 10*(114).

Rousselet, G. A., Macé, M. J.-M., Thorpe, S. J., & Fabre-Thorpe, M. (2007). Limits of ERP differences in tracking object processing speed. *Journal of Cognitive Neuroscience, 19*, 1-18.

Rousselet, G. A., Pernet, C. R., Bennett, P. J., & Sekuler, A. B. (2008). Parametric study of EEG sensitivity to phase noise during face processing. *BMC Neuroscience, 9*(98), doi:10.1186/1471-2202-9-98.

Rousselet, G. A., Pernet, C. R., Caldara, R., & Schyns, P. (2011). Visual object categorization in the brain: what can we really learn from ERP peaks? *Frontiers in Human Neuroscience, 5:93*, doi: 10.3389/fnhum.2011.00093.

Rousselet, G., Gaspar, C., Wieczorek, K., & Pernet, C. R. (2011a). Modeling single-trial ERP reveals modulation of bottom-up face visual processing by top-down task contraints (in some subjects). *Frontiers in Psychology, 2*(137), doi: 10.3389/fpsyg.2011.00137.

Rousselet, G., Macé, M., & Fabre-Thorpe, M. (2004). Animal and human faces in natural scenes: How specific to human faces is the N170 component. *Journal of vision, 4*(1), 13-21.

Rugg, M., & Morcom, A. M. (2005). The relationship between brain activity, cognitive performance and aging. In R. Cabeza, L. Nyberg, & D. Park, *Cogntive Neroscience of Aging* (pp. 132-154). Oxford, NY.: Oxford University Press, Inc.

Sadeh, B., Podlipsky, I., Zhdanov, A., & Yovel, G. (2010). Event-Related Potential and functional MRI measures of face-selectivity are highly correlated: a simultaneous ERP-fMRI investigation. *Human Brain Mapping, 31*, 1490–1501.

Said, F. S., & Weale, R. (1959). The variation with age of the spectral transmissivity of the living human crystalline lens. *Gerontologia, 3*, 213-231.

Salami, A., Eriksson, J., Nilsson, L.-G., & Nyberg, L. (2012). Age-related white matter microstructural differences partly mediate age-related decline in processing speed but not cognition. *Biochimica et Biophysica Acta, 1822*, 408-415.

Salat, D. H., Tuch, D. S., Greve, D. N., van der Kouwe, A. J., Hevelone, H. D., Zaleta, A. K., et al. (2005). Age-related alterations in white matter microstructure measured by diffusion tensor imaging. *Neurobiology of Aging, 26*(8), 1215-1227.

Salat, D., Grevea, D., Pacheco, J., Quinna, B., Helmera, K., Bucknera, R., et al. (2009). Regional white matter volume differences in nondemented aging and Alzheimer's disease. *Neuroimage, 44*(4), 1247–1258.

Salin, P.-A., & Bullier, J. (1995). Corticocortical connections in the visual system: structure and function. *Physiological Review, 75*(1), 107-154.

Salthouse, T. A. (1996). The processing-speed theory of adult age differences in cognition. *Psychological Review, 103*(3), 403-428.

Salthouse, T. A. (1998). Independence of age-realted inlfuences on cognitive abilities across the life span. *Developmental Psychology, 34*(5), 851-864.

Salthouse, T. A. (2000). Aging and measures of processing speed. *Biological Psychology, 54*, 35–54.

Salthouse, T. A. (2004). What and when of cognitive aging. *Current Directions in Psychological Science, 13*, 140–144.

Salthouse, T. A. (2011). Neuroanatomical substrates of age-related cognitive decline. *Psychological Bulletin, 137*(5), 753-784.

Salthouse, T. A., & Ferrer-Caja, E. (2003). What needs to be explained to account for age-related effects on multiple cognitive variables? *Psychology and Aging, 18*(1), 91-110.

Salthouse, T., & Czaja, S. (2000). Structural constraints on process explanations in cognitive aging. *Psychology and Aging, 15*, 44–55.

Sandell, J. H., & Peters, A. (2003). Disrupted myelin and axon loss in the anterior commissure of the aged rhesus monkey. *Journal of Comparative Neurology, 466*(1), 14-30.

Sato, T., Uchida, G., Lescroart, M. D., Kitazono, J., Okada, M., & Tanifuji, M. (2013). Object representation in inferior temporal cortex is organized hierarchically in a mosaic-like structure. *The Journal of Neuroscience, 33*(42), 16642–16656.

Schefrin, B. E., Tregear, S. J., Harvey, L. O., & Werner, J. S. (1999). Senescent changes in scotopic contrast sensitivity. *Vision Research, 39*, 3728–3736.

Schiller, P. H., Logothetis, N. K., & Charles, E. R. (1990a). Role of the color- opponent and broad-band channels in vision. *Visual Neuroscience, 5*, 321-346.

Schmolesky, M. T., Wang, Y., Hanes, D. P., Thompson, K. G., Leutgeb, S., Schall, J. D., et al. (1998). Signal timing across the macaque visual system. *Journal of Neurophysiology, 79*(6), 3272–3278.

Schmolesky, M., Wang, Y., Pu, M., & Leventhal, A. (2000). Degradation of stimulus selectivity of visual cortical cells in senescent rhesus monkeys. *Nature neuroscience, 3*, 384–390.

Scholte, H. S., Ghebreab, S., Waldorp, L., Smeulders, A. W., & Lamme, V. A. (2009). Brain responses strongly correlate with Weibull image statistics when processing natural images. *Journal of Vision, 9*(4), 1–15.

Schretlen, D., Pearlson, G. D., Anthony, J. C., Aylward, E. H., Augustine, A. M., Davis, A., et al. (2000). Elucidating the contributions of processing speed, executive ability, and frontal lobe volume to normal age- related differences in fluid intelligence. *Journal of the International Neuropsychological Society, 6*, 52–61.

Schroeder, C. E., Molhom, S., Lakatos, P., Ritter, W., & Foxe, J. J. (2004). Human–simian correspondence in the early cortical processing of multisensory cues. *Cognitive Processing, 5*, 140–151.

Schroeder, C. E., Steinschneider, M., Javitt, D. C., Tenke, C. E., Givre, S. J., Mehta, A. D., et al. (1995). Localization of ERP generators and identification. *Electroencephaphy Clinical Neurophysiology, 44*, 55–75.

Schwarzlose, R. F., Swisher, J. D., Dang, S., & Kanwisher, N. (2008). The distribution of category and location information across object-selective regions in human visual cortex. *Proceedings of the National Academy of Sciences of the USA, 105*(11), 4447-4452.

Schyns, P. G., Petro, L. S., & Smith, M. L. (2007). Dynamics of visual information integration in the brain for categorizing facial expressions. *Current Biology, 17*(18), 1580–1585.

Schyns, P. G., Thut, G., & Gross, J. (2011). Cracking the code of oscillatory activity. *PLoS Biology, 9*(5), e1001064.

Schyns, P., Gosselin, F., & Smith, M. L. (2009). Information processing algorithms in the brain. *Trends in Cognitive Sciences, 13*(1), 21-26.

Sclar, G., Maunsell, H. R., & Lennie, P. (1990). Coding of image contrast in central visual pathways of the macaque monkey. *Vision Research, 30*(1), 1-10.

Se´verac-Cauquil, A., Edmonds, G. E., & Taylor, M. J. (2000). Is the face-sensitive N170 the only ERP not affected by selective attention? *NeuroReport, 11*, 2167–2171.

Sehatpour, P., Molholm, S., Schwartz, T. H., Mahoney, J. R., Mehta, A. D., Javitt, D. C., et al. (2008). A human intracranial study of long-range oscillatory coherence across a frontal– occipital–hippocampal brain network during visual object processing. *Proceedings in National Academy of Sciences of the United States of America, 105*(11), 4399-4404.

Sekuler, R., & Sekuler, A. B. (2000). Age-related changes, optical factors, and neural processes. In A. E. Kazdin, *Encyclopedia of Psychology* (pp. 180-183). Oxford, NY.: American Psychological Association/Oxford University Press.

Sereno, M. E., Trinath, T., Augath, M., & Logothetis, N. K. (2002). Three-dimensional shape representation in monkey cortex. *Neuron, 33*(4), 635–652.

Sereno, M. I., & Tootell, R. B. (2005). From monkeys to humans: what do we now know about brain homologies? *Current Opinion in Neurobiology, 15*, 135–144.

Serre, T., Kreiman, G., Kouh, M., Cadieu, C., Knoblich, U., & Poggio, T. (2007). A quantitative theory of immediate visual recognition. *Progress in Brain Research, 165*, 33-56.

Séverac-Cauquil, A., Edmonds, G. E., & Taylor, M. J. (2000). Is the face-sensitive N170 the only ERP not affected by selective attention? *Neuroreport, 11*, 2167–2171.

Shaw, N. A., & Cant, B. R. (1980). Age-dependent changes in the latency of the pattern visual evoked potential. *Electroencephalography Clinical Neurophysiology, 48*(2), 237-41.

Shibata, T., Nishijo, H., Tamura, R., Miyamoto, K., Eifuku, S., Endo, S., et al. (2002). Generators of visual evoked potentials for faces and eyes in the human brain as determined by dipole localization. *Brain Topography, 15*(1), 51-63.

Silvanto, J., Schwarzkopf, D. S., Gilaie-Dota, S., & Rees, G. (2010). Differing causal roles for lateral occipital cortex and occipital face area in invariant shape recognition. *European Journal of Neuroscience, 32*(1), 165–171.

Silverman, B. W. (1986). Density Estimation for Statistics and Data Analysis. In B. W. Silverman, *Monographs on Statistics and Applied Probability* (pp. 1-22). London: Chapman and Hall.

Sloane, M. E., Owsley, C., & Alvarez, S. L. (1988). Aging, senile miosis and spatial contrast sensitivity at low luminance. *Vision Research, 28*(11), 1235-1246.

Smith, M. L., Gosselin, F., & Schyns, P. G. (2007). From a face to its category via a few information processing states in the brain. *NeuroImage, 37*, 974-984.

Smith, M. L., Gosselin, F., & Schyns, P. G. (2012). Measuring internal representations from behavioral and brain data. *Current Biology, 22*, 191–196.

Sokol, S., Moskowitz, A., & Towle, V. L. (1981). Age-related changes in the latency of the visual evoked potential: influence of check size. *Electroencephalography Clinical Neurophysiology, 51*, 559–562.

Spear, P. D. (1993). Minireview: Neural basis of visual deficits during aging. *Vision Research, 33*(18), 2589-2609.

Spear, P. D. (1993). Neural bases of visual deficits during aging. *Vision Research, 33*(18), 2589-2609.

Strassburger, T. L., Lee, H. C., Daly, E. M., Szczepanik, J., Krasuski, J. S., Mentis, M. J., et al. (1997). Interactive effects of age and hypertension on volumes of brain structures. *Stroke, 28*, 1410–1417.

Sugase, Y., Yamane, S., Ueno, S., & Kawano, K. (1999). Global and fine information coded by single neurons in the temporal visual cortex. *Nature, 400*(6747), 869-873.

Sugita, Y. (2008). Face perception in monkeys reared with no exposure to faces. *Proceedings of the National Academy of Sciences USA, 105*(1), 394-398.

Szczepanowska-Nowak, W., Hachol, A., & Kasprzak, H. (2004). System for measurement of the consensual pupil light reflex. *Optica Applicata, 34*(4), 619-634.

Tadmor, Y., & Tolhurst, D. J. (1993). Both the phase and the amplitude spectrum may determine the appearance of natural images. *Vision Research, 33*(1), 141-145.

Taki, Y., Kinomura, S., Sato, K., Goto, R., Wub, K., Kawashima, R., et al. (2010). Correlation between gray/white matter volume and cognition in healthy elderly people. *Brain and Cognition, 75*(2), 170-176.

Tanaka, J. W., & Curran, T. (2001). A neural basis for expert object recogntion. *Psychological Science, 12*(1), 43-47.

Tanaka, K. (1993). Neuronal mechanisms of object recognition. *Science, 262*(5134), 685-688.

Tanaka, K. (1997). Columnar organizatioin in inferotemporal cortex. In K. S. K. S. Rockland, J. H. Kaas, & A. Peters, *Extrastriate Cortex in Primates* (pp. 469-498). New York and London: Plenum Press.

Tanaka, K. (2003). Columns for complex visual object features in the Inferotemporal cortex: clustering of cells with similar but slightly different stimulus selectivities. *Cerebral Cortex*, 90–99.

Tanaka, T., Nishida, S., Aso, T., & Ogawa, T. (2013). Visual response of neurons in the lateral intraparietal area and saccadic reaction time during a visual detection task. *European Journal of Neuroscience, 37*, 942-956.

Tang, Y., Nyengaard, J. R., Pakkenberg, B., & Gundersen, J. G. (1997). Age-induced white matter changes in the human brain: a stereological investigation. *Neurobiology of Aging, 18*(6), 609 – 615.

Tanskanen, T., Nasanen, R., Montez, T., Paallysaho, J., & Hari, R. (2005). Face recognition and cortical responses show similar sensitivity to noise spatial frequency. *Cerebral Cortex, 15*, 526--534.

Tenke, C. E., & Kayser, J. (2012). Generator localization by current source density (CSD): Implications of volume conduction and field closure at intracranial and scalp resolutions. *Clinical Neurophysiology, 123*(12), 2328–2345, doi:10.1016/j.clinph.2012.0.

Thierry G., M. C. (2007). Controlling for interstimulus perceptual variance abolishes N170 face selectivity. *Nature Neuroscience, 10*, 505-511.

Thomas, C., Avidan, G., Humphreys, K., Jung, K. J., Gao, F., & Behrmann, M. (2009). Reduced structural connectivity in ventral visual cortex in congenital prosopagnosia. *Nature Neuroscience, 12*(1), 29-31.

Thomas, C., Moya, L., Avidan, G., Humphreys, K., Jung, K. J., & Behrmann, M. (2008). Reduction in white matter connectivity, revealed by Diffusion Tensor Imaging, may account for age-related changes in face perception. *Journal of Cognitive Neuroscience, 20*(2), 268-84.

Thompson, P. M., Mega, M. S., Woods, R. P., Zoumalan, C. I., Lindshield, C. J., Blanton, R. E., et al. (2001). Cortical change in Alzheimer's disease detected with a disease-specific population-based brain atlas. *Cerebral Cortex, 11*(1), 1-16.

Thorpe, S. (2010). Speed of processing in sensory systems. In E. B. Goldstein, *Encyclopedia of Perception, vol.1&2* (pp. 932-935). Thousand Oaks, CA.: SAGE Publications, Inc.

Tisserand, D. J., van Boxtel, M. P., Pruessner, J. C., Hofman, P., Evans, A. C., & Jolles, J. (2004). A voxel-based morphometric study to determine individual differences in gray matter density associated with age and cognitive change over time. *Cerebral Cortex, 14*(9), 966–973.

Tobimatsu S, C. G., & Cone, S. G. (1988). Effects of pupil diameter and luminance changes on pattern electrretinograms and visual evoked potentials. *Clinical Vision Science, 2*, 293-302.

Tobimatsu, S. (1995). Aging and pattern visual evoked potentials. *Optometry and vision science, 72*(3), 192-197.

Tobimatsu, S., Kurita-Tashima, S., Nakayama-Hiromatsu, M., Akazawa, K., & Kato, M. (1993). Age related changes in pattern visual evoked potentials: differential effects of luminance, contrast and check size. *Electroencephalography Clinical Neurophysiology, 88*, 12-19.

Tobimatsu, S., Kurita-Tashima, S., Nakayama-Hiromatsu, M., Akazawa, K., & Kato, M. (1993). Age-related changes in pattern visual evoked potentials: differential effects of luminance, contrast and check size. *Electroencephalography Clinical Neurophysiology, 88*, 12-19.

Tootell, R. B., Hamilton, S. L., Silverman, M. S., & Switkes, E. (1988). Functional anatomy of macaque striate cortex. 1. Ocular dominance, binocular interaction, and baseline conditions. *Journal of Neuroscience, 8*, 1500–1530.

Tootell, R. B., Tsao, D., & Vanduffel, W. (2003). Neuroimaging weighs in: humans meet macaques in "primate" visual cortex. *The Journal of Neuroscience, 23*(10), 3981-3989.

Tovee, M. J. (2008). *An introduction to the visual system.* Cambridge, UK: Cambridge University Press.

Trick, G. L., Trickl, L., & Haywood, K. M. (1986). Altered pattern evoked retinal and cortical potentials associated with human. *Current Eye Research, 5*(10), 717-724.

Tsao, D. Y., & Livingstone, M. S. (2008). Mechanisms of face perception. *Annual Reviews Neuroscience, 31*, 411–437.

Tsao, D. Y., Freiwald, W. A., Knutsen, T. A., Mandeville, J. B., & Tootell, R. B. (2003). Faces and objects in macaque cerebral cortex. *Nature Neuroscience, 6*(9), 989-995.

Tsao, D. Y., Freiwald, W. A., Tootell, R. B., & Livingstone, M. S. (2006). A cortical region consisting entirely of face-selective cells. *Science, 311*, 670-674.

Tsao, D. Y., Moeller, S., & Freiwald, W. A. (2008). Comparing face patch systems in macaques and humans. *Proceedings of the National Academy of Sciences of the USA, 105*(49), 19514-19519.

Ts'o, D. Y., Roe, A. W., & Gilbert, C. D. (2001). A hierarchy of thefunctional organization for color, form and disparity in primatevisual area V2. *Vision Research, 41*, 1333–1349.

Tsunoda, K., Yamane, Y., Nishizaki, M., & Tanifuji, M. (2001). Complex objects are represented in macaque inferotemporal cortex by the combination of feature columns. *Nature Neuroscience, 4*(8), 832-838.

Ullman, S. (2006). Object recognition and segmentation by a fragment-based hierarchy. *Trends in Cognitive Sciences, 11*(2), 58-64.

Ullman, S., Vidal-Naquet, M., & Sali, E. (2002). Visual features of intermediate complexity and their use in classification. *Nature Neuroscience, 5*(7), 1–6.

Ungerleider, L. G., & Mishkin, M. (1982). Two cortical visual systems. In D. J. Ingle, R. J. Mansfield, & M. S. Goodale, *The Analysis of Visual Behavior* (pp. 549–586). Cambridge: MIT Press.

Ungerleider, L. G., & Pasternak, T. (2003). Ventral and dorsal cortical processing streams. In L. M. Chalupa, & J. S. Werner, *The visual neurosciences* (pp. 541-562). Cambridge, MA.: MIT Press.

Ungerleider, L. G., Gaffan, D., & Pelak, V. S. (1989). Projections from inferior temporal cortex to prefrontal cortex via the uncinate fascicle in rhesus monkeys. *Experimental Brain Research, 76*, 473–484.

Ungerleider, L. G., Galkin, T. W., & Mishkin, M. (1983). Visuotopic organization of projections from striate cortex to inferiorand lateral pulvinar in rhesus monkey. *The Journal of Comparative Neurology, 217*(2), 137-157.

van de Nieuwenhuijzen, M. E., Backus, A. R., Bahramisharif, A., Doeller, C. F., Jensen, O., & van Gerven, M. A. (2013). MEG-based decoding of the spatiotemporal dynamics of visual category perception. *Neuroimage, 83*, 1063-1073.

van de Vijver, I., Cohen, M. X., & Ridderinkhof, R. (2014). Aging affects medial but not anterior frontal learning-related theta oscillations. *Neurobiology of Aging, 35*, 692-704.

van den Heuvel, D. M., ten Dam, V. H., de Craen, A. J., Admiraal-Behloul, F., Olofsen, H., & Bollen, E. L. (2006). Increase in periventricular white matter hyperintensities parallels decline in mental processing speed in a non-demented elderly population. *Journal of Neurology, Neurosurgery and Psychiatry, 77*, 149–153.

Van Essen, D. C. (2003). Organization of visual areas in macaque and human cerebral cortex. In L. M. Chalupa, & J. S. Werner, *The visual neurosciences* (pp. 507-521). Cambridge, MA: The MIT Press.

Van Essen, D. C., Newsome, W. T., Maunsell, J. H., & Bixby, J. L. (1986). The projections from striate cortex (V1) to areas V2 and V3 in the macaque monkey: asymmetries, areal boundaries and patchy connections. *Journal of Computational Neurology, 244*, 451–480.

van Rijsbergen, N. J., & Schyns, P. (2009). Dynamics of trimming the content of face representations for categorization in the brain. *PLOS Computational Biology, 5*(11), e1000561.

VanRullen, R. (2006). On second glance: Still no high-level pop-out effect for faces. *Vision Research, 46*(18), 3017-3027, author reply 3028-3035.

VanRullen, R. (2011). Four common conceptual fallacies in mapping the time course of recognition. *Frontiers in Psychology, 2*(365), doi: 10.3389/fpsyg.2011.00365.

VanRullen, R., & Thorpe, S. J. (2001). The time course of visual processing: from early perception to decision making. *Journal of Cognitive Neuroscience, 13*(4), 454-461.

Verhaeghen, P., & Salthouse, T. (1997). Meta-analyses of age–cognition relations in adulthood: estimates of linear and nonlinear age effects and structural models. *Psychological Bulletin, 122*, 231–249.

Vizioli, L., Rousselet, G. A., & Caldara, R. (2010). Neural repetition suppression to identity is abolished by other-race faces. *Proceedings of the National Academy of Sciences of the United States of America*, doi: 10.1073/pnas.1005751107.

Voss, M. W., Erickson, K. I., Chaddock, L., Prakash, R. S., Colcombe, S. J., Morris, K. S., et al. (2008). Dedifferentiation in the visual cortex: An fMRI investigation of individual differences in older adults. *Brain Research, 1244*, 121-131.

Wandell, B. A. (1995). *Foundations of Vision.* Stanford, CA.: Sinauer Associates, Inc.

Wang, G., Tanaka, K., & Tanifuji, M. (1996). Optical imaging of functional organization in the monkey inferotemporal cortex. *Science, 272*, 1665–1668.

Wang, G., Tanifuji, M., & Tanaka, K. (1998). Functional architecture in monkey inferotemporal cortex revealed by in vivo optical imaging. *Neuroscience Research, 32*, 33-46.

Wang, Q., Sporns, O., & Burkhalter, A. (2012). Network Analysis of Corticocortical Connections Reveals Ventral and Dorsal Processing Streams in Mouse Visual Cortex. *The Journal of Neuroscience, 32*(13), 4386-4399.

Wang, Y., Fujita, I., & Murayama, Y. (2000). Neuronal mechanisms of selectivity for object features revealed by blocking inhibition in inferotemporal cortex. *Nature Neuroscience, 3*, 807 - 813.

Wang, Y., FujitaI., Tamura, H., & Murayama, Y. (2002). Contribution of GABAergic inhibition to receptive field structures of monkey inferior temporal neurons. *Cerebral Cortex, 12*, 62-74.

Wang, Y., Zhou, Y., Ma, Y., & Leventhal, A. G. (2005). Degradation of Signal Timing in Cortical Areas V1 and V2 of Senescent Monkeys. *Cerebral Cortex, 15*, 403--408.

Watanabe, S., Kakigi, R., & Puce, A. (2003). The spatiotemporal dynamics of the face inversion effect: a magneto- and electro-encephalographic study. *Neuroscience, 116*, 879-895.

Watson, A. B., & Yellott, J. I. (2012). A unified formula for light-adapted pupil size. *Journal of Vision, 12*(10), 1–16.

Weale, R. A. (1992). *The senescence of human vision.* Oxford, U.K.: Oxford University Press.

Webster, M. J., Bachevalier, J., & Ungerleider, L. G. (1993). Subcortical connections of inferior temporal areas TE and TEO in macaque monkeys. *The Journal of comparative Neurology, 335*(1), 73-91.

Webster, M. J., Bachevalier, J., & Ungerleider, L. G. (1994). Connections of inferior temporal areas TEO and TE with parietal and frontal cortex in macaque monkeys. *Cerebral Cortex, 4*(5), 470-83.

Webster, M. J., Bachevalier, J., & Ungerleider, L. G. (1995). Transient subcortical connections of inferior temporal areas TE and TEO in infant macaque monkeys. *The Journal of Comparative Neurology, 352*(2), 213-226.

Wichmann, F. A., Braun, D. I., & Gegenfurtner, K. R. (2006). Phase noise and the classification of natural images. *Vision Research, 46*, 1520–1529.

Wichmann, F. A., Drewes, J., Rosas, P., & Gegenfurtner, K. R. (2010). Animal detection in natural scenes: critical features revisited. [Research Support, Non-U.S. Gov't]. *Journal of Vision, 10(4)*(6), 1-27, doi: 10.1167/10.4.6.

Widman, A., & Schroger, E. (2012). Filter effects and filter artifacts in the analysis of electrophysiological data. *Frontiers in Psychology, 3*(233), doi: 10.3389/fpsyg.2012.00233.

Wiese, H., Schweinberger, S., & Hansen, K. (2008). The age of the beholder: ERP evidence of an own-age bias in face memory. *Neuropsychologia, 46*, 2973–2985.

Wilcox, R. R. (2005). *Introduction to Robust Estimation and Hypothesis Testing.* San Diego, CA: Elsevier Academic Press.

Wilcox, R. R. (2006). Graphical methods for assessing effect size: Some alternatives to Cohen's d. *Journal of Experimental Education, 74*(4), 353–367.

Wilcox, R. R. (2011). Comparing Two Dependent Groups: Dealing with Missing Values. *Journal of Data Science, 9*(1), 1-13.

Wilcox, R. R. (2012). *Introduction to Robust Estimation and Hypothesis Testing.* San Diego, CA: Academic Press.

Wilcox, R. R., & Muska, J. (1999). Measuring effect size: A non-parametric analogue of omega(2). *The British journal of mathematical and statistical psychology, 52*, 93–110.

Wilcox, R. R., & Tian, T. S. (2011). Measuring effect size: a robust heteroscedastic approach for two or more groups. *Journal of Applied Statistics, 38*(7), 1359–1368. doi:10.1080/02664763.2010.498507.

Winn, B., Whitaker, D., Elliott, D. B., & Phillips, N. J. (1994). Factors Affecting Light-Adapted Pupil Size in Normal Human Subjects. *Investigative Ophthalmology & Visual Science, 35*(3), 1132-.

Wood, C. C. (1987). Generators of event-related potentials. In A. M. Halliday, S. R. Butler, & R. Paul, *A textbook of clinical neurophysiology* (pp. 435-567). New York: Wiley.

Yamamoto, S., & Kashikura, K. (1999). Speed of face recognition in humans: an event-related potentials study. *NeuroReport: Cognitive Neuroscience and Neuropsychology, 10*(17), 3531-3534.

Yamane, Y., Carlson, E. T., Bowman, K. C., Wang, Z., & Connor, C. E. (2008). A neural code for three-dimensional object shape in macaque inferotemporal cortex. *Nature Neuroscience, 11*(11), 1352-1360.

Yamane, Y., Tsunoda, K., Matsumoto, M., Phillips, A. N., & Tanifuji, M. (2006). Representation of the spatial relationship among object parts by neurons in macaque inferotemporal cortex. *Journal of Neurophysiology, 96*, 3147–3156.

Yiannikas, C., & Walsh, J. C. (1983). The variation of the pattern shift visual evoked response with the size of the stimulus field. *Electroencephalography and Clinical Neurophysiology, 55*, 427–435.

Yovel, G., & Freiwald, W. (2013). Face recognition systems in monkey and human: are they the same thing? *F1000Prime Reports, 5*(10), doi:10.12703/P5-10.

Yu, S., Wang, Y., Li, X., Zhou, Y., & Leventhal, A. G. (2006). Functinal degradation of extrastriate visual cortex in senescent rhesus monkeys. *Neuroscience, 140*, 1023-1029.

Zanto, T. P., & Gazzaley, A. (2009). Neural supression of irrelevant information underlies optimal working memory performance. *The Journal of Neuroscience, 29*(10), 3059-3066.

Zanto, T. P., Pan, P., Liu, H., Bollinger, J., Nobre, A. C., & Gazzaley, A. (2011). Age-Related Changes in Orienting Attention in Time. *The Journal of Neuroscience, 31*(35), 12461–12470.

Zhou, H., Friedman, H., & von der Heydt, R. (2000). Coding of border ownership in monkey visual cortex. *The Journal of Neuroscience, 20*, 6594–6611.

APPENDIX A

Supplementary Materials for Section 2.

SUPPLEMENTARY TABLES

Subject	β_1 F	β_2 H	β_3 F amp	β_4 F ϕ	β_5 F int	β_6 H amp	β_7 H ϕ	β_8 H int	ε
MAG 1	-2.4	0.9	1	-5.2	-0.6	0.6	-1.7	-0.1	-1.6
MAG 2	0.2	1.9	0.5	-4.4	0.1	1.1	-2.2	-0.4	2.2
GAR 1	-1	0.5	0	-3.6	0.1	0.1	-2.4	0.1	-0.4
GAR 2	-1.1	0.9	0.1	-3.4	0.1	0.5	-1.9	0.1	-0.2
KWI 1	-0.4	1.8	0.4	-3.3	-0.1	0.4	-2.2	-0.3	1.4
KWI 2	2.1	3.5	1.1	-2.8	-0.9	1.7	-2.1	0.1	5.6
TAK 1	1.5	2.3	0	-3.9	0.3	-0.1	-3.3	0	3.8
TAK 2	1.6	3.2	-0.5	-3.9	0	-0.6	-2.5	-0.6	4.8
CMG 1	0.7	3.3	0.4	-3.7	-0.1	-0.2	-0.7	0.1	4
CMG 2	1.7	4.1	-0.5	-3.1	-0.7	-0.1	-1	-0.1	5.8
WJW 1	0.2	4	-0.7	-5.8	-0.1	-0.2	-2.2	0.1	4.2
WJW 2	0.4	4.4	0.2	-7	0.9	-0.6	-3.5	-1.2	4.8
BTM 1	-2.1	-0.7	0.8	-4.9	0.3	0.3	-4.4	0	-2.8
CXM 1	-1.4	-0.1	0.4	-5.3	0	0.5	-4.5	0	-1.6
MEAN 1	**-0.6**	**1.5**	**0.3**	**-4.5**	**0**	**0.2**	**-2.7**	**0**	**0.9**
MEAN 2	**0.8**	**3**	**0.2**	**-4.1**	**-0.1**	**0.3**	**-2.2**	**-0.4**	**3.8**

Supplementary Table 1. *Beta coefficients associated with each predictor of the first (main) regression model. Results are reported at the electrode and the latency of the max R^2. Numbers 1 and 2 after the subjects' names indicate the session.*

Envelope

PHASE	P1		N1		P2	
	Faces	Houses	Faces	Houses	Faces	Houses
Session 1	0.02	0.01	0.15	0.06	0.08	0.06
	[0.01, 0.03]	[0.01, 0.02]	[.12, 0.17]	[0.05, 0.1]	[0.06,0.1]	[0.04, 0.08]
Session 2	0.01	0.01	0.11	0.05	0.07	0.04
	[0.01, 0.02]	[0.01, 0.02]	[0.09, 0.15]	[0.04, 0.06]	[0.04, 0.08]	[0.03, 0.06]

Max R^2 electrode

PHASE	P1		N1		P2	
	Faces	Houses	Faces	Houses	Faces	Houses
Session 1	0.006	0.003	0.15	0.06	0.07	0.05
	[0.001, 0.02]	[0.001, 0.01]	[0.11, 0.17]	[0.04, 0.1]	[0.05, 0.1]	[0.03, 0.08]
Session 2	0.006	0.006	0.11	0.04	0.06	0.04
	[0.002, 0.01]	[0.002, 0.01]	[0.09, 0.15]	[0.03, 0.05]	[0.04, 0.08]	[0.03, 0.06]

Supplementary Table 2. *Unique variance explained by phase spectrum. Median ERP variance uniquely explained by phase in the P1, N1 and P2 time windows for faces and houses with 95% percentile bootstrap confidence interval in brackets. Data are reported for the max R^2electrode and for the envelope (max across all electrodes).*

Envelope

AMPLITUDE	P1		N1		P2	
	Faces	Houses	Faces	Houses	Faces	Houses
Session 1	0.01	0.01	0.02	0.02	0.02	0.02
	[0.01, 0.02]	[0.01, 0.02]	[0.01, 0.02]	[0.01, 0.03]	[0.01, 0.02]	[0.02, 0.04]
Session 2	0.01	0.01	0.01	0.02	0.02	0.03
	[0.01, 0.02]	[0.01, 0.02]	[0.01, 0.02]	[0.01, 0.03]	[0.01, 0.03]	[0.02, 0.04]

Max R^2 electrode

	P1		N1		P2	
	Faces	Houses	Faces	Houses	Faces	Houses
Session 1	0.002	0.002	0.004	0.003	0.009	0.02
	[0.001, 0.003]	[0.001, 0.01]	[0.003, 0.005]	[0.002, 0.006]	[0.005, 0.02]	[0.01, 0.03]
Session 2	0.002	0.003	0.004	0.005	0.01	0.02
	[0, 0.003]	[0, 0.006]	[0.002, 0.005]	[0.002, 0.01]	[0.01, 0.03]	[0.02, 0.04]

Supplementary Table 3. Unique variance explained by amplitude. Median ERP variance uniquely explained by amplitude in the P1, N1 and P2 time windows for faces and houses. See Table 6 caption for details.

Subject	β_1 F	β_2 H	β_3 amp	β_4 ϕ	β_5 cat x amp	β_6 cat x ϕ	ε
MAG 1	0.9	-2.4	0.8	-3.4	0.2	-1.7	-1.6
MAG 2	1.9	0.3	0.8	-3.3	-0.3	-1.1	2.2
GAR 1	0.5	-1	0	-3	-0.1	-0.6	-0.4
GAR 2	0.9	-1.1	0.3	-2.7	-0.2	-0.7	-0.2
KWI 1	1.8	-0.4	0.4	-2.7	0	-0.6	1.4
KWI 2	3.3	2.1	1.4	-2.4	-0.3	-0.3	5.4
TAK 1	2.2	1.3	0.1	-3.6	0.1	-0.4	3.4
TAK 2	3.2	1.6	-0.6	-3.2	0	-0.7	4.8
CMG 1	3.3	0.7	0.1	-2.2	0.3	-1.5	4
CMG 2	4.1	1.7	-0.3	-2	-0.2	-1	5.8
WJW 1	4	0.2	-0.4	-4	-0.3	-1.8	4.2
WJW 2	4.4	0.4	-0.2	-5.3	0.4	-1.7	4.8
BTM 1	-0.7	-2.1	0.5	-4.7	0.3	-0.3	-2.8
CXM 1	-0.2	-1.4	0.4	-4.9	0	-0.4	-1.6
MEAN 1	**1.5**	**-0.6**	**0.2**	**-3.6**	**0.1**	**-0.9**	**0.8**
MEAN 2	**3**	**0.8**	**0.2**	**-3.2**	**-0.1**	**-0.9**	**3.8**

Supplementary Table 4.*.Beta coefficients associated with each predictor of the second regression model, at the electrode and the latency of the max R^2. Numbers 1 and 2 after the subjects' names indicate the session.*

SUPPLEMENTARY FIGURES

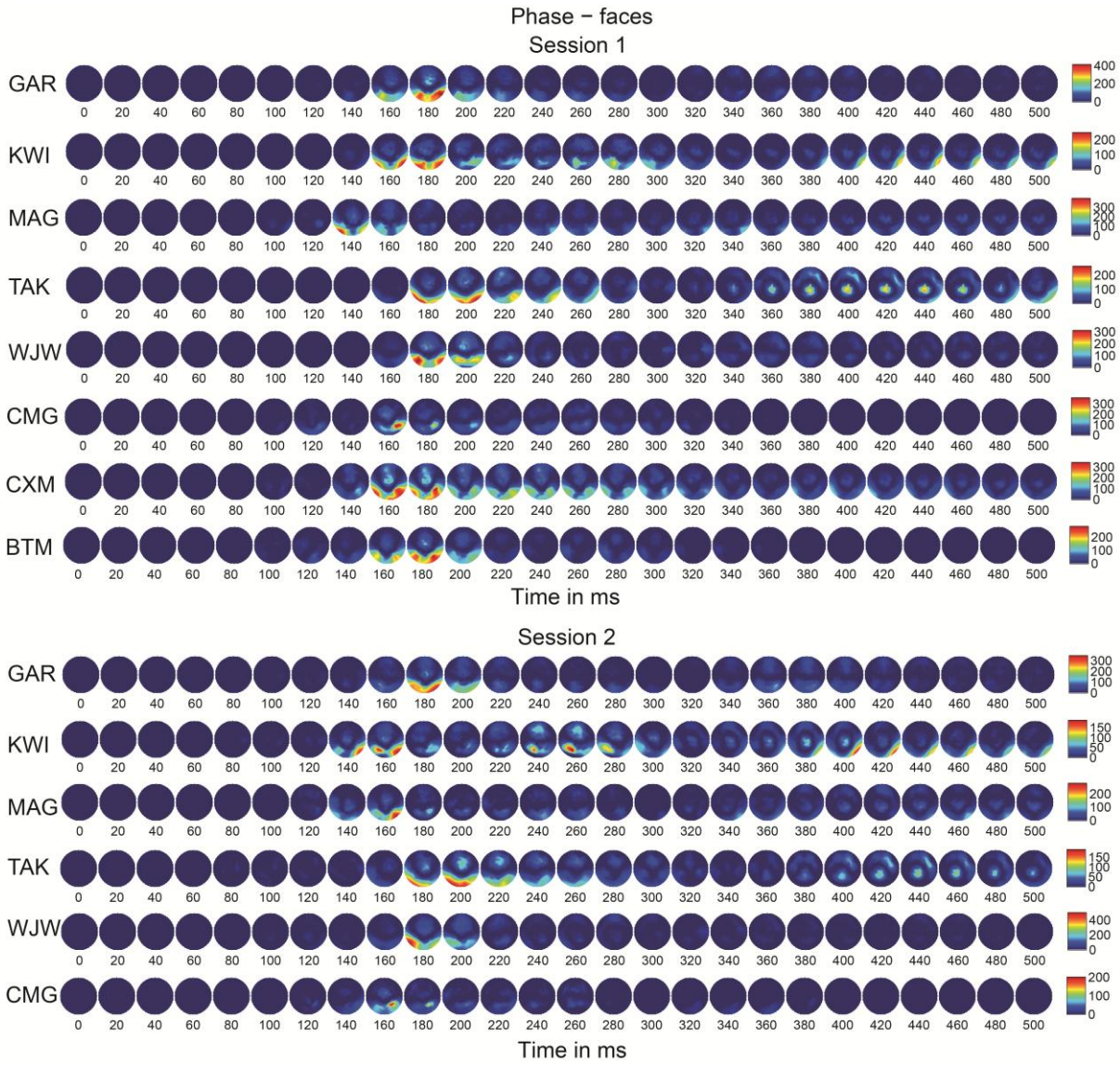

Supplementary Figure 1. *Scalp distributions of sensitivity to phase spectrum in face stimuli. Effects are expressed in colour-coded F values: from non-significant effects (dark blue) to the strongest significant effects (deep red) for session 1 and session 2. Each row represents one subject. The effects are shown between time 0 (=stimulus presentation) and 500ms post stimulus.*

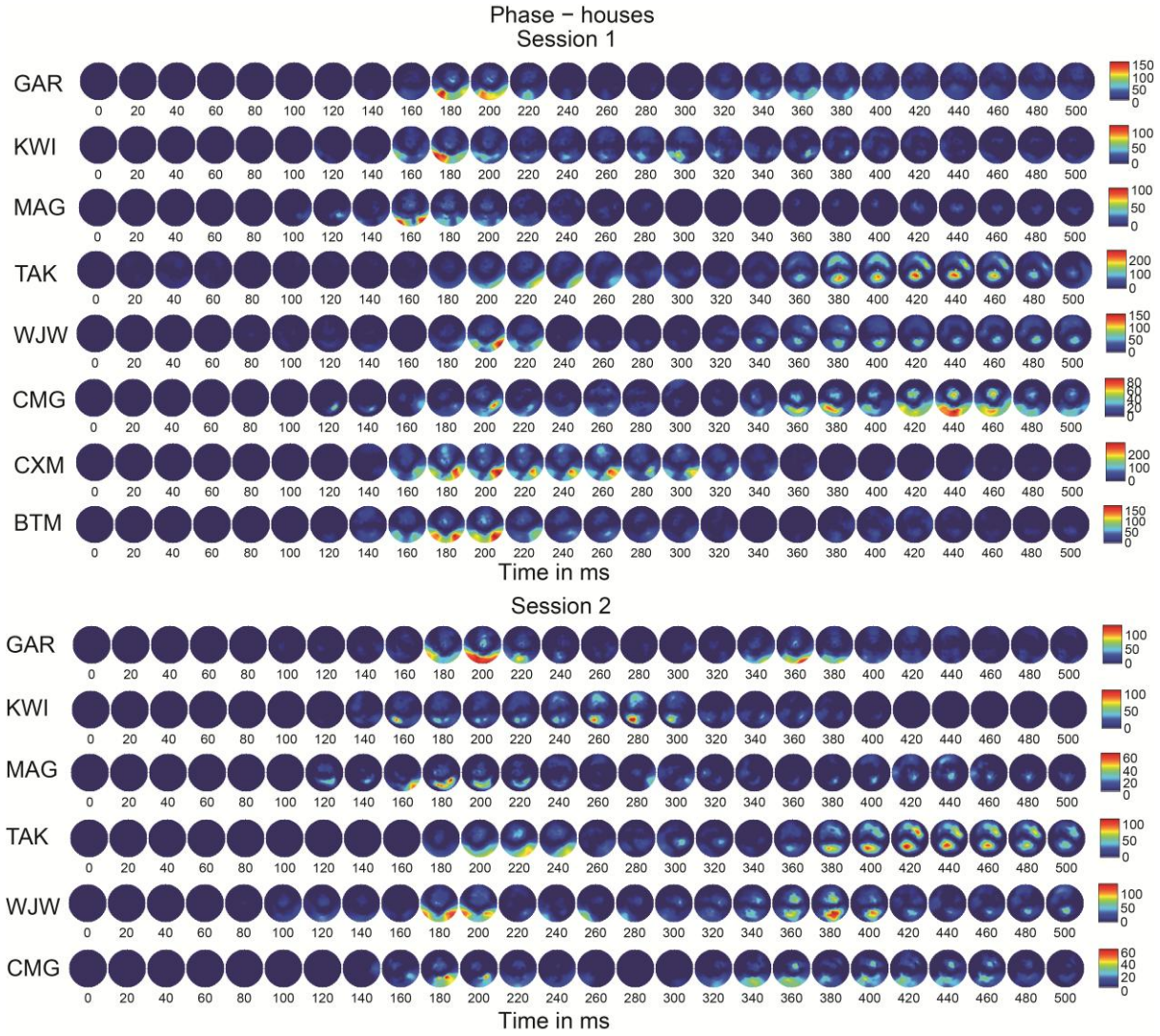

Supplementary Figure 2. *Scalp distributions of sensitivity to phase spectrum in house stimuli. See Supplementary Figure 1 caption for details.*

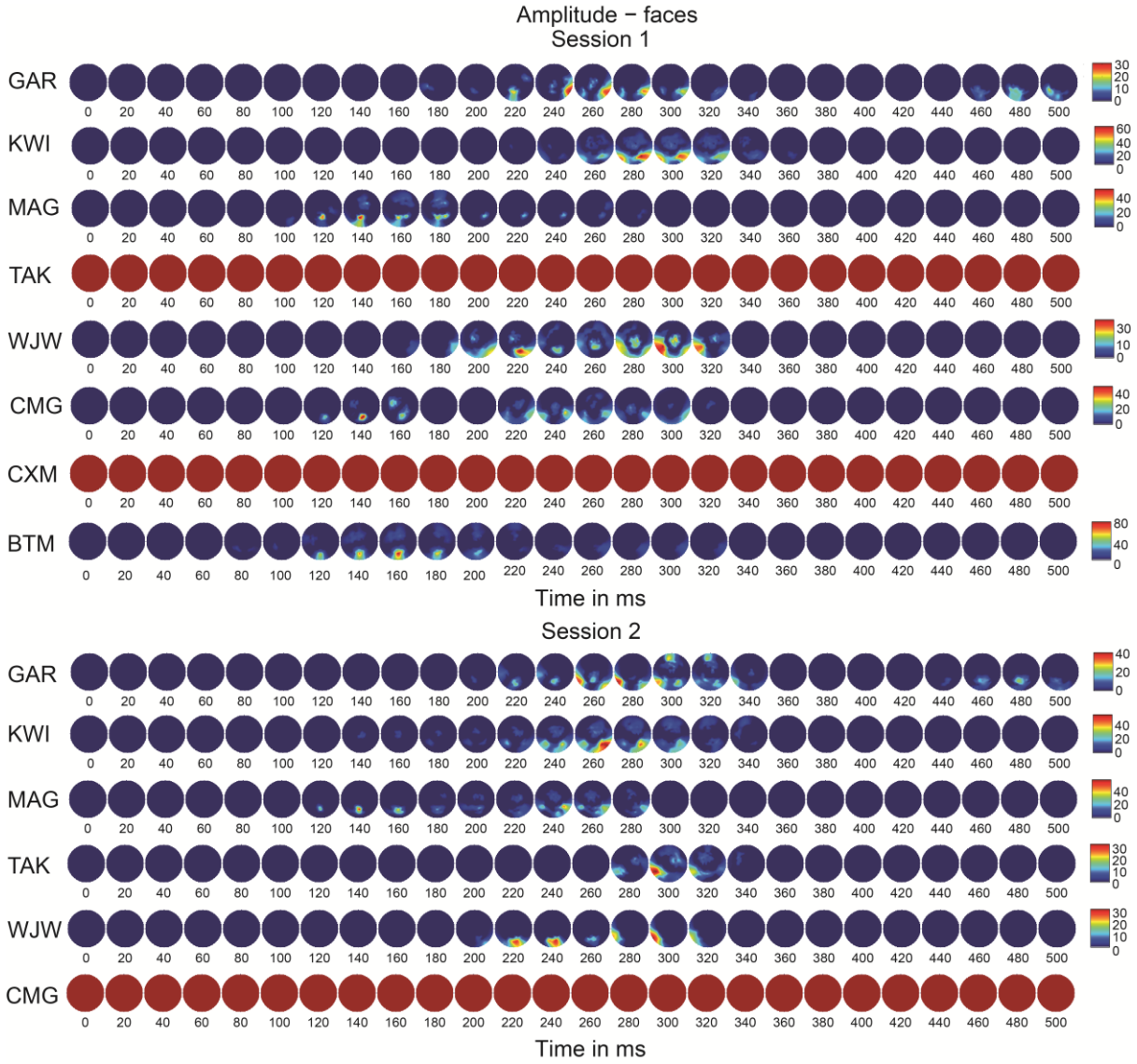

Supplementary Figure 3. *Scalp distributions of sensitivity to amplitude spectrum in face stimuli. See Supplementary Figure 1 caption for details.*

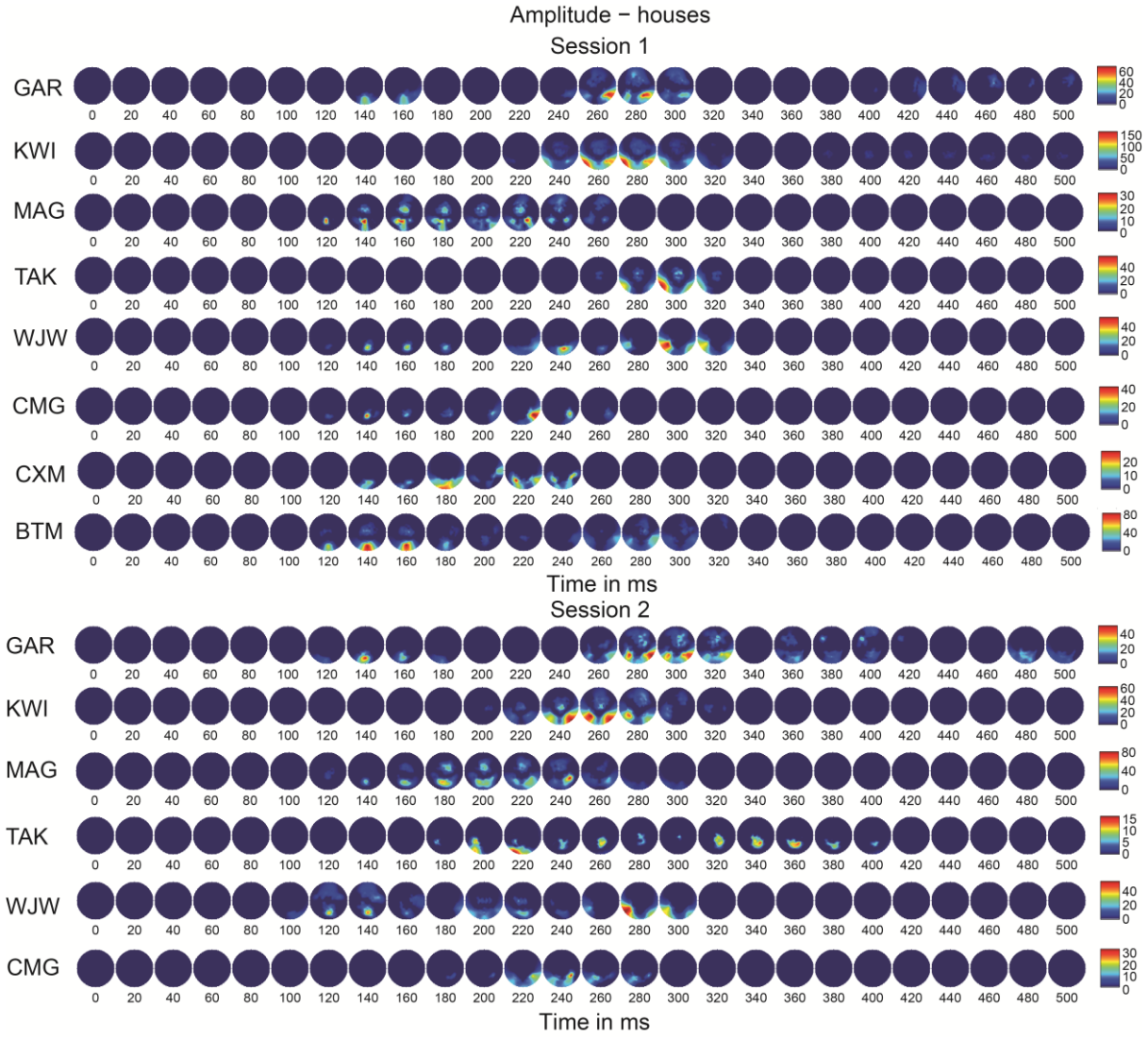

Supplementary Figure 4. *Scalp distributions of sensitivity to amplitude spectrum in house stimuli. See Supplementary Figure 1 caption for details.*

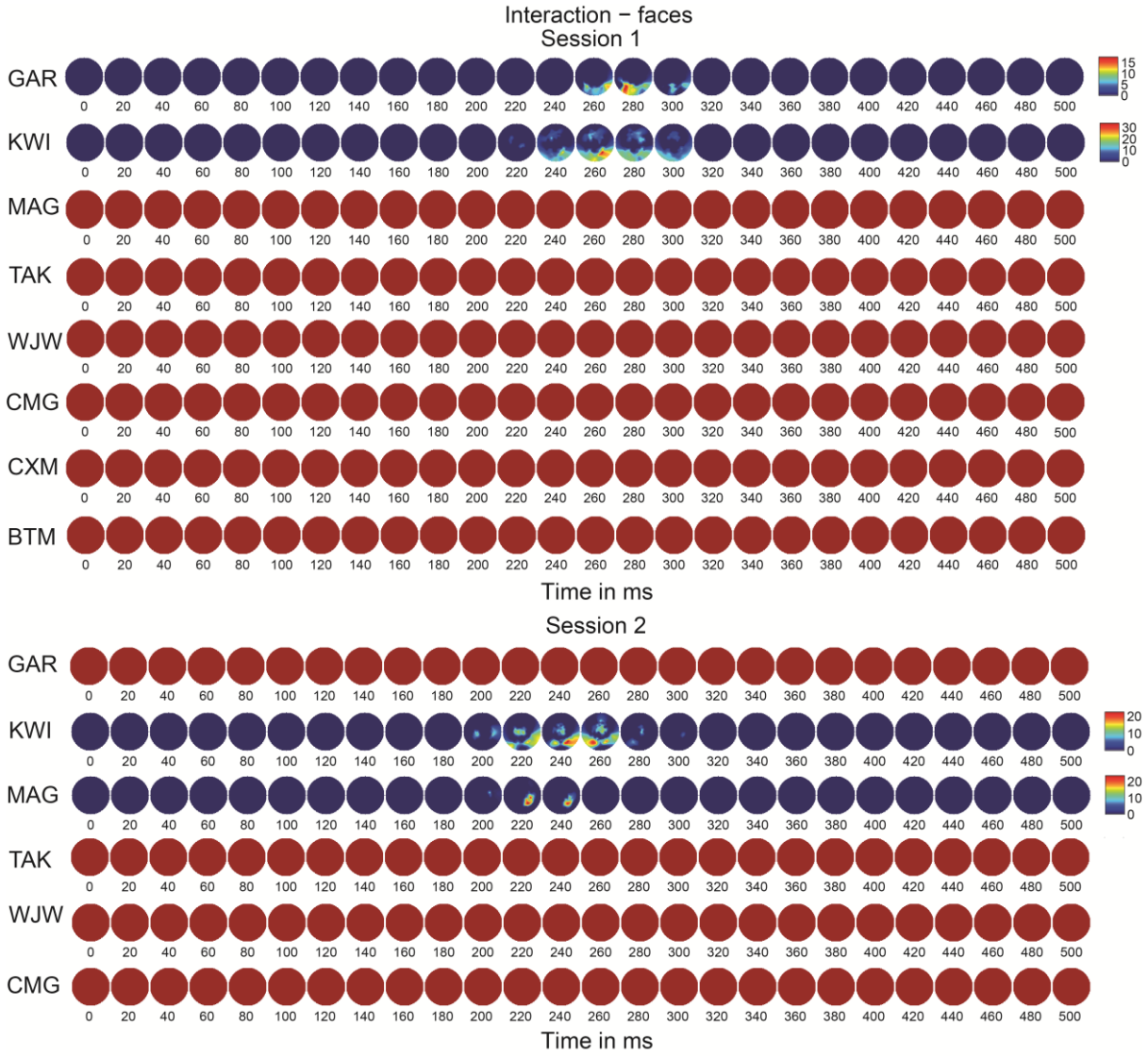

Supplementary Figure 5. *Scalp distributions of sensitivity to phase x amplitude interaction in face stimuli. See Supplementary Figure 1 caption for details.*

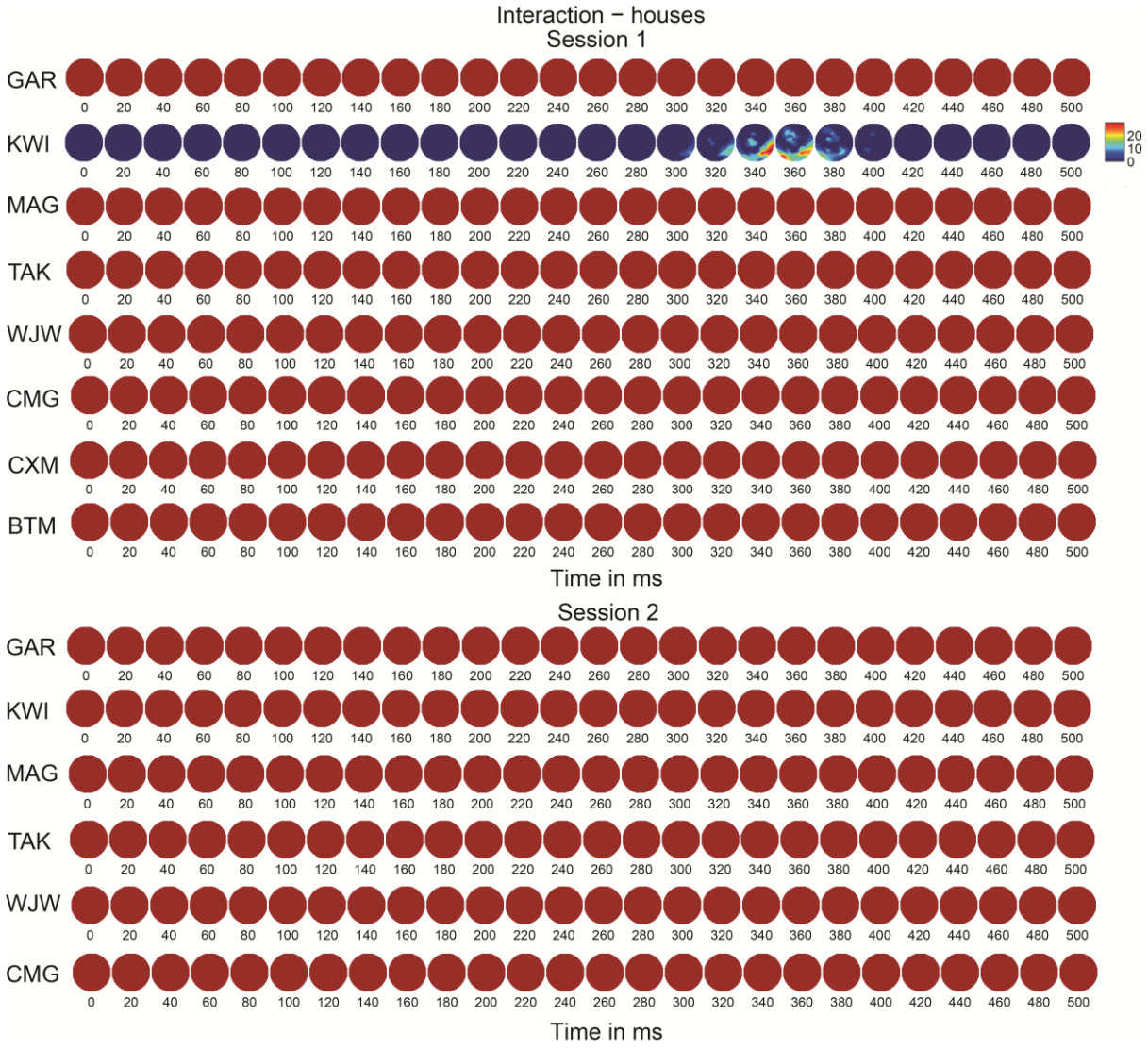

Supplementary Figure 6. *Scalp distributions of sensitivity to phase x amplitude interaction in house stimuli. See Supplementary Figure 1 caption for details.*

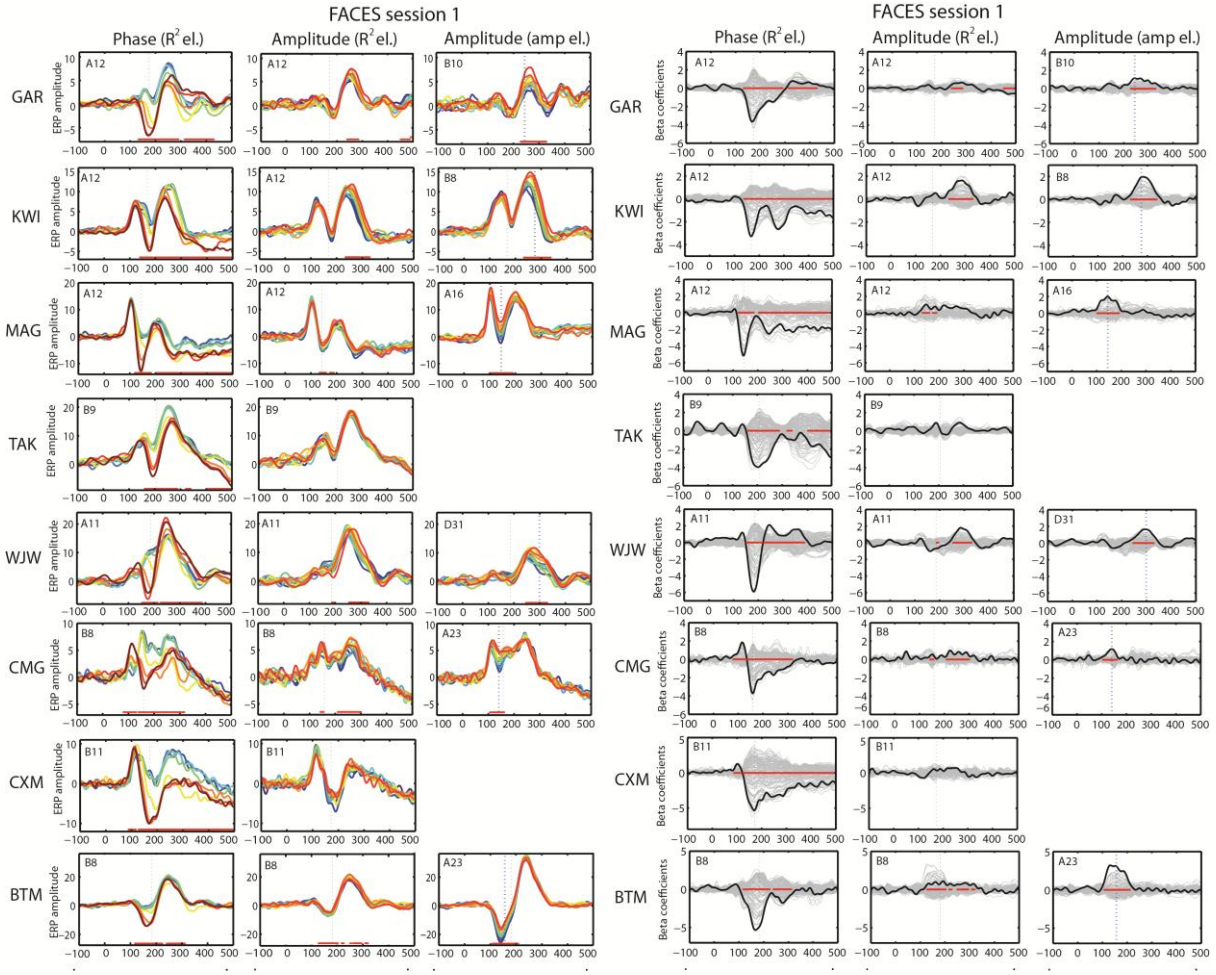

Supplementary Figure 7. *ERPs and beta coefficients from the main model for session 1, faces stimuli. Data at the max R^2 electrode (columns 1, 2, 4, 5) and the electrode with max amplitude effects (columns 3 and 6) for all subjects (rows). Column 1 - ERPs for 8 levels of phase averaged across all amplitude levels; columns 2, 3 – ERPs for 11 levels of amplitude averaged across all phase levels; columns 4, 5, 6 – time courses of beta coefficients on all electrodes (grey lines) with betas for the max R^2 electrode (columns 4, 5) or max amplitude effect electrode (column 6) highlighted with a thick black line. Red horizontal lines show time windows where the effects were significant. The number in upper left corner of each box tells which electrode was the max R^2 electrode (columns 1, 2, 4, 5) and max amplitude effect electrode for that subject.*

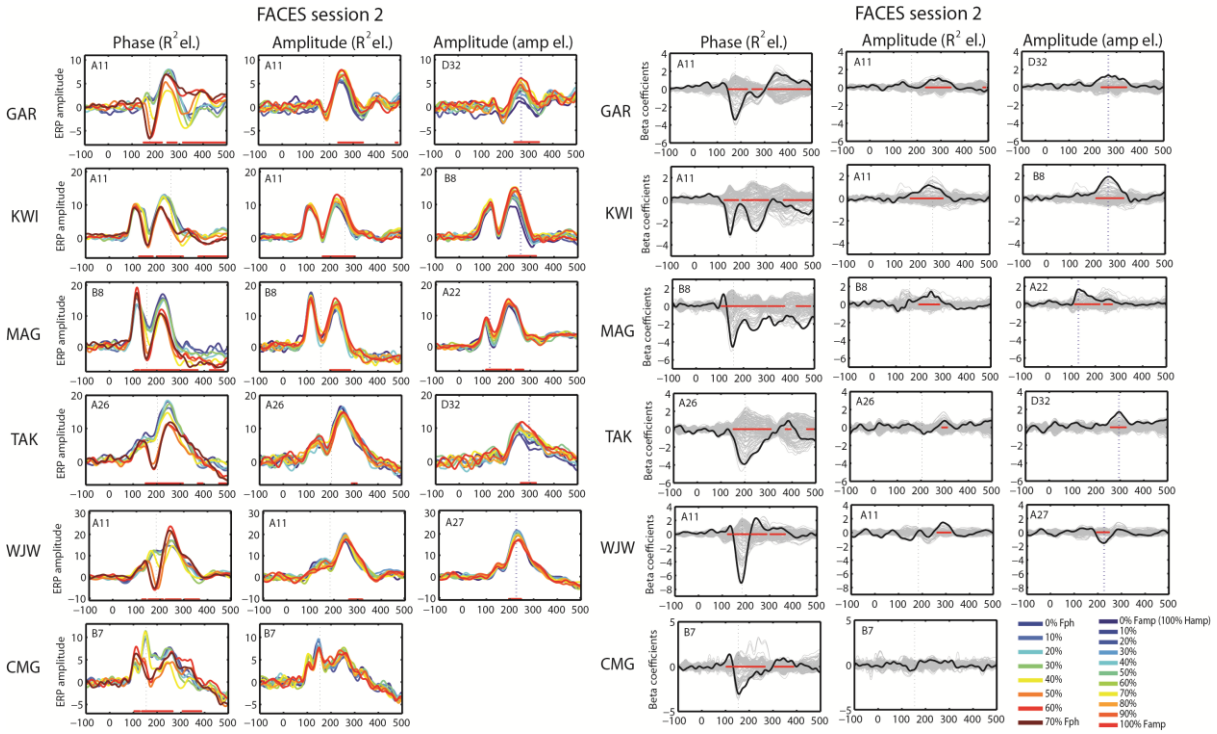

Supplementary Figure 8. *ERPs and corresponding beta coefficients (main model) - data for session 2, faces stimuli. See Supplementary Figure 7 caption for details.*

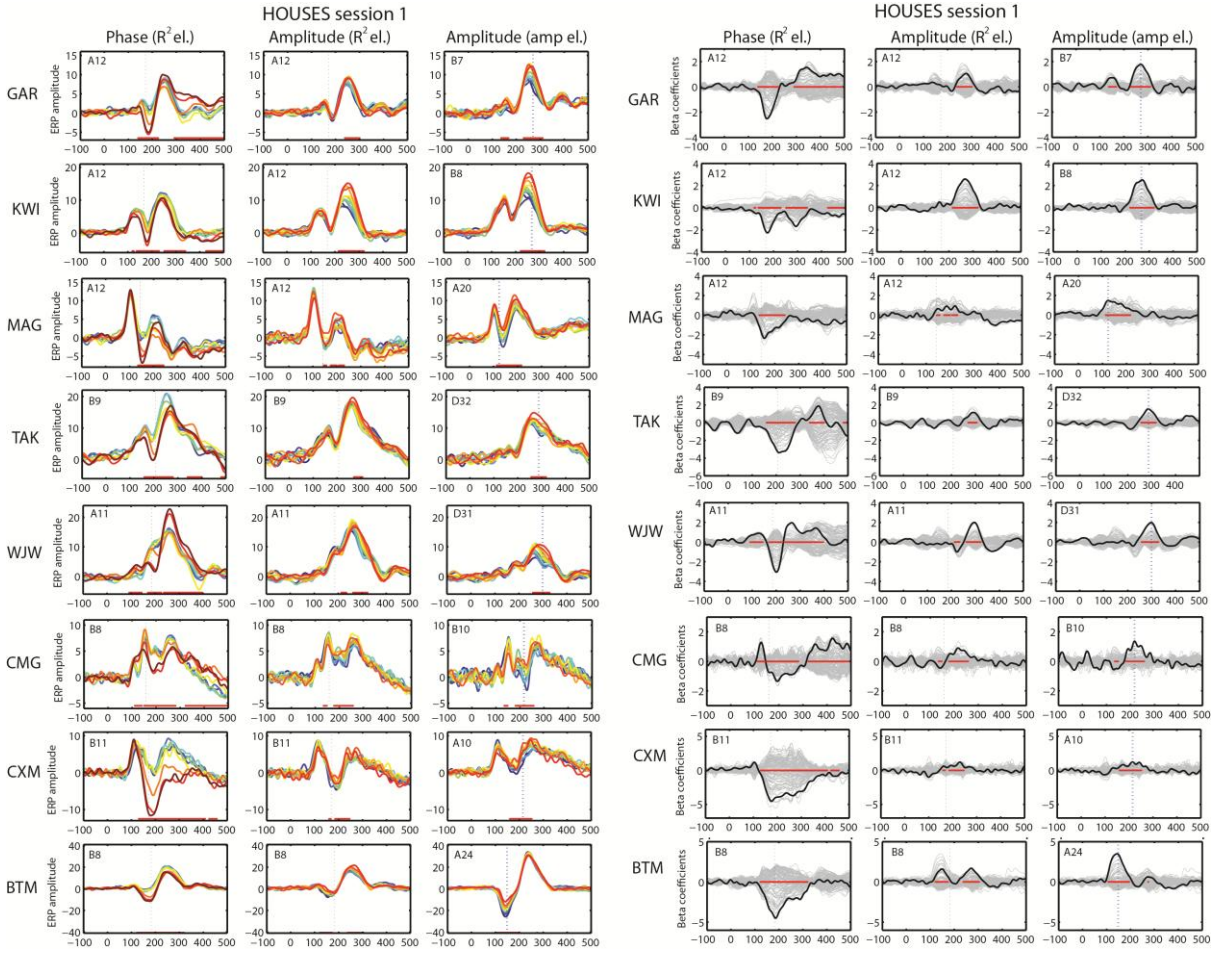

Supplementary Figure 9. *ERPs and corresponding beta coefficients (main model) - data for session 1, houses stimuli. See Supplementary Figure 7 caption for details.*

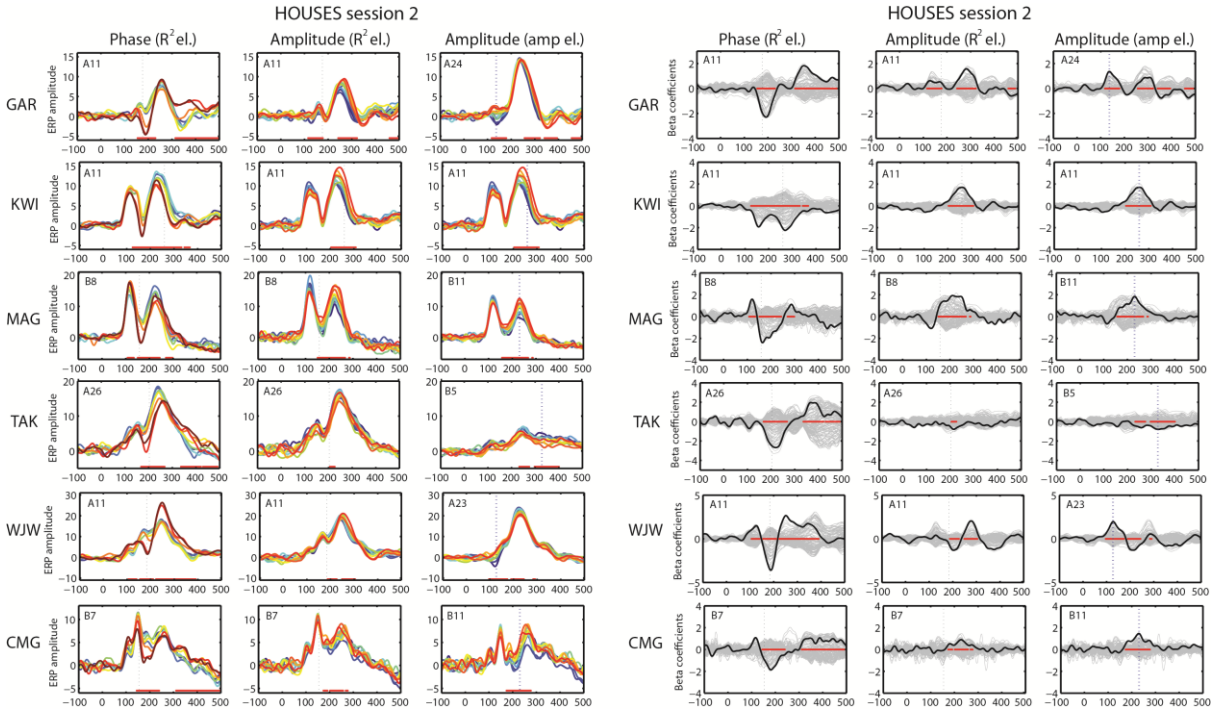

Supplementary Figure 10. *ERPs and corresponding beta coefficients - data for session 2, houses stimuli. See Supplementary Figure 7 caption for details.*

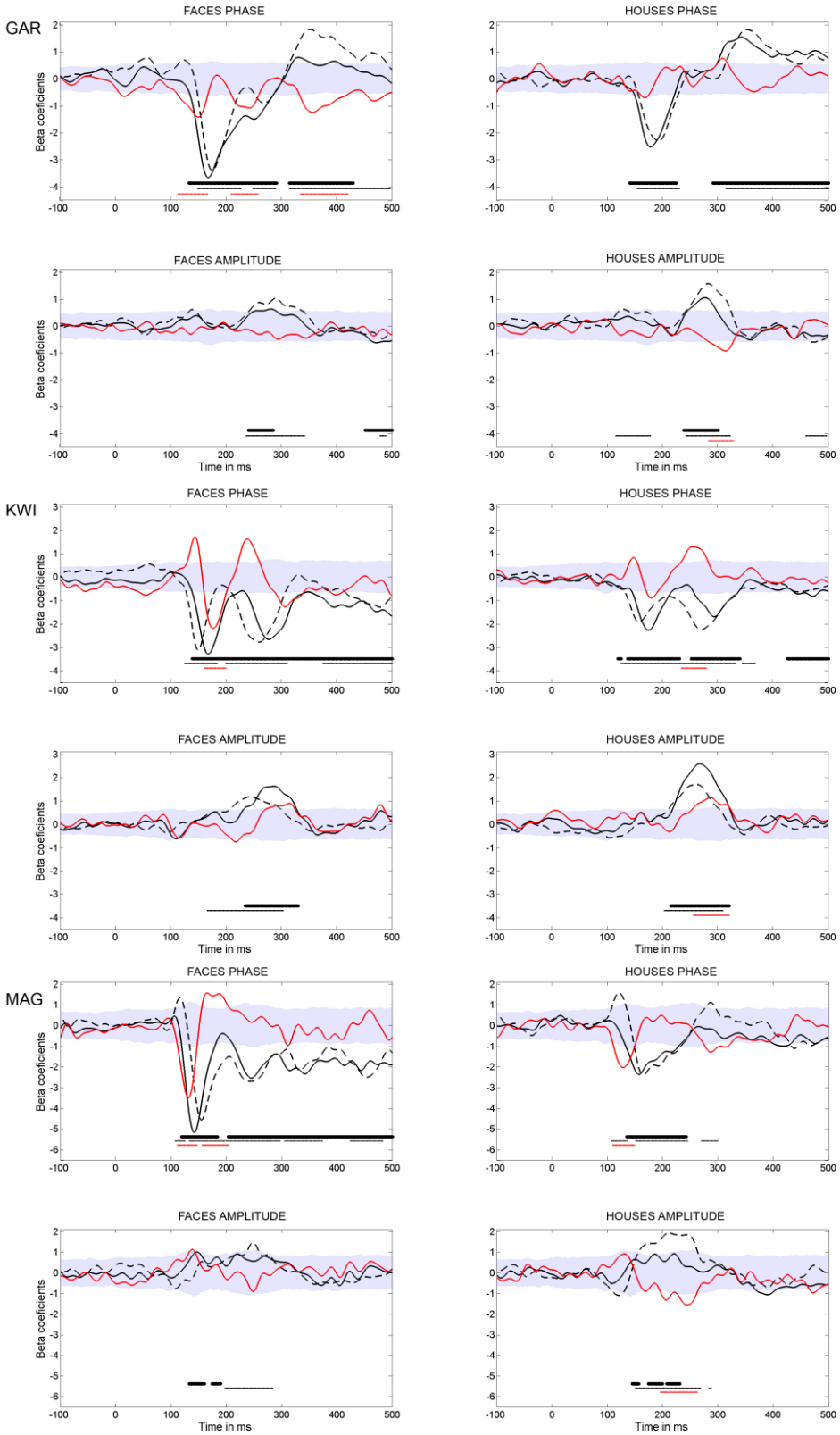

Supplementary Figure 11. *Cross-session reliability of beta coefficients associated with phase and amplitude spectra for faces and houses from the main regression model. Beta coefficients for the two sessions are plotted in black (session 1=solid; session 2=dashed) and the difference between them is plotted in red. Horizontal lines indicate time windows of significant beta coefficients (session 1=thick black; session 2=thin black; difference=red).*

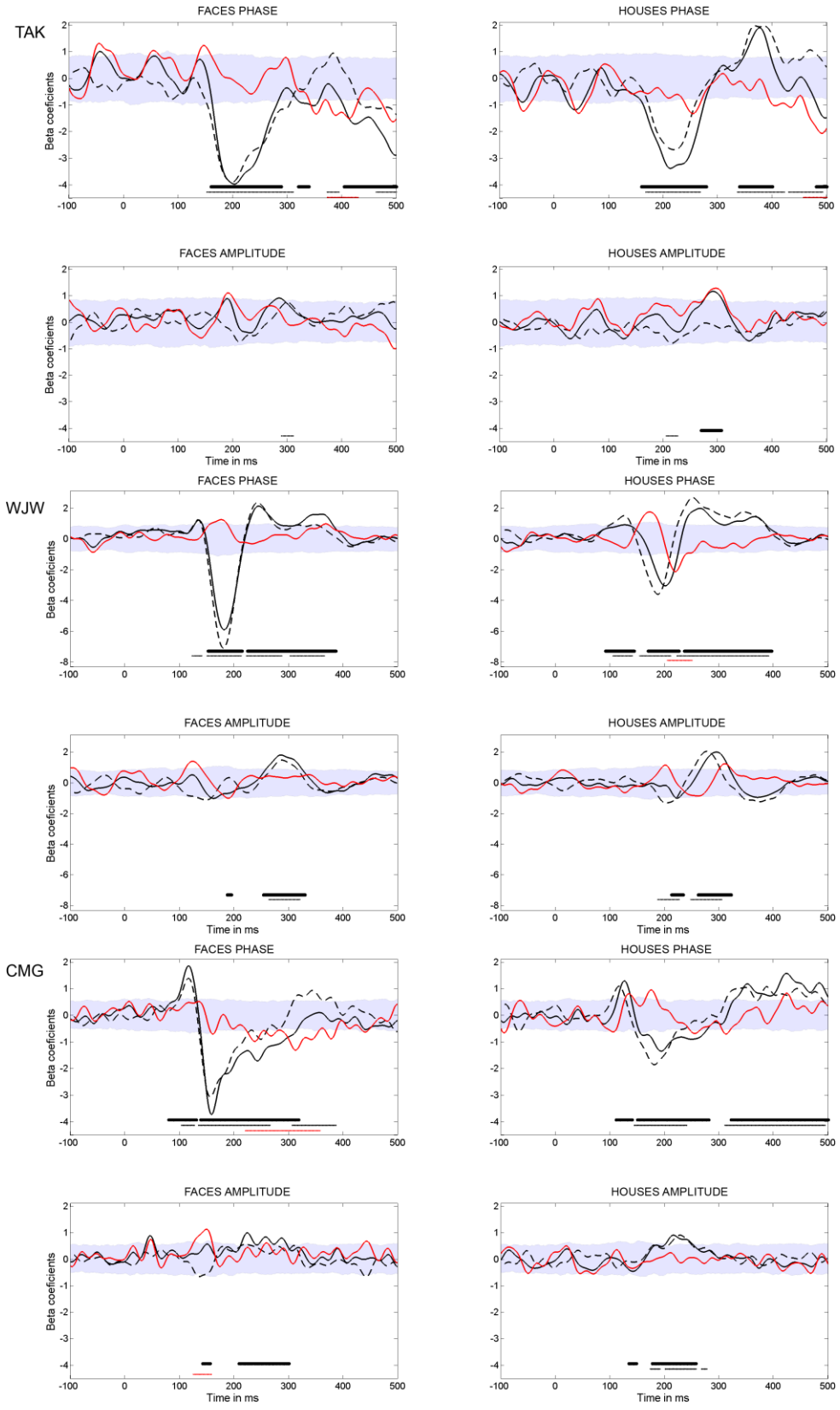

Supplementary Figure 12. *Cross-session reliability of beta coefficients (main model). See Supplementary Figure 11 caption for details.*

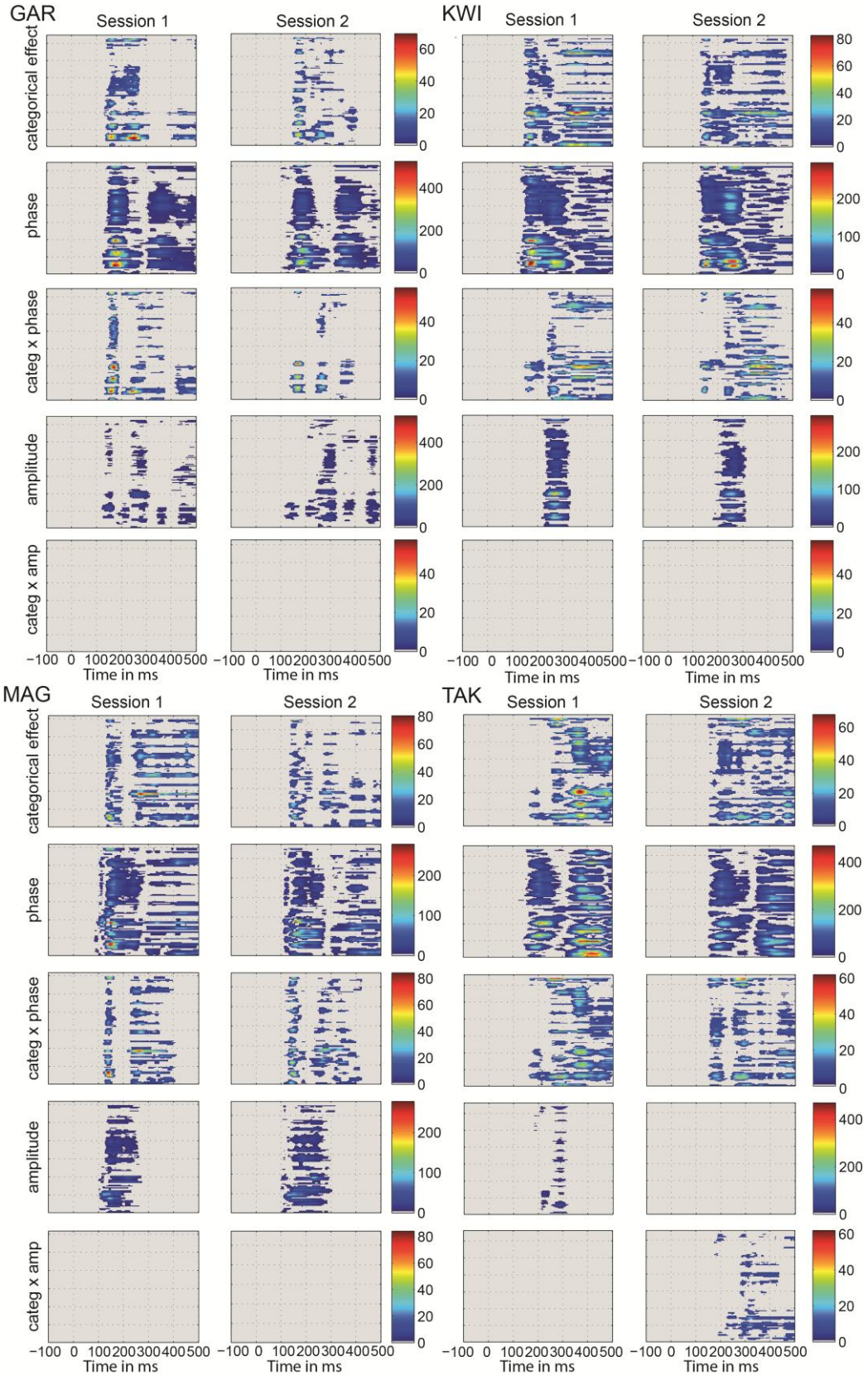

Supplementary Figure 13. *Categorical interaction analysis results for subjects GAR, KWI, MAG and TAK. For each subject, the results are presented in 10 subplots, with 2 sessions in columns, and 5 predictors in rows. Each subplot shows colour-coded F values at all electrodes along the Y axis, and from -100 to 500ms along the X axis. Non-significant effects are indicated with a grey background.*

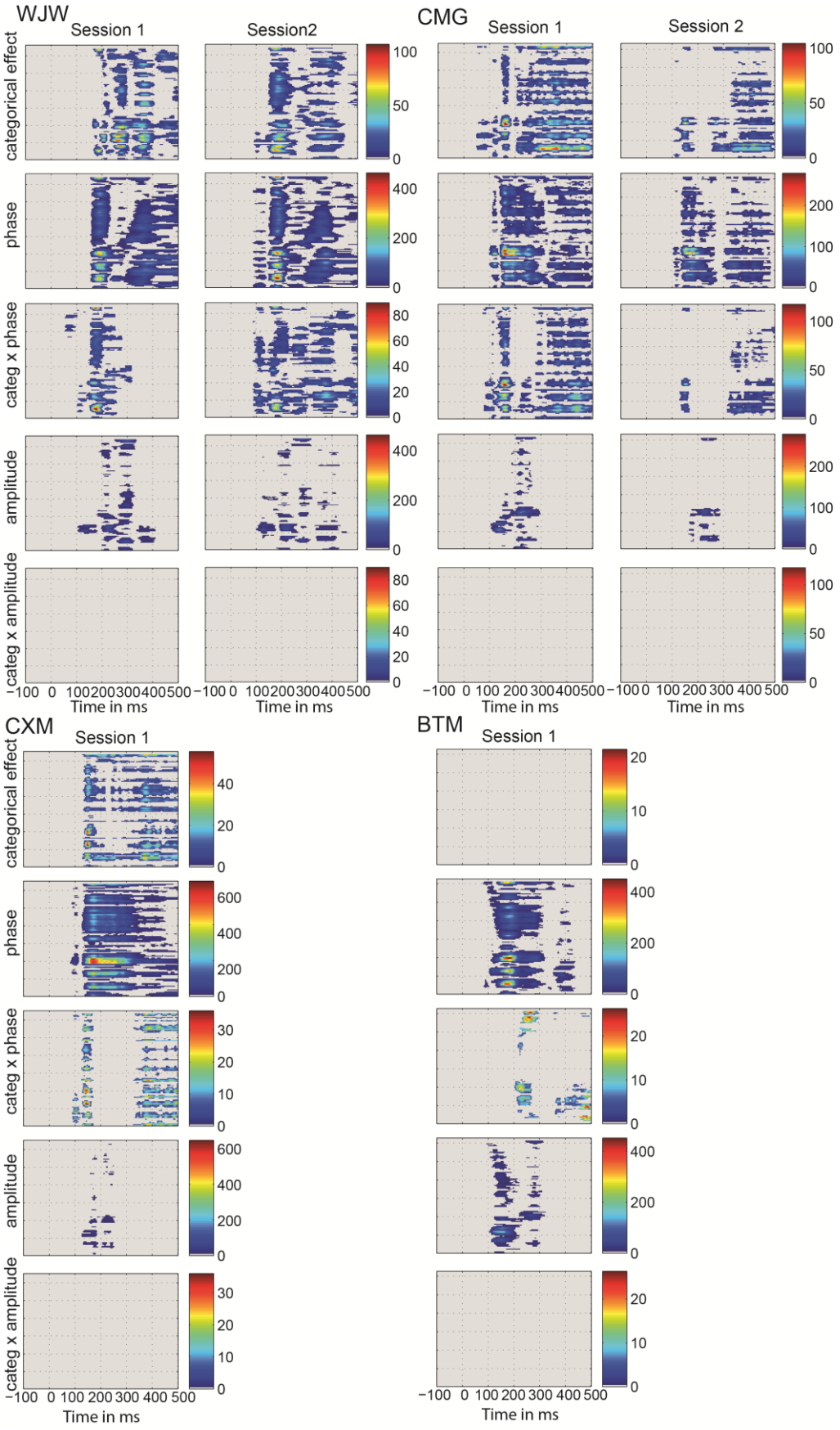

Supplementary Figure 14. *Categorical interaction analysis results for subjects WJW, CMG, CXM and BTM. See Supplementary Figure 13 caption for details.*

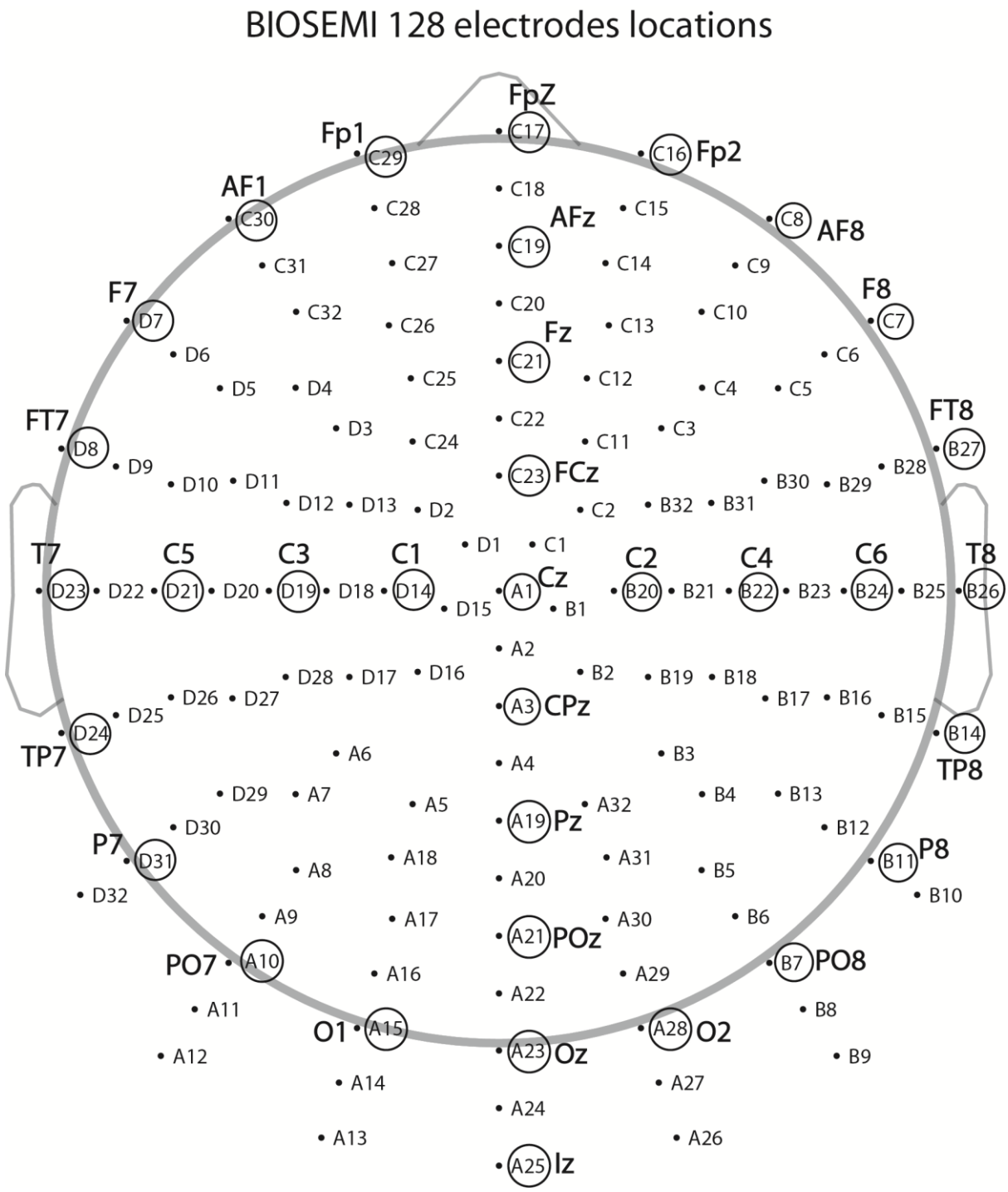

Supplementary Figure 15. *Electrode map for the Biosemi Active Electrode Amplifier System with 128 electrodes with corresponding labelling from the 10/10 system (circled electrodes).*

APPENDIX B

Supplementary material for Sections 3 and 4.

SUPPLEMENTARY TABLES

	Pupil size		Retinal illuminance		Onset		Amplitude		50IT	
ge	intr	slope	intr	slope	intr	slope	intr	slope	intr
3	5.93	-12.48	1471	0.06	95.8	-0.01	13.38	1.05	160.01
4,	[5.47,	[-17.82,	[1163.5,	[-0.24,	[81.83,	[-0.06,	[10.20,	[0.75,	[144.5,
2]	6.41]	-7.33]	1791.4]	0.43]	110.84]	0.06]	16.68]	1.33]	175.12]
4	6.67	-9.01	964.43	0.3	86.7	-0.01	13.92	0.96	172.48
5,	[6.16,	[-12.81,	[766.44,	[-0.01,	[71.13,	[-0.09,	[10.91,	[0.73,	[158.58,
3]	7.21]	-5.87]	1207.8]	0.67]	102.22]	0.05]	17.55]	1.23]	184.03]
4	7.11	-5.52	575.06	0.21	92.02	-0.01	13.19	1.05	173.68
5,	[6.71	[-7.2,	[459.26,	[-0.17,	[74.97,	[-0.07,	[10.09,	[0.77,	[155.64,
3]	,7.56]	-3.61]	678.15]	0.64]	110.84]	0.06]	16.7]	1.36]	89.57]
4	7.37	-2.78	299.1	0.029	104.9	0.01	12.01	1	181.41
5,	[6.95,	[-3.74,	[236.2,	[-0.21,	[92.13,	[-0.05,	[8.62,	[0.78,	[170.71,
3]	7.82]	-1.74]	355.64]	0.33]	116.43]	0.07]	15.21]	1.22]	195.97]
4	7.55	-1.5	162.65	0.1	106.28	0.01	11.77	1.01	190.81
5	[7.11,	[-2.01,	[131.0,	[-0.11,	[92.36,	[-0.06,	[8.1,	[0.72,	[174.12,
3]	8.01]	-1.00]	192.92]	0.53]	115.79]	0.08]	15.66]	1.34]	207.35]
4	7.62	-0.75	84.55	0.06	112.32	-0.01	12.61	1.02	196.18
5,	[7.13,	[-1.07,	[66.55,	[-0.15,	[92.48,	[-0.07,	[9.49,	[0.79,	[184.14,
3]	8.09]	-0.46]	103.47]	0.78]	123.97]	0.05]	16.19]	1.26]	207.78]
4	7.73	-0.39	44.43	0.38	108.15	0.01	11.49	1.04	203.78
5,	[7.25,	[-0.57,	[35.07,	[0.12,	[93.2,	[-0.05,	[8.50,	[0.75,	[189.14,
3]	8.21]	-0.25]	54.17]	0.7]	119.59]	0.07]	14.74]	1.34]	219.85]
4	7.81	-0.21	24.43	0.62	105.29	0.005	10.92	0.94	219.81
6,	[7.34,	[-0.31,	[19.66,	[0.31,	[85.09,	[-0.05,	[8.41,	[0.72,	[208.37,
4]	8.27]	-0.18]	29.53]	1.38]	121.35]	0.06]	14.39]	1.19]	231.00]
3	5.43	-9.49	1184	0.08	91.56	-0.01	13.64	0.75	181.17
4,	[4.85,	-[13.98,	[919.68,	[-0.18,	[75.68,	[-0.07,	[10.47,	[0.36,	[158.96,
2]	5.94]	-5.47]	1463]	0.41]	105.43]	0.05]	17.16]	1.18]	203.35]

Supplementary Table 1. Age regression fits in the b2d session. *Confidence intervals around the slopes and intercepts (intr) are given in square brackets.*

	Pupil size		Retinal illuminance		Onset		Amplitude		50IT		Peak latency	
lum	slope	intr	slope	intr	slope	intr	slope	intr	slope	intr	slope	intr
60.8 (first)	-0.03 [-0.04, -0.02]	5.95 [5.36, 6.52]	-11.15 [-15.72, -6.47]	1433.51 [1175.8, 1699.7]	0.27 [0.03, 0.55]	82.6 [69.27, 95.015]	0 [-0.06, 0.06]	13.31 [10.81, 16.04]	1.07 [0.64, 1.38]	158.71 [143.04, 177.20]	1.27 [0.61, 2.05]	116.86 [85.84, 140.73]
0.59	-0.05 [-0.06, -0.03]	8.11 [7.65, 8.55]	-0.24 [-0.30, -0.15]	27.07 [22.08, 30.32]	0.40 [0.13, 0.73]	115 [102.03, 127.27]	0 [-0.05, 0.071]	11.4 [8.50, 13.87]	1.22 [0.92, 1.5]	201.04 [186.37, 216.25]	1.59 [0.90, 2.39]	159.05 [117.92, 199.8]
1.12	-0.05 [-0.05, -0.03]	7.79 [7.30, 8.23]	-0.40 [-0.49, -0.27]	45.95 [38.65, 51.02]	0.36 [0.07, 0.64]	112.25 [100.67, 124.71]	0.01 [-0.03, 0.073]	11.63 [8.92, 13.98]	1.07 [0.75, 1.37]	202.72 [186.12, 219.639]	1.52 [0.73, 2.26]	160.34 [121.43, 202.8]
2.17	-0.05 [-0.05, -0.03]	7.61 [7.07, 8.12]	-0.79 [-0.97, -0.52]	87.66 [71.65, 98.50]	0.48 [0.18, 1.09]	95.12 [76.86, 108.51]	0.01 [-0.05, 0.07]	11.54 [8.54, 14.442]	1.01 [0.68, 1.35]	197.07 [179.46, 215.15]	1.76 [1.09, 2.35]	136.12 [104.71, 166.55]
4.19	-0.04 [-0.05, -0.03]	7.43 [6.93, 7.84]	-1.38 [-1.72, -0.94]	156.50 [130.49, 176.04]	0.18 [-0.10, 0.72]	98.38 [82.77, 115.94]	0.01 [-0.05, 0.079]	11.99 [9.29, 14.50]	0.95 [0.64, 1.22]	193.34 [177.53, 211.16]	1.78 [1.28, 2.25]	130 [104.17, 153.75]
8.16	-0.04 [-0.05, -0.03]	7.03 [6.59, 7.46]	-2.35 [-2.96, -1.52]	268.91 [225.32, 304.02]	0.29 [0.05, 0.58]	89.68 [77.68, 101.03]	0.01 [-0.04, 0.07]	11.96 [9.14, 14.67]	0.91 [0.54, 1.27]	189.41 [171.03, 208.82]	1.48 [0.9, 2.07]	135.69 [108.40, 159.63]
16	-0.04 [-0.05, -0.03]	6.7 [6.23, 7.17]	-4.01 [-5.15, -2.70]	476.12 [405.92, 548.24]	0.11 [-0.18, 0.44]	94.4 [79.92, 108.07]	0.01 [-0.04, 0.08]	12.26 [9.41, 15]	1.03 [0.68, 1.338]	173.77 [157.81, 193.44]	1.42 [0.78, 2.17]	123.24 [91.80, 147.64]
31	-0.04 [-0.04, -0.02]	6.27 [5.74, 6.71]	-6.57 [-8.83, -4.203]	813.75 [686.97, 952.64]	0.14 [-0.17, 0.49]	90.43 [74.02, 105.44]	0.02 [-0.04, 0.08]	12.32 [9.39, 15.16]	0.90 [0.55, 1.23]	174.92 [157.12, 194.47]	1.17 [0.55, 1.87]	130.69 [99.69, 156.913]
60.8 (last)	-0.03 [-0.04, -0.02]	5.74 [5.21, 6.19]	-10.62 [-14.42, -6.55]	1335.97 [1104.7, 1552.8]	0.16 [-0.12, 0.44]	86.33 [73.8, 98.53]	0.01 [-0.04, 0.07]	12.37 [9.70, 15.62]	0.97 [0.68, 1.194]	168.77 [156.02, 183.20]	1.20 [0.66, 1.88]	124.06 [98.03, 144.64]

Supplementary Table 2. Age regression fits in the d2b session*. Confidence intervals of the slopes and intercepts (intr) are given in square brackets.*

	Pupil size		Retinal illuminance		Onset		Amplitude		50IT		Peak latency	
lum	**slope**	**intr**	**slope**	**intr**	**slope**	**intr**	**slope**	**intr**	**slope**	**intr**	**slope**	**intr**
31	0.01 [0, 0.01]	-0.76 [-0.98, -0.568]	-3.46 [-5.978, -0.77]	506 [341, 646]	-0.24 [-0.54, 0.04]	9.09 [-2.81, 22.93]	0.01 [-0.02, 0.04]	-0.54 [-2.02, 0.80]	0.09 [-0.13, 0.31]	-12.48 [-24, -2]	0.04 [-0.6, 0.45]	-13.08 [-26.95, 4.91]
16	0.01 [0, 0.02]	-1.18 [-1.42, -0.928	-6.96 [-11.13, -3.13]	896 [674, 1144]	-0.15 [-0.44, 0.14]	3.77 [-11.34, 19.8]	0 [-0.02, 0.03]	0.2 [-1.14, 1.48]	0 [-0.2, 0.18]	-13.67 [-22.17, -4.25]	0.06 [-0.76, 0.66]	-20.83 [-42.03, 2.45]
8.16	0.01 [0, 0.02]	-1.44 [-1.68, -1.17	-9.69 [-14.52, -5.24]	1172 [906, 1450]	0.03 [-0.27, 0.31]	-9.11 [-20.51, 4.16]	-0.02 [-0.05, 0.01]	1.38 [0.15, 2.76]	0.04 [-0.15, 0.24]	-21.41 [-32.41, -11.20]	-0.36 [-0.90, 0.15]	-10.24 [-30.94, 6.85]
4.19	0.01 [0, 0.02]	-1.62 [-1.91, -1.3	-10.97 [-16.23, -6.25]	1308 [1013, 1617]	-0.04 [-0.43, 0.21]	-10.48 [-20.24, 3.21]	-0.02 [-0.06, 0.02]	1.62 [-0.5, 4.02]	0.03 [-0.22, 0.3]	-30.81 [-45.70, -15.94]	-0.34 [-0.95, 0.26]	-23.14 [-51.4, -0.59]
2.17	0.01 [0, 0.02]	-1.69 [-1.94, -1.40	-11.72 [-17.11, -6.92]	1386 [1090, 1704]	0 [-0.59, 0.20]	-16.53 [-25.61, 1.74]	0.01 [-0.03, 0.04]	0.77 [-1.30, 2.94]	0.03 [-0.2, 0.25]	-36.18 [-47.32, -24.50]	-0.12 [-0.89, 0.53]	-43.99 [-73.02, -15.72]
1.12	0.01 [0, 0.02]	-1.8 [-2.05, -1.51	-12.08 [-17.64, -7.13]	1426 [1122, 1753]	-0.31 [-0.7, 0.1]	-12.36 [-28.21, 3.93]	-0.02 [-0.06, 0.04]	1.9 [-0.49, 4.4]	0 [-0.29, 0.26]	-43.78 [-57.68, -28.7]	-0.42 [-1.18, 0.27]	-40.82 [-71.2, -11.15]
0.59	0.01 [0, 0.02]	-1.88 [-2.17, -1.6]	-12.26 [-17.85, -7.22]	1446 [1136, 1776]	-0.56 [-1.20, -0.16]	-9.49 [-27.28, 10.26]	-0.01 [-0.059, 0.04]	2.46 [0.27, 4.74]	0.11 [-0.2, 0.39]	-59.81 [-74.10, -44.38]	0.28 [-0.52, 0.97]	-79.82 [-113.6, -47.54]
60.8 (last)	0 [-0.01, 0]	0.5 [0.19, 0.85]	-2.98 [-6.69, -0.04]	286.37 [112.1, 522.70]	-0.02 [-0.28, 0.27]	4.23 [-7.73, 16.74]	0.01 [-0.019, 0.032]	-0.25 [-1.36, 1.10]	0.3 [0.05, 0.54]	-21.17 [-34.07, -6.89]	0.02 [-0.57, 0.53]	-9.01 [-26.44, 10.35]

Supplementary Table 3. *Age regression slopes and intercepts differences between the first brightest luminance (60.8 cd/m^2) and all the other luminance conditions in the b2d session.*

	Pupil size		Retinal illuminance		Onset		Amplitude		50IT		Peak latency	
lum	**slope**	**intr**	**slope**	**intr**	**slope**	**intr**	**slope**	**intr**	**slope**	**intr**	**slope**	**intr**
0.59	0.02 [0,0.02]	-2.16 [-2.61, -1.66]	-10.91 [-15.46, -6.4]	1406 [1171, 1659]	-0.13 [-0.47, 0.14]	-32.38 [-45.87, -19.18]	0 [-0.04, 0.04]	1.92 [0.10, 3.69]	-0.15 [-0.54, 0.16]	-42.34 [-59.82, -23.97]	-0.31 [-1.1, 0.40]	-42.19 [-85.6, -2.77]
1.12	0.01 [0,0.02]	-1.83 [-2.26, -1.4]	-10.75 [-15.28, -6.22]	1387 [1152, 1639]	-0.09 [-0.37, 0.23]	-29.66 [-43.89 -17.78]	-0.01 [-0.05, 0.03]	1.69 [0.08, 3.42]	0 [-0.33, 0.3]	-44.01 [-60, -27.41]	-0.24 [-0.82, 0.42]	-43.48 [-82.4, -14.58]
2.17	0.01 [0,0.02]	-1.66 [-2.05, -1.20]	-10.36 [-14.81, -5.87]	1345 [1118, 1596]	-0.21 [-0.72, 0.04]	-12.53 [-25.25, 6.77]	-0.01 [-0.03, 0.02]	1.78 [0.42, 3.14]	0.05 [-0.29, 0.36]	-38.36 [-54.12, -20.52]	-0.48 [-1.13, 0.16]	-19.26 [-50.8, 9.19]
4.19	0.01 [0,0.02]	-1.48 [-1.88, -1.05]	-9.77 [-14.06, -5.36]	1277 [1051, 1518]	0.09 [-0.35, 0.41]	-15.78 [-33.14, -2.37]	-0.01 [-0.04, 0.03]	1.33 [0.02, 2.8]	0.11 [-0.16, 0.38]	-34.63 [-48.41, -22.76]	-0.51 [-1.07, 0.11]	-13.14 [-37.6, 5.95]
8.16	0.01 [0,0.02]	-1.08 [-1.44, -0.72]	-8.8 [-12.80, -4.72]	1164 [954, 1398]	-0.02 [-0.28, 0.24]	-7.08 [-20.63, 7.01]	-0.01 [-0.04, 0.02]	1.36 [0.04, 2.71]	0.15 [-0.13, 0.46]	-30.7 [-46.89, -17.54]	-0.21 [-0.69, 0.29]	-18.82 [-42.5, 0.04]
16	0.01 [0,0.01]	-0.75 [-1.11, -0.37]	-7.14 [-11.01, -3.42]	957 [765, 1178]	0.16 [-0.14, 0.48]	-11.8 [-26.59, 2.97]	-0.01 [-0.05, 0.02]	1.06 [-0.27, 2.48]	0.04 [-0.22, 0.28]	-15.06 [-28.24, -1.70]	-0.15 [-0.72, 0.34]	-6.38 [-23.8, 13.14]
31	0 [0,0.01]	-0.32 [-0.67, 0.045]	-4.58 [-7.85, -1.38]	619 [459, 812]	0.13 [-0.16, 0.41]	-7.83 [-20.80, 6.54]	-0.02 [-0.05, 0.01]	0.99 [-0.33, 2.52]	0.16 [-0.16, 0.51]	-16.21 [-35.32, 1.38]	0.11 [-0.32, 0.62]	-13.83 [-36.1, 4.17]
60.8 (last)	0 [0,0]	0.22 [-0.11, 0.55]	-0.53 [-3.24, 2.30]	97 [-61, 264]	0.11 [-0.15, 0.39]	-3.74 [-16.43, 9.28]	-0.01 [-0.05, 0.02]	0.95 [-0.39, 2.24]	0.1 [-0.21, 0.36]	-10.06 [-24.90, 6.02]	0.07 [-0.27, 0.38]	-7.2 [-18.9, 3.72]

Supplementary Table 4. *Age regression slopes and intercepts differences between the first brightest luminance and all the other luminance conditions in the d2b session.*

	B2D				D2B			
	50IT / pupil size		**Peak lat / pupil size**		**50IT / pupil size**		**Peak lat / pupil size**	
luminance	slope	intercept	slope	intercept	slope	intercept	slope	intercept
60.8 (first)	-1.67 [-8.68, 7.47]	-0.08 [-6.22, 5.34]	1.7 [-12.44, 18.7]	0.02 [-9.72, 10.62]	-6.19 [-15.19, 6.08]	-0.49 [-7.45, 7.27]	0.50 [-29, 0.44]	-13.73 [-10.113, 13.31]
31	1.73 [-3.89, 7.85]	0.03 [-4.84, 4.49]	3.05 [-11.49, 17.98]	0.27 [-9.85, 11.87]	-3.18 [-8.62, 3.89]	0.14 [-4.50, 5.29]	-0.21 [-21.43, 12.42]	-6.86 [-11.93, 11.26]
16	-1.66 [-8.73, 7.90]	-0.04 [-5.20, 5.29]	-7.92 [-23.02, 10.73]	-0.53 [-12.20, 10.6]	-5.56 [-11.82, 1.78]	0.23 [-4.97, 5.71]	0.14 [-20.09, 10.14]	-7.38 [-10.66, 10.81]
8.16	-0.22 [-7.43, 8.68]	0.06 [-4.58, 5.03]	8.36 [-12.92, 26.35]	-0.4 [-13.02, 12]	-5.83 [-11.73, 0.65]	0.11 [-5.03, 6.07]	-0.16 [-22.50, 4.33]	-9.71 [-10.53, 9.55]
4.19	1.03 [-6.67, 8.88]	0.06 [-5.88, 6.37]	-8.31 [-25.88, 12.85]	-0.21 [-10.85, 9.94]	-1.91 [-9.46, 7.59]	-0.31 [-5.90, 5.88]	0.02 [-25.42, 10.44]	-5.6 [-10.56, 10.62]
2.17	-1.04 [-8.03, 5.57]	0.03 [-4.58, 4.51]	-15.9 [-27.21, -2.46]	-0.41 [-12.35, 10.29]	0.12 [-7.54, 8.23]	0.03 [-6.13, 6.40]	-0.63 [-20.89, 6.95]	-9.48 [-11.14, 10.59]
1.12	-2.36 [-9.17, 5.74]	-0.003 [-5.48, 5.19]	-13.21 -24.65, -1.54]	-0.43 [-10.16, 9.72]	-1.32 [-8.06, 6.13]	0.09 [-6.64, 6.39]	-0.04 [-13.67, 14.18]	-1.71 [-13.37, 17.43]
0.59	-5.11 [-12.90, 1.85]	0.33 [-3.89, 5.54]	-16.06 -30.34, 2.54]	0.21 [-13.33, 15.37]	-2.11 [-9.19, 8.29]	-0.10 [-5.55, 5.64]	-0.13 [-15.4, 13.20]	0.15 [-11.81, 14.95]
60.8 (last)	-4.72 [-14.67, 5.12]	0.005 [-6.99, 6.37]	-12.75 -26.72, 3.73]	0.02 [-10.34, 9.97]	-1.95 [-8.89, 5.45]	-0.05 [-4.52, 5.25]	0.06 [-20.41 10.87]	-4.8 [-9.52, 10.96]

Supplementary Table 5. *Slopes and intercepts of regressions of 50IT and peak latency against pupil size, after partialling out the effects of age. Confidence intervals of the slopes and intercepts are given in square brackets.*

B2d sessions			***D2b sessions***		
luminance	***50IT***	***Peak latency***	***luminance***	***50IT***	***Peak latency***
60.8 (first)	*-50 [-64, -34]*	*-84 [-100, -33]*	**60.8 (first)**	*-53 [-72, -33]*	*-80 [-100, -27]*
31	*-38 [-48, -28]*	*-76 [-94, -19]*	**0.59**	*-8 [-26, 10]*	*-51 [-74, 5]*
16	*-38 [-53, -20]*	*-70 [-89, -12]*	**1.12**	*-11 [-27, 8]*	*-55 [-79, 7]*
8.16	*-27 [-38, -18]*	*-69 [-85, -18]*	**2.17**	*-13 [-32, 6]*	*-67 [-86, -20]*
4.19	*-21 [-34, -4]*	*-66 [-83, -9]*	**4.19**	*-21 [-38, -1]*	*-65 [-89, -13]*
2.17	*-13 [-26, -3]*	*-53 [-75, 7]*	**8.16**	*-26 [-47, -3]*	*-69 [-92, -20]*
1.12	*-9 [-22, 8]*	*-49 [-72, 12]*	**16**	*-37 [-54, -17]*	*-76 [-96, -29]*
0.59	*8 [-1, 20]*	*-9 [-51, 56]*	**31**	*-37 [-58, -16]*	*-70 [-94, -20]*
60.8(last)	*-37 [-51, -18]*	*-71 [-93, -13]*	**60.8(last)**	*-40 [-56, -20]*	*-76 [-97, -28]*

Supplementary Table 6. *50IT and peak latency differences (ms), between young (<30) and old (>60) subjects. Differences in median processing speed (50IT) and median peak latency of face-texture ERP difference between young subjects in all luminance conditions, and old subjects in the first brightest condition (luminance = 60.8 cd/m^2). For each difference the 95% bootstrap confidence interval is given in square brackets.*

		Young, no pinhole (first)	**Young, 1 mm**	**Young, 2 mm**	**Young, 3 mm**	**Young, 4 mm**	**Young, 5 mm**	**Young, no pinhole (last)**
b2s pinhole	**(Old, b2d session)**	-43 [-56, -27]	32 [17, 45]	-14 [-39, 16]	-14 [-41, 11]	-21 [-45, -5]	-34 [-54,-15]	-22 [-42, -5]
	(Old, d2b session)	-47 [-64, -30]	28 [12, 47]	-18 [-44, 16]	-18 [-45, 9]	-25 [-50, -6]	-39 [-59,-14]	-26 [-48, -7]
s2b pinhole	**(Old, b2d session)**	-43 [-59, -26]	19 [-15, 36]	-27 [-41, -6]	-23 [-35, -6]	-28 [-48, -4]	-16 [-38, 5]	-36 [-53, -18]
	(Old, d2b session)	-47 [-65, -27]	14 [-16, 37]	-32 [-47, -7]	-27 [-40, -7]	-32 [-55, -6]	-20 [-43, 1]	-41 [-58, -19]

Supplementary Table 7. *Differences in 50IT between young subjects in the pinhole experiment and old subjects in the luminance experiment. The results are presented for all the pinhole conditions of each experimental session (s2b and b2s), and for luminance condition 1 (60.8 cd/m^2) of both sessions (b2d and d2b).*

SUPPLEMENTARY FIGURES

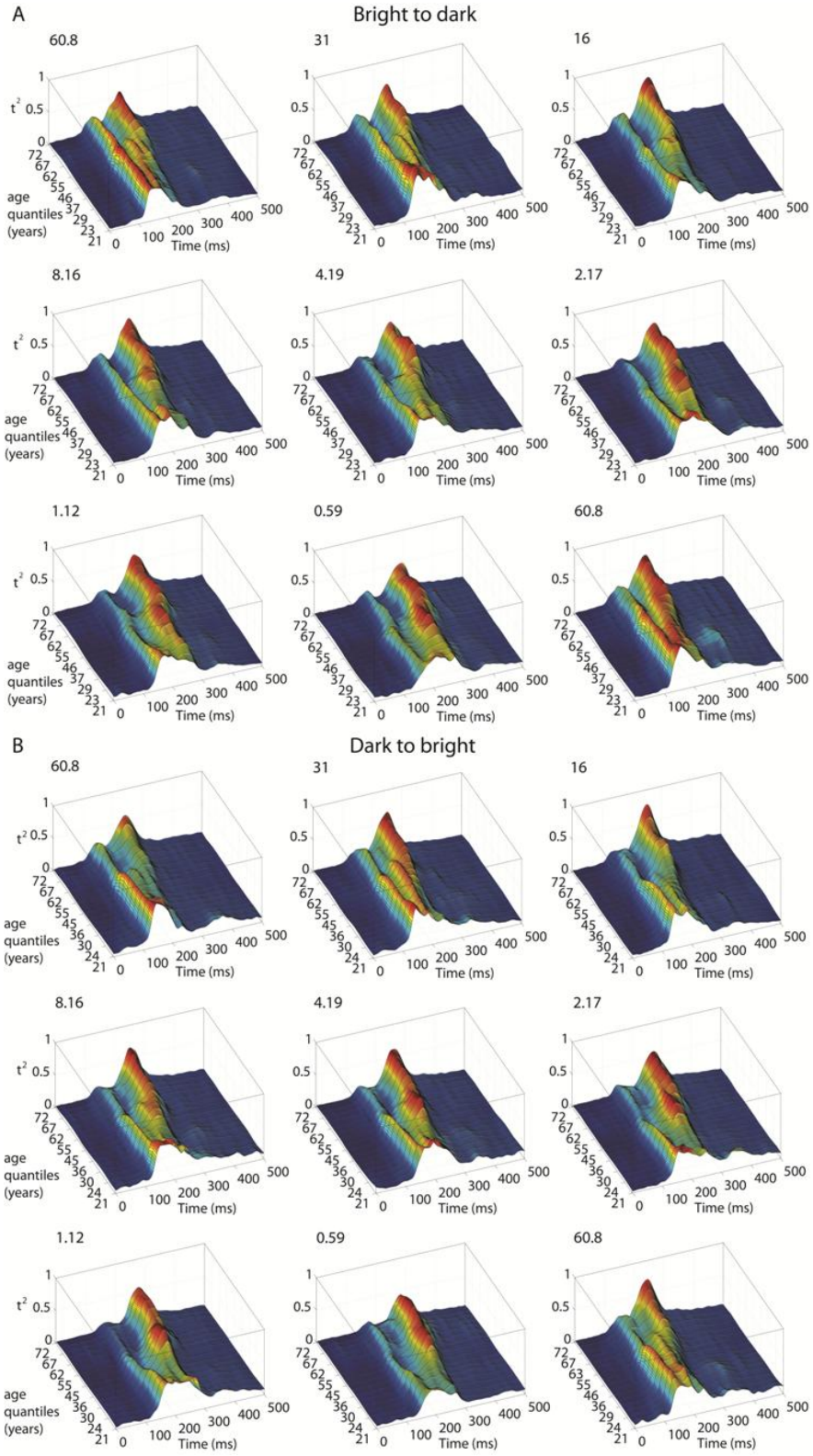

Supplementary Figure 1. *3D landscapes of t^2 functions. Each subplot depicts how the time-course (X axis) of normalised t^2 functions (Z axis) changes with age (Y axis), at the luminance indicated in the top left corner of the subplot.* ***(A)*** *B2d session.* ***(B)*** *D2b session. The process of generating the figure is described in section 3.1.7 of the thesis.*

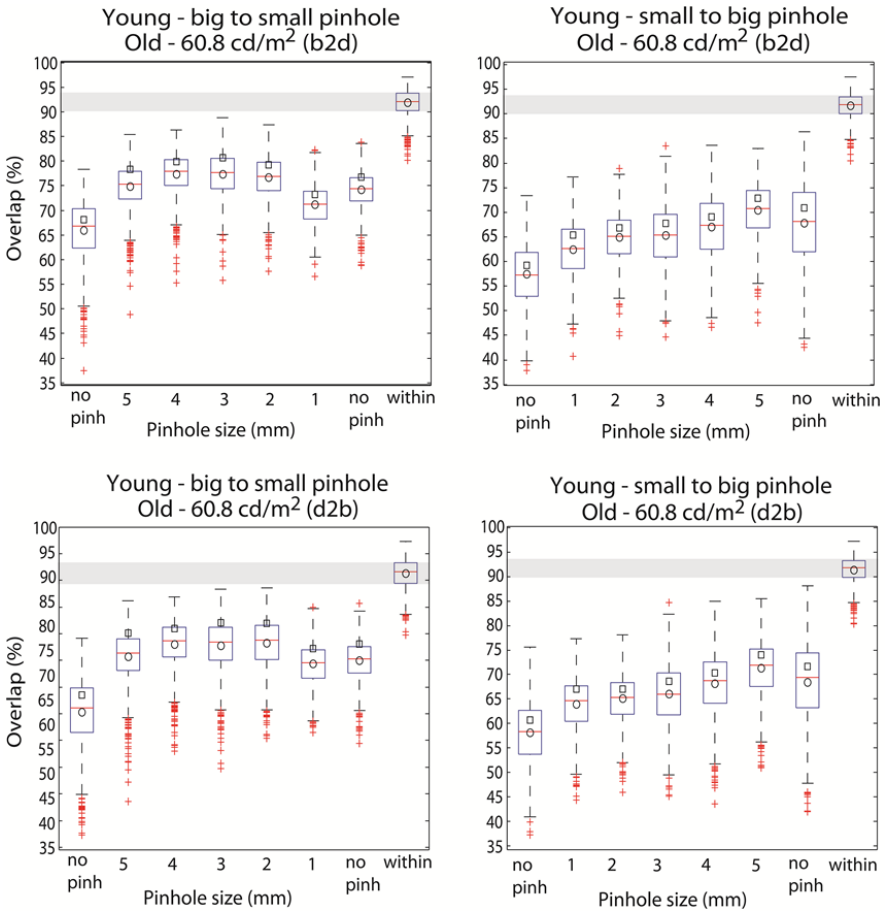

Supplementary Figure 2. *Boxplots of t^2 function overlaps. Boxplots depicting distributions of t^2 function overlaps between young subjects in each pinhole condition and old subjects from the luminance experiment, in the brightest condition (60.8 cd/m^2) of b2d and d2b sessions. The last boxplot in each subplot shows the overlap within the group of old subjects.*

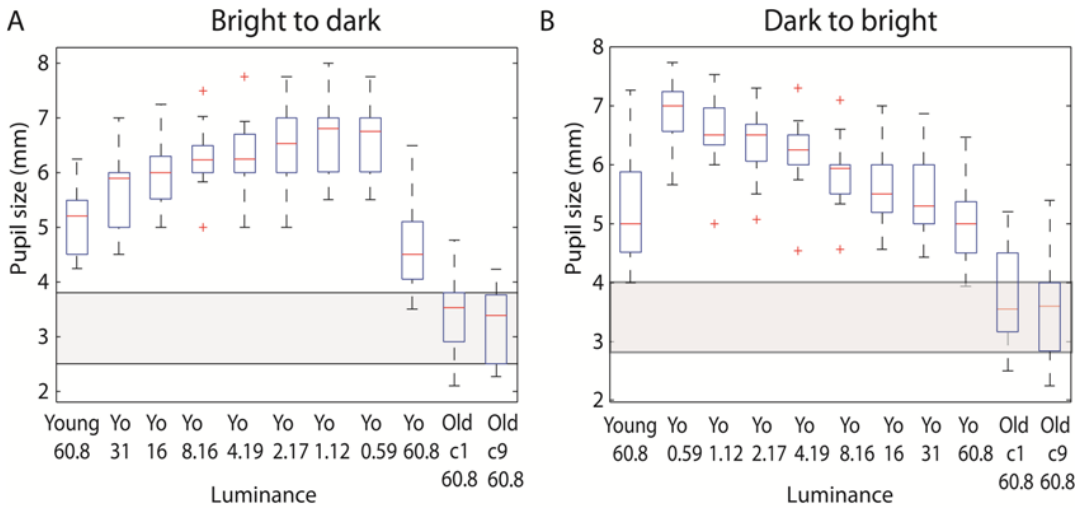

Supplementary Figure 3. *Pupil size of young and old subjects. The first nine boxplots in each subplot depict the distributions of pupil sizes in young subjects, at nine luminances for b2d (A) and d2b (B) sessions. The last two boxplots in each subplot show results in old subjects in the two brightest conditions (luminance=60.8 cd/m^2).*